

STUDIES OF SOME METAL CARBOXYLATE COMPLEXES

By

David Lincoln Martin, B.Sc.

Thesis presented for the degree of  
Doctor of Philosophy

University of Edinburgh

March 1961



# ABSTRACT OF THESIS

Name of Candidate DAVID LINCOLN MARTIN

Address \_\_\_\_\_

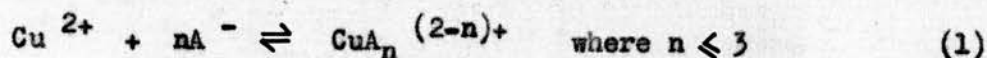
Degree DOCTOR OF PHILOSOPHY Date March 1961.

Title of Thesis STUDIES OF SOME METAL CARBOXYLATE COMPLEXES.

A wide variety of physicochemical evidence suggests that copper(II) acetate and its higher homologues exist as dimers in the crystalline state, in certain organic solvents, and possibly even in aqueous solution. A precise equilibrium study has been made of copper(II) formate, acetate, propionate, and n-butyrate in order to establish which species exist in aqueous solution. Competition between protons and Cu(II) ions for the carboxylate anions was followed at  $25.00 \pm 0.05^\circ\text{C}$ . in 3.00M sodium perchlorate with a glass electrode, and hydrogen ion concentrations were measured with a precision of  $\pm 0.003$  pH unit.

Before making the above investigation, it was necessary to study the analogous proton-carboxylate equilibria. The pH of carboxylate buffers in the constant ionic medium appears to be a function of their concentration. The formation of monomeric monocarboxylic acids HA predominates at carboxylate concentrations less than  $5 \times 10^{-2}\text{M}$ . At higher concentrations up to 1M appreciable concentrations of the proton bis (monocarboxylato)- species  $\text{HA}_2$  and the dimers  $\text{H}_2\text{A}_2$  exist. The species  $\text{H}_2\text{A}_3$  and  $\text{H}_3\text{A}_3$  have been identified in propionic and n-butyric buffers. All these species have been characterised by their formation constants. The species are assumed to associate by hydrogen bonding and the dimers appear to exist in/extended rather than the cyclic form. Further evidence for the extended form of the dimer has been deduced from calorimetric measurements of the heat changes on association in the acetate system.

For Cu(II) concentrations between  $10^{-2}$  and  $10^{-1}\text{M}$ , and free formate or acetate concentrations up to about 0.6M, neither polynuclear Cu(II) complexes nor mononuclear complexes of the anion  $\text{HA}_2$  were detectable. The experimental results are explicable in terms of the step-wise equilibria,



In the propionate system the same species exist together with the dimer  $\text{Cu}_2\text{A}_4$ . No polynuclear species are detectable in the butyrate system before precipitation occurs. The cadmium(II) acetate system has also been investigated; an earlier report of dimers in the literature cannot be substantiated.

The acetic acid and copper(II) acetate systems have also been studied in a 50% v/v dioxan/0.6M sodium perchlorate medium. In addition to the proton-carboxylate complexes found in aqueous solution,  $\text{H}_2\text{A}_3$ ,  $\text{H}_3\text{A}_3$ ,  $\text{H}_3\text{A}_4$ , and  $\text{H}_4\text{A}_4$  exist in acetic acid in this medium up to an acetate concentration of 0.5M. The formation constants have been obtained. In the copper(II) acetate system the experimental data indicate that polynuclear, mixed, and hydroxo complexes may exist. The stability constants of the mononuclear species  $\text{CuA}$  and  $\text{CuOH}$  have been evaluated; unfortunately, the equilibria in this system are so complicated that the evaluation of further formation constants appears to be impossible at present.

## CONTENTS

Acknowledgement

Symbols

Summary

Section 1.	INTRODUCTION.	
1(a)	Metal Complexes and Stability Constants	1
1(b)	Reversible Step Equilibria	2
1(c)	Association of Carboxylic Acids	5
1(d)	Dimerisation of Copper (II) <i>n</i> -Alkanoates	22
1(e)	The Scope of the Present Work	31
Section 2.	METHODS OF COMPUTATION.	32
2(a)	Graphical Treatment of the Data $\bar{n}$ , $\alpha$	34
2(b)	Curve-fitting Techniques	36
2(c)	Integration Method of Determining the Average Composition of Polynuclear Species	53
Section 3.	EXPERIMENTAL.	
3(a)	Reagents	55
3(b)	Apparatus	62
3(c)	Potentiometric Procedure	68
Section 4.	CARBOXYLIC ACID EQUILIBRIA IN WATER.	
4(a)	Potentiometric Titration Results	81
4(b)	Calorimetric Titration Results	110
4(c)	Discussion	132



Section 5.	METAL-CARBOXYLATE EQUILIBRIA IN WATER.	
5(a)	Potentiometric Titration Results	141
5(b)	Discussion	161
Section 6.	EQUILIBRIA IN 50% V/V AQUEOUS DIOXAN.	
6(a)	Preliminary Measurements	165
6(b)	Acetic Acid Equilibria	168
6(c)	Copper (II) Acetate	194
Bibliography		197

#### ACKNOWLEDGEMENTS

I am deeply grateful to Dr. F. J. C. Rossotti for all his advice, guidance, and encouragement during the course of this research.

The calorimetric work was carried out jointly with Fil. kand. K. Schlyter at the Royal Institute of Technology, Stockholm, Sweden, and I thank Professor L. G. Sillen of the Institute for his interest in this research. The measurements of the cadmium (II) acetate system were made by Mr. R. McLellan.

In addition, I am grateful to the Department of Scientific and Industrial Research for a maintenance allowance, and to the University of Edinburgh for the award of a Hope Prize and a travel allowance.

## SYMBOLS

A	Total carboxylate concentration
$A_1$	Total carboxylate concentration in the mononuclear species
a	Free ligand concentration
B	Total metal ion concentration
b	Free metal ion concentration
$C_B$	Concentration of alkali used in potentiometric acid-base titration
$C_H$	Concentration of acid used in potentiometric acid-base titration
$C_H^1$	Concentration of perchloric acid present in a metal-carboxylate solution
$C_{HA}$	Concentration of carboxylic acid in titration vessel
$C_{HClO_4}$	Concentration of perchloric acid solution
$C_{NaA}$	Concentration of sodium carboxylate in titration vessel
D, L	Factors in variation of Henderson's equation
E	Measured potential in mV
$E_J$	Liquid junction potential
$E_0$	Standard potential of glass electrode with reference to the reference silver electrode
F	Faraday
g, p, v	Parameters
H	Total hydrogen ion concentration
h	Free hydrogen ion concentration
$h_c$	Free hydrogen ion concentration at the isohydric point
I	Ionic strength
J	Exchange energy associated with $\delta$ -bond
K	Ratio connecting the association constants of complexes

$K_a$	Acid dissociation constant of $H_pA_q$
$K_D$	Dimerisation constant, Eq. (1-10)
$K_n$	Stepwise stoichiometric stability constant
$K_{pq}$	Stepwise formation constant for proton-carboxylate systems
$K_T$	Trimerisation constant, Eq. (1-11).
$K_W$	Ionic product of water
$M$	Mole.l <sup>-1</sup>
$N$	Maximum number of ligands
$n$	Number of ligands
$\bar{n}$	Degree of formation of a system
$\bar{n}_c$	Value of $\bar{n}_H$ at the isohydric point
$\bar{n}_H$	Degree of formation of a proton-carboxylate system
$\bar{n}_{H(1)}$	Average number of protons per carboxylate in the mononuclear species
$\bar{p}_{poly}$	Average number of protons per carboxylate group
$\bar{q}_{poly}$	Average number of carboxylate groups
$R$	Ratio to be determined
$\bar{r}$	Reciprocal of the average degree of condensation of A
$S_{B_pA_q}$	Solubility product of $B_pA_q$
$V_A$	Volume of acid
$V_B$	Volume of alkali
$V_i$	Initial volume of titration solution
$V_T$	Total volume of titration solution
$Z$	Average number of OH ions bound per copper atom

$A^*, a^*, h^*$	Normalised variables
$\alpha_n$	Relative proportions of species $BA_n$ in solution
$\alpha_{pq}$	Relative proportions of species $HpAq$ in solution
$\beta_n$	Overall stability constant
$\beta_{pq}^H$	Overall formation constant for proton-carboxylate systems
$\delta_H$	Activity coefficient of the hydrogen ion
$\Delta G$	Free energy change
$\Delta H_{pq}$	Enthalpy change (stepwise)
$\Delta \mathcal{H}_{pq}$	Enthalpy change (overall)
$\Delta S_{pq}$	Entropy change

---

The following symbols were used in the calorimetric work, Sec.4(b).

A	Amperes
C	Heat capacity of the calorimeter and its contents
$\bar{C}$	Average value of C
$c_i$	Molarity of the ionic or molecular species i
$c_{pq}$	Molarity of complex, $HpAq$
$E_B$	Potential difference recorded by the potentiometer during the calibration
$E_W$	Bridge voltage
$\bar{E}$	$E_B$ at middle point of calibration
$I_G$	Current through galvanometer branch of the Wheatstone bridge
L	Excess enthalpy in cal. litre <sup>-1</sup> of solution
$L_T$	Excess enthalpy of titrant in cal. litre <sup>-1</sup>
$l_A$	Relative partial molar enthalpy of A in cal. mole <sup>-1</sup>
$l_i$	Relative partial molar enthalpy of any ionic or molecular species, i



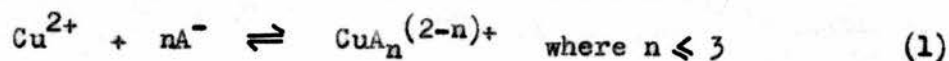
$m$	Position of the galvanometer light spot on the linear scale
$m_a$	Average value of the thermostat temperature expressed as a reading on the linear scale
$m_b$	Temperature of calorimeter solution just before an addition was made, expressed as a reading on the linear scale
$n_i$	Number of moles of any ionic or molecular species, $i$
$Q$	Amount of heat evolved or absorbed due to the addition of one solution to another
$R_{61}, R_{62}$	Constant resistances of the Wheatstone bridge
$R_{C3}$	Constant resistance temporarily replacing the thermometer resistance, $R_T$
$R_D$	Adjustable resistance kept constant during titrations
$R_G$	Internal resistance of the mirror galvanometer
$R_T$	Variable thermometer resistance
$S$	Error function, defined in Eq. (4-39)
$t_p$	"Student" factor, used in error calculations
$\mu$	Position of galvanometer light-spot corrected to circular scale
$\mu_0$	Value of $\mu$ for $I_G = 0$
$\tau_G$	Time (in sec) of calibration
$\Omega$	Ohms

### SUMMARY.

A wide variety of physicochemical evidence suggests that copper(II) acetate and its higher homologues exist as dimers in the crystalline state, in certain organic solvents, and possibly even in aqueous solution. A precise equilibrium study has been made of copper(II) formate, acetate, propionate, and n-butyrate in order to establish which species exist in aqueous solution. Competition between protons and Cu(II) ions for the carboxylate anions was followed at  $25.00 \pm 0.05^\circ\text{C}$ . in 3.00M sodium perchlorate with a glass electrode, and hydrogen ion concentrations were measured with a precision of  $\pm 0.003$  pH unit.

Before making the above investigation, it was necessary to study the analogous proton-carboxylate equilibria. The pH of carboxylate buffers in the constant ionic medium appears to be a function of their concentration. The formation of monomeric monocarboxylic acids HA predominates at carboxylate concentrations less than  $5 \times 10^{-2}\text{M}$ . At higher concentrations up to 1M appreciable concentrations of the proton bis(monocarboxylato)- species  $\text{HA}_2$  and the dimers  $\text{H}_2\text{A}_2$  exist. The species  $\text{H}_2\text{A}_3$  and  $\text{H}_3\text{A}_3$  have been identified in propionic and n-butyric buffers. All these species have been characterised by their formation constants. The species are assumed to associate by hydrogen bonding <sup>the</sup> and the dimers appear to exist in/extended rather than the cyclic form. Further evidence for the extended form of the dimer has been deduced from calorimetric measurements of the heat changes on association in the acetate system.

For Cu(II) concentrations between  $10^{-2}$  and  $10^{-1}\text{M}$ , and free formate or acetate concentrations up to about 0.6M, neither polynuclear Cu(II) complexes nor mononuclear complexes of the anion  $\text{HA}_2$  were detectable. The experimental results are explicable in terms of the step-wise equilibria,



In the propionate system the same species exist together with the dimer  $\text{Cu}_2\text{A}_4$ . No polynuclear species are detectable in the butyrate system before precipitation occurs. The cadmium(II) acetate system has also been investigated; an earlier report of dimers in the literature cannot be substantiated.

The acetic acid and copper(II) acetate systems have also been studied in a 50% v/v dioxan/0.6M sodium perchlorate medium. In addition to the proton-carboxylate complexes found in aqueous solution,  $\text{H}_2\text{A}_3$ ,  $\text{H}_3\text{A}_3$ ,  $\text{H}_3\text{A}_4$ , and  $\text{H}_4\text{A}_4$  exist in acetic acid in this medium up to an acetate concentration of 0.5M. The formation constants have been obtained. In the copper(II) acetate system the experimental data indicate that polynuclear, mixed, and hydroxo complexes may exist. The stability constants of the mononuclear species  $\text{CuA}$  and  $\text{CuOH}$  have been evaluated: unfortunately, the equilibria in this system are so complicated that the evaluation of further formation constants appears to be impossible at present.

SECTION 1.

INTRODUCTION

1 (a) METAL COMPLEXES AND STABILITY CONSTANTS.

A complex may be defined as a species which is formed by the association of two or more simpler species. There are limitations to this definition but generally it is quite adequate. In 1864 Guldberg and Waage<sup>1</sup> postulated the law of mass action which states that in a homogeneous system, the rate of chemical reaction is proportional to the active masses of the reacting substances. Since then the quantitative study of chemical equilibria has been based on this law.

Morse<sup>2</sup> and Sherrill<sup>3</sup>, two of Abegg's co-workers, were the first to show that step-wise formation of complexes occurred. They did this only a year or so after Bodländer and his co-workers<sup>4</sup> had reported the first stability constants of metal complexes. Bodländer also pioneered the use of the ionic medium (see Sec. 3 (c)), first reported in 1905 in a paper by Grossmann<sup>5</sup>.

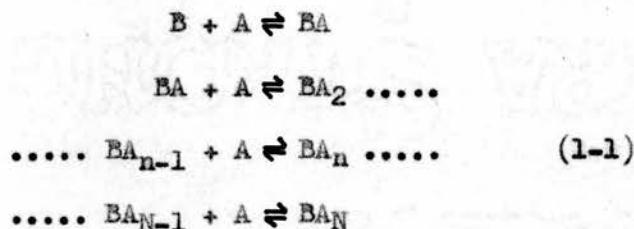
Niels Bjerrum also was studying metal complexes at this time and he was able to obtain the formation constants for six consecutive complexes in the system chromium (III) thiocyanate<sup>6,7</sup>. This work paved the way for the present analysis of systems in which several species coexist. Between 1920 and 1940 there was a lull in activity in the field of metal complexes until in 1941 Jannik Bjerrum<sup>8</sup> and Leden<sup>9</sup> described methods for computing step stability constants. Since 1941 there has been a renewal of interest in metal complexes and stability constants so that today an increasing number of workers is engaged in their study.



1 (b) REVERSIBLE STEP EQUILIBRIA

The present methods for determining the stability constants of complexes   owe much to the early work of the Bjerrums. The formation of metal complexes in solution may be discussed using Jannik Bjerrum's theory of step-wise equilibria<sup>8</sup>.

Consider the equilibrium between a central metal ion B and n ligands A. Complex formation is considered to take place by a series of consecutive reactions, each involving two of the intermediate species thus:



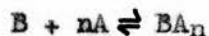
where N = maximum value of n. Charges are omitted for clarity.

The equilibrium constants for these consecutive reactions are known as the step equilibrium constants of the system. The stoichiometric stability constant,  $K_n$ , for the species  $BA_n$  is given by

$$K_n = [BA_n]/[BA_{n-1}]a \quad (1-2)$$

where a = concentration of free ligand.

The overall stability constant for the species  $BA_n$ , or thermodynamic equilibrium constant for the reaction



is  $\beta_n$  and is given by

$$\beta_n = [BA_n]/b a^n \quad (1-3)$$

where b = concentration of free central metal ion B.

$$\text{Thus } \beta_0 = K_0 = 1, \beta_1 = K_1 \text{ and } \beta_n = \prod_{1}^n K_n \quad (1-3a)$$

The quantity  $\bar{n}$  is called the degree of formation of the system and is defined as the average number of ligands bound to one central group. Thus, in the system outlined above where species BA, BA<sub>2</sub> .... BA<sub>N</sub> are formed

$$\bar{n} = \frac{[BA] + 2[BA_2] + \dots + N[BA_N]}{b + [BA] + [BA_2] + \dots + [BA_N]} \quad (1-3)$$

$$= \frac{\sum_{n=1}^{n=N} n[BA_n]}{\sum_{n=0}^{n=N} [BA_n]} \quad (1-4)$$

Substituting from eq. (1-2)

$$\begin{aligned} \bar{n} &= \frac{K_1ba + 2K_1K_2ba^2 + \dots + nK_1K_2 \dots K_nba^n}{b + K_1ba + K_1K_2ba^2 + \dots + K_1K_2 \dots K_nba^n} \\ &= \frac{\sum_{n=1}^{n=N} n\beta_n a^n}{\sum_{n=0}^{n=N} \beta_n a^n} \quad (1-5) \end{aligned}$$

Equation (1-5) is the formation function of the system and the plot of  $\bar{n}$  against  $-\log a$  is called the formation curve. The values of the stability constants can be calculated if the formation curve can be obtained experimentally.

In systems containing protons and a ligand A, stepwise formation of complexes such as HA, HA<sub>2</sub>, H<sub>2</sub>A<sub>2</sub>, .... H<sub>p</sub>A<sub>q</sub>, where p and q are integers, may take place. Stability constants may be obtained from measurements of  $\bar{n}_H$ , the average number of protons bound to each ligand. Now

$$\bar{n}_H = \frac{H - h + K_w h^{-1}}{A} \quad (1-6)$$

where H = total analytical concentration of hydrogen ions

h = concentration of free hydrogen ions

K<sub>w</sub> = ionic product of water

A = total concentration of ligand A

Thus

$$\bar{n}_H = \frac{[HA] + [HA_2] + 2[H_2A] + \dots + P[H_pA_q]}{a + [HA] + [H_2A] + 2[HA_2] + \dots + Q[H_pA_q]}$$

where P and Q are the maximum values of p and q respectively.

Then

$$\bar{n}_H = \frac{\sum_{p=1}^{p=P} \sum_{q=1}^{q=Q} p[H_pA_q]}{\sum_{p=0}^{p=P} \sum_{q=1}^{q=Q} q[H_pA_q]}$$

The overall stability constant for the species  $H_pH_q$  is  $\beta_{pq}^H$  and is given by

$$\beta_{pq}^H = [H_pA_q]/h^p a^q \quad (1-8)$$

whence

$$\bar{n}_H = \sum_{p=1}^{p=P} \sum_{q=1}^{q=Q} p \beta_{pq}^H h^p a^q / \sum_{p=0}^{p=P} \sum_{q=1}^{q=Q} q \beta_{pq}^H h^p a^q \quad (1-9)$$

If data (A, H, h) are available it is convenient to plot curves  $\bar{n}_H(\log h)_A$  i.e. to plot  $\bar{n}_H$  as a function of log h and join all points with the same value of A by a separate curve.

## 1 (c) ASSOCIATION OF CARBOXYLIC ACIDS

It has been known for many years that carboxylic acids are associated in the vapour phase and in some organic solvents. The type of association and the equilibrium between single and associated molecules have been studied extensively and a review of the subject has been published<sup>10</sup>. Formic, acetic, propionic, and n-butyric acids have been studied in the present investigation. Previous work on these acids is reviewed in this section.

### Association in the Vapour Phase.

Bineau<sup>11</sup> appears to have been the first to investigate the vapour phase association of a carboxylic acid. However, reliable data were not obtained until the end of the nineteenth century when Ramsay and Young<sup>12</sup> showed that acetic acid was associated. Since then there have been many investigations and some of the data obtained for the four acids are summarised in Table 1-1. Vapour density and spectroscopic methods have been used most. The temperature range is quoted and it can be seen that this varies quite widely from investigation to investigation. The range of pressure used also varies considerably but in all cases the pressure is low enough for dimerisation to be the main reaction taking place. The overall heats of association,  $-\Delta H_D^\circ$ , of the dimer and of the trimer are given. The change in the standard entropies  $\Delta S_n^\circ$  are given also.

In Table 1-1 the abbreviations in the "method used" column are

AA	Acoustic absorption	UV	Ultraviolet spectra
CAP	Heat capacity	VC	Virial coefficient
IR	Infrared spectra	VD	Vapour density
PVT	Pressure-volume-temperature	VP	Vapour pressure
R	Raman spectra		

TABLE 1-1

Standard heats and entropies of association of carboxylic acids in the vapour phase.

Reference	Method	Temperature Range °C	$-\Delta H_2^0$ k.cal.mole <sup>-1</sup>	$-\Delta S_2^0$ cal.deg. <sup>-1</sup> mole <sup>-1</sup>	$-\Delta H_3^0$ k.cal. mole <sup>-1</sup>	$-\Delta S_3^0$ cal.deg. <sup>-1</sup> mole <sup>-1</sup>
-----------	--------	-------------------------	---	---	---	---

TABLE 1-1A FORMIC ACID

11			17.4 <sup>a</sup>			
15	VD	110-215	16.0 <sup>b</sup>			
16	PVT; UV	25-84	14.1	36		
17	VD	10-156	14.1	36		
18	VD	25-80	17.4 <sup>b</sup>			
19	IR	50-150	12.4±0.7			
20	VD	25	14.4 <sup>c</sup>	36.7 <sup>j</sup>		
21	VC	75-185	14.5			
22	R		12.4			
23	IR		13.9			
24	PVT	50-150	14.1±0.2	36		
19 <sup>k</sup>	IR	50-150	12.8±0.7			

TABLE 1-1B ACETIC ACID

12,25	VD	0.280	12.4 <sup>d</sup>			
27	VP	70-80	17.5 <sup>e</sup>			
29	VD	40-200	15			
30	VD	137-197	14			
26	VD	110-184	13.8	28.8 <sup>j</sup>		
31	VD	25-40	16.4			
32	IR		f			
33	VD	25	15.9	39.2 <sup>j</sup>		
34	VD	50-170	13.7 <sup>g</sup>	33.2 <sup>j</sup>	22.8	58.9 <sup>j</sup>
21	VC	75-185	13.8			
36	VD	80-200	13.8±0.1	33.1 <sup>j</sup>	22.7	58.7 <sup>j</sup>
37	PVT	50-150	15.3	38.1 <sup>j</sup>		
38	PVT	350-435	13.5	15.5 <sup>j</sup>	20.5	25.0 <sup>j</sup>
39	PVT	120-164	15.0±0.2	35.95±0.05		
40	CAP; IR	95-270	15.1±0.05	36		
41 <sup>m</sup>	IR	24 and 139	15.9±0.7			
35 <sup>n</sup>	VD	80-170	14.1	34.0 <sup>j</sup>	23.2	60.3 <sup>j</sup>

TABLE 1-1C PROPIONIC ACID

30	VD	137-197	15			
42	VD	45-65	18.5±1	46 <sup>j</sup>	24±3	59.3 <sup>j</sup>
24	PVT	50-150	15.2	36.4		
43	AA	20-50	17.2 <sup>h</sup>			
45 <sup>p</sup>	IR	25-125	14.1±0.5	33		



TABLE 1-1 (continued)

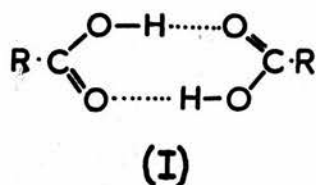
Reference	Method	Temperature Range °C	$-\Delta H_2^\circ$ k. cal. mole <sup>-1</sup>	$-\Delta S_2^\circ$ cal. deg. mole <sup>-1</sup>	$-\Delta H_3^\circ$ k. cal. mole <sup>-1</sup>	$-\Delta S_3^\circ$ cal. deg. mole <sup>-1</sup>
-----------	--------	-------------------------	---	---	---	---

TABLE 1-1D n-BUTYRIC ACID

30	VD	137-197	18.5			
46	VD	140-200	13.9	33	23	
19 <sup>9</sup>	IR	50-150	13.8±0.7			

- a Calculated by Gibbs<sup>13</sup> and Ramsperger and Porter<sup>14</sup>
- b Calculated by Ramsperger and Porter<sup>14</sup>
- c Calculated from measurements by Coolidge<sup>17</sup>
- d Calculated by Fenton and Garner<sup>26</sup>
- e Calculated by Bakr and McBain<sup>28</sup>
- f The experimental data agree approximately with those of MacDougall<sup>31</sup>
- g The original  $\Delta H_2^\circ$  value of 14.5±0.4 kcal. mole<sup>-1</sup> and  $\Delta H_4^\circ$  value of 27.0±2.4 kcal. mole<sup>-1</sup> were recalculated by Potter, Bender, and Ritter<sup>35</sup>
- h Calculated from measurements by Lamb and Huddart<sup>44</sup>
- j Calculated by Pimentel and McClellan<sup>47</sup>
- k Acid used was HCOOD
- m Acid used was CH<sub>3</sub>COOD
- n Acid used was CD<sub>3</sub>COOD
- p Acid used was C<sub>2</sub>H<sub>5</sub>COOD
- q Acid used was C<sub>3</sub>H<sub>7</sub>COOD

Considerable evidence indicates that the configuration of the dimer of the acids is a planar cyclic ring (I) thus:



R = H or an alkyl group.

The hydrogen is not symmetrically placed between the oxygen atoms and the C - O bonds are not all equal in length. ~~From X-ray diffraction measurements~~ Pauling and Brockway<sup>48</sup> calculated the O - H ..... O distance in formic acid to be  $2.67 \pm 0.04 \text{ \AA}$ , while Karle and Brockway<sup>49</sup> calculated  $2.73 \pm 0.05 \text{ \AA}$ , ~~from~~ electron diffraction measurements. Pauling and Brockway concluded that the carboxyl C - O bonds are of equal length,  $1.29 \pm 0.02 \text{ \AA}$ . However, Karle and Brockway found that they are of different lengths,  $1.25 \pm 0.03 \text{ \AA}$  and  $1.36 \pm 0.04 \text{ \AA}$ , and also that the bond lengths in acetic acid are the same as in formic acid except that the O - H ..... O distance is  $2.76 \pm 0.06 \text{ \AA}$ .

It can be seen from Table 1-1 that some workers have postulated the formation of trimers or tetramers. Ritter and Simons<sup>34</sup> believed that in acetic acid vapour a tetramer with  $\Delta H_4^\circ = 27 \text{ kcal.mole}^{-1}$  is the next higher species formed after the dimer. Johnson and Nash<sup>36</sup> postulated that a trimer is formed. Potter, Bender, and Ritter<sup>35</sup> considered that Ritter and Simons erred in postulating a tetramer and recalculated the latter's results assuming that a trimer is formed.

However, other workers e.g. Weltner<sup>40</sup> consider that no species higher than a dimer is formed and it has been pointed out<sup>10</sup> that some of the

measurements were made at relatively high pressures and although the higher polymers would be formed in greater proportion, deviations from ideality would increase also. Hence, some doubt is cast on the existence of the higher polymers in the vapour phase.

#### Association in the Solid State.

An X-ray analysis of solid formic acid by Holtzberg, Post, and Fankuchen<sup>50</sup> showed that the molecules in the crystal are arranged in the form of infinite chains, each molecule being linked to two neighbours by hydrogen bonds. The length of each hydrogen bond is  $2.58 \pm 0.03 \text{ \AA}$ ; other bond lengths are  $\text{C} - \text{O} = 1.26 \pm 0.03 \text{ \AA}$  and  $\text{C} = \text{O} = 1.23 \pm 0.03 \text{ \AA}$ . The  $\text{O} - \text{C} = \text{O}$  angle is  $123 \pm 1^\circ$ .

The chain like arrangement is in agreement with the measurements of Johnson and Cole<sup>51</sup> on the dielectric polarisation of solid and liquid formic acid. Their results indicated that there must be a significant contribution from polar configurations of molecules rather than from a system composed entirely of non-polar dimers.

The molecules in the crystal of acetic acid are also linked in infinite chains by hydrogen bonds. Spectroscopic work by Rigaux<sup>52</sup> indicates that acetic acid forms polymers rather than dimers and Jones and Templeton<sup>53</sup> have studied the structure by X-ray crystallography. This work shows the infinite chains with the length of the hydrogen bond  $= 2.61 \pm 0.02$ , the  $\text{C} - \text{O}$  bond  $= 1.24 \pm 0.02 \text{ \AA}$  and the  $\text{C} = \text{O}$  bond  $= 1.29 \pm 0.02 \text{ \AA}$ . The  $\text{O} - \text{C} = \text{O}$  angle is  $122 \pm 2^\circ$ .

#### Association in the Liquid Phase and in Solution.

Beckmann, Nernst, Auwers, and Hendrikson were the first to investigate the dimerisation of carboxylic acids in solution. In 1890 Beckmann<sup>54</sup> showed by an ebullioscopic method that carboxylic acids

are dimerised in such solvents as benzene and chloroform. Soon after, Nernst<sup>55</sup> and Hendrixson<sup>56</sup> using distribution methods and Auwers<sup>57</sup> using a cryoscopic method confirmed this work.

In 1897 Beckmann<sup>58</sup> studied acetic acid in benzene cryoscopically and concluded that dimers are formed and in 1905 Herz and Fischer<sup>59</sup>, from partition measurements between water and various organic solvents such as benzene, toluene, and o-, m-, and p-xylene, found that acetic acid is dimerised in the organic phase in all these systems. Hantzsch<sup>60</sup> studied formic acid and acetic acid in alcohol, ether, and light petroleum. Waentig and Pescheck<sup>61</sup> measured the solubility of acetic acid in a variety of solvents and concluded that the acid is monomeric in ether, ethyl alcohol, and benzaldehyde, and dimeric in benzene, toluene, carbon tetrachloride, nitrobenzene, and chloroform. In 1926 Trautz and Moschel<sup>30</sup> studied the four acids in benzene and nitrobenzene cryoscopically and evaluated dimerisation constants in benzene. They postulated that trimers of the acids are formed in these solvents but they found that the trimerisation constants increased with concentration.

Following this early work a considerable amount of attention has been paid to the dimerisation of the acids in solution. The solvents used most have been benzene, carbon tetrachloride, and chloroform, and among the methods used have been cryoscopy, ebullioscopy, dielectric polarisation, specific heats, acoustic absorption, infrared and Raman spectra, and nuclear magnetic resonance measurements. The four acids will now be considered separately.

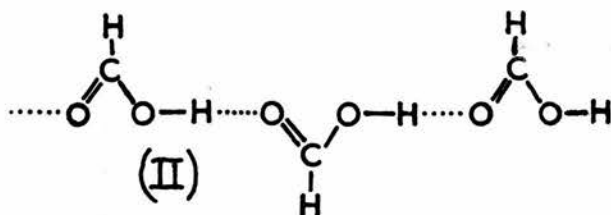
For 186

Formic Acid

Infrared and Raman spectra measurements of the acid in carbon tetrachloride solution have been made by Badger and Bauer<sup>32, 62</sup>, Kinsey and Ellis<sup>63</sup>, Batuev<sup>64</sup>, Chulanovskii and Simova<sup>65</sup>, and Chapman<sup>66</sup>, and it appears that the monomer predominates at low concentrations, the dimer being formed only at higher concentrations. From an examination of infrared spectra Chulanovskii and Simova postulated a new type of vibration, possibly of the binding hydrogen atom perpendicular to the plane of the dimer. This vibration, in the absence of an influence of the oxygen atoms of the two molecules, may go over into free rotation around the O - H axis.

The only measurements made in benzene solution have been of the dielectric constant at 30°C. by Pohl, Hobbs, and Gross<sup>67</sup>, who found the dimerisation constant  $\log K_D = -2.1$ . This contrasts with the value  $\log K_D = -3.9$  calculated by Trautz and Moschel<sup>30</sup>. Pohl, Hobbs, and Gross also measured the dimerisation constant in heptane solution and found  $\log K_D = -4.3$ . Wilson and Wenzke<sup>68</sup> from dielectric constant measurements and Batuev<sup>69</sup> from Raman spectra have concluded that formic acid is not dimerised in dioxan solution.

In the pure liquid, dimers or polymers appear to be formed. Huggins<sup>70</sup> considers that Kumler's work on the dielectric constant<sup>71</sup> indicates that chain polymerisation takes place thus





Evidence has also been cited from infrared spectra<sup>62, 66</sup> and Raman spectra<sup>72</sup> that the acid exists as long chain polymeric molecules and not as monomer or dimer. Sound velocity and dipole moment measurements<sup>73</sup> indicate a mean degree of association of about 5.

Peddle and Turner<sup>74</sup> were the first to report association of the acid in aqueous solution. They found that association is slight though it increases with increasing concentration. Raman spectra showed<sup>64</sup> that in 10-15% solutions of aqueous formic acid the dimers present in the pure acid break up, though not completely. There have been two attempts to evaluate the dimerisation constant of formic acid in aqueous solution. In each case a conductivity method at 25°C. was used. From measurements by Saxton and Darken<sup>75</sup>, Katchalsky, Eisenberg, and Lifson<sup>76</sup> calculated  $\log K_D = -1.40$  whilst Cartwright and Monk<sup>77</sup> calculated  $\log K_D = -2.08$ .

#### Acetic Acid

Since 1926 more attention has been paid to acetic acid than to the other three acids. Acetic acid dimerises in solution in benzene, chloroform, carbon tetrachloride and in diethyl ether<sup>78</sup>, cyclohexane<sup>79</sup>, carbon disulphide<sup>80</sup>, heptane<sup>67</sup>, chlorobenzene<sup>81</sup>, nitrobenzene<sup>81</sup>, isopropyl ether<sup>82</sup>, acetophenone<sup>83</sup>, 1:1 dichloroethane<sup>84, 85</sup>, nitromethane<sup>86, 87</sup>, and acetonitrile<sup>86, 87</sup>. There are conflicting views about dimerisation in solvents such as ether, dioxan, and alcohols. Smyth and Rogers<sup>78</sup> and Fénéant<sup>86, 87</sup> consider that dimers exist in ether solution but Tokareva and Kozlov<sup>85</sup> disagree. However, it is possible that the latter used solutions in their distribution measurements which were too weak, the maximum concentration being 10% acid in the solvent whereas Smyth and Rogers surveyed the entire concentration range. Wilson and Wenzke<sup>68</sup> and Batuev<sup>69</sup> believe that dimers are not present in dioxan and other

workers<sup>88, 89, 90</sup> postulate that instead there is some type of compound formed between the acid and the solvent. However, infrared<sup>91</sup> and Raman<sup>86, 87, 92, 93</sup> spectra measurements indicate that dimers do exist in dioxan solution.

While dimers have been found to exist in several organic solvents, there has been little support for the assertions of Herz and Lewy<sup>94</sup> and Trautz and Moschel<sup>30</sup> that higher species such as trimer, tetramer, and pentamer are formed. Meisenheimer and Dörner<sup>95</sup> found that at high concentration in benzene the degree of association rose to 2.15. From cryoscopic measurements in benzene Davies and Griffiths<sup>96</sup> have postulated that trimers or tetramers co-exist with the dimer. They believe the trimer to be the more likely.

The solvents used most in the study of the dimerisation of acetic acid have been benzene, carbon tetrachloride, and chloroform. It appears that in the first two of these solvents dimers are formed at low concentrations ( $< 0.05$  mole  $l^{-1}$ ). In chloroform dimerisation occurs at slightly higher concentrations.

Table 1-2 shows the dimerisation constant and heat and entropy of dimerisation of acetic acid in various solvents. The solvents are listed in order of increasing dielectric constant. The temperature at which the dielectric constant quoted was measured is added as a superscript. The abbreviations used in Tables 1-2, 1-3, and 1-4 are

AA	Acoustic absorption	EMF	Electromotive force
BPE	Boiling point elevation	IR	Infrared spectra
C	Cryoscopy	NMR	Nuclear magnetic resonance
CN	Conduction of electricity	R	Raman spectra
D	Distribution or partition between the solvent named and water.	UA	Ultrasonic absorption
		VP	Vapour pressure

DC Dielectric constant

DEN Density

The dimerisation constant,  $K_D$ , and the trimerisation constant,  $K_T$ , are given by

$$K_D = \frac{[H_2A_2]}{[HA]^2} \quad (1-10)$$

and

$$K_T = \frac{[H_3A_3]}{[HA]^3} \quad (1-11)$$

The <sup>VALUES</sup>units of the standard entropy change  $\Delta S_2^\circ$  depend on the units of  $K_D$  from which it is calculated. In order to compare the standard entropies in the gas phase with those in solution, it is necessary that they relate to the same standard state. The values of  $\Delta S_2^\circ$  in the gas phase (Table 1-1) have been calculated from values of  $K_D$  in atmospheres. Therefore, for the solution data it is necessary to add about 11 cal. deg.<sup>-1</sup> mole<sup>-1</sup> to the values of  $\Delta S_2^\circ$  calculated from values of  $K_D$  in mole fraction units<sup>10</sup>. This correction has been applied to the values of  $\Delta S_2^\circ$  in Table 1-2.

In the first five columns only of Tables 1-2, 1-3, and 1-4, a blank space means that the entry above is to be carried down.

TABLE 1-2.

Thermodynamic functions for the association of acetic acid in various solvents.

Solvent	Dielectric Constant	Reference	Method	Temp. °C.	LogK <sub>D</sub>	-ΔH <sub>2</sub> <sup>o</sup> kcal.mole <sup>-1</sup>	-ΔS <sub>2</sub> <sup>o</sup> E.U.
Hexane	1.89 <sup>25</sup>	81	D	25	2.93	8.98±0.54	23.1
				35	2.71		
				45	2.52		
Heptane	1.93 <sup>20</sup>	67	DC	30	4.57		
Cyclohexane	2.015 <sup>25</sup>	84	NMR	25	4.19		
Paraffin wax	2.10	97	IR	99-189		13.4±0.3	34.6
Carbon		80	D	25	2.21 <sup>a</sup>		
tetrachloride	2.23 <sup>25</sup>	81	D	25	2.68	7.56±0.74	19.4 <sup>b</sup>
				35	2.51		
				45	2.34		
		99	IR	18-75		9.3±1	
		100	IR	25	3.60±0.12		
		101	IR	25	3.38		
		102	IR		3.00-3.42		
		84	NMR	25	3.59		
Benzene	2.274 <sup>25</sup>	80	D	17	2.40	9.7	28.7 <sup>b</sup>
				24.09	2.25		
				25.00	2.22		
				30.40	2.11		
				34.46	2.01		
				45.00	1.79		
				62.00	1.44		
		103	D	25	2.70		
		81	D	25	2.11	8.80±0.20	24.2 <sup>b</sup>
				35	1.91		
				45	1.74		
		96	D	6.27	2.63*	8.89±0.2	26.2 <sup>b</sup>
				25	2.18		
				45.08	1.78		
			C	5.55	2.62		
		104	BPE	30	2.59	10.5±1	
		97				8.7 <sup>u</sup>	23.0
		67	DC	30	2.57		
		80 <sup>d</sup>		0	2.88		
				10	2.61		
				20	2.35		
				30	2.12		
				40	1.89		
				50	1.68		
				60	1.49		
				70	1.30		
		67 <sup>h</sup>	DC	30	2.47		

TABLE 1-2 (continued)

Solvent	Dielectric Constant	Reference	Method	Temp. °C	Log K <sub>D</sub>	-ΔH <sub>2</sub> <sup>g</sup> kcal. mole <sup>-1</sup>	-ΔS <sub>2</sub> <sup>g</sup> E.U.
Carbon disulphide	2.62 <sup>25</sup>	80	D	25	2.63 <sup>a</sup>	7.05±0.43	17.6 <sup>b</sup>
		81	D	17	2.86		
				27	2.69		
				37	2.51		
Isopropyl ether	3.88 <sup>25</sup>	82	D	20	-0.37	5.25±0.34	13.6 <sup>b</sup>
Diethyl ether	4.26 <sup>25</sup>	78	D	25	-0.43		
Chloroform	4.72 <sup>25</sup>	80	D	25	0.84 <sup>e</sup>		
		103	D	25	1.05		
		102	IR		2.00-2.62		
Chlorobenzene	5.62 <sup>25</sup>	81	D	25	2.15	5.02±0.34	13.4 <sup>b</sup>
				35	2.03		
				45	1.92		
1:1 Dichloroethane	9.1 <sup>18</sup>	84	NMR	25	1.21	5.25±0.34	13.6 <sup>b</sup>
Nitrobenzene	34.82 <sup>25</sup>	81	D	25	0.87		
				35	0.74		
				45	0.62		
Water	78.54 <sup>25</sup>	96	D	25	-1.42	0	13.0 <sup>b</sup>
			C	6-45	-1.45 <sup>f</sup>		
		108	C		-0.34 <sup>†</sup>		
		76	CN	25	-0.80		
		77	CN	25	-1.28±0.05		
		109	EMF	25	-1.26		
		110	DEN	20	1.95		
		111	VP	25	-0.73		
		96	VP	25	-1.30±0.06 <sup>g</sup>		
		112, 113	R	15 and 100			
Liquid Acid	6.15 <sup>20</sup>	43	UA	20	3.04 <sup>b</sup>	11.5 6.21	
				30	2.88 <sup>b</sup>		
				40	2.73 <sup>b</sup>		
				50	2.59 <sup>b</sup>		
				60	2.46 <sup>b</sup>		

- a Calculated from Herz and Kurzer<sup>98</sup>  
 b Calculated by Pimentel and McClellan<sup>47</sup>  
 c Quoted from references 10 and 105  
 d Calculated from Smyth and Rogers<sup>78</sup>  
 e Calculated from Rothmund and Wilsmore<sup>106</sup>  
 f Calculated from Jones and Bury<sup>107</sup>  
 g Calculated from MacDougall and Blumer<sup>111</sup>  
 \* LogK<sub>T</sub> = 3.63  
 † LogK<sub>T</sub> = -0.89  
 h Acid used was CH<sub>3</sub>COOD

In Table 1-2 it can be seen that values for  $K_D$ , determined by different methods in the same solvent often vary widely. Sometimes different workers using the same methods are not in agreement. The disparity between the values obtained with other methods may be due to the fact that water and the organic solvents used are not completely immiscible. The organic phase is in fact saturated with water and this affects the results.

The value of  $K_D$  tends to decrease and the value of  $\Delta H_2^\circ$  to increase with increasing dielectric constant of the solvent. However, for solvents with a dielectric constant less than 3, the value of  $\Delta H_2^\circ$  is fairly constant at about 9.0 kcal. mole<sup>-1</sup>. The value of  $\Delta S_2^\circ$  tends to increase with increasing dielectric constant of the solvent, but the trend is irregular.

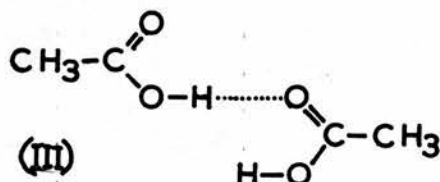
Both the heat-content change and the standard entropy change in solution are less than the corresponding changes in the gas phase. This shows that the hydrogen bonds require less energy for dissociation in organic solvents than they do in the vapour. However, although the smaller heat-change effect favours the monomer at the expense of the dimer, it is compensated by the smaller entropy change on dissociation, the changes in  $\Delta H_2^\circ$  and  $T\Delta S_2^\circ$  being of comparable magnitude and opposite effect<sup>10</sup> on  $K_D$ . The smaller entropy and heat-content changes have been attributed to solvation<sup>10</sup> which is likely to be more pronounced for the monomers, where there are the local dipoles of the hydroxyl and carboxyl group, than for the dimers where the polarisable groups are masked. [ In benzene the resultant dipole moment of the monomer is 1.7D compared with 1.0D for the dimer<sup>67</sup>]. A decrease of entropy, therefore, will arise from the solvation of the monomer and the energy of the monomer will be lowered more than that of the dimer by solvation. Thus  $\Delta H_2^\circ$  will be smaller in solution than it is in the gas phase. The trends of  $\Delta H_2^\circ$



and  $4S_2^o$  with dielectric constant are thus explicable by solvation.

In aqueous solution the dimerisation constant is very much smaller than in other solvents. Again there is some disparity between the results obtained and Davies and Griffiths<sup>96</sup> have concluded that earlier workers' results<sup>76, 108, 111</sup> are based on over simplified treatments or inadequate data.

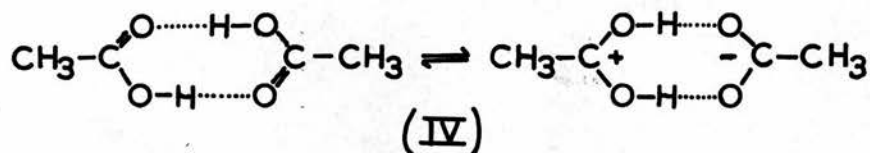
The structure of the acid dimer in the liquid phase and in solution has been studied widely. Latimer and Rhodebush<sup>114</sup> were the first to suggest that a hydrogen bond is present in associated acetic acid. Thereafter it was believed that the dimer is cyclic in form as in the vapour phase. In 1946 Batuey postulated, from Raman spectra, that acetic acid shows a chain type association in its liquid form<sup>69, 72</sup> and also in solution in dioxan<sup>88</sup>. Chulanovskii and Simova<sup>65</sup> noticed in the infrared spectrum of acetic acid, the same vibration which they had attributed to free rotation about the O - H axis in formic acid. Lamb and Pinkerton<sup>115</sup> suggested that the dissociation of the double molecules may proceed in two or more stages and that the relaxation mechanism observed in ultrasonic absorption measurements on acetic acid is associated with the breakage of only one hydrogen bond. On the basis of Raman spectra of the pure acid and solutions in organic solvents, Fénéant<sup>86, 92</sup> rejected Batuey's suggestion and postulated that with increasing dilution an open form of the dimer (III) increases in concentration, eventually rupturing to give the monomer. In aqueous solution it was postulated<sup>116</sup>





that a water molecule attaches itself to each extremity of the acid molecule and that this  $B - 2H_2O$  form is more stable than the simple open dimer (III).

Harris and Alder<sup>117</sup> noted that the dielectric constant of liquid acid acetic is higher than would be expected if the non-polar dimer were the only species present. They suggested that self-ionisation takes place thus



Support for Fénéant's scheme for the dissociation of the cyclic dimer to the monomer through the open dimer has come from the dilatometric measurements of Ragni, Ferrari, and Papoff<sup>118</sup>. Further studies of the Raman spectra of the pure acid and its aqueous solution by Cucurezeanu<sup>119, 120</sup> supports Fénéant's suggestion. This work shows that in the pure liquid the monomer is not formed completely till the temperature has reached 200°C. An equimolecular solution of acetic acid and water consists of open dimers with small amounts of cyclic dimer and monomer<sup>121</sup>.

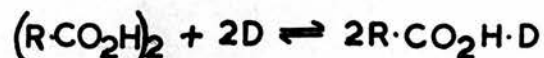
### Propionic Acid

Propionic acid appears to be dimerised in water and in organic solvents except dioxan<sup>68, 69</sup>. Although Trautz and Moschel<sup>30</sup> stated that trimers of the acid were formed in benzene and nitrobenzene solution, there has been no further evidence for their existence apart from the fact <sup>that</sup> Blinc and Blinc<sup>73</sup> found the degree of association in the pure acid to be 2.1. These authors, therefore, suggested that small amounts of polymer might be present.

Propionic acid is more associated than acetic acid in all solvents (Compare Tables 1-2 and 1-3). There are the same tendencies for  $K_D$  to

decrease and  $\Delta H_2^\circ$  to increase with increasing dielectric constant of the solvent that were noted for acetic acid.  $\Delta S_2^\circ$  is again about 22 E.U.

The configuration of the dimer has been studied very little. Where dimers have been found to exist, results have been interpreted on the assumption that the dimer is cyclic. In some strong donor solvents such as acetone and acetonitrile the dimeric acid takes part in an equilibrium involving a hydrogen-bonded complex with the monomer thus:



where D is the strong donor

TABLE 1-3

Thermodynamic functions for the association of propionic acid in various solvents.

Solvent	Dielectric Constant	Reference	Method	Temp. °C	Log $K_D$	$-\Delta H_2^\circ$ kcal. mole <sup>-1</sup>	$\Delta S_2^\circ$ E. U.
Light Petroleum	1.8-2.0 <sup>25</sup>	81	D	20	2.13	9.37±0.06	24.0 <sup>a</sup>
				30	1.94		
				40	1.69		
				50	1.48		
Carbon tetrachloride	2.23 <sup>25</sup>	81	D	20	2.60	7.43±0.25	18.5 <sup>a</sup>
				30	2.71		
				40	2.55		
				50	2.39		
Benzene	2.274 <sup>25</sup>	101	IR	25	3.39	7.75±0.56	22.6 <sup>a</sup>
		122	D	25	2.26		
		81	D	20	2.21		
				30	2.03		
				40	1.86	10.5±1	
				50	1.68		
				30	2.62 <sup>b</sup>		
		104	BPE	30	2.60		
Toluene	2.366 <sup>25</sup>	67	DC	30	2.58	6.66±0.12	22.1 <sup>a</sup>
		122	D	25	2.42		
	4.72 <sup>25</sup>	122	D	25	1.82		
				20	1.53		
Chloroform		81	D	30	1.37	6.66±0.12	22.1 <sup>a</sup>
				40	1.21		
				50	1.07		
				77	0.17		
Chlorobenzene	5.62 <sup>25</sup>	101	IR	25	2.27	6.29±0.21	17.6 <sup>a</sup>
		81	D	20	2.24		
				30	2.07		
				40	1.94		
Nitrobenzene	34.82 <sup>25</sup>	81	D	50	1.80	5.87±0.57	22.3 <sup>a</sup>
				25	0.82		
				50	0.50		
				77	0.17		
Water	78.54 <sup>25</sup>	30	C		b	9.33	
		76	CN	25	-0.64		
		77	CN	25	-1.30±0.06		
		109	EMF	25	-1.01		
Liquid Acid	3.30 <sup>10</sup>	43	UA	8	4.62 <sup>a</sup>	9.33	
				21	4.29 <sup>a</sup>		
				31	4.06 <sup>a</sup>		
				41	3.84 <sup>a</sup>		
				51	3.63 <sup>a</sup>	3.9	16.0 <sup>a</sup>
				44	UA, AA		

a Calculated by Pimentel and McGlellan<sup>47</sup>b Value of Log  $K_T$  varies with concentration.

Butyric Acid

Butyric acid is the most associated of the four acids and as early as 1911 Peddle and Turner<sup>74</sup> reported that it is distinctly associated even in dilute solution. Trauty and Moschel<sup>30</sup> reported that trimers of the acid exist in solution in benzene and nitrobenzene but this has not been confirmed by other workers. However, in 1929 Grindley and Bury<sup>128</sup> postulated that micelles are formed at an acid concentration of about 15 mole% in water and this was confirmed by Bury and Davies<sup>129</sup>.

There have been several attempts to evaluate  $K_D$  in aqueous solution (see Table 1-4). The results are in fair agreement though the value obtained by Katchalsky, Eisenberg, and Lifson<sup>76</sup> is somewhat lower than the others. Davies and Griffiths<sup>123</sup> recalculated the cryoscopic data of Jones and Bury<sup>107</sup> and found that in aqueous solution dimers exist at concentrations between 0 and 1.4 molal. Thereafter tetramers are formed  $\log K_{2,4} = \log \frac{[H_4A_4]}{[H_2A_2]^2} = 0.40$  and then 12-mers with  $\log K_{4,12} = \log \frac{[H_{12}A_{12}]}{[H_4A_4]^3} = 1.41$ . Then at concentrations higher than 3.4 molal, micelles of 80-mers are formed.

Further evidence for micelle formation in aqueous solution at concentrations higher than 12 mole % has come from ultrasonic measurements<sup>130</sup> and from the increase in solubility of a dye in increasing concentrations of butyric acid<sup>131</sup>. At low acid concentrations the dye is only slightly soluble but the solubility increases noticeably at acid concentrations above 2M. This behaviour is attributed to the fact that above this concentration micellar aggregates of butyric acid form.

TABLE 1-4

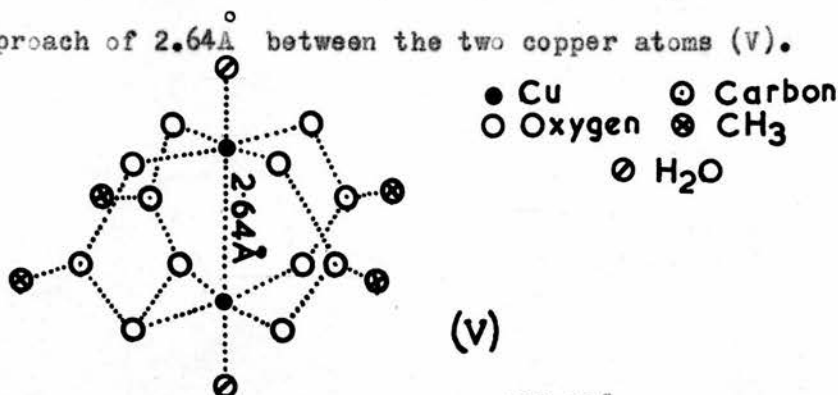
Thermodynamic functions for the association of n-butyric acid in various solvents.

Solvent	Dielectric Constant	Reference	Method	Temp °C.	LogK <sub>D</sub>	$-\Delta H_2^\circ$ kcal. mole <sup>-1</sup>	$-\Delta S_2^\circ$ E.U.
Paraffin Wax	2.19 <sub>25</sub>	97	IR	98±161			
Benzene	2.27 <sub>4</sub>	122	D	25	2.30	13.4±0.3	34.6
		123	D	6.32	2.72		
			D	0, 25, 60		11.0±1.0 <sup>a</sup>	
		30	C	5.5	2.66 <sup>b</sup>		
		104	BPE	30	2.64	10.5±1	
		67	DC	30	2.64		
Toluene	2.366 <sub>25</sub>	122	D	25	2.58		
Chloroform	4.72 <sub>25</sub>	122	D	25	2.00		
		125	D	25	1.68 <sup>c</sup>		
Nitrobenzene	34.82 <sub>25</sub>	30	C	5.5	<sup>b</sup>		
Water	78.54	127	D	25	0.00		
		123	C	0	-0.04		
			C	0	-0.02 <sup>±</sup>		
					0.02		
		76	CN	25	0.56		
		77	CN	25	-0.04 <sup>±</sup>		
					0.02		
		109	EMF	25	0.18		

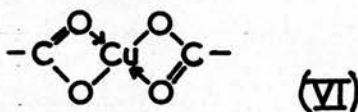
- a Calculated from Bektourov<sup>124</sup>.  
 b Value of LogK<sub>D</sub> varies with concentration.  
 c Calculated from (126).

1 (d) DIMERISATION OF COPPER (II) n-ALKANOATES.

In 1953 Van Niekerk and Schoening<sup>132</sup> determined the structure of crystalline copper (II) acetate monohydrate by X-ray diffraction. They found that this compound is dinuclear, its most striking feature being the close approach of 2.64 Å between the two copper atoms (V).



For some years prior to this, various workers<sup>133-138</sup> had reported on the magnetic susceptibility of copper (II) acetate and all, with one exception<sup>134</sup>, found the molar susceptibility to be considerably lower than that found in other copper salts. The temperature variation of the magnetic susceptibility was found to be anomalous also. Amiel, Ploquin, and their co-workers<sup>139, 140</sup> attribute the lowering of the magnetic susceptibility to the partial masking of the copper in a non-electrolytic internal complex (VI).



Just before Van Niekerk and Schoening published their work, Bleaney and Bowers<sup>141</sup> suggested that isolated pairs of copper ions are coupled together by exchange forces with each copper ion bonded by four oxygen atoms in a plane. This is exactly the arrangement described by Van Niekerk and Schoening.

The paramagnetic resonance absorption of copper (II) acetate is anomalous also<sup>141-145</sup>, and a similar explanation to that of Bleaney and Bowers has been advanced. Subsequently, infrared spectra measure-

ments<sup>146, 147</sup> have provided fresh confirmation of the dinuclear structure. From their magnetic susceptibility measurements Figgis and Martin<sup>148</sup> suggested that the bond between the adjacent copper atoms is a very weak covalent  $\delta$ -bond, formed by lateral overlap of  $3d_{x^2-y^2}$  orbitals. The bond is so weak that the dinuclear configuration can be maintained only by the four bridging acetate groups, the exchange energy being calculated as 1 kcal. mole<sup>-1</sup>. Ross<sup>149</sup> has confirmed the existence of the  $\delta$ -bond in copper(II) acetate from an analysis of the results of Bleaney and Bowers<sup>141</sup> and of Abe and Shimada<sup>145</sup> whose work preceded the publication of the molecular structure of copper(II) acetate monohydrate.

Copper(II) propionate<sup>149-151</sup> and n-butyrate<sup>151</sup> resemble copper(II) acetate in their magnetic behaviour. Optical absorption measurements on the acetate and propionate<sup>152, 153</sup> and n-butyrate were claimed to show the existence of the copper-copper bond. Of interest was the fact that absorptiometric measurements<sup>155, 156</sup> showed copper(II) mono- and dibromoacetate to be dinuclear but copper(II) tri-chloroacetate to be mononuclear.

Dimers of copper(II) alkanoates are formed in solution in organic solvents. Tsuchida and Yamada<sup>152, 157</sup> concluded that such species as  $\text{Cu}_2(\text{R-CO}_2)_4\text{X}_2$ , where  $\text{R}=\text{CH}_3$ ,  $\text{C}_2\text{H}_5$ , or  $n\text{-C}_3\text{H}_7$ , and  $\text{X}=\text{H}_2\text{O}$ ,  $\text{C}_2\text{H}_5\text{OH}$ , or  $\text{CHCl}_3$ , are formed in solution in ethanol or chloroform.

Cryoscopic measurements and absorption spectra<sup>158</sup> indicated that in dioxan solution copper(II) acetate, propionate, n-butyrate, and n-valerate are dinuclear. The absorption spectrum of copper(II) n-butyrate<sup>157, 158</sup> showed that it is dinuclear in solution in carbon tetra-



chloride, chloroform, acetone, and alcohol. Magnetic susceptibility measurements<sup>159</sup> at room temperature showed that copper (II) acetate is dinuclear in ethanol and dioxan, mononuclear in pyridine, while in methanol, the magnetic susceptibility lay between that usually observed for the mononuclear salts and dinuclear salts.

Graddon<sup>160, 161</sup> has found that the distribution of copper (II) propionate between water and chloroform gives distribution constants of the form

$$k = \sqrt[4]{\frac{\text{Concentration of copper in aqueous phase}}{\text{Concentration of copper in chloroform phase}}}$$

The fourth-root function in the distribution constants shows that the salt is dinuclear in chloroform solution. It appears to exist in the organic phase not as an unsolvated molecule but as the propionic acid solvate,  $\text{Cu}_2(\text{C}_2\text{H}_5\text{CO}_2)_4 \cdot (\text{C}_2\text{H}_5\text{CO}_2\text{H})_2$ .

The behaviour of copper (II) acetate and its higher homologues in aqueous solution is less certain. From potentiometric measurements with a glass electrode at 18°C., Pedersen<sup>162</sup> reported that  $\text{CuCH}_3\text{CO}_2^+$  and  $\text{Cu}(\text{CH}_3\text{CO}_2)_2$  are formed. Spectrophotometric measurements confirmed this and also indicated that complexes such as  $\text{Cu}(\text{CH}_3\text{CO}_2)_3^-$  and  $\text{Cu}(\text{CH}_3\text{CO}_2)_4^{2-}$  and polynuclear complexes are formed in sufficiently concentrated solutions. Fronaeus has made potentiometric and spectrometric measurements<sup>163</sup> and ion exchange measurements<sup>164</sup> in a 1 M sodium perchlorate medium at 20°C. and like Pedersen has found species formed up to  $\text{Cu}(\text{CH}_3\text{CO}_2)_4^{2-}$ . Fronaeus also found that the dinuclear complexes  $\text{Cu}_2(\text{CH}_3\text{CO}_2)^{3+}$  and  $\text{Cu}_2(\text{CH}_3\text{CO}_2)_2^{2+}$  were formed.

It has been postulated from conductivity measurements at 0°C.<sup>165</sup> and 30°C.<sup>166</sup> and spectrophotometric measurements at 20°C.<sup>165, 167</sup> that

only the species  $\text{CuCH}_3\text{CO}_2^+$  and  $\text{Cu}(\text{CH}_3\text{CO}_2)_2$  are formed in aqueous solution. Martin and Whitley<sup>158</sup> reported that their cryoscopic measurements on the series copper (II) acetate to copper (II) n-butyrate showed that the dinuclear structure present in the solid state is destroyed in water. The magnetic susceptibility of copper (II) acetate in aqueous solution is 1.93 B.M.<sup>159</sup> and this is taken to indicate that the salt is mononuclear in aqueous solution. While Pedersen and Fronaeus surveyed wide ranges of concentration, all the solutions used by the above workers were rather weak. It is unlikely, therefore, that any of their measurements were made at concentrations where the polynuclear species could be expected to exist.

Table 1-5 summarises the values for the constants for copper acetate obtained by the various workers. The method used for the measurements is shown in the third column of the Table by the following abbreviations:

emf      emf measurements other than glass electrode measurements  
gl        glass electrode  
i.ex      ion exchange  
sol       solubility  
sp        spectrophotometer

The abbreviations used in the fourth column of the Table refer to the medium in which the measurements were made thus:  $\rightarrow 0$  constants extrapolated or corrected to zero ionic strength.

1 M -  $\text{NaClO}_4$  } measurements made in the presence of a  
2 M -  $\text{NaNO}_3$  } constant concentration of inert salt

The stability constants,  $\beta_1'$  and  $\beta_2'$  for the species  $\text{Cu}_2(\text{CH}_3\text{CO}_2)^{3+}$  and  $\text{Cu}_2(\text{CH}_3\text{CO}_2)_2^{2+}$  respectively are given by

$$\beta_n' = \frac{[\text{Cu}_2(\text{CH}_3\text{CO}_2)_n]}{[\text{Cu}]^2 \cdot [\text{CH}_3\text{CO}_2]^n}$$

where n=1 or 2

TABLE 1-5

Stability constants obtained for copper (II) acetate complexes

Reference	Method	Medium	Temperature	Log $K_1$	Log $K_2$	Log $\beta_2$	Log $K_3$	Log $\beta_3$	Log $K_4$	Log $\beta_4$	Log $\beta_1^1$	Log $\beta_2^1$
			°C									
162	gl	$\rightarrow 0$	18	2.16	1.04	3.20						
163	emf	1M-NaClO <sub>4</sub>	20	1.67	0.98	2.65	0.42	3.07	-0.19	2.88	1.70	3.04
163	sp	1M-NaClO <sub>4</sub>	20	1.62	0.98	2.60						
164	l. ex	1M-NaClO <sub>4</sub>	20	1.65	1.00	2.65	0.36	3.01				
168	sol	$\rightarrow 0$	25	2.24								
166	emf		30	2.40	0.90	3.30						
165	emf		0	2.52	0.99	3.51						
167	sp		20	2.48	0.94	3.42						
169	gl	2m-NaNO <sub>3</sub>	24, 26	2.78								

Copper(II) formate differs from the other copper alkanoates in that it seems to be mononuclear not only in aqueous solution but also in the solid state and in organic solution. The crystal structure<sup>170</sup> shows that copper(II) formate tetrahydrate is mononuclear. The magnetic moment<sup>151</sup>, 1.6 B.M., is intermediate between that, 1.38 B.M., for its higher homologues which are dinuclear and that for magnetically dilute copper(II) compounds, (1.9 B.M.). The moment jumps to 1.9 B.M. in aqueous solution<sup>158</sup> suggesting that strong intermolecular exchange forces are present in the crystalline compound.

Absorption spectra<sup>152</sup> indicate that there is no copper-copper linkage in crystalline copper(II) formate nor in its solution in alcohol or chloroform. Species of the type  $\text{Cu}(\text{H}\cdot\text{CO}_2)^+$ ,  $\text{Cu}(\text{H}\cdot\text{CO}_2)_2$ ,  $\text{Cu}(\text{H}\cdot\text{CO}_2)_3^-$ , and  $\text{Cu}(\text{H}\cdot\text{CO}_2)_4^{2-}$  have been identified<sup>171</sup> in 2M sodium perchlorate solution at 25° and the formation constants evaluated though the limits of error are rather wide.

Further magnetic and cryoscopic measurements<sup>158</sup> of aqueous solutions of copper(II) formate indicate that it exists as a monomer in water. However the solutions used in this work were of low concentration. The magnetic moment is low (1.01 B.M.) in dioxan and the presence of an absorption band corresponding to the copper-copper linkage indicates that copper(II) formate adopts the dinuclear structure in dioxan solution<sup>158</sup>. Martin and Whitley believe that the donor and non-ionising properties of dioxan favour formation of discrete dinuclear  $[\text{Cu}_2(\text{H}\cdot\text{CO}_2)_4 \cdot (\text{C}_4\text{H}_8\text{O}_2)_2]$  molecules and they have confirmed this by isolating from solution crystals which contain dioxan and which have a magnetic moment about 1 B.M.

Further study has shown that several forms of copper(II) formate can be prepared in aqueous formic acid depending upon the conditions of

isolation<sup>172</sup>. Only mononuclear forms can be isolated but when copper carbonate is dissolved in concentrated formic acid, the resulting solution has a blue-green colour which changes to blue in a few minutes. Pale blue square plates which seem to have the structure  $\text{Cu}(\text{H}\cdot\text{CO}_2)_2\cdot 4\text{HCO}_2\text{H}$  then crystallise.

The absorption spectrum of the blue-green solution was characterised by the presence of a band which in heavier dinuclear copper (II) alkanoates was ascribed<sup>152, 157</sup> to the copper-copper linkage. The occurrence of a similar band in the blue-green solution is taken to indicate the existence of dinuclear copper (II) formate in solution, most probably in  $[\text{Cu}_2(\text{H}\cdot\text{CO}_2)_4\cdot (\text{H}\cdot\text{CO}_2\text{H})_2]$  molecules. Owing to the unstable nature of the solution, the magnetic moment of the copper (II) ion could not be measured. An attempt was made to stabilise the blue-green solution and to isolate the dinuclear compound by replacing water with acetone but this was unsuccessful. The absorption spectrum of this solution suggests that acetone molecules have replaced formic acid (or water) in the structure to form  $[\text{Cu}_2(\text{H}\cdot\text{CO}_2)_4\cdot (\text{CH}_3\cdot\text{CO}\cdot\text{CH}_3)_2]$  molecules.

The same workers<sup>173</sup> have "conditioned" copper (II) formate into adopting the dinuclear copper (II) acetate-type structure. The observed reluctance of anhydrous or hydrated copper (II) formate to adopt the dinuclear structure may arise from the comparatively low  $\sigma$ -electron density on formate oxygen atoms, leading to a relatively large residue of positive charge on each copper atom after the formation of the compound. In the dinuclear structure the two copper atoms are relatively close together and so a large residual electrostatic charge on the copper atoms will render the structure unstable. This excess of positive charge has been reduced considerably, thus favouring



the dinuclear structure, by forming heterocyclic monoamine copper (II) formates. The amines used, pyridine,  $\alpha$ -,  $\beta$ -,  $\gamma$ -picoline and also dioxan, have a high  $\sigma$ -electron charge density on the nitrogen atom and form a dative bond to copper.

The compounds formed are emerald-green in colour and have low magnetic moments of 1.0 - 1.1 B.M. The temperature variation of the magnetic susceptibility is anomalous and these facts indicate that dimers are formed. It is noted, too, that the copper-copper  $\delta$ -bond formed has a greater binding energy than the  $\delta$ -bond in heavier copper *n*-alkanoates. In the formate compounds the exchange energy,  $J$ , associated with <sup>the</sup> $\delta$ -bond is of the order 1.5 - 2.0 kcal. mole<sup>-1</sup> whereas in the heavier copper *n*-alkanoates  $J$  is  $0.88 \pm 0.09$  kcal. mole<sup>-1</sup>. At room temperature the magnetic moments of the formate derivatives are much lower (0.9 B.M. compared with 1.4 B.M.), and the temperature of maximum susceptibility is much higher (500°K compared with 250°K). Therefore, there is a greatly enhanced overlap between the Cu-Cu,  $3d_{\sigma}$ - $3d_{\sigma}$  orbitals which may arise in two ways. First the copper-copper distance in the formate derivatives may be decreased from the value  $2.64\text{\AA}$  observed in copper (II) acetate monohydrate toward the value of  $2.55\text{\AA}$  observed in metallic copper. Secondly, the copper-copper distance may remain  $2.64\text{\AA}$  but the  $3d_{\sigma}$ - $3d_{\sigma}$  overlap may be enhanced by the modified ligand field produced by the replacement of acetate by formate oxygen atoms and the presence of the terminal ligands.

The variation in the colour of solutions of copper (II) alkanoates with concentration is of interest and has received considerable attention<sup>174-177</sup>. Kondo and Kubo<sup>159</sup> have noted that ethanol and dioxan solutions of copper (II) acetate which showed anomalous magnetic behaviour are green in colour, while

aqueous and pyridine solutions which showed normal magnetic behaviour are blue in colour.

Solid copper (II) acetate monohydrate is blue-green<sup>148</sup> or dark green<sup>132</sup> in colour while copper (II) propionate monohydrate is dark green, copper (II) n-butyrate monohydrate is green<sup>151</sup>, and anhydrous copper (II) n-valerate is blue-green<sup>158</sup>. However, copper (II) formate is pale blue.

Copper (II) n-butyrate and n-valerate are blue-green in benzene solution<sup>158</sup> and solutions of copper (II) formate, acetate, propionate, n-butyrate, and n-valerate in dioxan are blue-green in colour. The aqueous solution which Martin and Waterman<sup>172</sup> believed contained dinuclear copper (II) formate,  $[\text{Cu}_2(\text{H}\cdot\text{CO}_2)_4\cdot(\text{H}\cdot\text{CO}_2\text{H})_2]$ , is blue-green in colour. The copper (II) formate monoamine solutions, which the same authors examined<sup>173</sup> and which <sup>be</sup> were found to/dinuclear, are emerald green in colour.

Thus, it appears that copper (II) n-alkanoates which are dinuclear or solutions containing dinuclear copper (II) n-alkanoates are blue-green or green in colour while mononuclear copper n-alkanoates and their solutions are blue.



1 (e) THE SCOPE OF THE PRESENT WORK.

From the preceding account it can be seen that there is some doubt about the existence of polynuclear copper (II) carboxylate complexes in aqueous solution. On somewhat slender evidence the Japanese and Australian workers have reported that the polynuclear complexes do not exist but they appear to have overlooked the earlier reports by two notable solution chemists, Fronaeus and Pedersen, that polynuclear complexes are formed in aqueous solution. Therefore, in the present work a precise equilibrium study has been made of the formate-, aceto-, propionate-, and butyrate-copper (II) systems in an attempt to seek further evidence for the formation of the dinuclear and polynuclear complexes in aqueous solution. As the existence of dinuclear and polynuclear complexes has also been reported<sup>178</sup> in the acetate-cadmium (II) system, a precise equilibrium study was also made of this system by the same method. The most convenient method of studying the systems was to follow competition between protons and copper (II) ions or cadmium (II) ions for the carboxylate anions at 25°C. with a glass electrode.

A necessary preliminary to the study of the metal complexes was the precise investigation of the proton-carboxylate equilibria in the absence of metal ions. Further information on the proton-acetate equilibria was obtained from measurements on a high precision calorimeter.

The proton-acetate equilibria and the acetate-copper (II) system have also been studied in a 50% v/v water/dioxan mixture in which dinuclear and polynuclear complexes might be expected to form more readily than in aqueous solution.

SECTION 2.

METHODS OF COMPUTATION.

## 2. METHODS OF COMPUTATION.

Many methods for computing stability constants have been developed and a full description of these methods will be published by Rossotti and Rossotti<sup>179</sup>.

Some methods of computation have been derived and used for the first time in the work described in this thesis. These methods along with other, previously developed, methods used in the present study are described below. Some further methods used in evaluating the equilibrium constants in the carboxylate equilibria in a dioxan-water medium are described in Sec. 6 (b)

In order to compute stability constants it is desirable to have data which are as accurate as possible and which cover a wide range of concentration. Thereafter the aim is to find the values of the stability constants which best express all the experimental measurements. If possible, more than one method of calculation should be used, as different methods sometimes give very different results.

In this work, the stability constants are obtained from the formation curve of the system,  $\bar{n}(\log a)$ . Equation (1-5) may be rearranged in the form

$$\sum_{n=0}^{n=N} (\bar{n} - n) \beta_n a^n = 0 \quad (2-1)$$

Now when  $N=2$ , e.g. in the copper (II) n-butyrate system [Sec. 5 (a)], it has been shown<sup>180</sup> that the formation curve is symmetrical about its mid-point. In this special case, Eqs. (2-1) and (1-3a) may be combined to

$$\bar{n} + (\bar{n} - 1)K_1a + (\bar{n} - 2)K_1K_2a^2 = 0 \quad (2-2)$$

whence

$$K_1 = \frac{\bar{n}}{a[(1 - \bar{n}) + (2 - \bar{n})K_2a]} \quad (2-3)$$

and

$$K_2 = \frac{\bar{n} + (\bar{n} - 1)K_1 a}{a(2 - \bar{n})K_1 a} \quad (2-4)$$

Thus the calculation of one of these constants depends on the value of the other. Simultaneous equations derived from Eq. (2-2) can be used to evaluate  $K_1$  and  $K_2$  from experimental data but the method has the disadvantage that where two experimental points, both slightly erroneous, are treated, the resulting constants may be far removed from the general average. The method is laborious and time-consuming also.

Another method which has been used previously is Bjerrum's "half  $\bar{n}$ " method<sup>8</sup>. If  $K_1 \gg K_2$  then the value of  $(-\log a)$  when  $\bar{n} = 0.5$  gives  $\log K_1$ , and the value of  $(-\log a)$  when  $\bar{n} = 1.5$  gives  $\log K_2$ . However, this method gives only approximate results when  $K_1 < 10^3 K_2$ , and it has the further disadvantage that the constants are evaluated from only two points on the formation curve.

Graphical methods of computation have the advantage that much of the experimental data can be considered simultaneously. Recently, curve-fitting techniques have been widely used<sup>179, 181</sup>. The application of graphical and curve-fitting methods to the systems studied in this work is outlined below.

## 2 (a) GRAPHICAL TREATMENT OF THE DATA $\bar{n}$ , $a$ .

A graphical method for computing successive stability constants from experimental values of the degree of formation by successive extrapolations has been described by Rossotti and Rossotti<sup>182</sup>. This method is useful for systems in which more than two complexes coexist.

Rearrangement of Eq. (2-1) gives

$$\frac{\bar{n}}{(1-\bar{n})a} = \beta_1 + \beta_2 \frac{2-\bar{n}}{1-\bar{n}}a + \sum_{n=3}^{n=N} \frac{n-\bar{n}}{1-\bar{n}} \beta_n a^{n-1} \quad (2-5)$$

Hence the plot of  $\bar{n}/(1-\bar{n})a$  against  $(2-\bar{n})a/(1-\bar{n})$  tends to a straight line of intercept  $\beta_1$  and of slope  $\beta_2$  as  $a \rightarrow 0$ . In general, an accurate value of any constant  $\beta_t$  can be obtained. If Eq. (2-1) is divided by  $(t-\bar{n})a$ , where  $t$  is an integer of value  $0 < t < N$ , and rearranged

$$\sum_{n=0}^{n=t-1} \left( \frac{\bar{n}-n}{t-\bar{n}} \right) \beta_n a^{n-t} = \beta_t + \sum_{n=t+1}^{n=N} \left( \frac{n-\bar{n}}{t-\bar{n}} \right) \beta_n a^{n-t} \quad (2-6)$$

If the values of  $\beta_1, \beta_2, \dots, \beta_{t-1}$  have been calculated previously, then the left-hand side of Eq. (2-6) is known. A plot of this term against  $(t+1-\bar{n})a/(t-\bar{n})$  gives  $\beta_t$  as the intercept and an approximate value of  $\beta_{t+1}$  as the limiting slope as  $a \rightarrow 0$ .

In the study of some of the copper(II)  $n$ -alkanoates, it was thought possible that three species  $BA$ ,  $BA_2$ , and  $BA_3$  were present, with overall stability constants  $\beta_1, \beta_2$ , and  $\beta_3$  respectively. An accurate value of  $\beta_1$  was obtained using Eq. (2-5) as described above.  $\beta_2$  and  $\beta_3$  were obtained in turn by substituting  $t = 2$  and  $3$  into Eq. (2-6). When  $t = 3$  is substituted in Eq. (2-3) the resulting plot gives  $\beta_3$  as the intercept and  $\beta_4$  as the slope. In the systems studied the straight line obtained in this plot was horizontal showing that  $\beta_4 = 0$ .

This method of calculating stability constants is not always satisfactory. It is laborious and requires a large number of precise experimental points, well spaced over the range  $0 < \bar{n} < N$ .

## 2 (b) CURVE-FITTING TECHNIQUES.

### $\bar{n}(\log a)$ data for a single complex

In a system where a single complex is formed i.e.  $N=1$ , the shape of the formation curve is unique. A particularly useful method of obtaining the equilibrium constant of the single complex is by fitting the experimental formation curve,  $\bar{n}(\log a)$ , to a normalised curve. The equation for the normalised curve has been derived by Sillén<sup>183</sup>. If only one complex is formed, Eq. (1-5) reduces to

$$\bar{n} = \frac{\beta_1 a}{1 + \beta_1 a} = \frac{a^*}{1 + a^*} \quad (2-7)$$

where

$$\log a^* = \log a + \log \beta_1 \quad (2-8)$$

Thus  $\bar{n}$  is a function only of the normalised variable  $a^*$ . The curve  $\bar{n}(\log a^*)$  is calculated from Eq. (2-7) and moved along the abscissa of the experimental plot until the best fit is obtained. Then the value of  $\log a^*$  coinciding with  $\log a^* = 0$  is the value of  $-\log \beta_1$ , cf. Eq. (2-8).

### $\bar{n}(\log a)$ data for two complexes.

In a system where two complexes only are formed, Eq. (1-5) reduces to

$$\bar{n} = \frac{\beta_1 a + 2\beta_2 a^2}{1 + \beta_1 a + \beta_2 a^2} \quad (2-9)$$

In this work, the method used to evaluate  $\beta_1$  and  $\beta_2$  in such systems has been the projection<sup>strip</sup> method<sup>184, 185</sup>.

Setting the normalised variable

$$a^* = a\beta_2^{\frac{1}{2}} \quad (2-10)$$



and the parameter

$$p = \beta_1 \beta_2^{-\frac{1}{2}} = (K_1/K_2)^{\frac{1}{2}} \quad (2-11)$$

Eq. (2-1) can be rewritten

$$p = \left( \frac{\bar{n}}{1-\bar{n}} \right) \frac{1}{a^*} - \left( \frac{2-\bar{n}}{1-\bar{n}} \right) a^* \quad (2-12)$$

Thus  $\bar{n}$  is a function of the normalised variable  $a^*$  and the parameter  $p$  which fixes the shape of the formation curve  $\bar{n}(\log a)$ . The family of theoretical curves  $\log p(\log a^*)_{\bar{n}}$  is calculated from Eq. (2-12) using a number of convenient values of  $\bar{n}$ . The data for this family of curves have been calculated and quoted by Rossotti and Rossotti<sup>185</sup>.

The plots of  $\log p$  against  $\log a$  and  $\bar{n}$  against  $\log a$  are made using the same abscissa scale. For each value of  $\bar{n}$  used in the calculation of the family of theoretical curves, the corresponding value of  $\log a$  and the experimental uncertainty in this value is marked off on the  $\log a$  axis [see Sec. 5(a), Fig. 5.1]. The projection strip  $(\log a)_{\bar{n}}$  is then superimposed on the family of theoretical curves, parallel to the  $\log a^*$  axis, so that the best fit is obtained for all the values of  $\bar{n}$  shown [see Sec. 5(a), Fig. 5.2].

The ordinate which corresponds to the best position of fit of the strip gives the value of  $\log p$ . The point of intersection of the  $\log p$  axis ( $\log a^* = 0$ ) with the projection strip gives the value of  $-\frac{1}{2} \log \beta_2$ . The maximum limits of error in the values of  $p$  and  $-\frac{1}{2} \log \beta_2$  may be estimated from the vertical and horizontal distances respectively through which the projection strip may be moved, whilst allowing the calculated values of  $(\log a)_{\bar{n}}$  to remain within the experimental uncertainty.

#### The determination of three equilibrium constants.

If, over a certain range of the variable  $a$ , a number of experimental points  $(a, f)$  have been measured and  $f$  and  $a$  are related by

$$f(a) = k_0 + k_1 a + k_2 a^2 \quad (2-13)$$

$k_0$ ,  $k_1$  and  $k_2$  being the unknown constants to be determined, then Eq. (2-13)

may be expressed in terms of the two normalised variables

$$f^* = p_1 f$$

$$a^* = p_2 f$$

and of a third parameter,  $p_3$ , where  $p_1$ ,  $p_2$ , and  $p_3$  are related to the stability constants<sup>183</sup>. The origin of the experimental function  $\log f(\log a)$  is fixed by  $p_1$  and  $p_2$ , and its shape by  $p_3$ . The values of the parameters may be found by comparing the experimental data  $\log f(\log a)$  with the family of normalised curves  $\log f^*(\log a^*)p_3$ . The maximum limits of error in the parameters are given by the permissible vertical and horizontal displacement of the origin. In his paper Sillén<sup>183</sup> discusses modifications of the method when the function is

$$f(a) = k_0 + k_1 a^{-1} + k_2 a^{-2} \quad (2-14a)$$

$$f(a) = (k_0 + k_1 a + k_2 a^2)^{-1} \quad (2-14b)$$

$$f(a) = (k_0 + k_1 a^{-1} + k_2 a^{-2})^{-1} \quad (2-14c)$$

when  $k_0=0$ , or  $k_2=0$ , or when treating the polynomial

$$f^* = p_1 f a^{-1}$$

$$\text{and } a^* = p_2 a$$

This method is not applicable directly to data  $\bar{n}(\log a)$  but may be applied to functions derived from them [see Sec. 6(b) .]

In analysing the data for systems in which several species coexist the problem of deciding which reactions occur and of calculating the relevant equilibrium constants arises. If curve-fitting methods are used, the data are fitted to normalised curves for different likely combinations of species until an acceptable fit is obtained. Some idea of the species present can often be gained from the shape of the experimental formation curve. Several combinations of species must be tried as it is sometimes possible to obtain equally acceptable fits with more than one combination.

Normalised curves for species A, HA, HA<sub>2</sub>, H<sub>2</sub>A<sub>2</sub>.

From the experimental data  $\bar{n}_H(\log h)$  for the four carboxylic acids studied in aqueous solution see [Sec. 4(a)] it was postulated that a possible combination of species formed is A, HA, HA<sub>2</sub>, and H<sub>2</sub>A<sub>2</sub>. The data were analysed using normalised curves of the type  $\log A^* (\log h^*)^{-\frac{186}{\bar{n}_H}}$ . This method has also been used in studying inorganic isopolyacids<sup>187</sup>.

For the present case, the family of normalised curves is derived as follows, charges being omitted here and elsewhere for clarity.

$$A = a + [HA] + 2[HA_2] + 2[H_2A_2] \quad (2-15)$$

$$= a + \beta_{11}^H h a + 2 \beta_{12}^H h a^2 + 2 \beta_{22}^H h^2 a^2 \quad (2-16)$$

$$H = h + [HA] + [HA_2] + 2[H_2A_2] \quad (2-17)$$

Combining Eqs. (1-6) and (2-17)

$$A\bar{n}_H = [HA] + [HA_2] + 2[H_2A_2] \quad (2-18)$$

$$= \beta_{11}^H h a + \beta_{12}^H h a^2 + 2 \beta_{22}^H h^2 a^2 \quad (2-19)$$

Equations (2-16) and (2-19) are normalised by setting

$$h^* = \beta_{11}^H h, \quad \frac{A^*}{A} = \frac{v}{\bar{n}_H} = \frac{\beta_{12}^H}{\beta_{11}^H}, \quad R = \frac{\beta_{22}^H}{\beta_{11}^H \beta_{12}^H}$$

Then Eq. (2-16) becomes

$$A^* = (1 + h^*)v + 2h^*(1 + Rh^*)v^2 \quad (2-20)$$

and Eq. (2-19) becomes

$$A^*\bar{n}_H = h^*v + h^*(1 + 2Rh^*)v^2 \quad (2-21)$$

Subtracting Eq. (2-21) from Eq. (2-20)  $x\bar{n}_H$  and solving for v

$$v = \frac{h^* - (1 + h^*)\bar{n}_H}{h^* [2\bar{n}_H(1 + Rh^*) - (1 + 2Rh^*)]} \quad (2-22)$$

Substituting Eq. (2-22) into Eq. (2-20) and solving for A\*

$$A^* = \frac{[\bar{n}_H(1 + h^*) - h^*][h^*(2R-1) + 1]}{h^* [(1 + 2Rh^*) - 2\bar{n}_H(1 + Rh^*)]}^2 \quad (2-23)$$

The experimental data  $\log A(\log h)_{\bar{n}_H}$  are superimposed on the family of curves

by  $\log A^*(\log h^*)_{\bar{n}_H, R}$  in such a position that the best fit is obtained. In

this position

$$\log A^* - \log A = \log \beta_{12}^H - \log \beta_{11}^H = \log K_{12}^H \quad (2-24)$$

$$\log h^* - \log h = \log \beta_{11}^H - \log K_{11}^H \quad (2-25)$$

where  $K_{12}^H$  is the equilibrium constant for the reaction



Also  $K_{22}^H$  is the equilibrium constant for the reaction



The values of  $\beta_{22}^H$  is obtained from the value of  $R$  used to obtain the best fit. The value of  $R$  may sometimes be calculated precisely from the formation curves; in other cases  $R$  must be found by successive approximations [see Sec. 4(a)]. The value of  $K_{22}^H$  is obtained from Eq. (2-28).

$$R = \frac{\beta_{22}^H}{\beta_{11}^H \beta_{12}^H} = \frac{K_{22}^H}{K_{11}^H} \quad (2-28)$$

The maximum limits of error in the values of the constants are given by the permissible vertical and horizontal displacements of the origin of the normalised curves, whilst maintaining an acceptable fit.

Normalised curves for species A,  $HA_2$ .

In the case where the species formed are A and  $HA_2$  we may set

$$\frac{A^*}{A} = \frac{y}{a} = \beta_{12}^H$$

$$\frac{A^*}{A} = \frac{y}{a} = \frac{H}{12}$$

and the analogue of Eq. (2-20) is

$$A^* = v + 2hv^2 \quad (2-29)$$

The analogue of Eq. (2-21) is

$$A^* \bar{n}_H = hv^2 \quad (2-30)$$

whence

$$A^*(1-2\bar{n}_H) = v \quad (2-31)$$

Substituting Eq. (2-31) into Eq. (2-29) and solving for  $A^*$

$$A^* = \frac{\frac{v}{\bar{n}_H}}{h(1-2\bar{n}_H)^2} \quad (2-32)$$

The experimental data  $\log A(\log h)_{\bar{n}_H}$  are superimposed on the family of curves  $\log A^*(\log h)_{\bar{n}_H}$  in such a position that the best fit is obtained. In this position the value of  $\log \beta_{12}^H$  is obtained from Eq. (2-24a).

$$\log A^* - \log A = \log \beta_{12}^H \quad (2-24a)$$

The maximum limits of error in the value of the constants are obtained in the same way as in the previous case.

Normalised curves for species A, HA, HA<sub>2</sub>, and H<sub>2</sub>A<sub>3</sub>.

In the study of acetic acid in dioxan-water mixture [see Sec. 6(b)] the formation of the species A, HA, HA<sub>2</sub>, and H<sub>2</sub>A<sub>3</sub> was postulated at low values of  $\bar{n}_H$  ( $0 \leq \bar{n}_H \leq 0.40$ ).

Here

$$A = a + [HA] + 2[HA_2] + 3[H_2A_3] \quad (2-33)$$

$$= a + \beta_{11}^H ha + 2\beta_{12}^H ha^2 + 3\beta_{23}^H h^2 a^3 \quad (2-34)$$

$$H = h + [HA] + [HA_2] + 2[H_2A_3] \quad (2-35)$$

Combining Eqs. (1-6) and (2-35)

$$A\bar{n}_H = [HA] + [HA_2] + 2[H_2A_3] \quad (2-36)$$

$$= \beta_{11}^H ha + \beta_{12}^H ha^2 + 2\beta_{23}^H h^2 a^3 \quad (2-37)$$

Normalising Eqs. (2-34) and (2-37) by setting

$$h^* = \beta_{11}^H h, \quad \frac{A^*}{A} = \frac{v}{a} = \frac{\beta_{11}^H}{\beta_{12}^H} \quad \text{and} \quad R = \frac{\beta_{23}^H}{(\beta_{12}^H)^2}$$

whence

$$A^* = (1 + h^*)v + h^*v^2(2 + 3Rh^*v) \quad (2-38)$$

$$\text{and} \quad A^*\bar{n}_H = h^*v + h^*v^2(1 + 2Rh^*v) \quad (2-39)$$

Subtracting Eq. (2-39)  $\times 3$  from Eq. (2-38)  $\times 2$

$$A^*(2 - 3\bar{n}_H) = (2 - h^*)v + h^*v^2 \quad (2-40)$$

and solving for  $v$

$$v = \frac{h^* - 2 + \sqrt{(2-h^*)^2 + 4h^*A^*(2 - 3\bar{n}_H)}}{2h^*} \quad (2-41)$$

Subtracting Eq. (2-38)  $\times \bar{n}_H$  from Eq. (2-39)

$$0 = h^* - \bar{n}_H(1 + h^*) + R(h^*)^2v^2(2 - 3\bar{n}_H) + h^*v(1 - 2\bar{n}_H) \quad (2-42)$$

whence

$$v = \frac{(2\bar{n}_H - 1) + \sqrt{(1-2\bar{n}_H)^2 - 4R(2 - 3\bar{n}_H)[h^* - (1 + h^*)\bar{n}_H]}}{2h^*R(2 - 3\bar{n}_H)} \quad (2-43)$$

Eliminating  $v$  by equating Eqs. (2-41) and (2-43), the following expression for  $A^*$  is obtained.

$$2Rh^*(2 - 3\bar{n}_H)^2 A^* = \left[ \frac{2\bar{n}_H - 1}{R(2 - 3\bar{n}_H)} + 2 - h^* \right] \sqrt{(1 - 2\bar{n}_H)^2 - 4R(2 - 3\bar{n}_H)[h^* - (1 + h^*)\bar{n}_H]} + \frac{(2\bar{n}_H - 1)^2}{R(2 - 3\bar{n}_H)} + 6\bar{n}_H - (2 + h^*) \quad (2-44)$$

The experimental data  $\log A(\log h)_{\bar{n}_H}$  are superimposed on the family of curves

$\log A^*(\log h^*)_{\bar{n}_H, R}$  in such a position that the best fit is obtained. In the



(43)

this position the values of  $\log \beta_{12}^H$  and  $\log K_{12}$  are obtained from Eq. (2-24) and the value of  $\log \beta_{11}^H$  from Eq. (2-25). The value of  $\beta_{23}^H$  is obtained from the value of R used to obtain the best fit. The maximum limits of error are calculated in the usual way.

Normalised curves for species A, HA, HA<sub>2</sub>, and HA<sub>3</sub>.

If the hypothesis is made that the species A, HA, HA<sub>2</sub>, and HA<sub>3</sub> coexist in equilibrium in a system then

$$A = a + [HA] + 2[HA_2] + 3[HA_3] \quad (2-45)$$

$$= a + \beta_{11}^H ha + 2 \beta_{12}^H ha^2 + 3 \beta_{13}^H ha^3 \quad (2-46)$$

$$H = h + [HA] + [HA_2] + [HA_3] \quad (2-47)$$

Combining Eqs. (1-6) and (2-47)

$$A\bar{n}_H = [HA] + [HA_2] + [HA_3] \quad (2-48)$$

$$= \beta_{11}^H ha + \beta_{12}^H ha^2 + \beta_{13}^H ha^3 \quad (2-49)$$

Normalising Eqs. (2-46) and (2-49) by setting

$$h^* = \beta_{11}^H ha, \quad \frac{A^*}{A} = \frac{v}{a} = \frac{\beta_{12}^H}{\beta_{11}^H}, \quad R = \frac{\beta_{11}^H \beta_{13}^H}{(\beta_{12}^H)^2}$$

we obtain

$$A^* = v(1 + h^*) + 2v^2 h^* + 3Rv^3 h^* \quad (2-50)$$

$$A^* \bar{n}_H = v h^* + v^2 h^* + Rv^3 h^* \quad (2-51)$$

If v is eliminated from Eqs. (2-50) and (2-51) and the equations are then solved for A\*, we obtain

$$2R(1-3\bar{n}_H)^2 A^* = \left[ \frac{R(1-2h^*)(1-3\bar{n}_H) - h^*(2\bar{n}_H-1)}{Rh^*(1-3\bar{n}_H)} \right] \sqrt{(h^*)^2(1-2\bar{n}_H)^2 - 4Rh^*(1-3\bar{n}_H) [h^* - \bar{n}_H(1+h^*)]} \\ + 2h^*(2-3\bar{n}_H) - 1 - \frac{h^*(1-2\bar{n}_H)^2}{R(1-3\bar{n}_H)} \quad (2-52)$$



The experimental data  $\log A(\log h)_{\bar{n}_H}$  are superimposed on the family of curves  $\log A^*(\log h^*)_{\bar{n}_H, R}$  in such a position that the best fit is obtained. In this position the values of  $\beta_{11}^H$ ,  $\beta_{12}^H$ , and  $K_{12}^H$  are obtained from Eqs. (2-24) and (2-25). The value of  $\beta_{13}^H$  is calculated from the value of  $R$  used to obtain the best fit. The maximum limits of error are calculated in the usual way.

Normalised curves for species A, HA, and  $H_2A_2$ .

---

In the case where the species A, HA and  $H_2A_2$  coexist in equilibrium in a system

$$A = a + [HA] + 2[H_2A_2] \quad (2-53)$$

$$= a + \beta_{11}^H h a + 2 \beta_{22}^H h^2 a^2 \quad (2-54)$$

$$H = h + [HA] + 2[H_2A_2] \quad (2-55)$$

Combining Eqs. (1-6) and (2-55)

$$A\bar{n}_H = [HA] + 2[H_2A_2] \quad (2-56)$$

$$= \beta_{11}^H h a + 2 \beta_{22}^H h^2 a^2 \quad (2-57)$$

Subtracting Eq. (2-57) from Eq. (2-54) we obtain

$$A(1 - \bar{n}_H) = a \quad (2-58)$$

On substituting Eq. (2-58) into Eq. (2-57), we obtain the following linear function (2-59), from which values of  $\beta_{11}^H$  and  $\beta_{22}^H$  may be obtained.

$$\frac{\bar{n}_H}{(1 - \bar{n}_H)h} = \beta_{11}^H + 2 \beta_{22}^H A(1 - \bar{n}_H)h \quad (2-59)$$

The values of  $\beta_{11}^H$  and  $\beta_{22}^H$  may also be obtained by normalisation. Setting

$$h^* = \beta_{11}^H h \text{ and } \frac{A^*}{A} = \frac{v}{a} = \frac{\beta_{22}^H}{(\beta_{11}^H)^2}$$

we have by substitution into Eq. (2-59)

$$A^* = \frac{\bar{n}_H - h^*(1 - \bar{n}_H)}{2(h^*)^2(1 - \bar{n}_H)^2} \quad (2-60)$$

The experimental data  $\log A(\log h)_{\bar{n}_H}$  are superimposed on the family of curves  $\log A^*(\log h^*)_{\bar{n}_H, R}$  in such a position that the best fit is obtained. In this position the value of  $\beta_{11}^H$  is obtained from Eq. (2-25) and the value of  $\beta_{22}^H$  is obtained from Eq. (2-61) thus

$$\log A^* - \log A = \log \beta_{22}^H - 2 \log \beta_{11}^H \quad (2-61)$$

The maximum limits of error are calculated in the usual way.

#### Equilibrium constants related by some ratio.

If a large number of species appear to coexist in a system, it is useful if some simplifying assumptions can be made and the system interpreted in terms of two or three parameters only. Usually the precision of the experimental data does not permit the determination of more than three parameters. In the study of acetic acid in the dioxan-water mixture [Sec. 6(b)], it appeared likely that species such as  $HA$ ,  $HA_2$ ,  $H_2A_2$ ,  $H_2A_3$ ,  $H_3A_3$ ,  $H_3A_4$ , and  $H_4A_4$  might be formed. As the successive oligomers differ only in the addition of one more proton or carboxylate ion, it is possible that there is a fairly simple relationship between the successive equilibrium constants. Four hypotheses were tested and the derivation of the corresponding normalised curves is outlined below.

In the four hypotheses, two constants  $K_a$  and  $K$  are defined.  $K_a$  is the same in each hypothesis and is the acid dissociation constant of  $H_qA_q$

$$K_a = \frac{[H_{q-1}A_q]}{[H_qA_q] h} \quad (2-62)$$

However,  $K$  is defined differently in each hypothesis. The mass-balance equations, (2-63) and (2-64) are thus

$$A = a + HA + 2HA_2 + 2H_2A_2 + 3H_2A_3 + 3H_3A_3 + 4H_3A_4 + \dots \quad (2-63)$$

$$A\bar{n}_H = HA + HA_2 + 2H_2A_2 + 2H_2A_3 + 3H_3A_3 + 3H_3A_4 + \dots \quad (2-64)$$

whence

$$A(1 - \bar{n}_H) = a + HA_2 + H_2A_3 + H_3A_4 + \dots \quad (2-65)$$

The normalised functions used are the same in every hypothesis, thus

$$(h^*)^{-1} = K_a h^{-1}$$

$$a^* = K_h a$$

$$A^* = AK$$

#### Hypothesis I

$$\text{Let } K^{q-1} = \frac{[H_q A_q]}{(ha)^q} \quad (2-66)$$

where  $q$  is an integer

Combining Eqs. (2-62), (2-65), and (2-66)

$$A(1 - \bar{n}_H) = K_a h^{-1} [HA + H_2A_2 + H_3A_3 + \dots] \quad (2-67)$$

$$= K_a h^{-1} [ha + Kh^2 a^2 + K^2 h^3 a^3 + \dots] \quad (2-68)$$

Multiplying both sides of Eq. (2-68) by  $K$

$$AK(1 - \bar{n}_H) = K_a h^{-1} [Kha + K^2 h^2 a^2 + K^3 h^3 a^3 + \dots] \quad (2-69)$$

Normalising Eq. (2-69)

$$A^*(1 - \bar{n}_H) = (h^*)^{-1} \sum_{q=1}^{\infty} (a^*)^q \quad (2-70)$$

$$= \frac{(h^*)^{-1} a^*}{1 - a^*} \quad \text{provided } a^* < 1 \quad (2-71)$$

Now

$$A = \sum_q q H_q A_q + \sum_q q H_{q-1} A_q \quad (2-63a)$$

Combining Eqs. (2-62) and (2-63a),

$$A = (1 + K_a h^{-1}) \sum q_H A_q \quad (2-72)$$

Combining Eqs. (2-66) and (2-72), and multiplying both sides by  $K$ , we obtain

$$AK = (1 + K_a h^{-1})(Kha + 2K^2 h^2 a^2 + 3K^3 h^3 a^3 + \dots) \quad (2-73)$$

Normalising Eq. (2-73)

$$A^* = [1 + (h^*)^{-1}] \sum_1^{\infty} q(a^*)^q \quad (2-74)$$

$$= \frac{[1 + (h^*)^{-1}] a^*}{(1 - a^*)^2} \quad (2-75)$$

From Eq. (2-71)

$$a^* = \frac{A A^* (1 - \bar{n}_H)}{(h^*)^{-1} + A^* (1 - \bar{n}_H)} \quad (2-71a)$$

Substituting for  $a^*$  in Eq. (2-75)

$$A^* = \frac{(h^*)^{-1} [(h^*)^{-1} - (1 - \bar{n}_H)(1 + (h^*)^{-1})]}{(1 - \bar{n}_H)^2 [1 + (h^*)^{-1}]} \quad (2-76)$$

When the experimental data  $\log A(\log h)_{\bar{n}_H}$  are superimposed on the family of curves  $\log A^*(\log h^*)_{\bar{n}_H}$ , calculated using Eq. (2-76), then in the position of best fit

$$\log h - \log h^* = \log K_a \quad (2-77)$$

$$\log A^* - \log A = \log K \quad (2-78)$$

The maximum limits of error are calculated in the usual way.

#### Hypothesis IA

A modified form of Hypothesis I allows the first acidity constant to differ from  $K_a$ . Let the first acidity constant =  $K_a K_1$

Then Eq. (2-70) becomes

$$A^*(1 - \bar{n}_H) = K_1 (h^*)^{-1} a^* + (h^*)^{-1} \sum_1^{\infty} (a^*)^q \quad (2-79)$$

$$= K_1 (h^*)^{-1} a^* + \frac{(h^*)^{-1} (a^*)^2}{(1 - a^*)} \quad (2-80)$$

$$= (h^*)^{-1} a^* [K_1 + \frac{a^*}{1 - a^*}] \quad (2-81)$$

provided  $a^* < 1$

Equation (2-74) becomes

$$A^* = a^*(1 + K_1(h^*)^{-1})^* + (1 + (h^*)^{-1}) \sum_{q=2}^{\infty} (a^*)^q \quad (2-82)$$

$$= a^*(1 + K_1(h^*)^{-1}) + \frac{[1 + (h^*)^{-1}](2 - a^*)(a^*)^2}{(1 - a^*)^2} \quad (2-83)$$

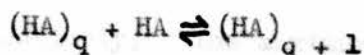
Solving Eq. (2-81) for  $a^*$  and substituting for  $a^*$  in Eq. (2-83) should give an equation for  $A^*$ , enabling curves of  $\log A^*(\log h^*)_{\bar{n}_H, K_1}$  to be calculated. However, the solution of Eq. (2-81) and the subsequent substitution in Eq. (2-83) are rather difficult and it was not considered worthwhile to devote time to the problem. The hypothesis, therefore, was not pursued.

#### Hypothesis II

$$K_a \text{ is again defined by Eq. (2-62) and } qK^{q-1} = \frac{[H_q A_q]}{(ha)^q} \quad (2-84)$$

where  $q$  is an integer

This implies that the first few additions of HA occur more easily than the later ones, i.e. the equilibrium constant for the reaction



is  $\frac{1+q}{q}K$  which decreases from  $\frac{3}{2}K$  to  $K$  as  $q$  increases from 2 to  $\infty$

Combining

Eqs. (2-62), (2-65), and (2-84) we obtained

$$A(1 - \bar{n}_H) = K_a h^{-1} [ha + 2Kh^2 a^2 + 2K^2 h^3 a^3 + \dots] \quad (2-85)$$

Multiplying both sides of Eq. (2-85) by  $K$

$$AK(1 - \bar{n}_H) = K_a h^{-1} [Kha + 2K^2 h^2 a^2 + 3K^3 h^3 a^3 + \dots] \quad (2-86)$$

Normalising Eq. (2-86)

$$A^*(1 - \bar{n}_H) = (h^*)^{-1} \sum_{q=1}^{\infty} q(a^*)^q \quad (2-87)$$

$$= \frac{(h^*)^{-1} a^*}{(1 - a^*)^2} \quad (2-88)$$

provided  $a^* < 1$

Combining Eqs. (2-62), (2-63a), and (2-84)

$$A = (1 + K_a h^{-1})(ha + 2^2 K h^2 a^2 + 3^2 K^2 h^3 a^3 + \dots) \quad (2-89)$$

Multiplying both sides of Eq. (2-89) by K and then normalising

$$A^* = (1 + (h^*)^{-1}) \sum_{q=1}^{\infty} q^2 (a^*)^q \quad (2-90)$$

and

$$A^* = \frac{(1 + (h^*)^{-1} a^* (1 + a^*))}{(1 - a^*)^3} \quad (2-91)$$

provided  $a^* < 1$

Solving Eq. (2-88) for  $a^*$  and substituting for  $a^*$  in Eq. (2-91)

we obtain

$$A^* = \frac{(h^*)^{-1} [(h^*)^{-1} - (1 - \bar{n}_H)(1 + (h^*)^{-1})] [(h^*)^{-1} + (1 - \bar{n}_H)(1 + (h^*)^{-1})]}{4(1 - \bar{n}_H)^3 (1 + (h^*)^{-1})^2} \quad (2-92)$$

The experimental data  $\log A(\log h)_{\bar{n}_H}$  are superimposed on the family of curves  $\log A^*(\log h^*)_{\bar{n}_H}$  calculated using Eq. (2-92). In the position of best fit the values of  $K_a$  and K are calculated from Eqs. (2-77) and (2-78) respectively. The maximum limits of error are calculated in the usual way.

### Hypothesis III.

$K_a$  is defined by Eq. (2-62) as before and

$$\frac{K^{q-1}}{q!} = \frac{[H_q A_q]}{(ha)^q} \quad (2-93)$$

where q is an integer.

This implies that the addition of the HA to  $(HA)_q$  to form  $(HA)_{q+1}$

becomes more and more difficult as q increases, i.e. the equilibrium constant for the reaction





is  $\frac{K}{q+1}$  which decreases from  $\frac{K}{3}$  to zero as  $q$  increases from 2 to  $\infty$

Combining Eqs. (2-62), (2-65), and (2-93) we obtain

$$A(1 - \bar{n}_H) = K_a h^{-1} \left( ha + \frac{Kh^2 a^2}{2!} + \frac{K^2 h^3 a^3}{3!} + \dots \right) \quad (2-94)$$

Multiplying both sides of Eq. (2-94) by  $K$  and then normalising

$$A^*(1 - \bar{n}_H) = (h^*)^{-1} \sum_{q=1}^{\infty} \frac{(a^*)^q}{q!} \quad (2-95)$$

$$= (h^*)^{-1} (e^{a^*} - 1) \quad (2-96)$$

Combining Eqs. (2-62), (2-63a), and (2-93) we obtain

$$A = (1 + K_a h^{-1}) \left( ha + \frac{2Kh^2 a^2}{2!} + \frac{3K^2 h^3 a^3}{3!} + \dots \right) \quad (2-97)$$

Multiplying both sides of Eq. (2-97) by  $K$  and normalising

$$A^* = (1 + (h^*)^{-1}) \sum_{q=1}^{\infty} q \frac{(a^*)^q}{q!} \quad (2-98)$$

$$= (1 + (h^*)^{-1}) a^* e^{a^*} \quad (2-99)$$

Solving Eq. (2-96) for  $a^*$  and substituting for  $a^*$  in Eq. (2-99) we obtain

$$A^*(1 - \bar{n}_H) + (h^*)^{-1} = (h^*)^{-1} \frac{(h^*)^{-1} A^*}{e[1 + (h^*)^{-1}][A^*(1 - \bar{n}_H) + (h^*)^{-1}]} \quad (2-100)$$

The family of curves  $\log A^*(\log h^*)_{\bar{n}_H}$  is calculated using Eq. (2-100).

To obtain the correct value of  $A^*$  for the substituted values of  $h^*$  and  $\bar{n}_H$

it is necessary to use successive approximations. The experimental data

$\log A(\log h)_{\bar{n}_H}$  are superimposed on the family of curves  $\log A^*(\log h^*)_{\bar{n}_H}$  and

in the position of best fit the values of  $K_a$  and  $K$  are calculated from Eq. (2-77)



and (2-78) respectively. The maximum limits of error are calculated in the usual way.

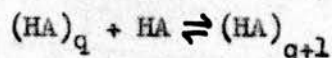
#### Hypothesis IV.

$K_a$  is defined by Eq. (2-62) as before and

$$\frac{K^{q-1}}{q} = \frac{[H_q A_q]}{(ha)^q} \quad (2-101)$$

where  $q$  is an integer.

This implies that the addition of HA to the first few oligomers is more difficult than it is to large oligomers, i.e. the equilibrium constant for the reaction



is  $\frac{q}{1+q} K$ , which increases from  $\frac{2}{3}K$  to  $K$  as  $q$  increases from 2 to  $\infty$ .

Combining Eqs. (2-62), (2-65), and (2-101) we obtain

$$A(1 - \bar{n}_H) = K_a h^{-1} (ha + \frac{K h^2 a^2}{2} + \frac{K^2 h^3 a^3}{3} + \dots) \quad (2-102)$$

Multiplying both sides of Eq. (2-102) by  $K$  and normalising

$$A^*(1 - \bar{n}_H) = (h^*)^{-1} \sum_{q=1}^{\infty} \frac{(a^*)^q}{q} \quad (2-103)$$

whence

$$A^*(1 - \bar{n}_H) = -(h^*)^{-1} \ln_e (1 - a^*) \quad (2-104)$$

Combining Eqs. (2-62), (2-63a), and (2-101) we obtain

$$A = (1 + K_a h^{-1}) (ha + \frac{2K h^2 a^2}{2} + \frac{3K^2 h^3 a^3}{3} + \dots) \quad (2-105)$$

Multiplying both sides of Eq. (2-105) by  $K$  and normalising

$$A^* = (1 + (h^*)^{-1}) \sum_{q=1}^{\infty} (a^*)^q \quad (2-106)$$



$$\text{Eq. (2-106)} = \frac{(1 + (h^*)^{-1})a^*}{(1 - a^*)} \quad (2-107)$$

Solving Eq. (2-104) for  $a^*$  and substituting for  $a^*$  in Eq. (2-107) we obtain

$$(A^* + 1 + (h^*)^{-1})e^{-A^*(1 - \bar{n}_H)h^*} = 1 + (h^*)^{-1} \quad (2-108)$$

The family of curves  $\log A^*(\log h^*)_{\bar{n}_H}$  is calculated using Eq. (2-108).

In order to obtain the correct value of  $A^*$  for the substituted values of  $h^*$  and  $\bar{n}_H$  it is necessary to use successive approximations. Seven figure logarithms are also necessary for this calculation. The experimental data  $\log A(\log h)_{\bar{n}_H}$  are superimposed on the family of curves  $\log A^*(\log h^*)_{\bar{n}_H}$ .

In the position of best fit the values of  $K_a$  and  $K$  are calculated from Eqs.

(2-77) and (2-78) respectively. The maximum limits of error are calculated in the usual way.

2 (c) INTEGRATION METHOD OF DETERMINING THE AVERAGE COMPOSITION OF  
POLYNUCLEAR SPECIES.

The average composition of polynuclear species may be obtained from the experimental curves  $\bar{n}_H(\log h)_A$ , without any special assumptions about the complexes, using formulae derived by Sillén<sup>188</sup> and quoted by Ingri et al.<sup>187</sup> These formulae define the quantities  $A_1$  and  $\bar{r}$  thus

$$\log A_1 = \log A - \int_{\log h_1}^{\log h_2} \left[ (\bar{n}_{H(1)} - \bar{n}_H) - \left( \frac{\delta \bar{n}_H}{\delta \log A} \right)_h \right] d \log h \quad (2-109)$$

and

$$\frac{1}{\bar{r}} = 1 - \left[ \int_{\log h_1}^{\log h_2} \left( \frac{\delta \bar{n}_H}{\delta \log A} \right)_h d \log h \right]_A \quad (2-110)$$

where

$A_1$  = total carboxylate concentration in the mononuclear species

$\bar{n}_{H(1)}$  = average number of protons per carboxylate group in the mononuclear species

$\bar{r}$  = the reciprocal of the average degree of condensation of A

$A_1$  and  $\frac{1}{\bar{r}}$  are calculated by plotting  $\left[ (\bar{n}_{H(1)} - \bar{n}_H) - \left( \frac{\delta \bar{n}_H}{\delta \log A} \right)_h \right]_A$

and  $\left( \frac{\delta \bar{n}_H}{\delta \log A} \right)_A$  respectively against  $\log h$  and evaluating the integrals.

The average number of protons per carboxylate group,  $\bar{p}_{poly}$ , may be calculated

$$\text{using the equation } \bar{p}_{poly} = \frac{\bar{n}_{Hpoly}}{\bar{r}_{poly}} = \frac{A\bar{n}_H - A_1\bar{n}_{H(1)}}{A\bar{r} - A_1} \quad (2-111)$$

The average number of carboxylate groups,  $\bar{q}_{poly}$ , may be calculated similarly,

$$\bar{q}_{poly} = \frac{1}{\bar{r}_{poly}} = \frac{A - A_1}{A\bar{r} - A_1} \quad (2-112)$$

In Eqs. (2-111) and (2-112)

$A\bar{n}_H$  = molar concentration of H bound to A

$A_1\bar{n}_H(1)$  = number of moles of H bound to A in the mononuclear species

$A\bar{r}$  = sum of the molar concentration of free A and of all complexes containing carboxylate groups.

SECTION 3.

EXPERIMENTAL.



### 3 (a) REAGENTS.

Reagents of Analar grade were used wherever possible. Some of the reagents used in the calorimetric work [Sec. 4(b)] were of the Merck "pro analysi" grade. It may be assumed that reagents were of one of these two grades, unless stated otherwise.

#### Water

Water from a glass still was passed through an "Elgastat" mixed-bed de-ioniser. According to the galvanometer attached to the de-ioniser, the eluate had a resistance of approx. 8 million ohms. Final traces of carbon dioxide were removed by boiling.

#### Potassium argentocyanide.

The sample used was prepared by Dr. F.J.C. Rossotti following the method of Brown<sup>189</sup>.

#### Sodium hydroxide.

A 50% sodium hydroxide solution was prepared from the solid and stored in a polythene bottle. After a few days sparingly soluble sodium carbonate which was present had settled. When required for preparing dilute solutions the 50% sodium hydroxide solution was filtered through a sintered glass filter, porosity 3, and transferred to a polythene bottle by pipette. All sodium hydroxide solutions were stored in polythene bottles and kept under an atmosphere of nitrogen.

#### Sodium hydrogen carbonate.

Solutions were prepared from the solid and filtered through a sintered filter, porosity 3, before potentiometric standardisation with perchloric acid.

#### Potassium hydrogen carbonate.

The solid was kept in a desiccator containing calcium chloride under an

atmosphere of carbon dioxide for several days before use. Potassium hydrogen carbonate was employed as a standard for the strong acids used in this work.

#### Sodium perchlorate.

The reagent grade anhydrous product of G.F. Smith & Co. was used. A concentrated solution was prepared and filtered through a sintered glass filter, porosity 3, to remove insoluble matter which contained some iron. The solution was boiled until, at about 137°C., a skin of sodium perchlorate formed on the surface. When the solution was cooled to 60°C.,  $\text{NaClO}_4 \cdot \text{H}_2\text{O}$  precipitated and was filtered off. The product was rinsed with a small amount of distilled water and recrystallised. The solution was free from chloride, chlorate, and other likely trace impurities. It was analysed by evaporation and drying weighed samples to constant weight at 125°C.

#### Sodium acetate.

A concentrated solution was prepared from sodium acetate trihydrate and water. The solution was filtered through a sintered glass filter, porosity 3, and analysed by evaporating, drying, and igniting weighed samples in 6 ml. platinum crucibles. After ignition, the sodium carbonate formed was titrated against standard hydrochloric acid using methyl orange indicator.

The prepared solution contained 3.084 Moles/1000 g. solution, and was free from chloride and iron.

#### Sodium propionate.

The B.D.H. product was recrystallised once from dilute propionic acid. The white, flaky crystals were washed with dilute propionic acid and a concentrated aqueous solution was prepared. The solution contained a little propionic acid but was free from chloride and iron.



Analysis of this solution by the method used for sodium acetate gave the following, rather scattered results, (in Moles/1000 g. solution): 4.237, 4.205, 4.231, 4.191, 4.229, 4.247, 4.199, 4.253, 4.240.

The solution was, therefore, analysed by potentiometric titration, described in Sec. 3 (c), and was found to contain  $4.324 \pm 0.005$  Moles/1000g. solution.

#### Sodium n-butyrate.

The B.D.H. product was recrystallised three times from water. A concentrated solution, free from chloride and iron, was prepared from the white, granular crystals and water. The solution was analysed potentiometrically, the concentration being  $4.173 \pm 0.005$  Moles/1000 g. solution.

#### Acetic acid.

The Analar acid was frozen, the last 10% to freeze and the last 10% to melt being rejected. The acid was used without further purification.

#### Propionic acid.

The B.D.H. product ( $n_D^{20} = 1.3870$ ) was distilled once using a Widmer column, the fraction boiling at  $141.0^\circ\text{C}$ . being collected. This fraction had a refractive index  $n_D^{20} = 1.3870$ . The first fraction (b.p.  $< 140^\circ\text{C}$ .) had  $n_D^{20} = 1.3883$ , and the residual higher boiling liquid had  $n_D^{20} = 1.3874$ .

Literature values of the boiling point and refractive index of the pure acid are  $140.8^\circ\text{C}$ . and 1.38650 respectively.

#### n-Butyric acid.

The B.D.H. product ( $n_D^{20} = 1.3978$ ) was distilled once using a Widmer column, the fraction boiling at  $163-164^\circ\text{C}$ . being collected. This fraction had  $n_D^{20} = 1.3979$ . The first low boiling fraction had  $n_D^{20} = 1.3985$ . Literature values of the boiling point and refractive index of the pure acid are  $163.25^\circ\text{C}$ . and 1.39796 respectively.

Formic acid.

The Analar acid was treated in the same way as acetic acid and then used without further purification. It had  $n_D^{20} = 1.3714$ , the literature value being  $n_D^{20} = 1.37140$ .

Dioxan.

The Fluka product (purified according to Hess and Frahm) was further purified by freezing, the last 10% to freeze and the last 10% to melt being rejected. Before freezing, the refractive index,  $n_D^{20}$ , was 1.4220, and after purification  $n_D^{20}$  was 1.4223. The literature value for  $n_D^{20}$  is 1.42241. The dioxan was tested for acid by the method quoted by Rosin<sup>190</sup>. A mixture of 10 ml. of dioxan and 10 ml. distilled water required 0.09 ml. of 0.1N sodium hydroxide for neutralisation, using one drop of phenolphthalein as indicator. Thus the acidity of the dioxan used was within the limit of 0.15 ml. 0.1N sodium hydroxide given by Rosin.

The stock solution and all solutions containing dioxan were kept under an atmosphere of nitrogen to prevent the formation of peroxide.

Silver perchlorate.

Silver nitrate was dissolved in the minimum of water and a saturated solution of ammonium carbonate was added drop by drop. The yellow silver carbonate which was precipitated was centrifuged and washed several times with distilled water. Excess of the precipitate was dissolved in dilute perchloric acid. The neutral solution was filtered and was free from chloride and nitrate.

The silver perchlorate was analysed by Volhard's method, using standard ammonium thiocyanate with ferric ammonium sulphate as indicator. The thiocyanate had previously been standardised against spectroscopically pure silver wire.

Copper(II) perchlorate.

Copper(II) nitrate was dissolved in water and a saturated solution of ammonium carbonate added, precipitating blue copper(II) carbonate. After washing with water, excess of the copper carbonate was dissolved in the minimum of perchloric acid. Sufficient perchloric acid was added to this solution to make the concentration of acid about 10mM. The solution was free from nitrate, chloride, and ammonium ions.

The copper was analysed by electrodeposition on a platinum cathode. 4-6 g. portions of solution, which contained about 0.25 g. copper, were weighed accurately and after dilution with water to 150 ml., 1 drop of 0.1N hydrochloric acid, 5 drops of concentrated sulphuric acid, 1 ml. concentrated nitric acid, and 0.5 g. urea were added. A platinum cathode and anode were used with an independent glass stirrer<sup>191</sup>. A current of 0.5A was used for 10 minutes and then 3A for about  $1\frac{1}{4}$  hours. An applied potential of 3V was used.

After electrolysis the cathode was washed with water, rinsed in alcohol, and dried in a steam oven for 10 minutes before weighing. The residual solution was tested for copper using diethyldithiocarbamate and re-electrolysed if necessary. Two stock copper(II) perchlorate solutions, whose concentrations were 496.0 and 738.3mM/1000 g. solution respectively were prepared. The acid content of the copper(II) perchlorate solutions was determined by potentiometric titration [see Sec. 3 (c)].

Cadmium(II) perchlorate.

Cadmium(II) chloride was dissolved in water and a saturated solution of ammonium carbonate added, slowly and with constant stirring, to precipitate cadmium carbonate. The precipitate, which was slightly gelatinous, was washed with distilled water and excess of it dissolved in perchloric acid.

The solution was free from chloride ions. The concentration of the solution was about 0.5M and the pH about 3.4.

The cadmium was analysed by two methods, by electrodeposition<sup>191</sup> and by volumetric titration.

(I) Analysis by electrodeposition.

About 2 g. of the cadmium solution was weighed accurately. A drop of phenolphthalein was added, followed by 0.1N sodium hydroxide until precipitation was complete and the solution had a permanent pink tinge. A 5% solution of potassium cyanide was added dropwise and with constant stirring until the precipitated cadmium hydroxide just dissolved. This solution was diluted to 100 ml. and electrolysed for 30 minutes using a platinum cathode and anode and an independent glass stirrer. The current was 0.2A at first and then was increased to 1.5-2.0A. An applied potential of 3V was used.

After electrolysis the cathode was washed with water, rinsed in alcohol, and dried for 10 minutes at 100°C.

(II) Volumetric analysis.

About 3 g. of the cadmium solution was weighed accurately. This solution was transferred to a column of the cation exchange resin Zeo-Karb 225, which had been converted to the hydrogen form. The acid solution equivalent to the original cadmium was eluted with water and titrated with 0.197N sodium hydroxide using phenolphthalein as indicator.

The results obtained from the two methods agreed to within 0.5%.

Nitrogen.

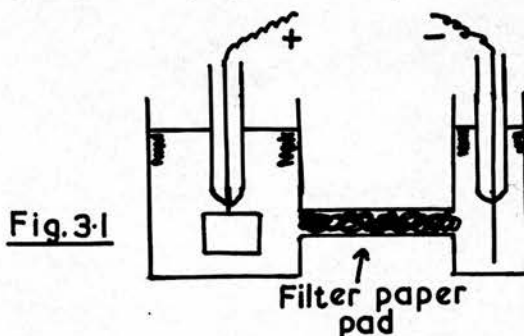
During a potentiometric titration, air was excluded from the system by a stream of nitrogen which also served to stir the solution. The nitrogen ~~which~~ was bubbled through a 40% sodium hydroxide solution to remove CO<sub>2</sub> and

and other acidic impurities and then through 3M sodium perchlorate to bring it to the correct vapour pressure.

For the measurements in the dioxan-water mixture, the nitrogen was bubbled through 40% sodium hydroxide solution, then through a 50% v/v dioxan-water solution and finally through a 50% v/v dioxan - 0.60M sodium perchlorate solution.

#### Silver reference electrodes.

Silver reference electrodes were prepared according to Brown<sup>189</sup>. A platinum wire, 1-2 cm. long, with one end sealed through a glass tube, was coated with silver by electrolysis from a 1% aqueous solution of potassium argentocyanide,  $\text{KAg}(\text{CN})_2$ , for 8 hours at 0.3mA. Free cyanide was removed from the solution before use by the addition of enough dilute silver nitrate to produce a faint precipitate of silver cyanide. At the platinum anode hydrocyanic acid is evolved and silver cyanide is precipitated. To prevent contamination of the rest of the solution by these products, a pad of filter paper was inserted along the narrow tube joining the two halves of the electrolytic cell (Fig. 3-1 ).



A number of electrodes may be prepared simultaneously by connecting them in series and using a current of 0.3mA for each electrode. After electrolysis, the electrode was washed in distilled water and then lightly chloridized by electrolysis in a 0.1N hydrochloric acid solution for 30 minutes at 0.3mA.



The electrodes were usually purplish-brown in colour though on occasion white ones were prepared. The reason for this variation is not apparent as all electrodes were prepared in identical fashion. However, the behaviour of the electrodes was the same whatever the colour and it was found that electrodes behaved satisfactorily for more than six months without renewal.

### 3 (b) APPARATUS.

Grade A burettes and volumetric flasks were used. Solutions were kept in rubber-stoppered Pyrex or Jena glass bottles, except alkaline solutions which were kept in polythene bottles.

The potentiometric titration cell used was of the type described by Forsling, Hietanen and Sillén<sup>192</sup>, see Fig. 3-2.

The titration vessel, A, had a capacity of 150-250 ml. The larger capacity vessel was used for measurements of aqueous solutions and the smaller capacity vessel was used for measurements of dioxan-water mixtures. The titration vessel contained openings for various auxiliary fittings.

The 25 or 50 ml. Grade A burette, B, had an extended tip which was bent just below the top so as to remove the burette stem from the area above the titration vessel, thus giving easier access to the other auxiliary equipment.

The glass electrode was a Radiometer shielded G202A type, suitable for use between pH 0-9. Before use, the electrode was immersed for 24 hours in 0.1N hydrochloric acid and then immersed for 24 hours in distilled water.

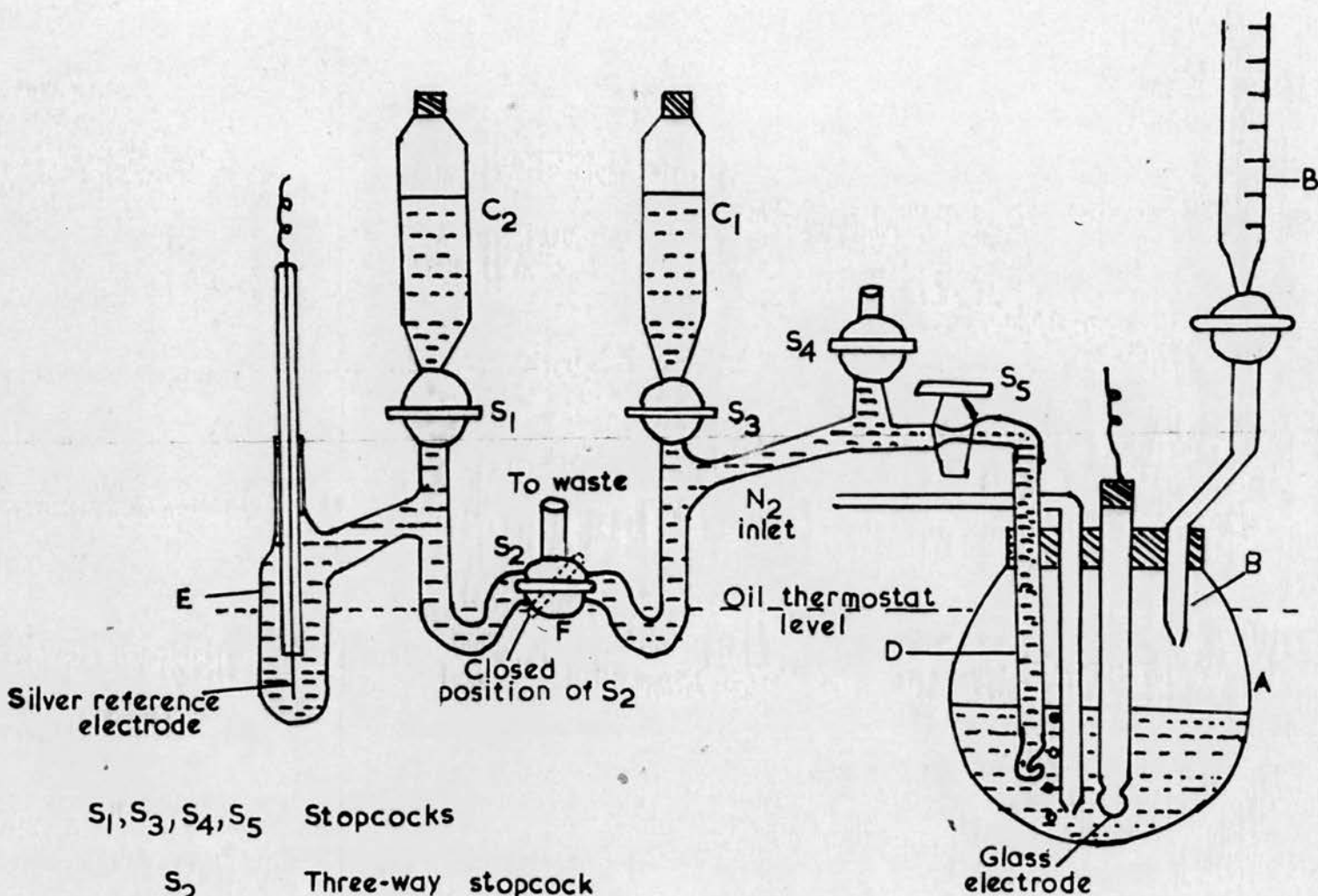
Thereafter the electrode was stored in distilled water. The treatment with acid was repeated occasionally.

The nitrogen inlet was extended as close as possible to the bottom of the titration vessel.

Fig 3.2

TITRATION CELL

'Wilhelm' Salt Bridge



- |   |                         |
|---|-------------------------|
| S <sub>1</sub> , S <sub>3</sub> , S <sub>4</sub> , S <sub>5</sub> | Stopcocks               |
| S <sub>2</sub>  | Three-way stopcock      |
| C <sub>1</sub> , C <sub>2</sub>                                   | Reservoirs              |
| A   | Titration vessel        |
| B   | Burette                 |
| D   | J-tube                  |
| E   | Silver electrode vessel |
| F   | Liquid junction         |



The J-tube of the "Wilhelm" salt bridge, described below, is the last auxiliary device shown in Fig. 3-2 . However, the titration vessels contained spare openings for second burettes or other fittings. The titration vessel was made gas-tight with rubber stoppers. The nitrogen outlet was a small slit in the rubber stopper holding the glass electrode in position.

The "Wilhelm" salt bridge occupies the left hand side of Fig. 3-2 . The solution to the right of the 3-way stopcock,  $S_2$ , was 3.00M sodium perchlorate, and that to the left of the stopcock was 2.99M sodium perchlorate + 0.01M silver perchlorate. These solutions were maintained by the reservoirs  $C_1$  and  $C_2$  respectively. The salt bridge was in contact with the titration solution via the J-tube, D. The silver reference electrode was firmly fixed in the electrode vessel, E, by a bored rubber stopper. The silver reference electrode and the glass electrode were connected to the potentiometer. Any waste solution from the salt bridge could be removed by manipulation of the three-way stopcock  $S_2$ .

When measurements of equilibria in dioxan-water mixtures were made the solutions in the right and left hand sides of the salt bridge were 50% v/v dioxan - 0.60M sodium perchlorate and 50% v/v dioxan - 0.59M sodium perchlorate + 0.01M silver perchlorate, respectively.

Before each titration the liquid junction at F was renewed by suitable movements of the stopcocks  $S_1$ ,  $S_2$ , and  $S_3$ . The solution at the J-tube side was renewed before each titration by closing  $S_2$  to that side and then manipulating  $S_3$ ,  $S_4$ , and  $S_5$ . During a titration, the salt bridge and titration vessel were immersed in an oil thermostat to the level shown by the dotted line in Fig. 3-2 . After a titration, the salt bridge was removed from the thermostat bath and stored in the thermostat room. The 3-way stop-

cock,  $S_2$ , was turned to a diagonal position (see Fig. 3-2 ) so that none of its outlets was open. All other stopcocks were closed.

#### Potentiometer.

Potentials were measured to  $\pm 0.1$ mv with a Radiometer PHM 3k valve potentiometer, which had been calibrated against a Pye Precision Vernier potentiometer by Dr. F.J.C. Rossotti.

#### Thermostats.

Potentiometric titrations were carried out in an oil thermostat at  $25.00 \pm 0.05^\circ\text{C}$ . This thermostat and all solutions used in the titrations were kept in a room thermostated at  $25.0 \pm 0.5^\circ\text{C}$ .

#### Calorimeter.

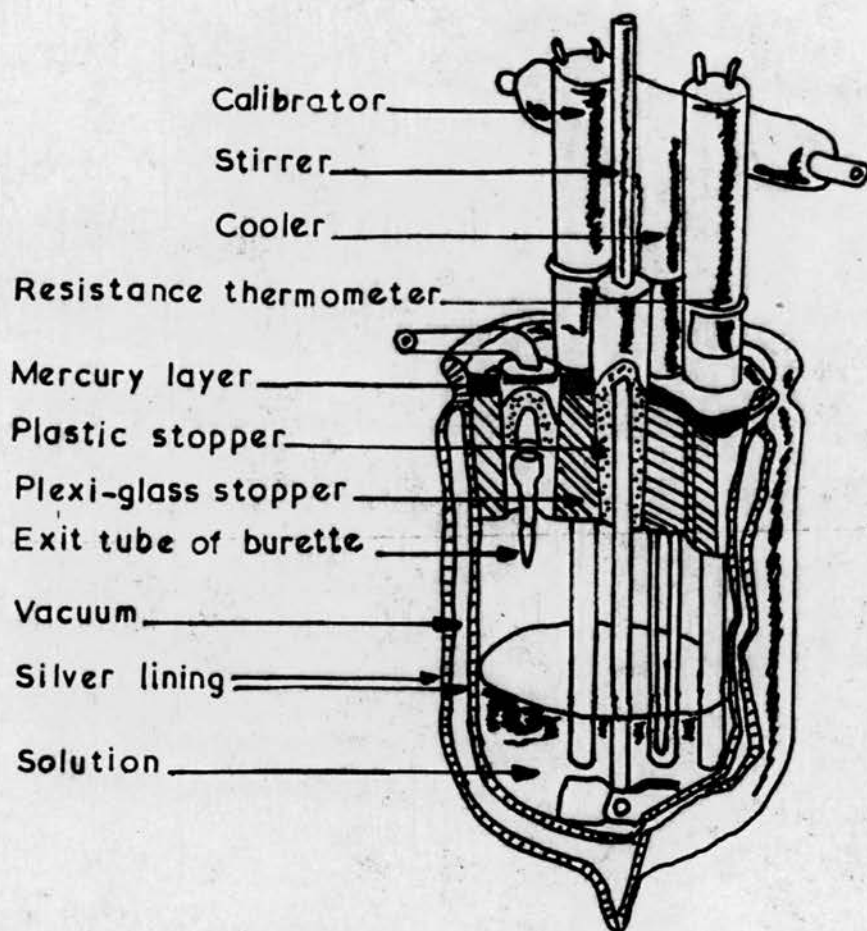
Calorimetric measurements were made on the instrument installed in the Inorganic Chemistry Department, Royal Institute of Technology, Stockholm. This precision calorimeter was equipped with a resistance thermometer, a thermostated burette, a mild cooler, and an auxiliary heater. It has been fully described by Schlyter<sup>193</sup>. The calorimeter vessel and its attachments are shown in Fig. 3-3.

The temperature sensitive part of the resistance thermometer was a nickel wire wound vertically on a cylindrical plastic support. The cylinder was placed in a thin walled pyrex tube partially filled with non-corrosive transformer oil. The top end of the shielding pyrex tube was sealed with a paraffin plug. The thermometer was attached to a Wheatstone bridge circuit. The resistance box and rheostats of the Wheatstone bridge and the thermometer were shielded by Faraday cages in order to eliminate parasitic currents. The thermometer was standardised by Schlyter against a high precision mercury thermometer.

A high-sensitivity mirror galvanometer, on a vibrationless mounting

Fig. 3-3

CALORIMETER VESSEL



acted as temperature indicator. A lamp containing a vertical, straight incandescent filament was used as the light source. The beam from this lamp passed through a positive lens and an iris diaphragm, and was reflected by the slightly concave galvanometer mirror. A sharp image of the incandescent filament was given on a linear scale at a horizontal distance of  $480 \pm 1$  cm. from the galvanometer mirror. The middle point of the scale was in front of the galvanometer. The reading of the light spot on the linear scale was corrected to a circular scale.

Disturbances of the measurements, which can be caused by the sudden occurrence of electromagnetic fields near exposed parts of the Wheatstone bridge, were eliminated by the Faraday cages already mentioned. Thermal voltages due to temperature differences between metal-metal junctions in the

Wheatstone bridge can also affect the measurements. Lange and Berga<sup>194</sup> found that variations in thermal voltages could be neglected if the soldered connections of the resistance thermometer, which cause the effects, were kept at atmospheric pressure. In the bridge circuit, thermal differences may be generated during a measurement and these have their largest values just after the current is switched on. Thereafter the temperature of the conducting wires gradually reaches a steady state through heat exchange with the surrounding thermostated air. The rest-position of the galvanometer light spot was found to vary just after the current was switched on, but after 3 hours the light spot was stationary at its rest-position. Thus variations in thermal voltages could be neglected if the current was switched on at least 3 hours before measurements were taken. In practice, the current was switched on 10-12 hours (overnight) before the start of a titration.

If, during titrations, a number of calibrations are carried out, the heat capacity of the calorimeter and its contents can be calculated from



observed data and plotted in a diagram against the volume added from the burette. This plot was found to be linear. Hence, temperature changes caused by a heat of reaction can be converted to a well-defined number of joules or calories evolved or absorbed.

The heat-generating part of the electric calibrator was a manganin wire attached to a pyrex rod. The ends of the manganin wire were soldered to copper wires and the heater was shielded by a thin-walled pyrex tube, partially filled with non-corrosive ricinus oil. The top of the calibrator was sealed with a paraffin plug.

The experiments were carried out in a room thermostated at  $25.0 \pm 0.2^\circ\text{C}$ . The calorimeter and thermostating burette bulb were immersed in distilled water thermostated to  $\pm 0.004^\circ\text{C}$ . The temperature of water contained in a glass vessel of similar design to the thermostated burette bulb and immersed in the thermostat, varied within  $\pm 0.002^\circ\text{C}$ .

The calorimeter vessel was a Dewar flask of about 700 ml. capacity. It was provided with a ground plexi-glass stopper, which contained ground openings for the resistance thermometer, the stirrer, the burette, the cooler, and the calibrator. The stopper was covered with a mercury seal about 5 cm. thick to ensure water-tightness. During experiments the calorimeter was attached to a stable ring-stand and totally immersed in the thermostat.

The stirrer was a pyrex rod fitted with two pyrex propeller blades at its lower end. The stirrer shaft was partially surrounded by a plastic joint, which could be fitted into one of the openings of the calorimeter stopper. The top end of the stirrer was attached by a latex tube to the drive shaft of an electric precision motor. An asbestos sheet was placed between the running motor and auxiliary devices to diminish the heat transfer from the motor to the calorimeter.

A simple burette device was used to add a reactant to the solution in the calorimeter. A 25 ml. burette was connected to a thermostated pyrex bulb of about 50 ml. capacity. The bulb was connected to the calorimeter by a ground joint and held in position by two steel springs. The calorimeter end of the glass tube was provided with a short glass capillary tube, the top of which had been treated with molten paraffin so that it delivered very small drops of solution of the order of 0.005 ml.

It was found that, to keep uncertainties in the measurements as low as possible, the temperature of the added reactant solution should not differ by more than  $\pm 0.02^{\circ}\text{C}$ . from the temperature of the solution in the calorimeter. By means of the air-cooler (see below) the temperature of the calorimeter solution was adjusted as closely as possible to that of the thermostated water immediately before each addition of reactant solution.

The reactant solution was brought to the temperature of the thermostated water by the burette bulb. The bulb was totally immersed in the thermostated water (Fig. 3-3 ). In the measurements to be described 2 ml. increments of reactant solution were added to the calorimeter solution at intervals of 20-30 minutes. The part of the solution in the burette stem was thermostated by air and its temperature differed from that of the thermostat water by  $0.4^{\circ}\text{C}$ . at most. An addition of the burette solution to the calorimeter resulted in the addition of 2 ml. of air-thermostated solution to the top of the 50 ml. bulb. After 20 minutes the temperature difference between the solution added to the bulb and the thermostat water had decreased from a maximum of  $0.4^{\circ}\text{C}$ . to  $0.003^{\circ}\text{C}$ .

The air-cooler used for reducing the temperature of the calorimeter solution to  $25^{\circ}\text{C}$ . consisted of a U-shaped, thin-walled glass tube. It was



connected to a water pump and a pre-cooler, and sealed with latex joints and a rubber-stopper. By means of the water pump, cold air, pre-cooled by passage round an ice-water mixture, was drawn through the cooler. The inlet tube and exhaust pipe of the cooler were heat-insulated by asbestos yarn.

The method of operation is described in more detail in Section 4(b) .

### 3 (c) POTENTIOMETRIC PROCEDURE.

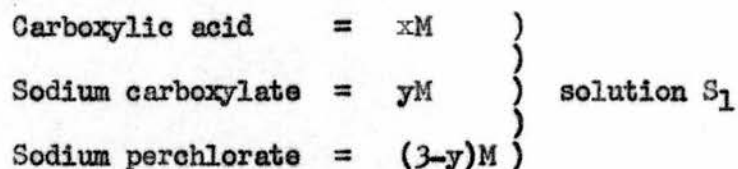
In studying complicated systems of complexes in solution, it is very useful to keep activity coefficients constant, so that the concentrations of the various reacting species can be calculated directly from emf measurements etc. and the law of mass action applied using concentrations instead of activities. The activity coefficients are controlled by using a supporting electrolyte, usually a 1:1 salt of an alkali metal, in large excess so that the ionic composition of the medium is kept as constant as possible. The composition of the medium may be varied slightly provided that either the formal ionic strength or the concentration of the bulk ion of opposite charge to the reactant of higher concentration is kept constant<sup>195, 196</sup>. The background salt should form either no complexes or very weak complexes with the reacting species and it should contribute little to the property being studied. Sodium perchlorate has often been used as the background salt; it is known to form weak complexes with some metals<sup>197</sup>. Equilibrium measurements cannot be used to distinguish between species with different amounts of solvent or ionic medium and so the formula [BA] represents the sum of all possible species with varying amounts of solvents, say water, and ionic medium, say sodium perchlorate. Thus

$$[BA] = \sum \sum \sum [BA(H_2O)_x(Na^+)_y(ClO_4^-)_z] \quad (3-1)$$

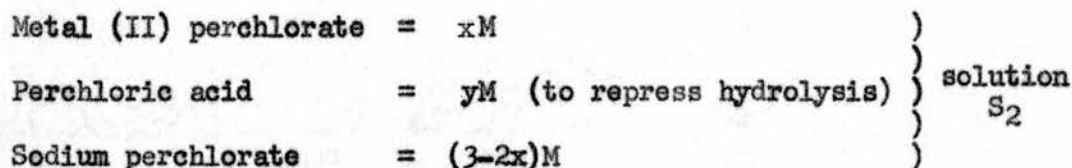
The constant ionic medium was used first by Grossmann<sup>5</sup> and since 1940 it has been used in many investigations. For this work sodium perchlorate was chosen as the inert medium and, except in copper (II) and cadmium (II) perchlorate solutions, the sodium ion concentration has been kept at 3.00M in aqueous solutions and at 0.60M in 50% v/v dioxan - water mixtures.

### 1. Aqueous solutions

A typical buffer had the following composition

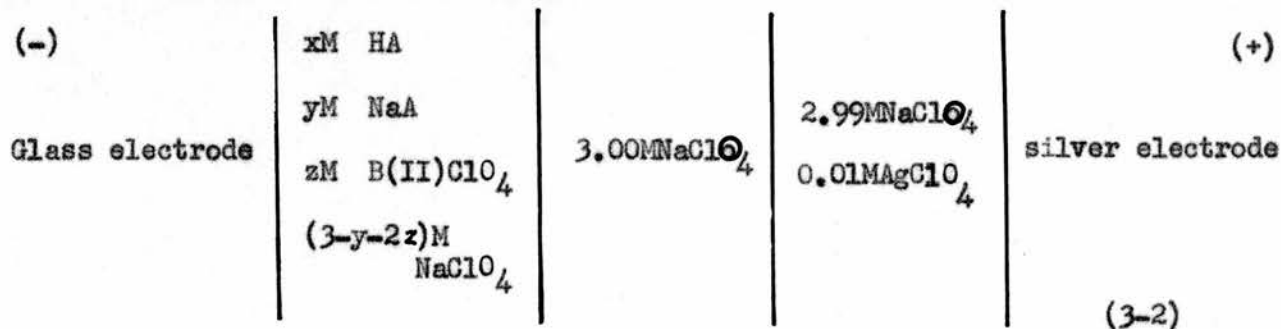


Copper (II) and cadmium (II) perchlorate solutions were prepared as follows:



Thus, in the metal solutions the perchlorate ion concentration was kept constant at 3.00M.

The complete cell used in the potentiometric measurements in aqueous solution was:



## 2. Dioxan-water mixtures.

Dioxan is miscible with water at all concentrations, but the solubility of sodium perchlorate in dioxan is quite low. The solubility of sodium perchlorate in the 50% v/v dioxan-water mixture at 25°C was investigated. It is just possible to prepare a 0.7M solution of sodium perchlorate in the mixture. It was decided, therefore, to use 0.60M sodium perchlorate as the constant ionic medium in the 50% v/v dioxan-water mixture. Thus a typical buffer in this medium had the following composition:

Carboxylic acid	=	xM	) solution S <sub>3</sub>
Sodium carboxylate	=	yM	
Sodium perchlorate	=	(0.60-y)M	
Dioxan comprises 50% by volume			

The complete cell used in the potentiometric measurements in the 50% v/v dioxan-water mixture was thus:

(-)				(+)
	xM HA			
	yM NaA			
Glass electrode	zM B(II)ClO <sub>4</sub>	0.60M NaClO <sub>4</sub>	0.59M NaClO <sub>4</sub>	
	(0.6-y-2z)M NaClO <sub>4</sub>	50% v/v dioxan	0.01M AgClO <sub>4</sub>	silver electrode
	50% v/v dioxan		50% v/v dioxan	
				(3-3)

For the cells (3-2) and (3-3) the relationship between the measured potential  $E$  (in mV) and the concentration,  $h$ , of free hydrogen ions is given by

$$E = E'_0 + E_J - \frac{RT}{F} \ln h - \frac{RT}{F} \ln \gamma_H \quad (3-4)$$

The term  $E'_0$  includes the difference between the standard potentials of the electrodes, and the asymmetry potential of the glass electrode.

$E_J$  is the liquid junction potential.

$R$  is the gas constant.

$T$  is the absolute temperature.

$F$  is the Faraday.

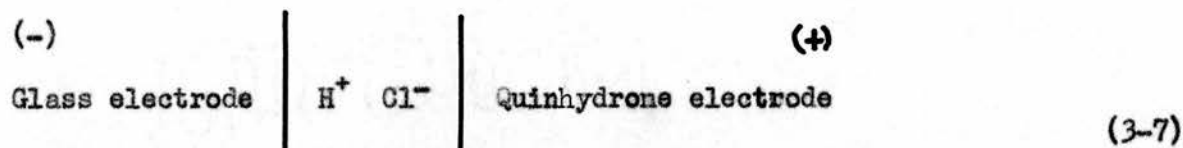
$\gamma_H$  is the activity<sup>COEFFICIENT</sup> of the hydrogen ion.

In a constant ionic medium, concentrations can replace activities and thus at 25°C Eq.(3-4) may be written

$$E = E_0 + E_J - 59.15 \log h \quad (3-5).$$

$$\text{where } E_0 = E'_0 - \frac{RT}{F} \ln \gamma_H \quad (3-6).$$

The range over which Eq.(3-5) was valid for the glass electrode was checked by using the cell



Equation (3-5) is valid for the quinhydrone electrode for  $pH \leq 8$ . Using the subscripts  $g$  and  $q$  to denote glass electrode and quinhydrone electrode, respectively, we have from Eq.(3-5)

$$E_g = E_{0(g)} - 59.15 \log h \quad (3-8)$$

$$E_q = E_{0(q)} - 59.15 \log h \quad (3-9)$$

Combining Eqs. (3-8) and (3-9)

$$E_g - E_q = E_{0(q)} - E_{0(g)} = \text{constant} \quad (3-10)$$

If the glass electrode behaves according to Eq.(3-5), the potentiometer should show a constant reading for acid solutions of  $pH \leq 8$  when both electrodes are connected to it. In this experiment 0.1N hydrochloric acid

in the titration vessel was titrated against 0.1N sodium hydroxide. The reading on the potentiometer remained constant at  $86.8 \pm 0.1$  mV till  $\text{pH} \approx 9$ . Thus the glass electrode was behaving satisfactorily.

Before starting any titration  $E_0$  was found by titrating acid and base of known concentrations. The method of titration varied slightly depending on the type of equilibria under investigation. The  $E_0$  tended to drift slowly from day to day but usually this was not very pronounced. For instance between 11/2/58 and 9/9/58 (93 determinations)  $E_0$  drifted slowly, varying between 258.8 and 261.9 mV.

#### Carboxylic acid equilibria in water.

17.50ml. of a perchloric acid solution of known concentration (usually about 15mM) and 17.50ml of 3.00M sodium perchlorate were mixed and titrated with a sodium hydrogen carbonate solution of known concentration (usually about 100mM). Between 2.00ml and 2.60ml of the sodium hydrogen carbonate was added and readings of the potential taken at 0.40ml increments at first and then at 0.20ml increments. From these measurements  $E_0$  was calculated (see p. 75 ).

Buffer solution  $S_1$  was then added in 0.05ml. or 0.10ml. increments at first, and then in increments such that there was an addition of either 50mM or 100mM of A. Titrations were usually stopped when  $A = 1000$  mM though occasionally some titrations were stopped at lower or higher concentrations.

#### Metal carboxylate equilibria in water.

The method was similar to that above except that metal ions were also present at a constant concentration.

17.50ml. of a perchloric acid solution of known concentration (usually about 15mM) and 17.50ml. of a metal perchlorate solution of known concentration and containing perchloric acid of known concentration (usually about 2mM) were mixed and titrated with sodium hydrogen carbonate of known concentration. The sodium hydrogen carbonate was added in the same increments as above. The metal ion concentration was held constant by adding equal increments of a solution of copper (II) perchlorate twice the concentration of that in the titration vessel. From these measurements  $E_0$  was calculated. The titration was stopped when the pH of the solution was about 1 unit below that of the buffer to be added. This buffer was then added in suitable increments such that E changed by a few mV at a time. Equal increments of the metal perchlorate were added. The titration was stopped when very large increments of buffer produced only small changes in pH or when precipitation occurred.

Measurements in dioxan-water mixture.

The methods used in the dioxan-water mixture were identical ~~to~~ <sup>with</sup> those above except that in order to conserve dioxan, a smaller "Wilhelm" salt bridge and a smaller titration vessel were used. All solutions used contained 50% v/v dioxan. At the start of the  $E_0$  titration, in the case of the carboxylic acid equilibria, the total volume in the titration vessel was either 20.00ml. or 25.00ml. instead of 35.00ml. The concentration of perchloric acid used was between 16mM. and 20mM, 15.00ml. being the usual volume taken. The other 5.00ml. or 10.00ml. was 0.60M sodium perchlorate. The acid was titrated with sodium hydroxide of known concentration (about 100mM.), the alkali being added in 0.20ml. increments up to a total of 2.40-3.00ml.



In the metal carboxylate titrations the initial volume in the titration vessel was 25.00ml. (12.50ml. of perchloric acid of known concentration,  $\sim 16\text{mM.}$ , and 12.50ml. of metal perchlorate containing a known concentration of perchloric acid, 6-10mM.). This solution was titrated with sodium hydroxide of known concentration (about 80mM.), 0.10ml. increments being added up to 1.00ml. The metal concentration was kept constant as before.

Equilibrium was reached in all the potentiometric titrations within the time required for mixing of the solutions (approximately 15 seconds). Potentials remained constant for at least 3 hours. In all these titrations the glass electrode was not removed from the solution between the start of the  $E_0$  titration and the finish of the main titration. Titrations were usually carried out in duplicate.

#### End-point determination.

The equivalence point in a potentiometric acid-base titration was determined in this work by Gran's method <sup>198</sup>. At the start of a titration, the titration vessel contained  $V_A\text{ml.}$  of acid, concentration  $C_H$ , which was to be titrated with alkali, concentration  $C_B$ . Let the amount of alkali added be  $V_B\text{ml.}$  and the equivalence point  $V_E\text{ml.}$  Then at any point during the titration,

$$h = \frac{C_H V_A - C_B V_B}{V_A + V_B} \quad (3-11)$$

At the equivalence point

$$C_H V_A = C_B V_E \quad (3-12)$$

and

$$h = C_B \frac{V_E - V_B}{V_A + V_B} \quad (3-13)$$

Now

$$E = E_0 + E_J - 59.15 \log h \quad (3-5)$$

It has been found<sup>199</sup> that in acid solutions in 3.00M sodium perchlorate

$$E_J = 16.5h \pm 0.5 \text{ mV/mole} \quad (3-14)$$

while the present work has shown that in 0.60M sodium perchlorate in 50% v/v dioxan-water mixture

$$E_J = 26.2h \pm 0.4 \text{ mV/mole} \quad (3-15)$$

$E_J$  is significant, therefore, only at  $\text{pH} < 2$ , and could be neglected in these titrations which were carried out at  $\text{pH} > 2$ .

As  $E_0$  in Eq(3-5) is unknown, an arbitrarily chosen constant  $E_0''$  is substituted. Re-arranging Eq(3-5) we have

$$h = 10^{\frac{E_0'' - E}{59.15}} \quad (3-16)$$

Combining Eqs.(3-13) and (3-16)

$$(V_A + V_B) 10^{\frac{E_0'' - E}{59.15}} = C_B (V_E - V_B) \quad (3-17)$$

Thus a plot of  $(V_A + V_B) 10^{\frac{E_0'' - E}{59.15}}$  against  $V_B$  will give intercept  $V_E$ .

#### Calculation of $E_0$

When both  $C_H$  and  $C_B$  are known,  $E_0$  can be calculated.

Combining Eqs(3-5) and (3-11)

$$E_0 = E + 59.15 \log \left( \frac{V_A C_H - V_B C_B}{V_A + V_B} \right) \quad (3-18)$$

where  $E_J$  is neglected. Thus  $E_0$  can be calculated for each point in the titration. In a titration 10-16 additions of alkali were made and the corresponding values of  $E_0$ , which should be constant during a titration, were averaged. The experimental error in  $E_0$ , calculated by this method, is estimated to be  $\pm 0.2\text{mV}$ . A determination of  $E_0$  is shown below (Table 3-1).

Determination of the concentration of a sodium carboxylate by potentiometric titration.

An example of the determination of the concentration of the stock solution of a sodium carboxylate by potentiometric titration is shown below (Table 3-2). After the determination of  $E_0$ , a known volume of the sodium carboxylate was added to the titration vessel by burette. Perchloric acid of known concentration (about 100mM) was then added in suitable amounts. At the end-point all the sodium carboxylate originally present had been converted to the carboxylic acid. This method can be used for determining the concentration of the sodium carboxylate in the presence or absence of the corresponding carboxylic acid.

We define

$C_{HClO_4}$	the concentration of the perchloric acid solution added to the salt
$C_{HA}$	the concentration of the carboxylic acid in the titration vessel before perchloric acid is added
$C_A$	the concentration of the sodium carboxylate in the titration vessel before perchloric acid is added
$C_H$	the concentration of perchloric acid in the titration vessel at the end of the $E_0$ determination. This concentration is usually very small or negligible.
$V_A$	the volume of perchloric acid added
$V_i$	the initial volume of the titration solution (i.e. before perchloric acid is added).

$V_T$  the total volume of the titration solution.

Then at any point during the titration

$$\bar{n}_H = \frac{(C_{HA} + C'_H) \frac{V_1}{V_T} + C_{HClO_4} \frac{V_A}{V_T} - h}{(C_{HA} + C_A) \frac{V_1}{V_T}} \quad (3-19)$$

$$= \frac{C_{HA} + C'_H + C_{HClO_4} \frac{V_A}{V_1} - h \frac{V_T}{V_1}}{C_{HA} + C_A} \quad (3-20)$$

At the end point  $\bar{n}_H = 1.00$ , whence from Eq.(3-20) (3-20)

$$C_A = C_{HClO_4} \frac{V_A}{V_1} - h \frac{V_T}{V_1} + C'_H \quad (3-21)$$

When all the sodium salt has been neutralised the expression on the right-hand side of Eq.(3-21) reaches a constant value, which is the initial concentration of the sodium carboxylate.

#### Analysis of sodium formate solution.

17.50ml. of 14.62mM perchloric acid and 17.50ml. of 3.00M. sodium perchlorate were run into the titration vessel and titrated with 101.5mM sodium hydrogen carbonate. The Gran diagram is shown in Fig. 3-4 and the calculation of  $E_0$  is shown in Table 3-1.

3.40ml. of stock sodium formate solution, of concentration about 500mM was then added to the titration vessel and titrated with 100.5mM perchloric acid until the expression on the right hand side of Eq.(3-21) reached a constant value (see Table 3-2).

Fig 3.4

# ACID-BASE POTENTIOMETRIC TITRATION

Determination of the end-point by Gran's method

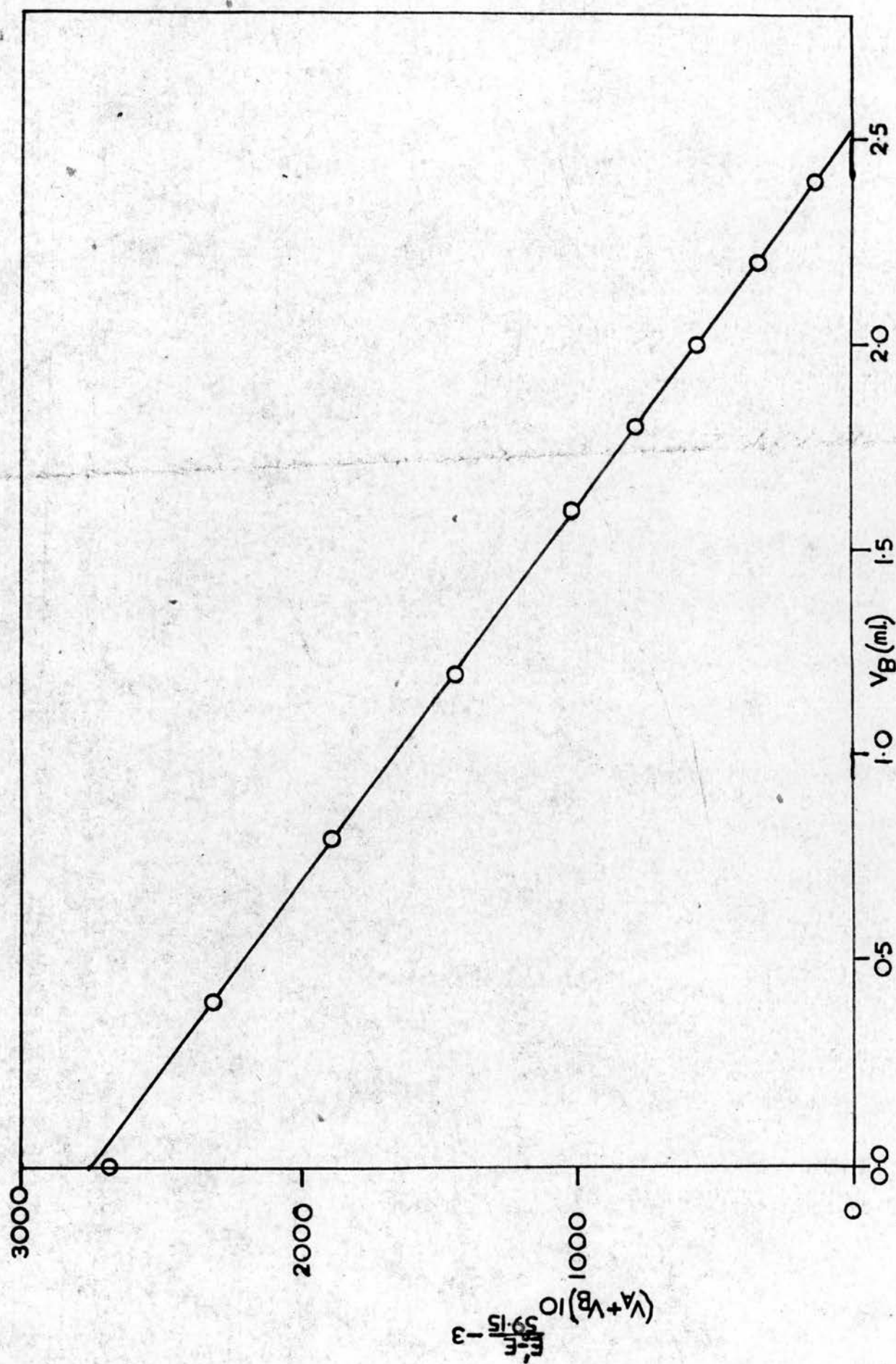


TABLE 3-1

Determination of  $E_0$ The arbitrary constant  $E_0'' = 500$  $C_H = 14.62\text{mM}$  $C_B = 101.5\text{mM}$ 

$V_B$	$V_T$	$E$	$E_0'' - E$	$\frac{E_0'' - E}{59.15} - 3$	$V_C - V_B C_B$	$3 + \log h$	$59.15(3 + \log h)$	$E_0$
ml.	ml.	mV		$(V_A + V_B)10$				
0.00	35.00	211.0	289.0	2686	0.2559	0.8639	51.11	262.1
0.40	35.40	215.2	284.8	2308	0.2152	0.7839	46.38	261.6
0.80	35.80	220.8	279.2	1881	0.1746	0.6882	40.71	261.5
1.20	36.20	227.9	272.1	1439	0.1340	0.5685	33.63	261.5
1.60	36.60	237.2	262.8	1014	0.09341	0.4068	24.07	261.3
1.80	36.80	243.9	256.1	784.7	0.07310	0.2981	17.64	261.5
2.00	37.00	252.2	247.8	571.2	0.05280	0.1544	9.13	261.3
2.20	37.20	265.1	234.9	347.6	0.03249	-0.0588	- 3.48	261.6
2.40	37.40	290.2	209.8	131.6	0.01218	-0.4872	-28.82	261.4
2.60	37.60	623.1						

Average  $E_0 = 261.5 \pm 0.3$ 

The use of  $(3 + \log h)$  in columns 7 and 8 of Table 3-1 is for convenience.

The units of  $h$  have been changed from moles to millimoles, the latter being more convenient to use when small concentrations of  $h$  are

involved. Thus whenever Eq(3-5) has been used in this work, the values of  $E$ ,  $E_0$ , and  $E_J$  have been expressed in mV, and the values of  $h$  in mM.



TABLE 3-2

Sodium formate titration

$$C_{\text{HClO}_4} = 100.5 \text{ mM}$$

$$E_0 = 261.5$$

$V_A$ mL	$V_T$ mL	$E$ mV	pH	$h$ mm	$h$ $\frac{V_T}{V_A}$	$C_{\text{HClO}_4/V_A}$	LHS Eq(3-21)	$\bar{n}_H$
-	37.60	623.1		End of $E_0$ titration				
5.00	41.00	505.2	7.119	0.00008	0.0567	3.40mL sodium formate added	12.20	0.294
10.00	46.00	338.2	4.297	0.0505	0.215	12.259	24.30	0.586
15.00	51.00	306.6	3.762	0.173	1.020	24.517	35.76	0.862
16.00	56.00	269.0	3.127	0.747	1.595	36.776	37.63	0.907
17.00	57.00	258.0	2.941	1.147	2.586	39.227	39.09	0.942
17.50	58.00	246.0	2.738	1.828	3.307	41.679	39.60	0.954
18.00	58.50	239.9	2.635	2.318	4.165	42.905	39.97	0.963
18.50	59.00	234.2	2.539	2.894	5.062	44.131	40.29	0.971
19.00	59.50	229.4	2.457	3.488	6.035	45.357	40.55	0.977
19.50	60.00	225.1	2.385	4.124	7.139	46.582	40.67	0.980
20.00	60.50	221.0	2.315	4.838	8.152	47.808	40.88	0.985
20.50	61.00	217.8	2.261	5.479	9.237	49.034	41.02	0.988
21.00	61.50	214.8	2.211	6.158	10.383	50.260	41.10	0.990
21.50	62.00	212.0	2.163	6.866	11.537	51.486	41.18	0.992
22.00	62.50	209.5	2.121	7.568	12.669	52.712	41.27	0.994
22.50	63.00	207.3	2.084	8.245	14.921	53.938	41.47	0.999
23.00	64.00	203.5	2.020	9.559	17.36	56.389	41.48	0.999
24.00	65.00	200.0	1.960	10.95	19.75	58.841	41.54	1.001
25.00	66.00	197.1	1.911	12.27	22.26	61.293	41.49	1.000
26.00	67.00	194.4	1.866	13.62	24.70	63.744	41.50	1.000
27.00	68.00	192.1	1.827	14.89	27.10	66.196	41.55	1.001
28.00	69.00	190.1	1.793	16.10		68.648		

The last six values in the L.H.S. Eq(3-21) column were considered constant and the average value is 41.505. Using this figure, the values of  $\pi_H$  in the last column of the table were calculated.

SECTION 4

CARBOXYLIC ACID EQUILIBRIA IN WATER

4(a) POTENTIOMETRIC TITRATION RESULTS.

It was soon evident from preliminary studies that the potential of a glass electrode immersed in a particular carboxylate buffer was not constant but was a function of the total carboxylate concentration. This effect might be caused by any one or a combination of three factors viz:

- (1) a liquid junction potential between the solution in the titration vessel, which was 3.00M with respect to sodium ions and to (perchlorate + carboxylate) ions, and the solution in the J- tube of the salt bridge which was 3.00M with respect to both sodium and perchlorate ions.
- (2) a variation in activity coefficients during the partial exchange of perchlorate for carboxylate ions.
- (3) a real variation in hydrogen ion concentration.

It is considered that (1) and (2) are not major factors in the variation of the potential for the reasons outlined below.

The well-known equation for the liquid junction potential derived by Henderson has been put into a convenient form by Büchi<sup>200</sup>.

$$E_J = - \frac{RT}{F} \frac{D'' - D'}{L'' - L'} \ln \frac{L'}{L''} \quad (4-1)$$

$$\text{where } D = \sum (C_1 l_1)_{\text{cations}} - \sum (C_1 l_1)_{\text{anions}}$$

$$L = \sum (C_1 Z_1 l_1)_{\text{cations}} + \sum (C_1 / Z_1 / l_1)_{\text{anions}}$$

$$C_1 = \text{molar concentration}$$

$$l_1 = \text{ionic conductivity}$$

$$Z_1 = \text{ionic charge}$$

The superscripts ' and '' refer to the solution nearer the negative and positive poles of the cell, respectively. For the cell (3-2) used in this work,

$$D'' \sim 3l_{Na^+} - 3l_{ClO_4^-}$$

$$D' \sim 3l_{Na^+} - (3-C_A)l_{ClO_4^-} - C_A l_{A^-}$$

$$L'' \sim 3l_{Na^+} + 3l_{ClO_4^-}$$

$$L' \sim 3l_{Na^+} + (3-C_A)l_{ClO_4^-} + C_A l_{A^-}$$

$$\text{where } C_A = [NaA]$$

Terms in  $h$  may be neglected as  $h \leq 10^{-3}M$ .

At best Henderson's equation is only approximate and calculated potentials cannot be used to correct experimental results accurately. Moreover the values obtained for  $E_j$  from Eq(4-1) using limiting conductivities are different in both magnitude and sign from those obtained using values of the conductivities appropriate to the concentrations of the constituents. For example, in a formate buffer of  $\pi_H = 0.05$ , at  $A = 1000mM$  the calculated liquid junction potential is  $+0.9mV$  using limiting conductivities and  $-4.4mV$  using the conductivities for this concentration. In a similar acetate buffer at  $A = 1000mM$  the values are  $+1.9mV$  and  $-2.3mV$  respectively<sup>201</sup>. These values correspond to an experimentally observed change in potential of about  $+8mV$ . It would seem more correct to use the conductivities appropriate to the concentrations of the constituents in the solutions rather than the limiting conductivities. Thus although there is the possibility of a liquid junction potential occurring, it appears to differ in both magnitude and sign from the experimentally observed potential change.

In addition, the variation of potential with total acetate concentration in a  $3.00M$  sodium perchlorate medium is larger than Sundén<sup>202</sup> and Sonesson<sup>203</sup> found for a  $2.00M$  medium and larger still than

Fronaeus<sup>163</sup> and Ahrlund<sup>204</sup> found for a 1.00M sodium perchlorate medium. If the effect were caused by a liquid junction potential it would be expected to be smallest in 3.00M sodium perchlorate and largest in 1.00M sodium perchlorate.

A rough calculation based on Harned's rule<sup>205</sup>, and the fact that not only the magnitude but also the sign of the variation in potential depends on the ratio of acid to salt in the buffer, indicate that the possibility of serious variations in the activity coefficients can be discounted. Harned's rule states that the logarithm of the activity coefficient of one electrolyte in a mixture of constant total molality is directly proportional to the molality of the other component, thus

$$\log \gamma_B = \log \gamma_B^0 - \alpha_B m_C \quad (4-2)$$

where  $\gamma_B$  = activity coefficient of electrolyte B.

$\gamma_B^0$  = molal activity coefficient of electrolyte B in a solution containing only B.

$\alpha_B$  = the slope of the plot of  $\log \gamma_B$  against molality of B at constant total molality.

$m_C$  = molality of electrolyte C.

In the present case,  $\gamma_H$ , the activity coefficient of the hydrogen ion in the ionic medium is being considered. By a readily justifiable extension of Harned's rule

$$\log \gamma_H = \log \gamma_H^0 - \alpha_{H,ClO_4} m_{ClO_4} - \alpha_{H,A} m_A \quad (4-3)$$

at constant ionic strength.

Then for 3.00M sodium perchlorate

$$\log \gamma_H = \log \gamma_H^0 - 3\alpha_{H,ClO_4} \quad (4-4)$$



and for a solution containing 2.00M sodium perchlorate and 1.00M sodium acetate,

$$\log \gamma_H = \log \gamma_H^0 - 2 \alpha_{H,ClO_4} - 1 \alpha_{H,A} \quad (4-5)$$

Subtracting Eq. (4-5) from Eq. (4-4)

$$\Delta \log \gamma_H = -\alpha_{H,ClO_4} + \alpha_{H,A} \quad (4-6)$$

where  $\Delta \log \gamma_H$  is the change in the logarithm of the hydrogen ion activity coefficient during a titration in which the initial and final solutions are 3.00M sodium perchlorate, and 2.00M sodium perchlorate + 1.00M sodium acetate respectively. The values of  $\alpha$  may be calculated using a relationship developed by Guggenheim<sup>206</sup> which for electrolytes of the same charge type takes the form

$$\alpha_{1,2^m} = 0.5 (\log \gamma_1^0 + \log \gamma_2^0) \quad (4-7)$$

where the subscripts 1, 2 are the ions of the electrolyte.

Thus for a 3.00M medium

$$\alpha_{1,2} = 0.167 (\log \gamma_1^0 + \log \gamma_2^0) \quad (4-7a)$$

Combining Eqs. (4-6) and (4-7a) we have

$$\begin{aligned} \Delta \log \gamma_H &= 0.167 (\log \gamma_A^0 - \log \gamma_{ClO_4}^0) \\ &= 0.167 (0.206) \\ &= 0.0344 \end{aligned} \quad (4-7b)$$

This value corresponds to an 8% change in  $\gamma_H$  or a change of potential of +2.0mV, which is much smaller than the change observed experimentally. It is of the same magnitude, but opposite in sign, to the value of the liquid junction potential calculated using the conductivities for the concentrations of the constituents. Thus if there is both a liquid junction potential and a variation in activity coefficients, the resultant changes in potential from these two effects will almost cancel leaving a

small net change. Similar results are obtained when these calculations are extended to the other three acids studied.

Therefore, as a working hypothesis, the observed variation in potential has been ascribed entirely to a real variation in  $h$  caused by polynuclear complex formation.

For each system  $\bar{n}_H$  was calculated at values of  $A$  up to  $A = 1000\text{mM}$  and on occasion at higher values of  $A$ . By definition,  $\bar{n}_H$  is the average number of protons bound to each carboxylate ion and it is calculated using Eq.(1-6). (The term  $K_W h^{-1}$  is negligible in the concentration range studied). Values of  $H$  and  $A$  are known from the previously determined concentrations of the acid and of the stock solution of the sodium salt. From the measurement of  $E$ ,  $h$  was calculated using Eq.(3-5).  
Acetic acid.

Table 4-1A shows the full experimental data for a typical titration of an acetate buffer. Tables 4-1B and 4-1C contain a selection of the experimental data  $(\bar{n}_H, \log h)_A$  for acetic acid obtained from the duplicated potentiometric titrations of the acetate buffers. The values of  $\log h$  and  $\bar{n}_H$  were calculated using Eqs(3-5) and (1-6) respectively. The results for  $A \leq 100\text{mM}$  are in Table 4-1B and the results for  $A \gg 100\text{mM}$  are in Table 4-1C. The experimental data  $(\bar{n}_H, \log h)_A$  at  $A = 10\text{ mM}$  and  $1000\text{mM}$  are plotted in Fig. 4.2

TABLE 4-1A

Titration of an acetate buffer.

17.50ml. of 14.85mM perchloric acid and 17.50ml. of 3.00M sodium perchlorate were mixed in the titration vessel and titrated with 101.5mM sodium hydrogen carbonate. The end-point in this titration

was 2.56ml of sodium hydrogen carbonate. The total amount of sodium hydrogen carbonate added in small increments was 2.50ml., and  $E_0$  was calculated from this titration. Suitable increments of a buffer with composition 1.996M sodium acetate +1.951M acetic acid were added. All solutions used had  $[Na^+]$  made up to 3.00M with sodium perchlorate.

$E_0 = 261.4mV$ .  $C'_H$  = residual perchloric acid left from the preliminary acid-base titration.

Volume of Buffer (ml.)	Total volume (ml.)	$C_A$ mM	$C_{HA}$ mM	A mM	$C'_H$ mM	E mV	pH	h mM	$\bar{H}H$
0.00	37.50	-	-	-	0.162	307.2	3.774	0.168	-
0.10	37.60	5.307	5.188	10.50	0.162	379.9	5.003	0.010	0.509
0.30	37.80	15.84	15.48	31.32	0.161	381.4	5.028	0.009	0.499
0.50	38.00	26.26	25.67	51.93	0.160	381.4	5.028	0.009	0.497
0.70	38.20	36.57	35.75	72.32	0.16	381.4	5.028	0.009	0.496
0.95	38.45	49.31	48.20	97.51	0.16	381.8	5.035	0.009	0.496
2.00	39.50	101.0	98.77	199.8	0.15	382.1	5.040	0.009	0.495
3.10	40.60	152.4	149.0	301.4	0.15	382.7	5.050	0.009	0.495
4.25	41.75	203.1	198.6	401.7	0.15	383.1	5.057	0.009	0.495
5.45	42.95	253.2	247.6	500.8	0.14	383.5	5.064	0.009	0.495
6.75	44.25	304.4	297.6	602.0	0.14	383.9	5.071	0.008	0.495
8.10	45.60	354.5	346.5	701.0	0.13	384.3	5.077	0.008	0.495
9.55	47.05	405.1	396.0	801.1	0.13	384.8	5.086	0.008	0.495
11.10	48.60	455.8	445.6	901.4	0.13	385.1	5.091	0.008	0.494
12.75	50.25	506.4	495.0	1001.4	0.12	385.5	5.098	0.008	0.494

TABLE 4-1B

Acetic acid

Experimental data ( $\bar{n}_H$ , logh)<sub>A</sub> obtained from potentiometric titrations of acetate buffers at  $A \leq 100\text{mM}$ . Duplicate titrations have not been tabulated.

Buffer	1			2			3			4			5		
[HA] mM	161.6			279.9			542.2			997.5			1474		
[NaA] mM	3000			2760			2759			2998			2995		
	A	$\bar{n}_H$	pH	A	$\bar{n}_H$	pH	A	$\bar{n}_H$	pH	A	$\bar{n}_H$	pH	A	$\bar{n}_H$	pH
	8.397	0.057	6.225	12.09	0.091	5.975	8.767	0.163	5.696	10.60	0.239	5.507	11.85	0.317	5.336
	12.58	0.055	6.244	16.10	0.091	5.985	17.49	0.164	5.711	21.14	0.244	5.507	23.64	0.323	5.336
	16.75	0.054	6.256	20.10	0.092	5.992	21.83	0.164	5.711	31.63	0.246	5.507	35.37	0.326	5.336
	20.91	0.053	6.271	24.09	0.092	5.997	26.16	0.164	5.713	42.06	0.247	5.507	58.64	0.327	5.336
	25.06	0.053	6.271	28.07	0.092	5.999	30.48	0.164	5.713	98.46	0.249	5.509	98.79	0.328	5.339
	33.32	0.052	6.271	32.04	0.092	5.999	34.79	0.164	5.713						
	41.55	0.052	6.271	35.99	0.092	5.999	102.2	0.164	5.728						
	101.9	0.052	6.288	101.7	0.092	6.017									
Buffer	6			7			8			9			10		
[HA] mM	1951			3999			5344			7461			9820		
[NaA] mM	1996			1341			1152			759.0			499.9		
	A	$\bar{n}_H$	pH	A	$\bar{n}_H$	pH	A	$\bar{n}_H$	pH	A	$\bar{n}_H$	pH	A	$\bar{n}_H$	pH
	10.50	0.509	5.003	14.20	0.760	4.531	8.650	0.836	4.308	11.24	0.896	4.072	13.74	0.949	3.751
	31.32	0.499	5.028	28.33	0.756	4.545	17.28	0.830	4.351	22.46	0.901	4.024	27.45	0.950	3.725
	51.93	0.497	5.028	42.38	0.753	4.547	34.46	0.826	4.351	33.64	0.903	4.019	41.11	0.951	3.725
	72.32	0.496	5.028	56.36	0.752	4.547	51.56	0.825	4.351	44.80	0.905	4.019	54.75	0.951	3.725
	97.51	0.496	5.035	70.26	0.751	4.547	102.3	0.824	4.351	67.01	0.906	4.019	68.34	0.951	3.725
				97.85	0.750	4.548				100.01	0.906	4.019	81.90	0.951	3.724
													95.43	0.951	3.722



TABLE 4-1C

Acetic acid

Experimental data ( $\bar{n}_H$ , logh)<sub>A</sub> obtained from potentiometric titrations of acetate buffers at A  $\geq$  100mM. Duplicate titrations have not been tabulated.

Buffer		1			2			3			4			5		
[HA] mM	[NaA] mM	161.6 3000			279.9 2760			542.2 2759			997.5 2998			1474 2995		
A		$\bar{n}_H$	pH	A	$\bar{n}_H$	pH		A	$\bar{n}_H$	pH	A	$\bar{n}_H$	pH	A	$\bar{n}_H$	pH
101.9		0.052	6.288	101.7	0.092	6.017		102.2	0.164	5.728	98.46	0.250	5.509	98.79	0.328	5.339
201.1		0.051	6.305	200.4	0.092	6.033		202.2	0.164	5.743	201.8	0.250	5.520	198.7	0.329	5.346
300.9		0.051	6.320	299.2	0.092	6.044		299.7	0.164	5.759	299.8	0.250	5.527	299.4	0.329	5.356
400.7		0.051	6.335	400.6	0.092	6.058		401.5	0.164	5.769	401.5	0.250	5.541	400.3	0.329	5.367
499.8		0.051	6.349	500.4	0.092	6.070		502.9	0.164	5.781	501.8	0.250	5.554	501.2	0.329	5.377
600.3		0.051	6.359	600.7	0.092	6.085		600.5	0.164	5.794	600.4	0.250	5.563	601.6	0.330	5.387
701.1		0.051	6.374	700.7	0.092	6.100		699.6	0.164	5.806	701.0	0.250	5.576	701.4	0.330	5.395
799.1		0.051	6.386	798.4	0.092	6.110		799.4	0.164	5.816	799.1	0.250	5.588	800.1	0.330	5.407
900.3		0.051	6.396	900.2	0.092	6.122		901.1	0.164	5.830	901.2	0.250	5.596	901.3	0.330	5.419
1001.1		0.051	6.409	999.6	0.092	6.134		1001.2	0.164	5.841	1002.9	0.250	5.608	1000.7	0.330	5.426
														1027	0.330	5.427
														1174	0.330	5.443
														1309	0.330	5.458
														1472	0.330	5.475

Buffer		6			7			8			9			10		
[HA] mM	[NaA] mM	1951 1996			3999 1341			5344 1152			7461 759.0			9820 499.9		
A		$\bar{n}_H$	pH	A	$\bar{n}_H$	pH		A	$\bar{n}_H$	pH	A	$\bar{n}_H$	pH	A	$\bar{n}_H$	pH
97.51		0.496	5.035	97.85	0.750	4.548		102.3	0.824	4.351	100.1	0.906	4.019	95.43	0.951	3.722
199.8		0.495	5.040	198.8	0.750	4.550		201.4	0.823	4.351	208.5	0.907	4.019	202.4	0.951	3.718
301.3		0.495	5.050	302.3	0.750	4.552		297.5	0.823	4.351	303.6	0.907	4.019	294.1	0.951	3.715
401.7		0.495	5.057	401.6	0.749	4.555		398.4	0.823	4.351	396.5	0.907	4.019	396.9	0.951	3.712
500.8		0.495	5.064	503.0	0.749	4.560		496.0	0.823	4.351	507.2	0.907	4.019	497.7	0.951	3.708
602.0		0.495	5.071	600.3	0.749	4.564		597.7	0.823	4.352	605.0	0.907	4.018	596.4	0.951	3.707
701.0		0.495	5.077	699.2	0.749	4.565		702.9	0.823	4.354	700.5	0.907	4.014	693.1	0.952	3.705
801.0		0.495	5.086	799.1	0.749	4.567		797.7	0.823	4.356	793.5	0.907	4.011	799.7	0.952	3.703
901.4		0.494	5.091	899.8	0.749	4.569		902.4	0.823	4.357	902.2	0.908	4.007	892.5	0.952	3.702
1001.3		0.494	5.098	1000.9	0.749	4.570		1003.3	0.823	4.359	1007.7	0.908	4.006	994.7	0.952	3.700
								1457	0.823	4.361						
								1493	0.823	4.361						
								1817	0.823	4.363						
								2232	0.823	4.366						

TABLE 4-1D

Acetic Acid

Values of  $\log \beta''^H$  calculated from the pH of buffers at  $A \leq 50\text{mM}$  using Eq. (4-8).

Buffer	$\log \beta''^H$	Buffer	$\log \beta''^H$
1	5.002	6	5.018
2	5.004	7	5.021
3	5.006	8	5.016
4	5.024	9	5.012
5	5.024	10	5.018

Calculation of the acid association constant  $\beta''^H$

The value of  $\beta''^H$  has been calculated in five ways.

(1) Bjerrum's "half -  $\bar{n}$ " method has been applied to Fig. 4-1 for  $A \leq 10\text{mM}$  by the method described in Sec. 2, p. 33. The value obtained is  $\log \beta''^H = 5.018$ .

(2) The curve ( $\bar{n}_H$ , logh) for  $A = 10\text{mM}$  fits exactly the normalised curve for a single complex, Eq. (2-7), as shown in Fig. 4-1. From Eq (2-8),  $\log \beta''^H = 5.018 \pm 0.004$ .

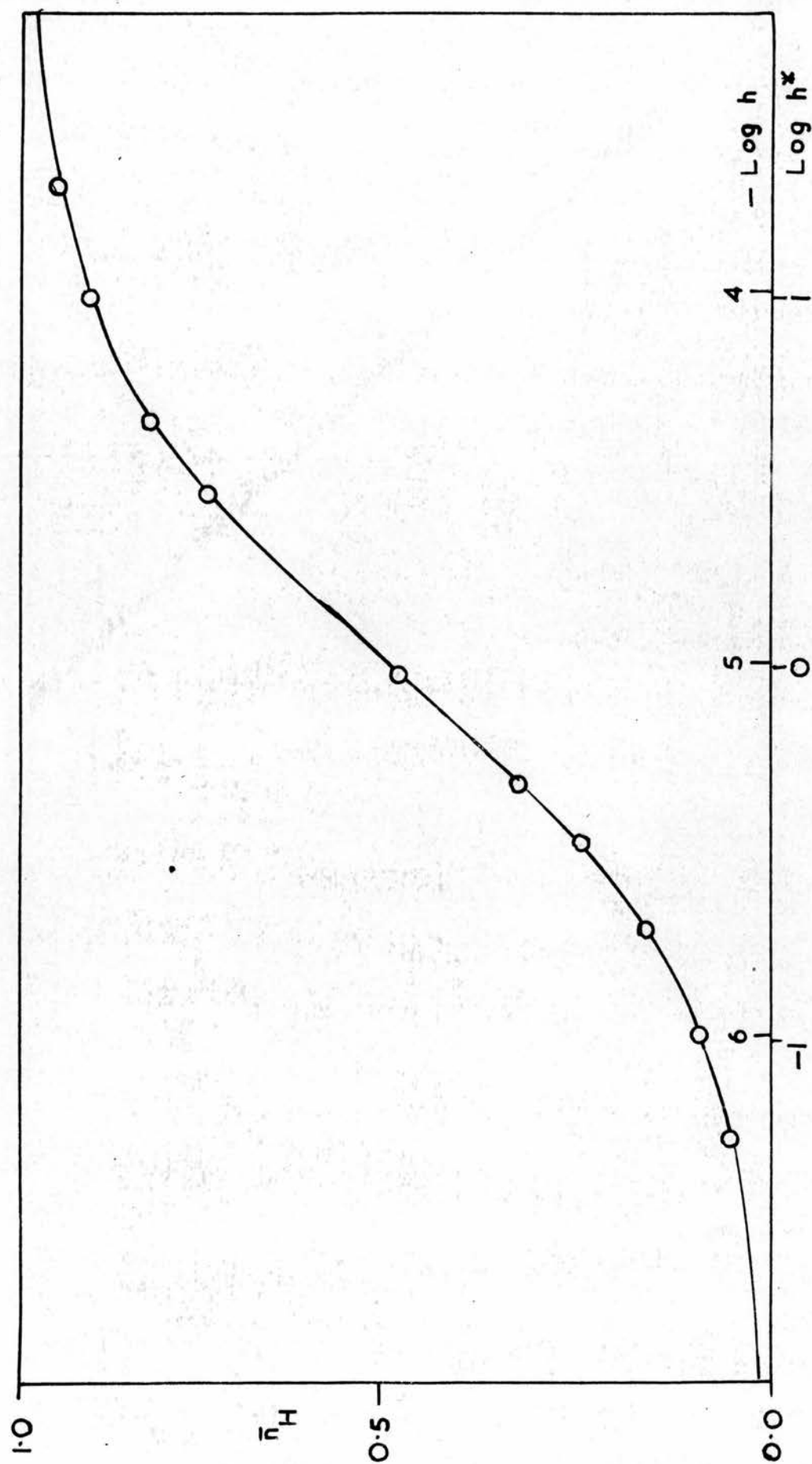
(3) In tables 4-1B and 4-1C it can be seen that at low concentrations of  $A$ , the values of  $\bar{n}_H$  and pH vary slightly but as the concentration increases the values become constant. Finally the pH varies once more and is a function of the total carboxylate concentration. The initial slight variation is caused by the residual acid or alkali from the acid-base titration for the determination of  $E_0$ . This acid or base residual concentration is very small but nevertheless affects the pH of a buffered solution at low values of  $C_{HA}$  and  $A$ . However, its effect usually becomes negligible at  $A > 100\text{mM}$ .



Fig 4.1

ACETIC ACID

Mononuclear Formation Curve



Where the pH of the buffer is constant at low concentrations of A, it is possible to calculate  $\log \beta_{II}^H$  from the well-known equation,

$$pH = \log \beta_{II}^H + \log \frac{[\text{salt}] + h}{[\text{acid}] - h} \quad (4-8)$$

The values of  $\log \beta_{II}^H$ , calculated for  $A \leq 50\text{mM}$  in the 10 buffers in Table 4-1B are shown in Table 4-1D. The average value of  $\log \beta_{II}^H$  is  $5.014 \pm 0.009$ .

(4) The pH of the acetate buffers examined remains constant at least up to  $A = 50\text{mM}$ . Therefore for  $A \leq 50\text{mM}$  it appears that only the species HA is present and the value of  $\beta_{II}^H$  can be calculated by rearranging Eq (1-9).

Putting  $P = 1$ ,  $Q = 1$ , we have

$$\bar{n}_H = \frac{\beta_{II}^H h a}{a (1 + \beta_{II}^H h)}$$

whence

$$\beta_{II}^H = \frac{\bar{n}_H}{(1 - \bar{n}_H)h} \quad (1-9a)$$

The experimental data at  $A \leq 50\text{mM}$  were substituted in this equation and the average of 51 results is  $\log \beta_{II}^H = 5.012 \pm 0.014$ .

(5) The experimental data  $\log A(\log h)\bar{n}_H$  were fitted to a family of normalised curves  $\log A^* (\log h^*)_{\bar{n}_H, R}$  (see below). The value of  $\log \beta_{II}^H$  obtained is  $5.01 \pm 0.005$ .

The preferred value of  $\log \beta_{II}^H$  is that obtained by method (3), i.e.  $5.014 \pm 0.009$ .

Analysis of the experimental data when  $A \gg 50\text{mM}$ .

In Tables 4-1B and 4-1C it can be seen that for  $50\text{mM} \leq A \leq 1000\text{mM}$  the pH of a buffer varies with the concentration. The curves  $(\bar{n}_H, \log h)_A$  for  $A > 50\text{mM}$  in Fig. 42 deviate from the mononuclear curve and this indicates that there is polynuclear complex formation. Some idea of the type or types of polynuclear species formed can be gained from the intersection point of the functions  $(\bar{n}_H, \log h)_A$ , cf. Fig. 42. This point is at  $\bar{n}_H = 0.855 \pm 0.005$  and all the curves intersect within these limits. Intersection points have been noted in similar functions for some inorganic polyacids 187, 207, 208.

Suppose several polynuclear species  $H_pA_Q$  are formed, where  $P \gg 1$ ,  $Q \gg 1$ . It has been shown 179 that if all the curves  $(\bar{n}_H, \log h)_A$  intersect at a unique point  $(\bar{n}_C, h_C)$ , then  $\bar{n}$  must be independent of  $A$  at that point. Further if  $Q$  has only two values  $Q'$  and  $Q''$ , and  $\bar{n}_{Q'}$ ,  $\bar{n}_{Q''}$  are the average number of protons for all species,  $H_pA_{Q'}$  and  $H_pA_{Q''}$ , containing carboxylate ions, then there will be a point of intersection where

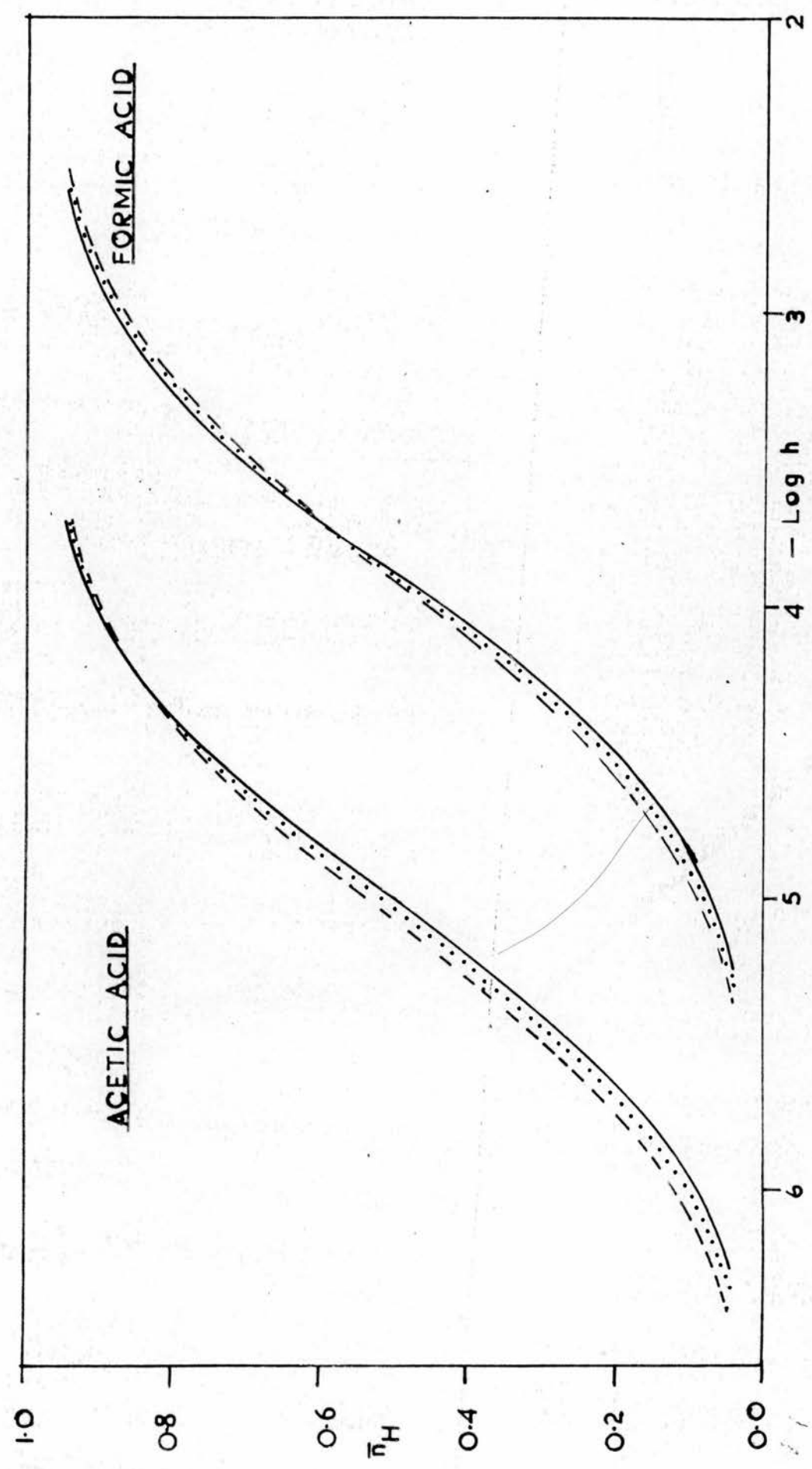
$$\bar{n}_C = \bar{n}_{Q'} = \bar{n}_{Q''}$$

If  $Q$  has more than two values it seems unlikely that all the functions  $(\bar{n}_H, \log h)_A$  will intersect at the same point. However Byé<sup>209</sup> has suggested that the curves might intersect within a very small range of values of  $h$  indistinguishable experimentally from a single point. Carpeni believed that the intersection point indicated an equilibrium between two polynuclear species only, rather than equilibria between species of two different degrees of condensation 207, 208. Therefore he termed the point  $(\bar{n}_C, h_C)$  the isohydric point.

Fig 4.2

Formation Curves for  $A=10\text{mM}$  and  $1000\text{mM}$

— 10mM      ..... 500mM  
- - - 1000mM



In the acetic acid system, stepwise formation of complexes higher than HA will lead first to  $H_2A$  or  $HA_2$ . Under the experimental conditions used in this work, the formation of  $H_2A$  would lead to a value of  $\bar{n}_H > 1$  unless  $\beta_{21}^H \gg \beta_{11}^H$ . In the latter case the formation curve would be "stepped" with a plateau at  $\bar{n}_H = 1$ <sup>183</sup>. In this work the value of  $\bar{n}_H$  tends to a maximum of unity and therefore the formation of  $H_2A$  appears unlikely. However, the formation of  $HA_2$  is much more feasible. If HA and  $HA_2$  were the only species formed in the system then the isohydric point would be  $\bar{n}_C = 0.50$ . On the other hand if the only species formed were HA and  $H_2A_2$  then the curves would be more nearly parallel and would coalesce at  $\bar{n}_H = 1$ . Acetic acid has an isohydric point at  $\bar{n}_H = 0.855$  and therefore the working hypothesis adopted was that both  $HA_2$  and  $H_2A_2$  are formed in addition to HA. Therefore at the isohydric point

$$\bar{n}_C = \bar{n}_1 = \frac{\beta_{11}^H h}{1 + \beta_{11}^H h} \quad (4-9)$$

whence

$$h = \frac{\bar{n}_C}{(1 - \bar{n}_C) \beta_{11}^H} \quad (4-10)$$

and

$$\bar{n}_C = \bar{n}_2 = \frac{\beta_{12}^H + 2\beta_{22}^H h}{2\beta_{12}^H + 2\beta_{22}^H h} \quad (4-11)$$

Substituting Eq(4-10) in Eq(4-11)

$$(2\bar{n}_C - 1) = \frac{2\bar{n}_C \cdot \beta_{22}^H}{\beta_{11}^H \cdot \beta_{12}^H} \quad (4-12)$$

$$\text{Setting } R = \frac{\beta_{22}^H}{\beta_{12}^H \beta_{12}^H} \quad (2-28)$$

and substituting in Eq(4-12)

$$R = \frac{2\bar{n}_G - 1}{2\bar{n}_G} \quad (4-13)$$

The values of  $\beta_{12}^H$  and  $\beta_{22}^H$  were obtained using the family of normalised curves, described in Sec. 2(b), Eq(2-23). It can be seen that various values of R do not have to be substituted in an attempt to find the family of curves which fits the data best since R can be found from the isohydric point. In acetic acid  $\bar{n}_G = 0.855$  and  $R = 0.415$ . The family of curves  $\log A^*(\log h^*)_{\bar{n}_H, R}$  with  $R = 0.415$  is shown in Fig.4.3 with the experimental data,  $\log A(\log h)_{\bar{n}_H}$ , represented by circles, superimposed in the position of best fit. Up to the limit of experimental measurements, the data fit the normalised curves with high precision.

In the position of best fit, when  $(\log A^*, \log h^*) = (0, 0)$ ,  $(\log A, \log h) = (0.34 \pm 0.03, -5.01 \pm 0.005)$ . Whence, using Eqs (2-24), (2-25), and (2-28),

$$\log \beta_{11}^H = 5.01 \pm 0.005$$

$$\log \beta_{12}^H = 4.67 \pm 0.03$$

$$\log \beta_{22}^H = 9.30 \pm 0.03$$

It is now possible to calculate the equilibrium constants for the following reactions,



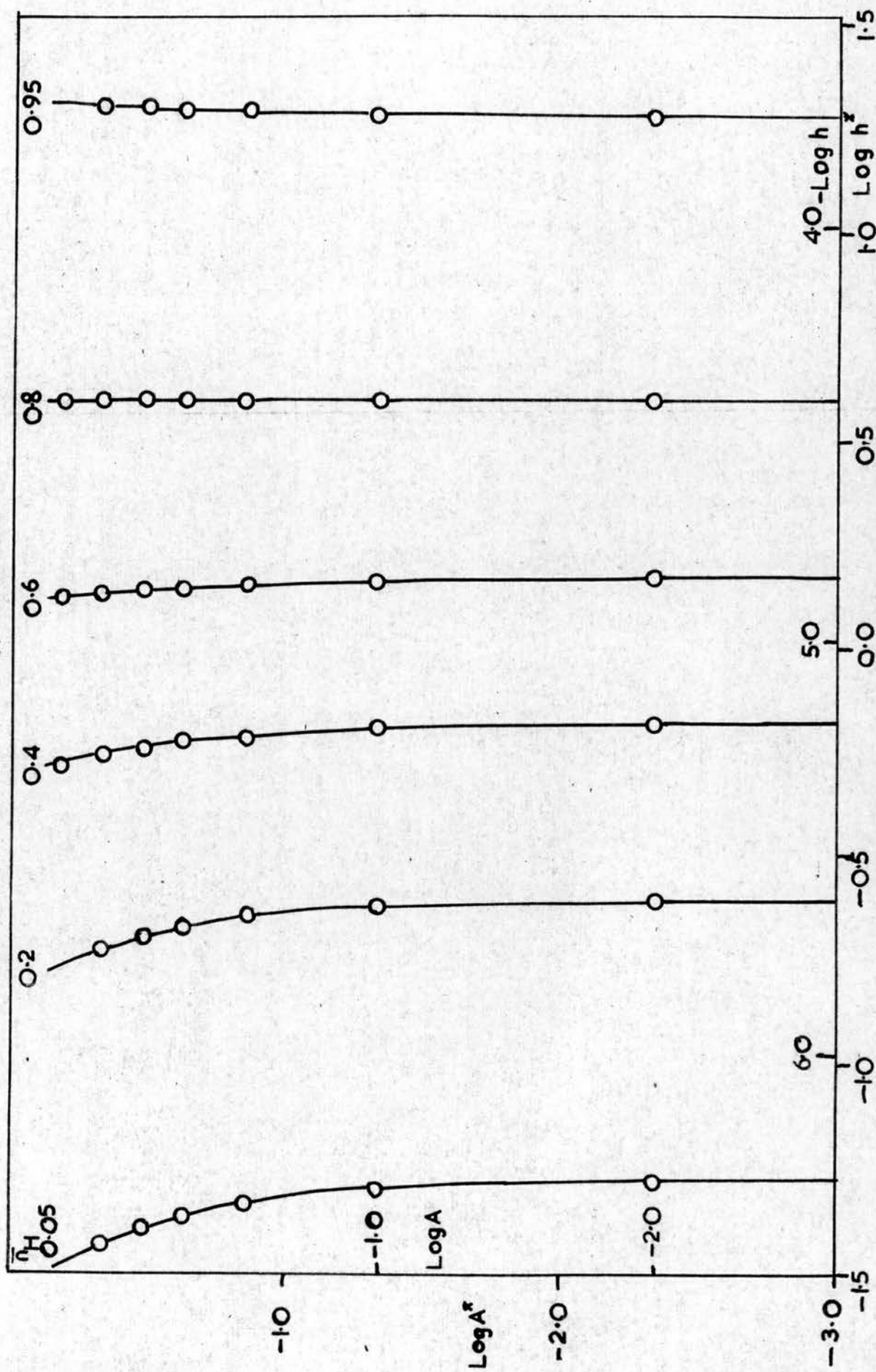


Fig 4.3

ACETIC ACID

○ Experimental Data  $\log A(\log h)_{\bar{n}_H}$

— Normalised curves  $\log A^*(\log h^*)_{\bar{n}_H, R=0.415}$ , calculated using Eq.(2-23).



$$\log K_{12} = \log \beta_2^H - \log \beta_{11}^H - \log A (\log A^* = 0, \log h^* = 0) = -0.34 \pm 0.03$$

$$\log K_{22} = \log \beta_{22}^H - \log \beta_{12}^H = \log R + \log \beta_{11}^H = 4.63 \pm 0.01$$

$$\log K_D = \log \beta_{22}^H - 2 \log \beta_{11}^H = -0.73 \pm 0.03.$$

An attempt was made to fit the experimental data to the combination of species, HA, HA<sub>2</sub>, H<sub>2</sub>A<sub>3</sub>, [Sec. 2(b), Eq(2-44)], and to the combination HA, HA<sub>2</sub>, HA<sub>3</sub>, [Sec. 2(b), Eq(2-52)]. The experimental data fit the families of normalised curves for these combinations fairly well at  $\bar{n}_H < 0.2$ , but at higher values of  $\bar{n}_H$ , no fits can be obtained. Hence, there is no evidence for the existence of the additional species HA<sub>3</sub> or H<sub>2</sub>A<sub>3</sub> in appreciable concentrations.

The proportions,  $\alpha_{p,q}$ , of the various species present in solution have been calculated.

$$\alpha_{pq} = \frac{q [H_p A_q]}{A} \quad (4-14)$$

i.e.  $\alpha_{pq}$  is the proportion of carboxylate in the different species, H<sub>p</sub>A<sub>q</sub>. Thus

$$\begin{aligned} \alpha_1 &= \frac{a}{A}, \quad \alpha_{11} = \frac{[HA]}{A}, \quad \alpha_{12} = \frac{2 [HA_2]}{A} \\ \alpha_{22} &= \frac{2 [H_2A_2]}{A} \end{aligned} \quad (4-15)$$

The value of  $a$  may be calculated from the mass-balance equations, Eqs(2-15) and (2-17). Subtracting Eq(3-17) from Eq(2-15) and rearranging

$$\begin{aligned} a &= \frac{\sqrt{1 + 4 \beta_{12}^H h(A-H+h)} - 1}{2 \beta_{12}^H h} \\ &= \frac{\sqrt{1 + 4 \beta_{12}^H A(1-\bar{n}_H)h} - 1}{2 \beta_{12}^H h} \end{aligned} \quad (4-16)$$

$$= \frac{W}{2\beta_{12}^H h} \quad (4-17)$$

Combining Eq(4-17) and the relationships (4-15)

$$\begin{aligned} \alpha_1 &= \frac{W}{2\beta_{12}^H hA} \\ \alpha_{11} &= \frac{W\beta_{11}^H}{2\beta_{12}^H A} = \frac{W}{2K_{12}A} \\ \alpha_{12} &= \frac{W^2}{2\beta_{12}^H hA} \\ \alpha_{22} &= \frac{W^2 R \beta_{11}^H}{2\beta_{12}^H A} = \frac{W^2 R}{2K_{12}A} \end{aligned} \quad (4-18)$$

In the calculation of  $W$ , Eq(4-17),  $\bar{n}_H$  was read from the appropriate formation curve, within the limits of the experimental measurements. Outside these limits  $\bar{n}_H$  was estimated using the theoretical curve for the formation of one complex only, cf. Eq(2-7). This method of estimation seems justified because the shape of the acetate formation curve for  $A \leq 1000\text{mM}$  at  $0.05 \leq \bar{n}_H \leq 0.10$  and  $0.90 \leq \bar{n}_H \leq 0.95$  is very similar to that of the formation curve for one complex. It was assumed, therefore, that the similarity between the curves continued for  $\bar{n}_H < 0.05$  and  $\bar{n}_H > 0.95$ . The values of  $\alpha_{pq}$  have been plotted against pH for  $A = 10\text{mM}$  and  $A = 700\text{mM}$ . These plots are shown in Fig. 4-4.

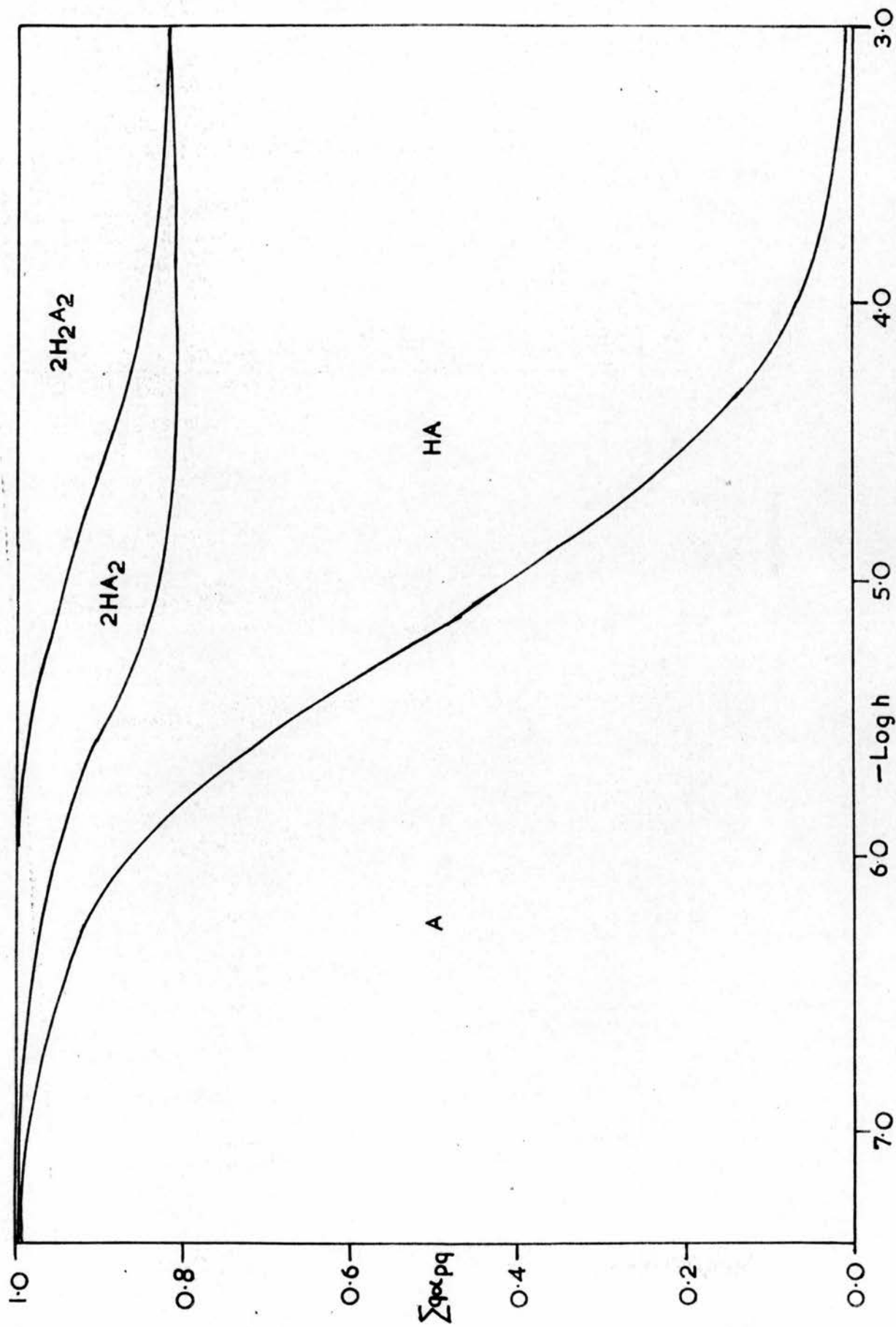
#### Formic acid.

The experimental data  $(\bar{n}_H, \log h)_A$  for formic acid are summarised in Tables 4-2A and 4-2B. Duplicate titrations have not been tabulated.

Fig. 4.4

ACETIC ACID

Relative proportions of the species  $\text{H}_2\text{A}$  present in solution at  $A=700\text{mM}$ .



The data for  $A \leq 100\text{mM}$  are given in Table 4-2A and the data for  $100\text{mM} < A \leq 1000\text{mM}$  in Table 4-2B. The corresponding formation curves are drawn in Fig. 4.2. The data were analysed in a similar manner to the acetic acid system.

TABLE 4-2A

Formic acid

Experimental data ( $\bar{n}_H$ , logh)<sub>A</sub> obtained from potentiometric titrations of formate buffers at  $A \leq 100\text{mM}$ . Duplicate titrations have not been tabulated.

Buffer			1			2			3			4			5		
[HA] mM [NaA] mM			134.3 3000			428.2 3000			655.4 3000			1475 3000			3046 3000		
A	$\bar{n}_H$	pH	A	$\bar{n}_H$	pH	A	$\bar{n}_H$	pH	A	$\bar{n}_H$	pH	A	$\bar{n}_H$	pH	A	$\bar{n}_H$	pH
8.325	0.029	5.279	9.105	0.118	4.775	4.848	0.164	4.570	11.90	0.332	4.207	8.051	0.494	3.918			
16.61	0.036	5.258	18.16	0.121	4.751	14.54	0.174	4.562	17.83	0.331	4.207	16.08	0.498	3.894			
41.19	0.040	5.252	36.13	0.123	4.741	24.18	0.176	4.562	47.23	0.330	4.207	24.09	0.500	3.893			
101.0	0.042	5.258	71.51	0.124	4.741	38.53	0.177	4.562	70.47	0.330	4.207	32.08	0.501	3.893			
						76.25	0.178	4.562	99.19	0.330	4.210	47.99	0.502	3.893			
						99.43	0.179	4.565				79.56	0.503	3.893			
												110.8	0.503	3.893			
Buffer			6			7			8			9					
[HA] mM [NaA] mM			4906 2440			7817 1560			9690 1000			9913 500.1					
A	$\bar{n}_H$	pH	A	$\bar{n}_H$	pH	A	$\bar{n}_H$	pH	A	$\bar{n}_H$	pH	A	$\bar{n}_H$	pH			
9.783	0.655	3.636	12.59	0.847	3.157	14.35	0.894	2.970	14.21	0.954	2.596						
19.54	0.656	3.615	25.14	0.841	3.176	28.66	0.897	2.951	28.37	0.953	2.596						
58.31	0.664	3.602	50.14	0.838	3.184	42.93	0.900	2.941	56.59	0.952	2.596						
96.67	0.665	3.600	99.76	0.836	3.188	57.17	0.901	2.934	98.64	0.952	2.594						
						99.64	0.903	2.926									



TABLE 4-2B

Experimental data ( $\bar{n}_H$ , logh)<sub>A</sub> obtained from potentiometric titrations of formate buffers at  $A \gg 100\text{mM}$ . Duplicate titrations have not been tabulated.

Buffer	1			2			3			4			5		
[HA] mM [NaA] mM	134.3 3000			428.2 3000			655.4 3000			1475 3000			3046 3000		
	A	$\bar{n}_H$	pH	A	$\bar{n}_H$	pH	A	$\bar{n}_H$	pH	A	$\bar{n}_H$	pH	A	$\bar{n}_H$	pH
	101.0	0.042	5.258	101.9	0.124	4.750	99.43	0.179	4.565	99.19	0.330	4.210	110.8	0.503	3.893
	199.3	0.042	5.270	201.9	0.125	4.760	202.3	0.179	4.574	199.5	0.330	4.217	202.6	0.503	3.893
	301.7	0.043	5.284	299.9	0.125	4.773	299.4	0.179	4.586	300.6	0.330	4.224	306.1	0.504	3.894
	400.4	0.043	5.296	399.3	0.125	4.780	398.9	0.179	4.592	401.9	0.330	4.229	392.0	0.504	3.898
	501.4	0.043	5.306	499.2	0.125	4.792	500.0	0.179	4.601	498.4	0.330	4.237	516.1	0.504	3.901
	600.5	0.043	5.319	599.0	0.125	4.800	601.8	0.179	4.609	599.4	0.330	4.242	582.8	0.504	3.904
	700.1	0.043	5.328	700.9	0.125	4.810	700.4	0.179	4.618	699.7	0.330	4.249	711.3	0.504	3.906
	799.1	0.043	5.336	801.1	0.125	4.821	798.8	0.179	4.624	798.9	0.330	4.256	834.0	0.504	3.908
	898.9	0.043	5.348	899.2	0.125	4.827	899.2	0.179	4.633	800.7	0.330	4.259	1063.1	0.504	3.913
	1000.3	0.043	5.355	999.4	0.125	4.834	1000.5	0.179	4.640	1000.6	0.330	4.263			

Buffer	6			7			8			9		
[HA] mM [NaA] mM	4906 2440			7817 1560			9690 1000			9913 500.1		
	A	$\bar{n}_H$	pH	A	$\bar{n}_H$	pH	A	$\bar{n}_H$	pH	A	$\bar{n}_H$	pH
	96.67	0.665	3.600	99.76	0.836	3.188	99.64	0.903	2.926	98.64	0.952	2.594
	200.1	0.667	3.592	197.4	0.835	3.189	197.5	0.905	2.910	195.4	0.952	2.586
	300.6	0.667	3.592	304.9	0.834	3.178	293.5	0.905	2.904	290.4	0.952	2.579
	398.4	0.667	3.588	398.3	0.834	3.174	401.1	0.905	2.894	396.8	0.951	2.569
	502.0	0.667	3.587	501.0	0.834	3.171	506.5	0.906	2.883	488.1	0.951	2.562
	602.5	0.667	3.587	601.6	0.834	3.162	596.9	0.906	2.877	590.4	0.951	2.552
	700.1	0.667	3.585	699.8	0.834	3.159	698.4	0.906	2.868	690.7	0.951	2.544
	802.7	0.668	3.583	806.4	0.834	3.156	797.7	0.906	2.860	788.9	0.951	2.534
	902.2	0.668	3.583	900.1	0.834	3.147	895.3	0.906	2.855	885.1	0.951	2.528
	998.7	0.668	3.582	1001.8	0.834	3.144	1002.6	0.906	2.850	991.1	0.951	2.518



TABLE 4-2C

Formic acid

Values of  $\log \beta_{11}^H$  calculated from the pH of buffers at  $A \leq 50\text{mM}$  using Eq.(4-8).

Buffer	$\log \beta_{11}^H$	Buffer	$\log \beta_{11}^H$
1	3.902	5	3.898
2	3.896	6	3.898
2a*	3.904	7	3.897
3	3.901	8	3.896
3a*	3.904	9	3.896
4	3.899		

\* Buffers 2a and 3a are additional buffers of similar composition to buffers 2 and 3. Buffer 2a has  $\bar{n}_H = 0.158$  and buffer 3a has  $\bar{n}_H = 0.200$ .

The value of  $\beta_{11}^H$  was calculated by the following methods,

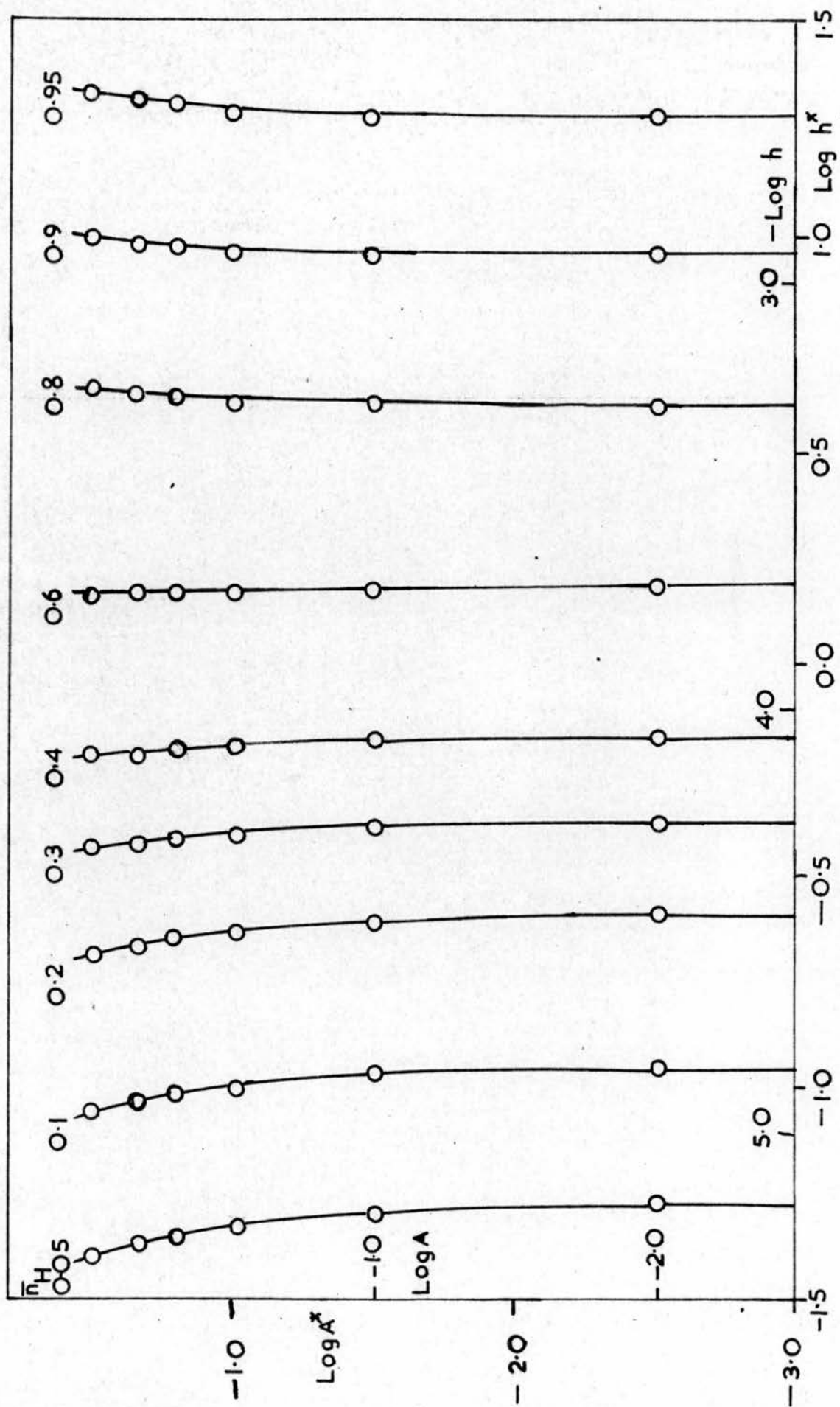
- (1) The curve  $(\bar{n}_H, \log h)$  for  $A \leq 10\text{mM}$  fits exactly the normalised curve for a single complex, Eq.(2-7), and from Eq.(2-8),  $\log \beta_{11}^H = 3.900 \pm 0.004$ .
- (2) Where the pH of a buffer is constant at low concentrations of A,  $\log \beta_{11}^H$  has been calculated using Eq.(4-8). The values of  $\log \beta_{11}^H$  at  $A \leq 50\text{mM}$  for the 9 buffers in Table 4-2A and two additional buffers with  $\bar{n}_H = 0.200$  and  $\bar{n}_H = 0.158$  are shown in Table 4-2C. The average value of  $\log \beta_{11}^H$  is  $3.900 \pm 0.005$ .
- (3) The value of  $\log \beta_{11}^H$  calculated using the curve-fitting method based on the postulate that the species HA, HA<sub>2</sub>, and H<sub>2</sub>A<sub>2</sub> are present is  $3.90 \pm 0.005$  (see below).

The preferred value of  $\log \beta_{11}^H$  is that calculated by method (2) i.e.  $3.900 \pm 0.005$ .

Fig 4.5

O Experimental Data  
 — Normalised curves

$\bar{n}_H$  FORMIC ACID  
 $\log A^*(\log h^*) \bar{n}_H$  calculated using Eq.(2-23)  
 $\log A^*(\log h^*) \bar{n}_H, R=0.18$



For  $A \geq 50\text{mM}$  the formation curves do not coincide with the calculated curve for a single complex only. In formic acid there is an isohydric point at  $\bar{n}_H = 0.61 \pm 0.01$  and the working hypothesis adopted was that the species  $HA$ ,  $HA_2$ , and  $H_2A_2$  are formed. The value of  $R$  obtained from Eq.(4-13) is 0.18. Up to the limit of the experimental measurements, the data  $\log A(\log h)_{\bar{n}_H}$  fit the family of normalised curves  $\log A^*(\log h^*)_{\bar{n}_H, R}$ , calculated using Eq(2-23) with  $R = 0.18$ , with high precision (Fig. 4-5 ). The values of the various equilibrium constants are given below.

In the position of best fit, when  $(\log A^*, \log h^*) = (0, 0.)$   $(\log A, \log h) = (0.50 \pm 0.04, -3.90 \pm 0.005)$ . Whence

$$\begin{array}{ll} \log \beta_{11}^H = 3.90 \pm 0.005 & \log K_{12} = -0.50 \pm 0.04 \\ \log \beta_{12}^H = 3.40 \pm 0.04 & \log K_{22} = 3.16 \pm 0.01 \\ \log \beta_{22}^H = 6.56 \pm 0.04 & \log K_D = -1.24 \pm 0.04. \end{array}$$

The values of  $\alpha_{pq}$  have been plotted against pH for  $A = 10\text{mM}$  and  $A = 700\text{mM}$ . These plots are shown in Fig. 4-6.

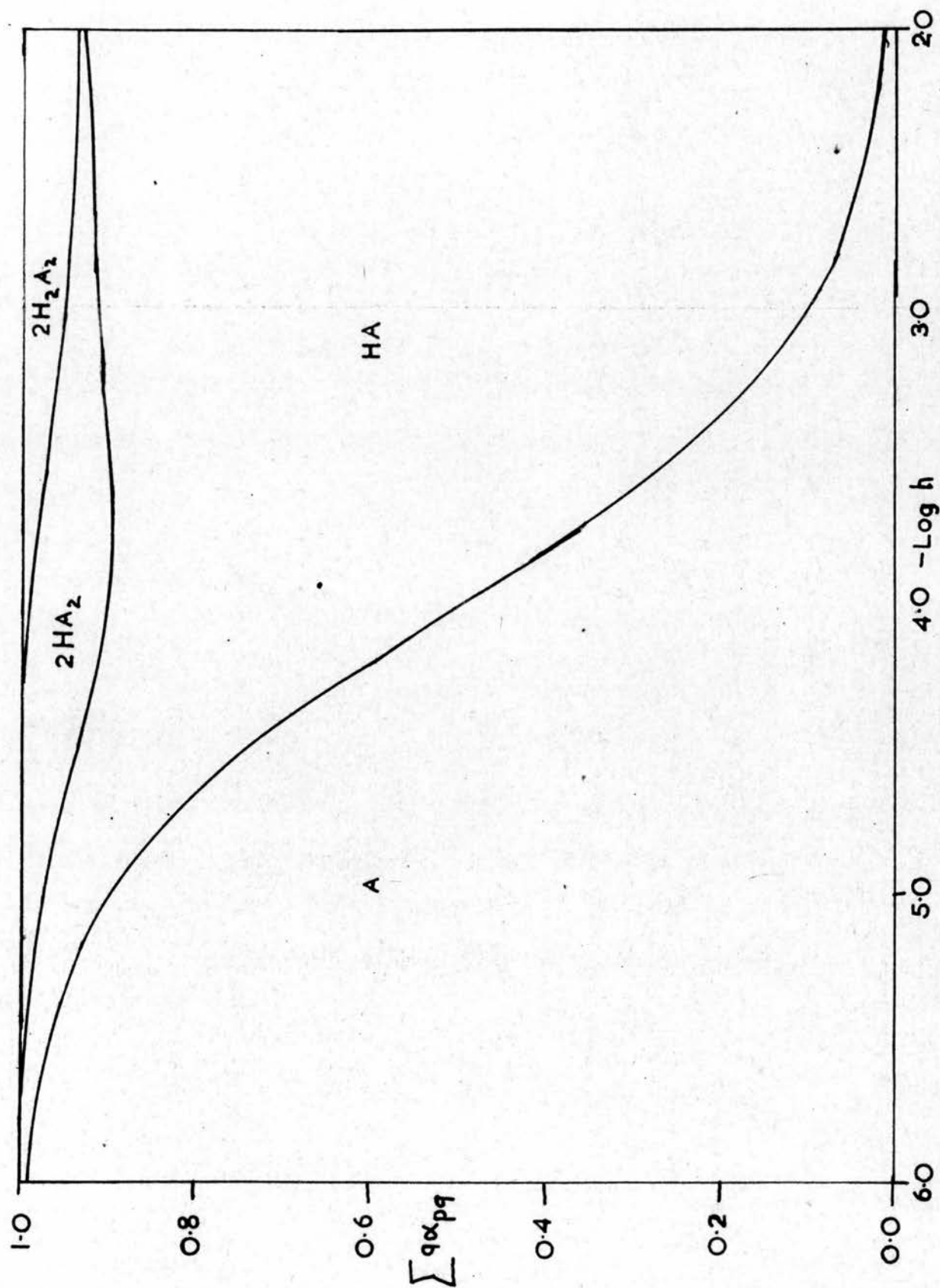
#### Propionic acid

A selection of the experimental data  $(\bar{n}_H, \log h)_A$  for propionic acid is given in Tables 4-3A and 4-3B. Duplicate titrations have not been tabulated. The data for  $A \leq 100\text{mM}$  are given in Table 4-3A and the data for  $100\text{mM} \leq A \leq 1000\text{mM}$  in Table 4-3B. The corresponding formation curves are drawn in Fig. 4-7.

Fig 4.6

FORMIC ACID

Relative proportions of the species  $H_pA_q$  present in solution at  $A=700\text{ mM}$



(100)

TABLE 4-3A

Propionic acid

Experimental data ( $\bar{n}_H$ , logh)<sub>A</sub> obtained from potentiometric titrations of propionate buffers at  $A \leq 100\text{mM}$ . Duplicate titrations have not been tabulated.

Buffer	1			2			3			4			5			6		
HA mM	321.5			747.9			1269			1996			4270			4939		
NaA mM	3000			3000			3000			3000			3000			2500		
	A	$\bar{n}_H$	pH	A	$\bar{n}_H$	pH	A	$\bar{n}_H$	pH	A	$\bar{n}_H$	pH	A	$\bar{n}_H$	pH	A	$\bar{n}_H$	pH
	8.810	0.076	6.247	9.941	0.190	5.784	11.32	0.289	5.547	13.25	0.391	5.351	19.28	0.579	5.023	9.958	0.668	4.832
	17.57	0.086	6.156	19.83	0.195	5.779	22.59	0.293	5.544	26.43	0.395	5.345	28.89	0.582	5.018	19.89	0.666	4.866
	26.29	0.090	6.141	29.67	0.197	5.769	33.79	0.295	5.530	33.00	0.396	5.343	38.47	0.583	5.010	29.80	0.665	4.866
	34.96	0.092	6.141	39.45	0.197	5.759	44.94	0.295	5.530	39.54	0.397	5.336	57.55	0.585	5.010	39.67	0.665	4.866
	43.59	0.093	6.141	49.19	0.198	5.759	99.80	0.296	5.541	52.59	0.397	5.336	104.8	0.586	5.012	49.53	0.665	4.871
	98.57	0.095	6.144	101.8	0.199	5.771				97.70	0.398	5.343				59.35	0.665	4.875
																78.93	0.665	4.876
																88.68	0.664	4.878
	7			8			9			10			11			12		
	5608			4834			7843			6995			5053			4937		
	2000			1020			1030			800.2			250.0			125.1		
	A	$\bar{n}_H$	pH	A	$\bar{n}_H$	pH	A	$\bar{n}_H$	pH	A	$\bar{n}_H$	pH	A	$\bar{n}_H$	pH	A	$\bar{n}_H$	pH
	10.10	0.725	4.744	15.53	0.815	4.523	19.90	0.888	4.283	10.35	0.882	4.293	14.10	0.952	3.857	13.48	0.974	3.583
	20.18	0.731	4.722	23.26	0.816	4.513	39.70	0.886	4.280	20.68	0.889	4.249	21.13	0.953	3.855	26.89	0.974	3.571
	30.23	0.733	4.721	30.97	0.820	4.503	59.42	0.885	4.280	30.97	0.892	4.241	28.14	0.953	3.855	40.22	0.975	3.570
	40.25	0.734	4.711	46.34	0.822	4.491	79.05	0.885	4.280	41.24	0.893	4.237	55.97	0.953	3.855	53.49	0.975	3.570
	50.25	0.735	4.711	61.62	0.823	4.491				51.49	0.894	4.231	97.18	0.953	3.855	66.69	0.975	3.570
	60.22	0.735	4.711	99.48	0.824	4.491				61.70	0.895	4.227				99.34	0.975	3.568
	99.84	0.736	4.714							82.06	0.896	4.227						
										102.3	0.896	4.227						



TABLE 4-3B

Propionic acid

Experimental data  $(\bar{n}_H, \log h)_A$  obtained from potentiometric titrations of propionate buffers at  $A \geq 100\text{mM}$ . Duplicate tirations have not been tabulated.

[illegible]



Fig 4.7

Formation Curves for  $A=10\text{mM}$  and  $1000\text{mM}$

— 10mM      ..... 500 mM  
 - - - - - 1000 mM

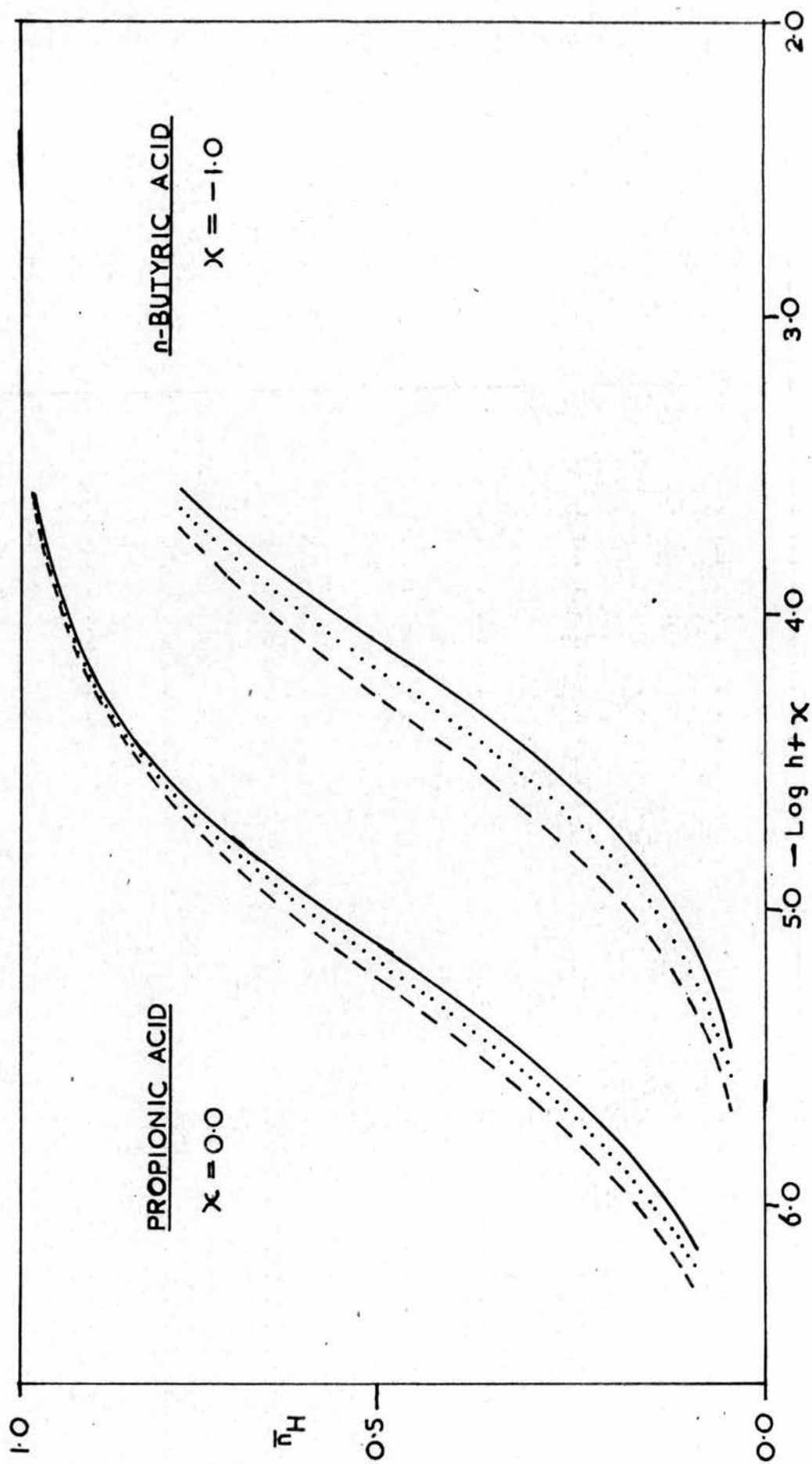


TABLE 4-3C

Propionic acid

Values of  $\log \beta_{II}^H$  calculated from the pH of buffers at  $A \leq 50\text{mM}$  using Eq. (4-8).

Buffer	$\log \beta_{II}^H$	Buffer	$\log \beta_{II}^H$
1	5.171	7	5.159
2	5.155	8	5.165
3	5.157	9	5.157
4	5.159	10	5.164
5	5.163	11	5.161
6	5.161	12	5.154

The value of  $\beta_{II}^H$  was calculated by the following methods.

1. The curve ( $\eta_H$ , logh) for  $A \leq 10\text{mM}$  fits exactly the normalised curve for a single complex Eq. (2-7), and from Eq. (2-8) the value of  $\log \beta_{II}^H = 5.160 \pm 0.005$ .

2.  $\log \beta_{II}^H$  has been calculated using Eq. (4-8) for each buffer at low concentrations of A. The values of  $\log \beta_{II}^H$  at  $A \leq 50\text{mM}$  for the 12 buffers in Table 4-3A are shown in Table 4-3C. The average value of  $\log \beta_{II}^H$  is  $5.161 \pm 0.006$ .

3. The value of  $\log \beta_{II}^H$  calculated using the curve-fitting method based on the postulate that the species HA, HA<sub>2</sub>, and H<sub>2</sub>A<sub>2</sub> are present is  $5.16 \pm 0.005$  (see below).

The preferred value of  $\log \beta_{II}^H$  is that calculated by method (2) i.e.  $5.161 \pm 0.006$ .

The data for  $A > 50\text{mM}$  have been interpreted and analysed in a similar manner to the data for formic and acetic acids but the formation curves show no isohydric point. Postulating, as before, that the species HA, HA<sub>2</sub>, and H<sub>2</sub>A<sub>2</sub>

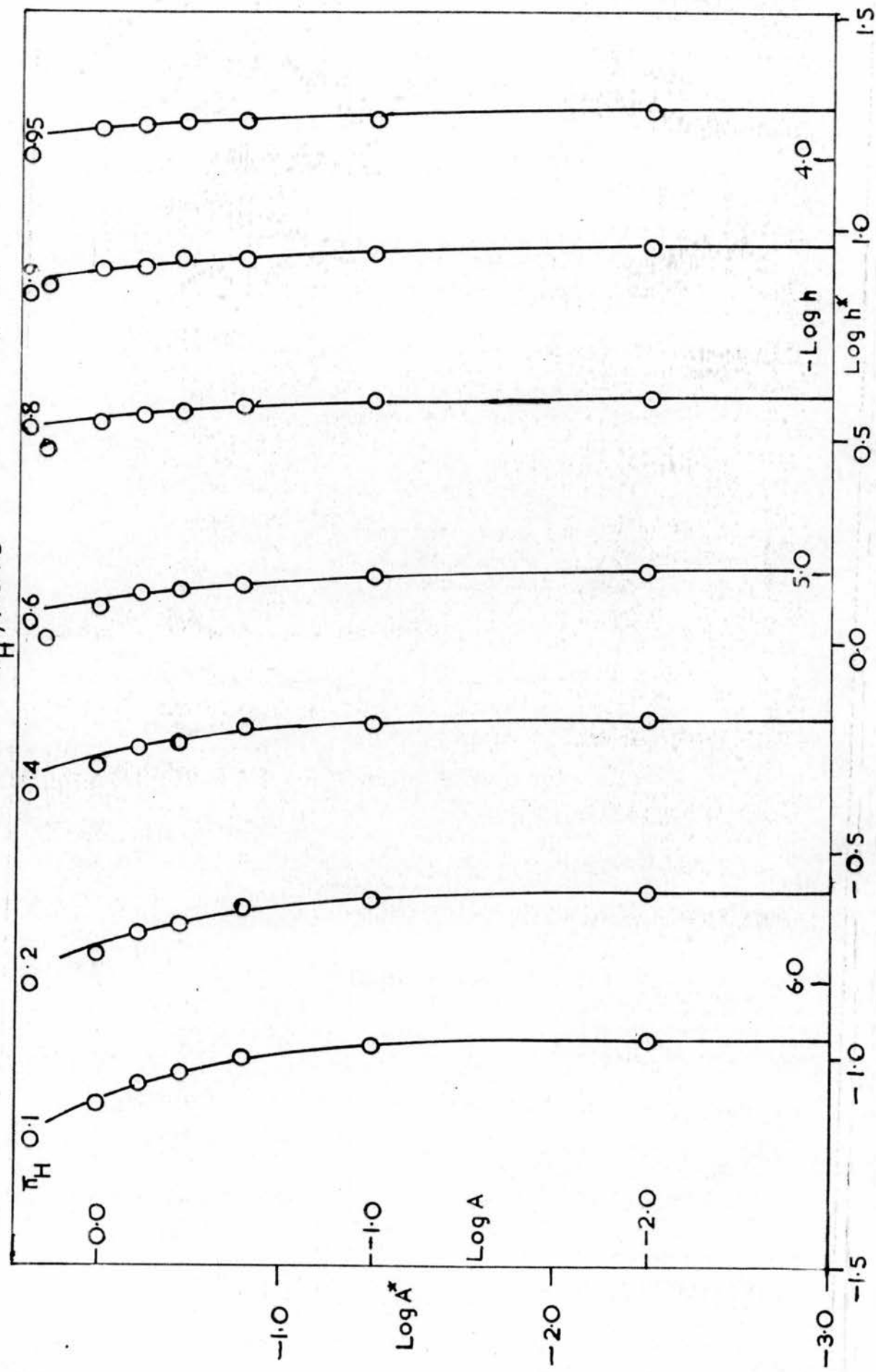
Fig 4.8

PROPIONIC ACID

O Experimental Data

$\log A(\log h)_{\bar{\pi}_H}$

— Normalised curves  $\log A^*(\log h^*)_{\bar{\pi}_H}, R=0.70$  calculated using Eq.(2-23).



are formed, the experimental data  $\log A (\log h)_{\text{NH}}$  were fitted to curves  $\log A^* (\log h^*)_{\text{NH}, R}$  calculated using Eq. (2-23) for various values of  $R$ . The best fit was obtained with the family of curves calculated with  $R = 0.70 \pm 0.05$  but it can be seen in Fig. 4.8 that although the experimental data fit with high precision for  $A \leq 700\text{mM}$ , at higher concentrations the experimental data deviate from the calculated curves. Decreasing or increasing  $R$  does not improve the fit. The constants calculated are given below. For  $A \leq 700\text{mM}$ , in the position of best fit when  $(\log A^*, \log h^*) = (0, 0)$ ,  $(\log A, \log h) = (0.35 \pm 0.03, -5.16 \pm 0.005)$ , whence

$$\begin{aligned} \log \beta_{11}^H &= 5.16 \pm 0.005 & \log K_{12} &= -0.35 \pm 0.03 \\ \log \beta_{12}^H &= 4.81 \pm 0.03 & \log K_{22} &= 5.01 \pm 0.03 \\ \log \beta_{22}^H &= 9.82 \pm 0.04 & \log K_D &= -0.50 \pm 0.04 \end{aligned}$$

The values of  $\alpha_{pq}$  have been plotted against pH for  $A = 10\text{mM}$  and  $A = 700\text{mM}$ . These plots are shown in Fig. 4-9

The reason for the experimental data at  $A > 700\text{mM}$  not fitting the calculated curves precisely may be the formation of higher species than  $\text{H}_2\text{A}_2$ . A reasonable postulate appears to be that  $\text{H}_2\text{A}_3$  is the next higher species formed thus:



The mass-balance equations, Eq. (2-16) and Eq. (2-19) may be extended,

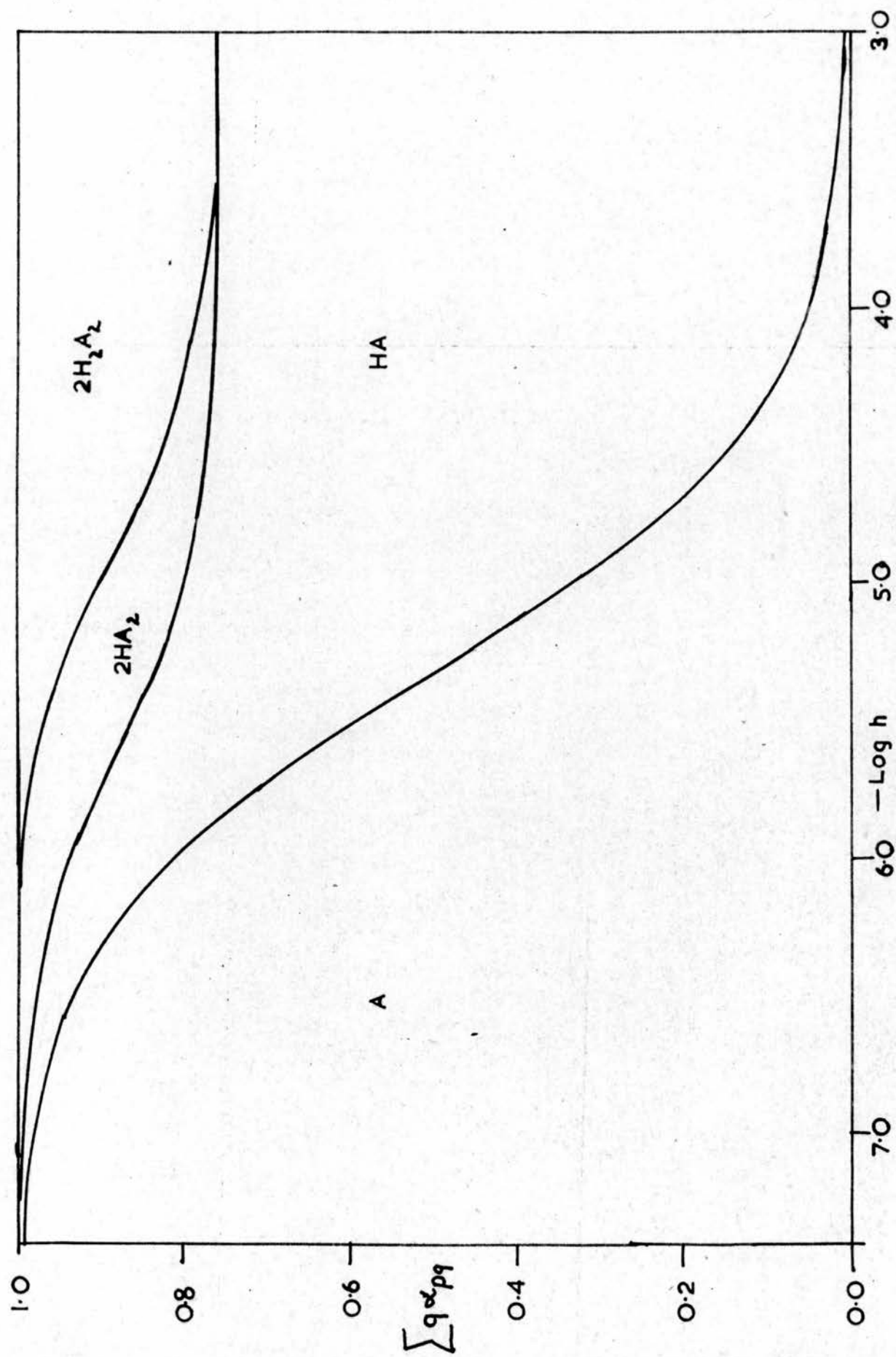
$$A = a + \beta_{11}^H ha + 2\beta_{12}^H ha^2 + 2\beta_{22}^H h^2 a^2 + 3\beta_{23}^H h^2 a^3 \quad (4-20)$$

$$A\text{H}_H = \beta_{11}^H ha + \beta_{12}^H ha^2 + 2\beta_{22}^H h^2 a^2 + 2\beta_{23}^H h^2 a^3 \quad (4-21)$$

Fig 49

PROPIONIC ACID

Relative proportions of the species  $H_pA_q$  present in solution at  $A=700mM$



From Eq. (4-20)

$$\beta_{23}^H = \frac{A-a-\beta_{11}^H ha-2\beta_{12}^H ha^2-2\beta_{22}^H h^2 a^2}{3h^2 a^3} \quad (4-22)$$

Subtracting Eq. (4-21) from Eq. (4-20) we have

$$A(1-\bar{n}_H) = a + \beta_{12}^H ha^2 + \beta_{23}^H h^2 a^3 \quad (4-23)$$

in which  $a$  and  $\beta_{23}^H$  are unknown. The values of  $a$  and  $\beta_{23}^H$  were obtained by successive approximations using Eqs. (4-22) and (4-23). The method can only be used in the concentration range where  $H_2A_3$  is likely to exist in appreciable concentration i.e.  $A \gg 700mM$  and  $\bar{n}_H > 0.3$ . The calculated values of  $\beta_{23}^H$  were found to increase with acidity. The most reasonable explanation of this phenomenon is that the neutral trimer  $H_3A_3$  also exists; neutral species such as  $HA$  and  $H_2A_2$  predominate in solutions of high acidity whereas the amounts of charged species like  $A$  and  $HA_2$  are relatively small (cf: Fig. 4-9). The appropriate modification of Eq. (4-22) is

$$\beta_{23}^H + \beta_{33}^H h = \frac{A-a-\beta_{11}^H ha-2\beta_{12}^H ha^2-2\beta_{22}^H h^2 a^2}{3h^2 a^3} \quad (4-24)$$

Thus a plot of the right-hand side of Eq. (4-24) against  $h$  gives  $\beta_{23}^H$  as intercept and  $\beta_{33}^H$  as slope. The value of  $\beta_{23}^H$  and  $\beta_{33}^H$  may also be calculated by successive approximations using Eq. (4-23) and Eq. (4-24). Both these methods give the following values

$$\text{Log } \beta_{23}^H = 9.8 \pm 0.2$$

$$\text{Log } \beta_{33}^H = 14.5 \pm 0.4.$$



n-Butyric acid.

A selection of the experimental data  $(\bar{n}_H, \log h)_A$  for butyric acid is given in Tables 4-4A and 4-4B. Duplicate titrations have not been tabulated. The data for  $A \leq 100\text{mM}$  are given in Table 4-4A and the data for  $100\text{mM} \leq A \leq 1000\text{mM}$  in Table 4-4B. It can be seen that the potentiometric measurements did not extend beyond  $\bar{n}_H = 0.78$ . The buffer at this point had an acid to salt ratio of about 5 to 1. Attempts to prepare concentrated buffers with a higher acid to salt ratio in the 3.00M sodium perchlorate medium were unsuccessful owing to the insolubility of the acid in the salt medium. Measurements above  $\bar{n}_H = 0.78$  were not therefore carried out.

TABLE 4-4A

n-Butyric acid

Experimental data ( $\bar{n}_H$ , logh)<sub>A</sub> obtained from potentiometric titrations of n-butyrate buffers at A ≤ 100mM. Duplicate titrations have not been tabulated.

Buffer	1			2			3			4		
[HA] mM	140.8			372.2			580.9			950.6		
[NaA] mM	3000			3000			3001			3000		
	A	$\bar{n}_H$	pH	A	$\bar{n}_H$	pH	A	$\bar{n}_H$	pH	A	$\bar{n}_H$	pH
	8.331	0.027	6.695	8.945	0.084	6.103	9.514	0.135	5.946	10.48	0.223	5.667
	12.48	0.033	6.602	17.84	0.097	6.098	14.25	0.144	5.906	20.90	0.232	5.650
	16.62	0.036	6.563	22.27	0.100	6.090	18.98	0.149	5.847	31.27	0.235	5.645
	20.75	0.039	6.533	26.69	0.102	6.082	28.38	0.153	5.847	41.59	0.236	5.625
	24.86	0.040	6.524	35.50	0.104	6.063	37.75	0.156	5.847	51.85	0.237	5.625
	33.06	0.041	6.507	44.25	0.105	6.051	47.07	0.157	5.847	102.4	0.239	5.632
	41.22	0.042	6.472	52.97	0.106	6.051	74.72	0.159	5.852			
	49.33	0.043	6.472	100.1	0.108	6.061	92.92	0.159	5.852			
	101.1	0.044	6.480									
Buffer	5			6			7			8		
[HA] mM	1876			3033			3883			3627		
[NaA] mM	3000			3000			2000			1000		
	A	$\bar{n}_H$	pH	A	$\bar{n}_H$	pH	A	$\bar{n}_H$	pH	A	$\bar{n}_H$	pH
	12.93	0.374	5.356	16.00	0.489	5.152	15.61	0.648	4.870	22.27	0.763	4.626
	19.38	0.378	5.348	23.97	0.494	5.135	31.13	0.654	4.853	18.38	0.770	4.613
	25.80	0.379	5.379	31.92	0.496	5.128	46.57	0.656	4.849	24.48	0.773	4.596
	38.60	0.381	5.329	47.75	0.498	5.121	61.93	0.657	4.846	36.62	0.777	4.575
	51.33	0.382	5.329	63.50	0.499	5.121	99.97	0.658	4.843	48.70	0.779	4.575
	101.6	0.383	5.343	102.5	0.501	5.128				60.72	0.780	4.575
										102.3	0.781	4.575

TABLE 4-4B

n-Butyric acid

Experimental data ( $\bar{n}_H$ , logh)<sub>A</sub> obtained from potentiometric titrations of n-butyrate buffers at A  $\geq$  100mM. Duplicate titrations have not been tabulated.

Buffer	1			2			3			4		
[HA] mM	140.8			372.2			580.9			950.6		
[NaA] mM	3000			3000			3001			3000		
	A	$\bar{n}_H$	pH	A	$\bar{n}_H$	pH	A	$\bar{n}_H$	pH	A	$\bar{n}_H$	pH
	101.1	0.043	6.480	100.1	0.108	6.061	92.92	0.159	5.852	102.4	0.239	5.632
	199.5	0.044	6.499	202.3	0.109	6.082	181.1	0.161	5.869	199.5	0.240	5.656
	302.0	0.044	6.523	302.1	0.110	6.102	265.0	0.161	5.887	300.9	0.240	5.678
	400.8	0.045	6.548	399.3	0.110	6.127	344.8	0.161	5.904	401.2	0.240	5.698
	498.9	0.045	6.570	500.3	0.110	6.149	420.9	0.162	5.921	500.1	0.240	5.720
	601.1	0.045	6.595	600.7	0.110	6.174				601.3	0.240	5.743
	700.8	0.045	6.619	700.0	0.110	6.198				700.2	0.240	5.764
	800.0	0.045	6.644	800.3	0.110	6.222				800.2	0.240	5.791
	899.9	0.045	6.668	900.6	0.110	6.247				900.5	0.241	5.814
	999.5	0.045	6.690	1000.0	0.110	6.271				1000.4	0.241	5.838
Buffer	5			6			7			8		
[HA] mM	1876			3033			3883			3627		
[NaA] mM	3000			3000			2000			1000		
	A	$\bar{n}_H$	pH	A	$\bar{n}_H$	pH	A	$\bar{n}_H$	pH	A	$\bar{n}_H$	pH
	101.6	0.383	5.343	102.5	0.501	5.128	99.97	0.658	4.843	102.3	0.781	4.575
	199.0	0.384	5.363	201.6	0.502	5.145	203.9	0.659	4.856	200.1	0.783	4.586
	304.0	0.384	5.382	297.4	0.502	5.162	304.2	0.659	4.873	299.3	0.783	4.599
	404.4	0.384	5.400	397.2	0.502	5.179	401.0	0.660	4.888	399.2	0.783	4.613
	500.4	0.385	5.421	500.3	0.502	5.199	501.0	0.660	4.905	499.5	0.783	4.628
	602.4	0.385	5.444	599.7	0.502	5.223	597.5	0.660	4.922	599.8	0.784	4.645
	699.8	0.385	5.465	701.8	0.502	5.243	702.7	0.660	4.946	699.8	0.784	4.660
	801.8	0.385	5.487	800.2	0.503	5.263	797.9	0.660	4.964	799.1	0.784	4.677
	899.1	0.385	5.512	900.8	0.503	5.285	901.0	0.660	4.983	901.6	0.784	4.694
	1000.0	0.385	5.534	1003.3	0.503	5.307	1000.0	0.660	5.001	998.7	0.784	4.712

TABLE 4-46

n-Butyric acid

Values of  $\log \beta_{11}^H$  calculated from the pH of buffers at  $A \leq 50\text{mM}$  using Eq.(4-8).

Buffer	$\log \beta_{11}^H$	Buffer	$\log \beta_{11}^H$
1	5.139	6a	5.121
2	5.142	7	5.136
3	5.133	7a	5.135
4	5.126	8	5.133
5	5.125	8a	5.141
6	5.126		

The formation curves are drawn in Fig. 4-7 . The value of  $\beta_{11}^H$  was calculated by the following methods.

1. The curve  $(\bar{n}_H, \log h)$  for  $A \leq 10\text{mM}$  fits exactly the normalised curve for a single complex Eq.(2-7), and from Eq.(2-8) the value of  $\log \beta_{11}^H = 5.130 \pm 0.005$ .
2.  $\log \beta_{11}^H$  has been calculated by Eq.(4-8) for each buffer at low concentrations of A. The values of  $\log \beta_{11}^H$  at  $A \leq 50\text{mM}$  for 11 buffers are shown in Table 4-4C. The average value of  $\log \beta_{11}^H$  is  $5.132 \pm 0.007$ .
3. The value of  $\log \beta_{11}^H$  calculated using the curve-fitting method based on the postulate that the species HA, HA<sub>2</sub>, and H<sub>2</sub>A<sub>2</sub> are present is  $5.13 \pm 0.005$  (see below).

The preferred value of  $\log \beta_{11}^H$  is that calculated by method (2) i.e.  $5.132 \pm 0.007$ .

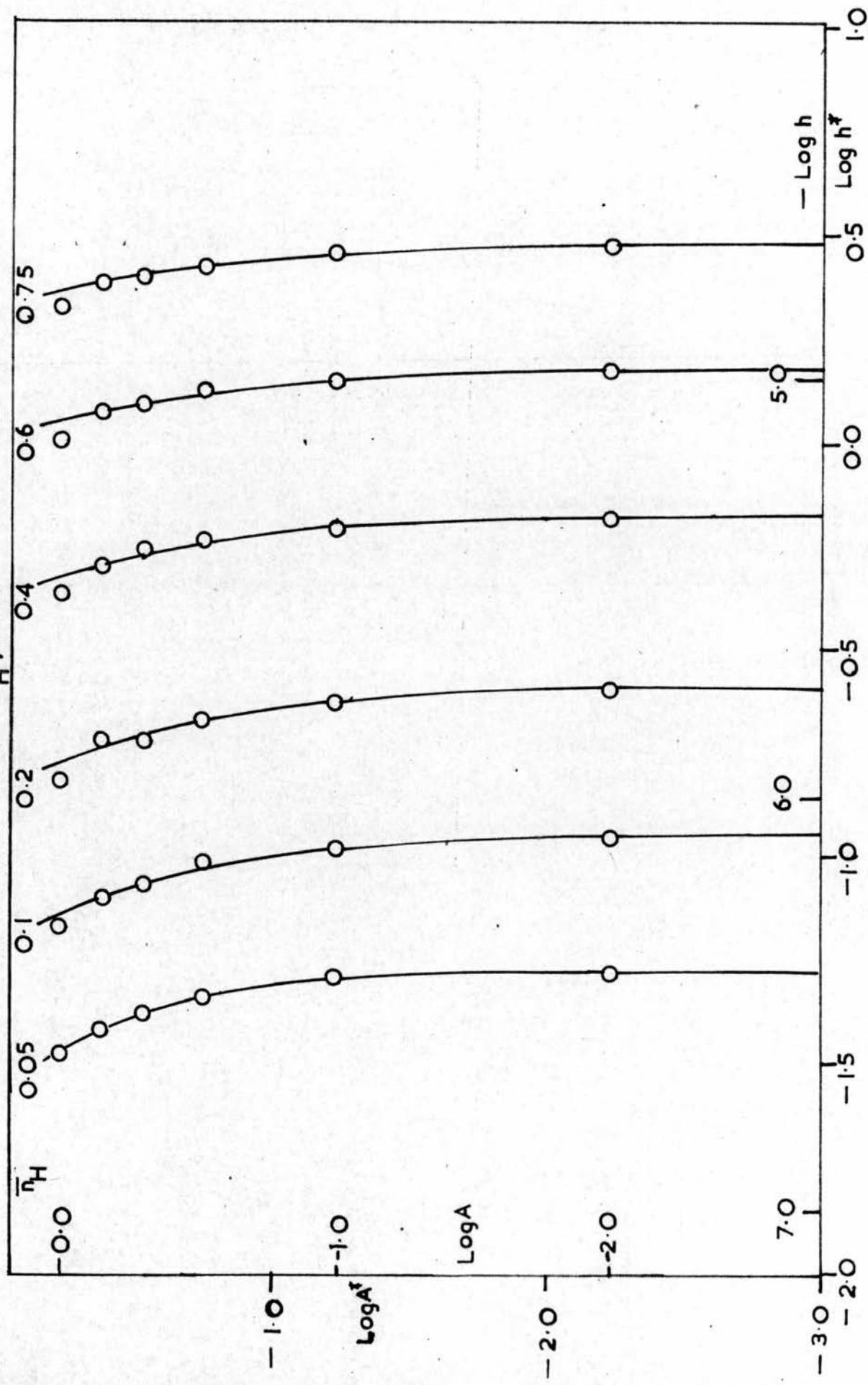
Fig 4.10

n-BUTYRIC ACID

O Experimental Data

— Normalised curves

$\log A^*(\log h^*)_{\bar{n}_H}$  calculated using Eq.(2-23)



As in the other acids the formation curves for  $A > 50\text{mM}$  do not coincide with the calculated curve for one complex and the data have been analysed and interpreted in a similar manner to the propionic acid system. There is again no isohydric point but it was postulated that  $\text{HA}$ ,  $\text{HA}_2$ , and  $\text{H}_2\text{A}_2$  are the only species formed and families of normalised curves  $(\log A^*, \log h^*)_{\bar{n}_H, R}$  for this postulate were calculated for various values of  $R$  using Eq. (2-23).

It was found that the experimental data  $(\log A, \log h)_{\bar{n}_H}$  fit the family of curves with  $R = 0.95 \pm 0.05$  with high precision for  $A \leq 700\text{mM}$  (Fig. 4-10). For  $700\text{mM} \leq A \leq 1000\text{mM}$  the experimental data do not fit the calculated curves precisely. The best fit for  $A \leq 700\text{mM}$  is obtained when  $(\log A^*, \log h^*) = (0, 0)$  and  $(\log A, \log h) = (0.24 \pm 0.03, -5.13 \pm 0.005)$ , whence

$$\log \beta_{11}^H = 5.13 \pm 0.005 \quad \log K_{12} = -0.24 \pm 0.03$$

$$\log \beta_{12}^H = 4.89 \pm 0.03 \quad \log K_{22} = 5.11 \pm 0.03$$

$$\log \beta_{22}^H = 10.00 \pm 0.04 \quad \log K_D = -0.26 \pm 0.04$$

The values of  $\alpha_{pq}$  have been plotted against pH for  $A = 10\text{mM}$  and  $A = 700\text{mM}$ . These plots are shown in Fig. 4-11.

The data for  $700\text{mM} \leq A \leq 1000\text{mM}$  have been interpreted in the same way as the propionic acid system. However, the interpretation proved even more difficult in this case as there were no data at  $\bar{n}_H > 0.78$  or at  $A > 1000\text{mM}$ . The values of  $\beta_{23}^H$  and  $\beta_{33}^H$  have been obtained both by successive approximations and graphically, using Eqs. (4-23) and (4-24). Both methods give the following values

$$\log \beta_{23}^H = 10.2 \pm 0.2$$

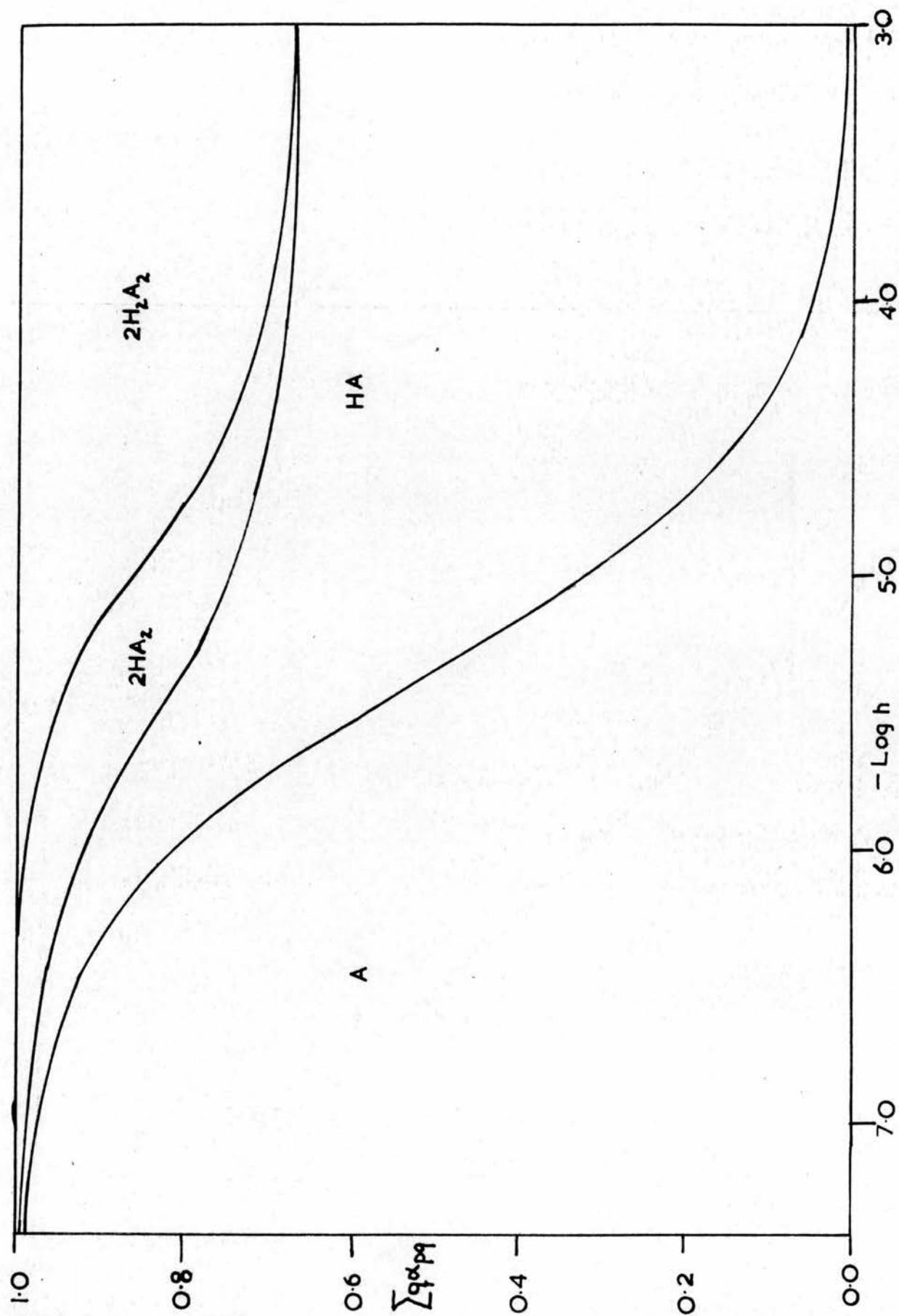
$$\log \beta_{33}^H = 15.0 \pm 0.3.$$



**Fig 4.11**

**n-BUTYRIC ACID**

Relative proportions of the species  $H_pA_q$  present in solution at  $A=700\text{mM}$



#### 4(b) CALORIMETRIC TITRATION RESULTS.

Certain preliminary operations were carried out on the day before a calorimetric titration. Solutions were introduced into the calorimeter and burette. The burette, cooler, calibrator, and stirrer were fitted to the calorimeter stopper, and the resistance thermometer was suspended in the thermostat water. The measuring current was switched on, and after at least three hours the bridge voltage,  $E_w$ , and the position of the light spot,  $m$ , were recorded. If necessary,  $m$  was brought close to the mid-point of the galvanometer scale by adjustment of one of the resistances in the Wheatstone bridge. The value of  $m$  was then recorded every 30 seconds during 15 minutes and plotted against time. Simultaneously, the constancy of the thermostat bath temperature was checked with the standard mercury thermometer. From these data, it was possible to estimate a good average value,  $m_a$ , of the thermostat temperature, expressed as a reading on the galvanometer scale. The mirror galvanometer was then switched off from the bridge circuit. The resistance thermometer was removed from the thermostat bath, carefully dried with filter paper and fitted into the Dewar. The plexi-glass stopper was sealed with mercury and the calorimeter placed in the thermostat. The stirrer was started and the battery, B2 (Fig. 4.12), was connected to the potentiometer. The switch, S4, was put in the blank resistance and no galvanometer was connected to any circuit. The apparatus was left overnight for 10-12 hours.

Heat generated by the resistance thermometer during the night caused the temperature of the calorimeter contents to rise considerably (about  $0.13^\circ$ ).

Fig 4.12

# CALIBRATION CIRCUIT

$S_1, S_2, S_3$ , and  $S_4$  = Switches

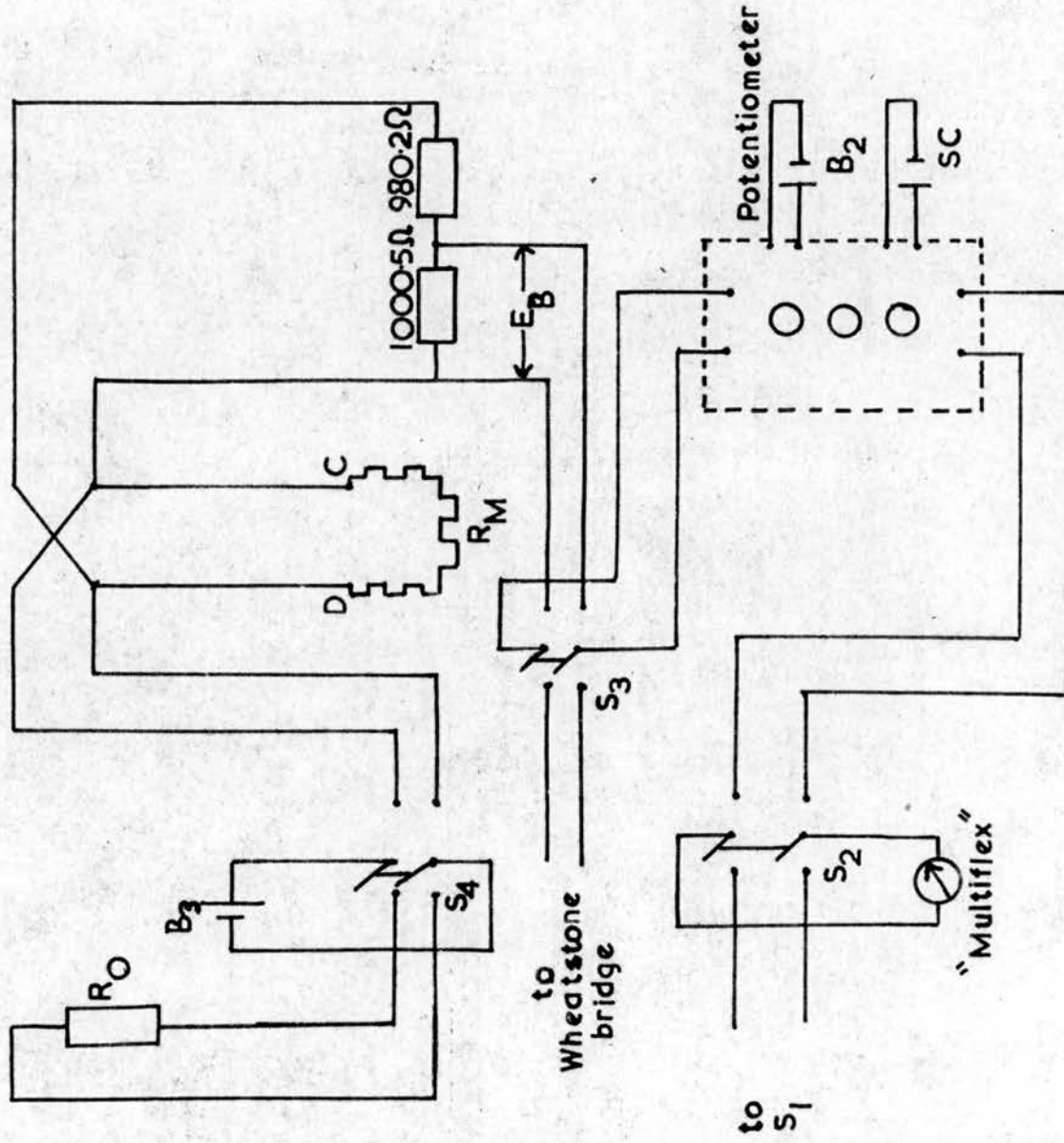
$B_2$  and  $B_3$  = Lead storage batteries (about 2V)

SC = Standard cell (1.01850 V)

$E_B$  = Potential difference, recorded by potentiometer

$R_M$  = Resistance of the manganin wire, CD

$R_O$  = Blank resistance



This temperature was reduced by the cooler to a value corresponding to  $m = 37-41\text{cm}$  on the scale. About 10 minutes later three consecutive calibrations were started. The calibration current was generated by a 2-volt lead storage battery, B3, which was switched on 10-12 hours before the start of the calibration when its voltage was stable. The position,  $m$ , of the galvanometer light spot was observed every 30 seconds during 5-7 minutes, during which time the battery was not connected to the calibrator. Times were measured by a double-pointer stop-clock. The battery was then connected to the calibrator, by means of a switch, for 3 minutes. During this time the potential difference,  $E_p$ , was measured very carefully at least four times. The battery was switched out and  $m$  observed once again during 5-7 minutes. The temperature rise caused by the calibration heat could be evaluated graphically.

The main enthalpy titration was then started. The Dewar contained about 225 ml. of solution initially and during the titration twelve 2 ml. portions were added by burette. Before every addition,  $m$  was adjusted by the cooler and calibrator so that  $(m-m_a)$  was as small as possible. The value of  $m$  was observed for 5-7 minutes. After an addition the value of  $m$  had changed considerably and it was once more observed for 5-7 minutes (Fig. 4.13). The correct value for  $\Delta m$ , the change in  $m$  due to the addition, was graphically evaluated from the observed data by the method shown in Figs. 4.14 & 4.15. Using Figs. 4-16 & 4-17 the value of  $\Delta\mu$ , the value of  $\Delta m$  corrected to a circular scale, was obtained. When the 12 additions had been made, another three or four calibrations were carried out. When the titration was finished the mirror galvanometer was switched off and the Dewar brought above the level

Fig 4.13

Variation of calorimeter temperature during three calibrations and two additions of titrant

Q = Calibration  
R = Reaction heat evolved  
C = Cooling  
Corr = Correction with calibrator

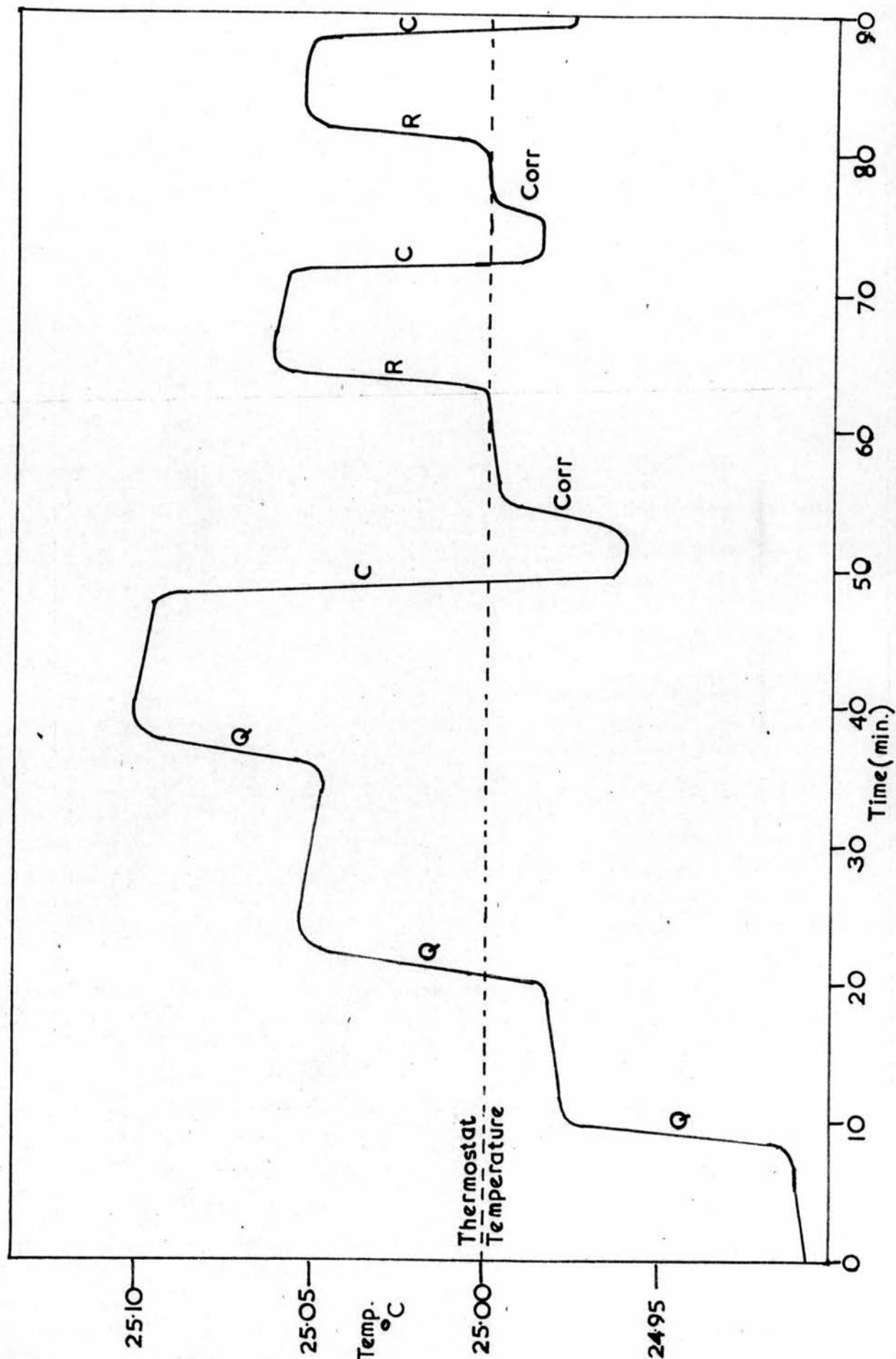




Fig 4.14

CONSTRUCTION OF  $\Delta m$  TITRATION I(a). POINT S.  
Only  $m_1$  and  $m_2$  are corrected later to circular scale (Fig 4.17)

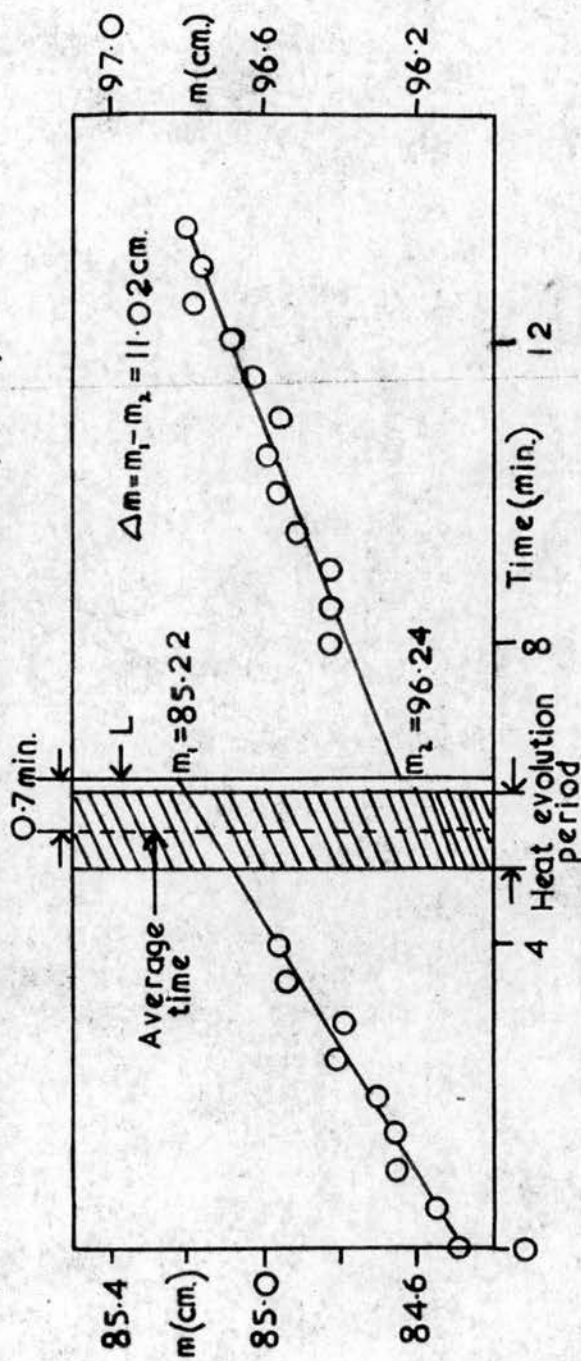


Fig 4.15

POSITION OF THE INTERSECTION LINE, L.

The position of L is chosen so that the areas A and B are equal: The distance from L to the average time (dashed line) of the heat evolution period is estimated to be  $(0.7 \pm 0.1)$  min. The same distance is obtained for heat evolution periods between 1-3 min.

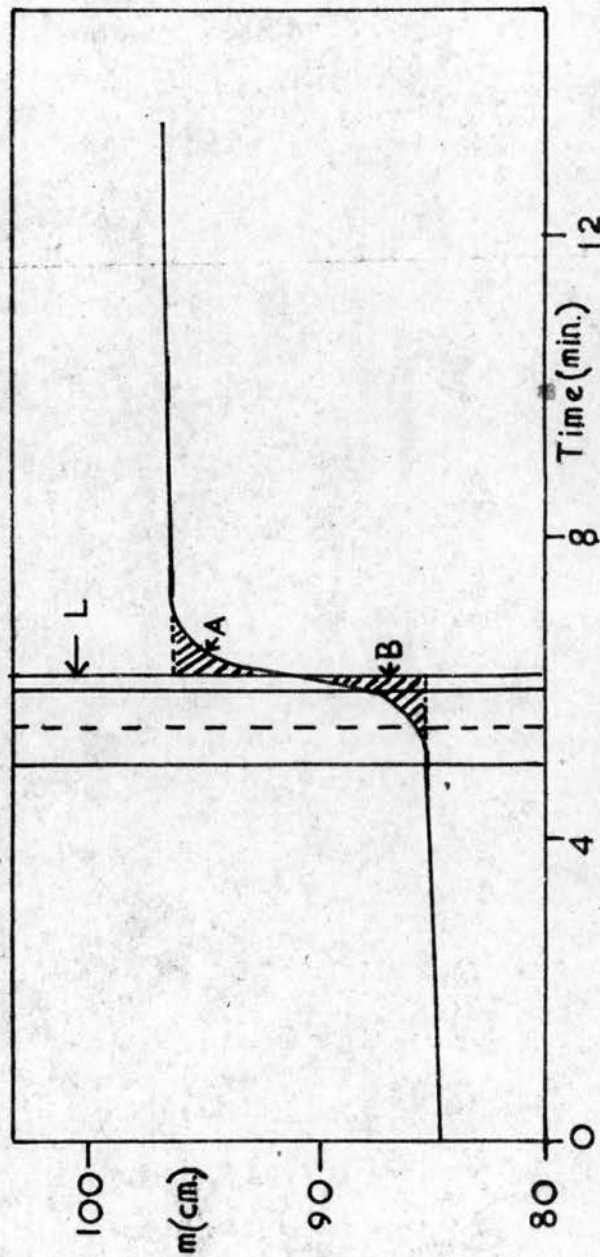




Fig 4.16

# GALVANOMETER MIRROR AND SCALE IN HORIZONTAL PROJECTION

G = Galvanometer mirror.

HS = Linear, horizontal galvanometer scale with the range 0-200 cm.

JT = Circular scale (radius =  $MG = P'G$ ).

PG = Beam, reflected by the galvanometer mirror.

M = Middle point of HS and JT.

$m$  = Position (in cm.) of the light-spot, P, on HS.

$\mu$  = Position (in cm.) of  $P'$  on JT.

$w$  = Angle PGM (in radians).

$s$  = Scale distance  $MG = (480 \pm 1)$  cm.

Angle  $PMG = 90^\circ$

For  $w=0$ ,  $m=\mu=100$  cm.

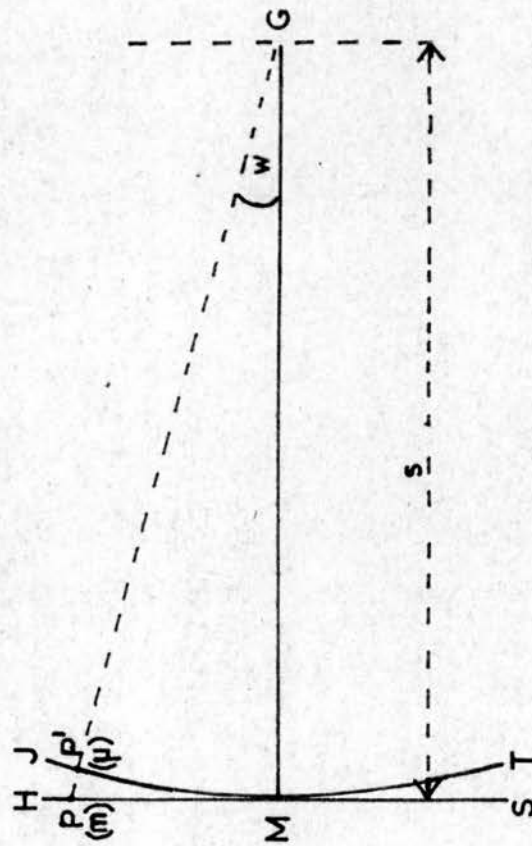
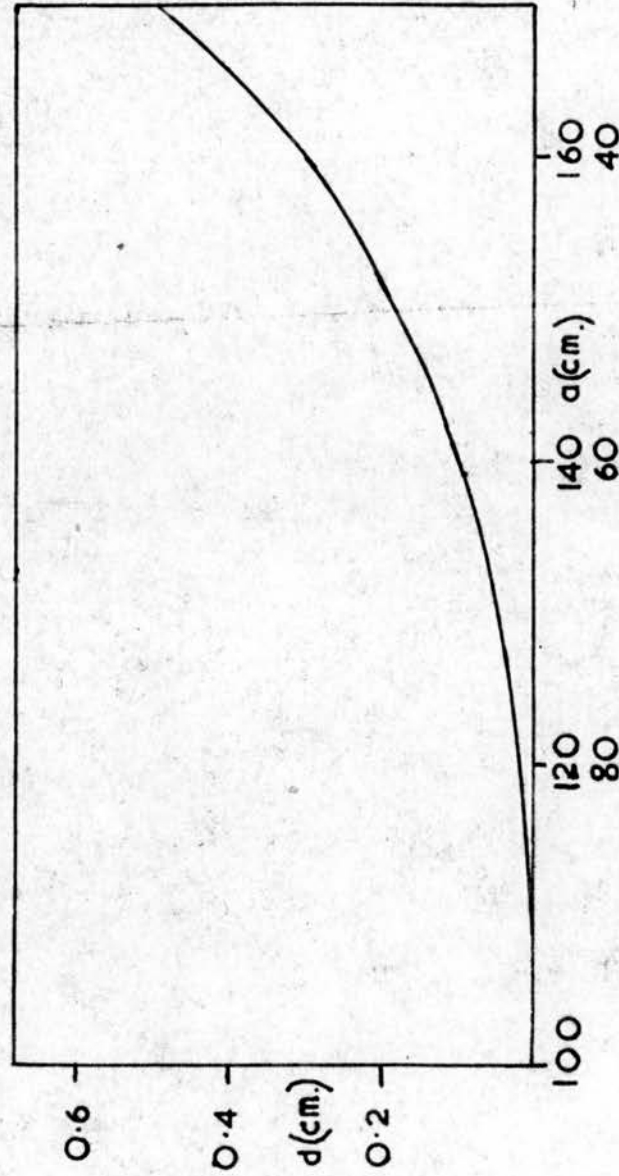


Fig 4.17

# DIAGRAM FOR CORRECTION TO CIRCULAR SCALE

For definitions of symbols, see Fig 4.16: The correction,  $d$ , is defined as  $d = PM - \widehat{PM}$ , or  $d = s \cdot \tan w - sw$ , where  $|m - 100| = s \cdot \tan w$ , and  $|\mu - 100| = sw$ . Using  $s = (480 \pm 1) \text{ cm}$ , and  $w = 0.00; 0.02; 0.04; 0.06 \dots$  radians, the value of  $d$  may be calculated and then plotted against the corresponding values of  $m$



of the thermostat water. The mercury was removed by suction and the resistance thermometer was placed in the thermostat water. Finally, the mirror galvanometer was switched on in the bridge and to check the value of  $m_a$ ,  $m$  was recorded every 30 seconds during 15 minutes and plotted against time. Each titration was repeated next day.

#### Calculation of results.

The thermometer resistance,  $R_T$  (in ohms), was compared with the temperature,  $t$ , indicated by the standard thermometer and the following equation was found to be valid for temperatures between 24.0 and 25.2°C.

$$R_T = (114.4300 \pm 0.0009) + (0.5660 \pm 0.0029) (t - 25.000) \quad (4-25)$$

The following symbols were used

$R_D, R_{C1}, R_{C2}$  = constant resistances (in  $\Omega$ ) in the Wheatstone bridge.

$R_T$  = variable resistance (in  $\Omega$ ) of the thermometer,  
Eq. (4-25).

$R_G$  = internal resistance (in  $\Omega$ ) of the mirror galvanometer

$I_G$  = current (in A) through the galvanometer branch

$E_W$  = bridge voltage (in V).

Schlyter<sup>193</sup> has derived the following equation for the current,  $I_G$ ,

$$I_G = \frac{E_W(R_{C1}R_T - R_{C2}R_D)}{(R_T + R_D) [R_G(R_{C1} + R_{C2}) + R_{C1}R_{C2}] + (R_{C1} + R_{C2}) R_T R_D} \quad (4-26)$$

Setting  $R_{C1} = R_C$  and

$$R_{C2} = R_C + e \quad (4-27)$$

the value of  $e$  is of the magnitude of  $10^{-2} \Omega$  and is negligible compared to  $R_G \sim 100 \Omega$ ,  $R_D \sim 114 \Omega$ , and  $R_C \sim 515 \Omega$ . Hence, when the terms (4-27) are substituted in Eq. (4-26)  $e$  can be neglected in the denominator and Eq. (4-26) simplifies to

$$I_G = \frac{E_W(R_T - R_D - R_D e / R_C)}{2R_D(2R_G + R_C + R_D) + (R_T - R_D)(2R_G + R_C + 2R_D)} \quad (4-28)$$

Schlyter has shown that the denominator in Eq. (4-28) can be included in a proportionality constant and

$$I_G = \text{const.} \cdot E_W \cdot (R_T - R_D - R_D e / R_C) \quad (4-29)$$

At the rest-position of the galvanometer light spot ( $I_G = 0$ ) the value of  $\mu$  is  $\mu_0$  and the difference  $(\mu - \mu_0)$  is proportional to  $I_G$ . Then

$$\mu - \mu_0 = C_G \cdot E_W \cdot (R_T - R_D - R_D e / R_C) \quad (4-30)$$

where  $C_G$  is a constant, the value of which was found by temporarily replacing the resistance thermometer with a known constant resistance,  $R_{C3}$ .

Several measurements with two different resistances  $R_D \pm \Delta R_D$  where

$R_D = R_{C3} \sim 114 \Omega$  and  $\Delta R_D \approx 0.1 \Omega$ , were made. Then

$$|\Delta \mu| = C_G \cdot E_W \cdot \Delta R_D \quad (4-31)$$

Hence,  $C_G$  may be calculated. During enthalpy titrations,  $R_D$  was kept constant and hence Eq. (4-31) may be written

$$\Delta \mu = C_G \cdot E_W \cdot \Delta R_T \quad (4-32)$$

Differentiating Eq. (4-25)

$$\Delta R_T = (0.5660 \pm 0.0029) \Delta t. \quad (4-33)$$

Assuming the change  $\Delta R_T$  to be entirely due to a certain temperature change  $\Delta t$ , we find, by combining Eq.(4-33) and the numerical value of  $C_G$  with Eq. (4-32)

$$\Delta t = 2.198 \times 10^{-3} \cdot \Delta \mu \cdot (E_W)^{-1} \quad (4-34)$$

The observation error of any temperature change was calculated<sup>193</sup> to be

$$\delta \Delta t = \pm 6.2 \times 10^{-5} \text{ degrees and} \quad (4-35)$$

the galvanometer sensitivity for the scale distance 480cm.,  $4.3 \times 10^{-10} \text{ A/mm.}$

$$(4-36).$$

In the calibrations the heat produced was calculated<sup>193</sup> to be

$$Q = (\bar{e})^2 \cdot T_c \cdot 6.2087 \times 10^{-2} \text{ cal.} \quad (4-37)$$

where  $T_c$  = time (in seconds) of calibration

$\bar{e} = E_B$  at the middle point of the calibration.

The heat capacity,  $C$ , of the calorimeter and its contents

$$C = \frac{Q}{\Delta t} \quad (4-38)$$

If the heat capacity of the calorimeter and its contents is plotted against the volume of solution added from the burette a straight line is obtained.

Thus temperature changes caused by any heat of reaction can be converted into the number of calories evolved or absorbed. The variation in temperature of the calorimeter and its contents during a calibration and subsequent titration is shown in Fig. 4-13 .

Six titrations were carried out as follows:-

<u>Burette solution</u>	<u>Calorimeter solution</u>
1(a) and 1(b) 9.897M acetic acid + 2.00M NaClO <sub>4</sub>	3.00M NaClO <sub>4</sub>
2(a) and 2(b) 9.897M acetic acid + 3.00M NaClO <sub>4</sub>	0.500M sodium acetate+2.50M NaClO <sub>4</sub>
3(a) and 3(b) 0.4919M perchloric acid + 2.50M NaClO <sub>4</sub>	0.025M sodium acetate+2.975M NaClO <sub>4</sub>

At the start of every titration the volume of solution in the calorimeter was 224.74 ml. In titrations 1(a), 1(b), 2(a), and 2(b),  $R_D = 115.58 \Omega$ . In titrations 3(a) and 3(b),  $R_D = 115.57 \Omega$ .



TABLE 4-5

The calculation of  $C$ , the heat capacity of the calorimeter and its contents. Titration 1(b). $V_B$  = volume of titrant added.

Point	$V_B$ (ml)	$E$ (Volts)	$T_c$ (secs)	$Q$ (cal)	$m_1$ $m_2$ (cm)	$\Delta m$ (cm)	$\Delta \mu$ (cm)	$E_H$ (volts)	$10^2 \Delta t$	$C$
1	0.00	1.01927	180.05	11.61	<sup>48.51</sup> 79.96	31.45	31.26	1.39218	4.935	235.3
2	0.00	1.01905	180.00	11.61	82.11 113.16	31.05	31.04	1.39220	4.901	236.9
3	0.00	1.01889	180.00	11.60	114.81 <sup>46.16</sup> 146.04	31.23	31.10	1.39222	4.910	236.3
16	25.00	1.01955	180.00	11.62	75.08 <sup>77.76</sup> 106.46	28.92	28.71	1.39220	4.533	256.3
17	25.00	1.01924	180.12	11.62	108.20 <sup>54.75</sup> 136.78	28.70	28.68	1.39222	4.528	256.6
18	25.00	1.01918	180.11	11.62	83.73 <sup>85.72</sup> 114.27	28.58	28.51	1.39224	4.501	258.2
19	25.00	1.01918	180.08	11.61	115.61 <sup>114.27</sup> 144.51	28.98	28.86	1.39211	4.557	254.8
20	25.00	1.01842	179.90	11.58	115.61	28.55	28.55	1.39213	4.508	256.9
21	25.00	1.01912	180.21	11.62	144.51	28.90	28.78	1.39215	4.544	255.7

Table 4-5 shows a typical set of data for the calculation of the heat capacity of the calorimeter and its contents. Points 1-3 were taken before, and points 16-21 after the main enthalpy titration. The values of  $\bar{e}$  were obtained from graphs of the type shown in Fig. 4-18, which refers to point 1. The values of  $E_B$  during the calibration are plotted against time; the data for point 1 are shown in Table 4-6.

---

TABLE 4-6

Titration 1(b), calibration point 1

Values of  $E_B$  and  $\tau$

$\tau$ sec.	$E_B$ volts
0.00	start
57.8	1.01950
87.1	1.01930
112.8	1.01915
138.4	1.01900
180.05	stop

---

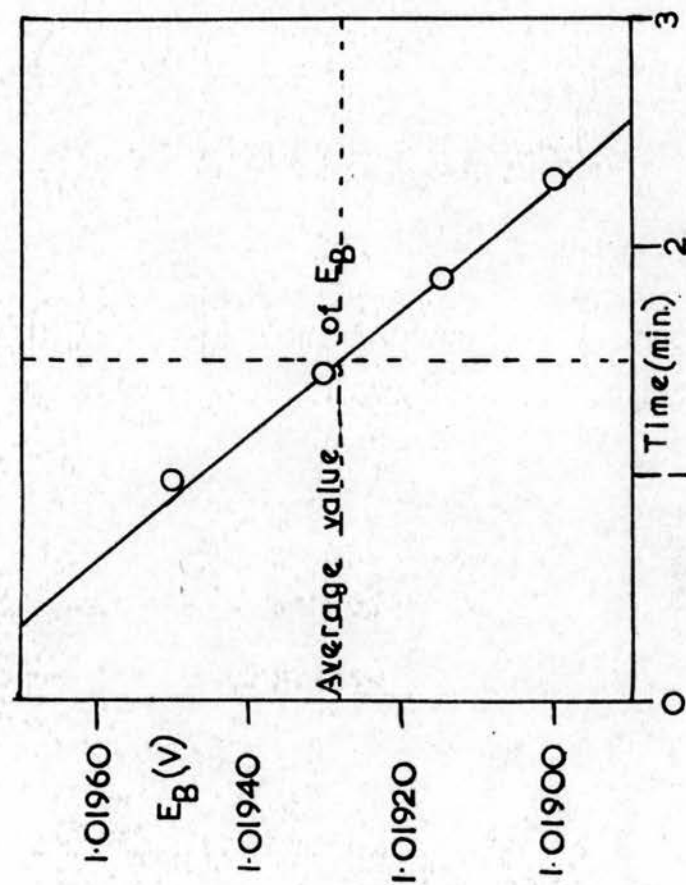
From Fig. 4-18  $\bar{e}$  is 1.01927V. The value of  $Q$  may now be calculated using Eq. (4-37). The plot of  $m$  against time is shown in Fig. 4-14. The position of  $L$  in Fig. 4-15 has been chosen so that the areas  $A$  and  $B$  are equal. The distance from  $L$  to the average time of the heat evolution period is estimated to be  $0.7 \pm 0.1$  min. The change,  $\Delta m$ , in the position of the galvanometer light spot due to the heat change is  $m_1 - m_2$ . For point 1  $\Delta m$  is 31.45cm. The value of  $\Delta t$  may be calculated by Eq. (4-34) and that of  $C$  by Eq. (4-38). Similar calibrations were carried out in

Fig 4.18

VARIATION OF  $E_B$  WITH TIME TITRATION I(b) POINT I

Construction of the average value of  $E_B$  which was substituted in

Eq.(4-37) to obtain Q.



titrations 2(a), 2(b), and 3(a) and all the values obtained for C are collected in Table 4-7. From these results,  $\bar{C}$ , the average value of c, together with its error, may be calculated.

TABLE 4-7

Values of the heat capacity, C, of the calorimeter and its contents.

$V_B = 0.0 \text{ ml.}$			$V_B = 25.0 \text{ ml.}$ (9.897M acetic acid)		
Titration	C cal. degree <sup>-1</sup>	$ \bar{C} - C $	Titration	C cal. degree <sup>-1</sup>	$ \bar{C} - C $
1(b)	235.3	1.9	1(b)	256.3	1.0
1(b)	236.9	0.3	1(b)	256.6	0.7
1(b)	236.3	0.9	1(b)	258.2	0.9
2(a)	237.7	0.2	1(b)	254.8	2.5
2(a)	238.0	0.8	1(b)	256.9	0.4
2(a)	238.9	1.7	1(b)	255.7	1.6
2(b)	238.3	1.1	2(a)	258.2	0.9
2(b)	236.3	0.9	2(a)	259.3	2.0
2(b)	238.4	1.2	2(a)	256.6	0.7
3(a)	236.7	0.8	2(b)	257.3	0.0
3(a)	237.2	0.0	2(b)	259.6	2.3
3(a)	236.2	1.0	2(b)	258.6	1.3
$\bar{C} = 237.2 \quad S = 0.316$			$\bar{C} = 257.3 \quad S = 0.422$		
<u>Error:</u> $n = 12$ , for which $t_p = 2.201$			<u>Error:</u> $n = 12$ , for which $t_p = 2.201$		
Using Eq. (4-39)			Using Eq. (4-39)		
$\bar{C} = 237.2 \pm 0.7 \text{ cal. degree}^{-1}$			$\bar{C} = 257.3 \pm 0.9 \text{ cal. degree}^{-1}$		

$V_B = 18.0 \text{ ml.}$  (3.00M sodium perchlorate).

Titration	C cal. degree <sup>-1</sup>	$ \bar{C} - C $
3(a)	253.4	0.8
3(a)	254.0	0.2
3(a)	255.2	1.0
$\bar{C} = 254.2 \quad S = 0.529$		
<u>Error:</u> $n = 3$ , for which $t_p = 4.303$		
Using Eq. (4-39)		
$\bar{C} = 254.2 \pm 2.2 \text{ cal. degree}^{-1}$		

In these measurements errors were calculated statistically. The variable  $x$  was measured  $n$  times and its arithmetical mean value,  $\bar{x}$ , was assumed to be very close to  $\xi$  which is defined as the accurate value of  $x$ . We have

$$x = \bar{x} \pm t_p \cdot S \quad (4-39)$$

where  $S$  is the error function<sup>210</sup>  $\pm \sqrt{\frac{\sum(\bar{x}-x)^2}{n(n-1)}}$

and  $t_p$  is the so-called "Student" factor, which can be obtained from statistical tables for given values of  $n$  and the confidence coefficient<sup>211</sup>. In the present work a confidence coefficient of 95% was used. For titrations 1(a), 1(b), 2(a), and 2(b) the slope of the plot of  $\bar{C}$  against  $v_B$  is

$$\frac{\Delta C}{\Delta V} = 0.804 \text{ cal. ml.}^{-1} \text{ deg.}^{-1}$$

For titrations 3(a) and 3(b) the slope of the plot of  $\bar{C}$  against  $v_B$  is

$$\frac{\Delta C}{\Delta V} = 0.944 \text{ cal. ml.}^{-1} \text{ deg.}^{-1}$$

The above value results from three calibration runs only. However Schlyter<sup>212</sup> has carried out about seventy calibration runs of the type in titrations 3(a) and 3(b) with an average value of the slope  $\Delta C/\Delta V$  of 0.968 cal. ml.<sup>-1</sup> deg.<sup>-1</sup>. This average value was therefore used in subsequent calculations.

The data for one of the main enthalpy titrations, titration 1(a) and 1(b) are tabulated in full in Table 4-8. The value of  $\Delta_m$  was calculated in the same way as in the calibration but after the correction of  $\Delta_m$  to

$\Delta_\mu$ , the value of  $\Delta_\mu$  was itself corrected thus:

$$\Delta\mu_{\text{corr}} = \Delta\mu + (m_b - m_a)F \quad (4-40)$$

where  $m_a$  = the galvanometer reading corresponding to the temperature of the burette solution i.e. the temperature of the thermostat water.

$m_b$  = the galvanometer reading corresponding to the temperature of the calorimeter solution just before an addition was made.

$$F = \frac{\Delta V \cdot \frac{\Delta G}{\Delta V}}{G}$$

Thus Eq.(4-34) is rewritten

$$\Delta t = \frac{\Delta\mu_{\text{corr}}}{E_W} \cdot 2.198 \times 10^{-3} \quad (4-41)$$

The results for titrations 2(a) and 2(b), and 3(a) and 3(b) have been summarised and are tabulated in Table 4-9. In Tables 4-8 and 4-9 it can be seen that there is rather good agreement between the values of  $\sum Q$  up to  $v_B = 23.0\text{ml.}$



TABLE 4-8

The calculation of  $Q$ , the heat produced in the enthalpy titration 1.

Titration 1(a)		$m_a = 79\text{cm.}$									
Point	$V_B(\text{ml})$	$m_2^{\text{ml}}(\text{cm})$	$\Delta m(\text{cm})$	$\Delta \mu(\text{cm})$	$m_b - m_a$	F	$\Delta \mu^{\text{corr}}$	$E_M(\text{volts})$	$\Delta t \cdot 10^2(^{\circ}\text{C})$	C	$Q(\text{cal})$
1	1.930	86.26 98.44 85.87	12.18	12.18	7	0.00673	12.23	1.39275	1.930	238.8	4.609
2	3.930	98.34 86.36	12.47	12.47	7	0.00669	12.52	1.39275	1.976	240.4	4.650
3	5.930	98.43 85.29	12.07	12.07	7	0.00664	12.12	1.39274	1.913	242.0	4.629
4	7.930	96.89 85.22	11.60	11.60	6	0.00660	11.64	1.39273	1.837	243.6	4.475
5	9.930	96.24 86.42	11.02	11.02	6	0.00656	11.06	1.39276	1.745	245.2	4.279
6	11.930	97.04 86.80	10.62	10.62	7	0.00652	10.67	1.39275	1.684	246.8	4.156
7	13.930	96.94 86.67	10.14	10.14	8	0.00647	10.19	1.39272	1.608	248.5	3.996
8	15.930	96.43 85.92	9.76	9.76	8	0.00643	9.81	1.39272	1.548	250.1	3.872
9	17.930	95.23 85.27	9.31	9.31	7	0.00639	9.35	1.39272	1.476	251.7	3.715
10	19.930	94.47 87.50	9.20	9.20	6	0.00635	9.24	1.39270	1.458	253.3	3.693
11	21.930	96.22 85.01	8.72	8.72	9	0.00631	8.78	1.39270	1.386	254.9	3.533
12	22.930	89.29	4.28	4.28	6	0.00314	4.30	1.39270	0.679	255.7	1.736
										$\Sigma Q = 47.40$	

TABLE 4-8 (continued)

Titration 1(b)

 $m_a = 80 \text{ cm.}$ 

Point	$V_B(\text{ml})$	$m_2(\text{cm})$	$\Delta m(\text{cm})$	$\Delta \mu(\text{cm})$	$m_B - m_a$	F	$\Delta \mu_{\text{corr}}$	$E_H(\text{volts})$	$\Delta t \cdot 10^2 (^\circ\text{C})$	C	$Q(\text{cal})$
4	0.920	82.30 88.24 83.08	5.94	5.93	2	0.00338	5.94	1.39219	0.938	238.0	2.257
5	2.910	95.86 83.71	12.78	12.77	3	0.00671	12.79	1.39222	2.019	239.6	4.838
6	4.910	96.11 82.31	12.40	12.39	4	0.00667	12.42	1.39220	1.961	241.2	4.730
7	6.910	94.18 82.39	11.87	11.86	2	0.00662	11.87	1.39220	1.874	242.8	4.550
8	8.910	93.67 81.20	11.28	11.27	2	0.00658	11.28	1.39220	1.781	244.4	4.353
9	10.910	92.30 82.40	11.10	11.09	1	0.00654	11.10	1.39220	1.752	246.0	4.310
10	12.910	92.96 82.24	10.56	10.55	2	0.00649	10.56	1.39220	1.667	247.7	4.129
11	14.910	92.38 82.42	10.14	10.13	2	0.00645	10.14	1.39220	1.601	249.3	3.991
12	16.910	92.12 82.31	9.70	9.69	2	0.00641	9.70	1.39221	1.531	250.9	3.841
13	18.910	91.55 81.94	9.24	9.23	2	0.00637	9.24	1.39220	1.459	252.5	3.684
14	20.910	90.77 82.32	8.83	8.82	2	0.00633	8.83	1.39220	1.394	254.1	3.542
15	22.910	90.68 82.21	8.36	8.35	2	0.00629	8.36	1.39220	1.320	255.7	3.375
16	24.910	90.53	8.32	8.31	2	0.00625	8.32	1.39222	1.314	257.3	3.381

$$\sum_{0}^{22.91} Q = 47.57$$

TABLE 4-9

The experimental data,  $\Delta t$ ,  $C$ , and  $Q$ , for titrations 2 and 3.

Titration 2(a)							Titration 2 (b)						
Point	$V_B$ (ml)	$\Delta \mu_{\text{corr}}$	$E_W$ (volts)	$\Delta t \cdot 10^2$	$C$	$Q$ (cal)	Point	$V_B$ (ml)	$\Delta \mu_{\text{corr}}$	$E_W$ (volts)	$\Delta t \cdot 10^2$	$C$	$Q$ (cal)
4	1.955	10.95	1.39194	1.729	238.8	4.129	4	1.00	5.78	1.39162	0.913	238.0	2.173
5	3.955	10.77	1.39194	1.701	240.4	4.089	5	3.00	11.15	1.39162	1.761	239.6	4.219
6	5.955	10.32	1.39194	1.630	242.0	3.945	6	5.00	10.55	1.39162	1.666	241.2	4.018
7	7.955	9.86	1.39193	1.557	243.6	3.793	7	7.00	10.16	1.39162	1.605	242.8	3.897
8	9.955	9.57	1.39193	1.511	245.2	3.705	8	9.00	9.69	1.39159	1.531	244.4	3.742
9	11.955	9.02	1.39194	1.424	246.8	3.514	9	11.00	9.34	1.39159	1.475	246.0	3.629
10	13.955	8.67	1.39194	1.369	248.5	3.402	10	13.00	9.05	1.39159	1.429	247.7	3.540
11	15.955	8.37	1.39189	1.322	250.1	3.306	11	15.00	8.66	1.39159	1.368	249.3	3.410
12	17.955	8.13	1.39189	1.284	251.7	3.232	12	17.00	8.28	1.39159	1.308	250.9	3.282
13	19.955	7.78	1.39189	1.229	253.3	3.113	13	19.00	7.85	1.39160	1.240	252.5	3.131
14	21.955	7.45	1.39189	1.176	254.9	2.998	14	21.00	7.68	1.39160	1.213	254.1	3.082
15	24.955	10.48	1.39189	1.655	257.3	4.258	15	23.00	7.30	1.39159	1.153	255.7	2.948
$\Sigma Q = 43.48$							16	25.00	6.99	1.39160	1.104	257.3	2.841
							$\Sigma Q = 43.91$						
Titration 3(a)							Titration 3(b)						
Point	$V_B$ (ml)	$\Delta \mu_{\text{corr}}$	$E_W$ (volts)	$\Delta t \cdot 10^2$	$C$	$Q$ (cal)	Point	$V_B$ (ml)	$\Delta \mu_{\text{corr}}$	$E_W$ (volts)	$\Delta t \cdot 10^2$	$C$	$Q$ (cal)
4	2.00	1.85	1.39112	0.292	239.1	0.698	1	1.00	0.97	1.39115	0.153	238.2	0.364
5	4.00	1.87	1.39110	0.295	241.1	0.711	2	3.00	1.85	1.39115	0.292	240.1	0.701
6	6.00	1.81	1.39110	0.286	243.0	0.695	3	5.00	1.88	1.39114	0.297	242.0	0.719
7	8.00	1.81	1.39110	0.286	244.9	0.700	4	7.00	1.85	1.39113	0.292	244.0	0.712
8	10.00	1.73	1.39110	0.273	246.9	0.674	5	9.00	1.75	1.39114	0.277	245.9	0.681
9	12.00	1.38	1.39110	0.218	248.8	0.542	6	11.00	1.56	1.39112	0.246	247.8	0.610
10	14.00	0.04	1.39110	0.006	250.8	0.015	7	13.00	0.43	1.39112	0.068	249.8	0.170
11	16.00	0.17	1.39110	0.027	252.7	0.068	8	15.00	0.02	1.39113	0.003	251.7	0.008
12	18.00	-0.02	1.39110	-0.03	254.6	-0.008							

The values of  $Q$  obtained in these measurements can now be combined with equilibrium constants obtained from the potentiometric titrations to calculate the heats of reaction in the system. The solution under investigation contains solvent, i.e. water, ionic medium, i.e. sodium perchlorate, the reactants H and A and certain complexes  $H_pA_q$  where  $p$  and  $q$  are integers. The relative heat content,  $L$ , per litre of solution (or the excess enthalpy expressed in cal. per litre of solution) is defined by Eq(4-42)

$$L = \sum c_i l_i \quad (4-42)$$

where  $c_i$  = the molarity of any molecular species,  $i$ .

$l_i$  = relative partial molar enthalpy of  $i$ .

The standard state is chosen arbitrarily so that  $l_i = 0$  for the solvent, ionic medium and the reactants H and A in dilute solution in the ionic medium. The amount of heat,  $Q$ , evolved or absorbed due to the addition of one solution to another will then be

$$Q = \sum n_i' l_i' - \sum n_i'' l_i'' \quad (4-43)$$

The superscripts ' and '' indicate the state before and after the addition, and  $n_i$  = number of moles of  $i$ .

The heat evolved is made up of the heats of reaction and the heats of dilution. If the heats of dilution are negligible, then the terms  $l_i$  will be independent of  $n_i$ . However, it is not possible to eliminate the heats of dilution completely. It seems reasonable to suppose that other ionic properties than activity coefficients and cationic mobilities remain constant in the ionic medium. Thus the simplifying assumption is made that  $l_i$  remains constant in a constant ionic medium within the range where the

activity factors remain constant. This assumption is reasonable because at constant temperature, each  $l_i$  will deviate from its value at the standard state by an amount proportional to the partial temperature derivative of the activity coefficient of  $i$ . Schlyter<sup>213</sup> found that the heat produced on adding 3.00M perchloric acid to about 225 ml. of 3.00M sodium perchlorate was very small, about 30 cal. per litre of 3.00M perchloric acid.

In the solutions under discussion all  $l_i$ 's are taken as constant. Since  $l_i = 0$  for the solvent, ionic medium and the reactants H and A, the only remaining terms,  $l_i$ , in Eq. (4-43) are those for  $H_pA_q$  which will be denoted by  $l_{pq}$  below. For the reactions



$$\Delta H_{pq} = l_{pq} - pl_H - ql_A = l_{pq} \quad (4-45)$$

where  $l_{pq}$  is expressed in cal. per mole.

Equation (4-42) can now be transformed to

$$L = \sum c_{pq} l_{pq} = Al_A \quad (4-42a)$$

where  $c_{pq}$  = molarity of the complex,  $H_pA_q$

$A$  = total molarity of A [Eq. (2-15)]

$l_A$  = relative partial molar enthalpy of A, expressed in cal. per mole.

In the standard state, (3.00M sodium perchlorate),  $L$  in Eq. (4-42a) is zero. A preliminary value,  $l_A^*$ , of the relative partial molar enthalpy of A may be calculated from the experimental measurements. Its relationship to the accurate value,  $l_A$ , and the values  $\Delta H_{11}$ ,  $\Delta H_{12}$ , and  $\Delta H_{22}$  which are to be determined will be derived. The symbols  $\Delta H_{pq}$  and  $\Delta H_{pq}$

are the enthalpy changes for the reactions for which the equilibrium constants are  $K_{pq}$  and  $\beta_{pq}^H$ . Now  $l_A^*$  may be defined by Eq.(4-46)

$$Q = n' l_A^{*'} - n'' l_A^{*''} \quad (4-46)$$

In these measurements the initial value of  $l$ , i.e.  $l_A^{*'}$ , is, by definition, zero. Hence, from Eq.(4-46)

$$- l_A^{*'} = \frac{Q}{n_A} \quad (4-47)$$

where  $n_A$  = number of moles of A

Assuming no volume change on mixing, the heat,  $Q$ , evolved due to the addition of the titrant to the calorimeter solution is obtained from the following heat balance:

$$Q = n'_A l'_A + (V'' - V') L_T - n''_A l''_A \quad (4-48)$$

where  $n'_A$  and  $n''_A$  = number of moles of A in the calorimeter.

$V'$  and  $V''$  = volume of solution in the calorimeter (in litres).

$L_T$  = excess enthalpy of the titrant (in cal. per litre).

Setting

$$Q_{\text{corr}} = Q - (V'' - V') L_T \quad (4-49)$$

we have, by substitution in Eq.(4-48)

$$Q_{\text{corr}} = n'_A l'_A - n''_A l''_A \quad (4-50)$$

where  $Q_{\text{corr}}$  is the value of  $Q$  corrected for the excess enthalpy of the titrant. Now

$$n''_A - n'_A = A_T (V'' - V') \quad (4-51)$$

where  $A_T$  = total concentration of A in the titrant.

Substituting Eq.(4-51) into Eq.(4-48), and combining with Eq.(4-46),

$$n'_A \left( l_A^{*'} + \frac{L_T}{A_T} - l'_A \right) = n''_A \left( l_A^{*''} + \frac{L_T}{A_T} - l''_A \right) \quad (4-52)$$



Thus during each titration the terms  $n_A (l_A^* + \frac{L_T}{A_T} - l_A)$  are constant.

Now at any point in a titration

$$n_A = n_0 + v_{B/A} A_T \quad (4-53)$$

where  $n_0$  = number of moles of A in the calorimeter at the start of a titration.

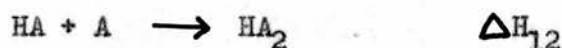
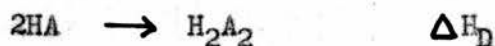
Combining Eqs. (4-52) and (4-53) it is seen that  $(n_0 + v_{B/A} A_T) (l_A^* + \frac{L_T}{A_T} - l_A)$  is also constant. (4-54)

is also constant.

From Eq. (4-42a)

$$Al_A = [H^+] l_{H^+} + a l_a + [HA] \cdot \Delta H_{11} + [HA_2] \cdot \Delta H_{12} + [H_2A_2] \Delta H_{22} \quad (4-55)$$

By the definition of the standard state,  $l_{H^+} = l_a = 0$ . The enthalpy changes for the various reactions are,



$$\text{and} \quad \Delta H_{22} = 2 \Delta H_{11} + \Delta H_D \quad (4-56)$$

$$\Delta H_{12} = \Delta H_{11} + \Delta H_{12} \quad (4-57)$$

Substituting Eqs. (2-17), (4-56), and (4-57) into Eq. (4-55)

$$Al_A = \Delta H_{11} \cdot (H - h) + \Delta H_D \cdot [H_2A_2] + \Delta H_{12} \cdot [HA_2] \quad (4-58)$$

Whence

$$l_A = \Delta H_{11} \cdot \left( \frac{H-h}{A} \right) + \Delta H_D \cdot \frac{[H_2A_2]}{A} + \Delta H_{12} \cdot \frac{[HA_2]}{A} \quad (4-59)$$

Substituting the terms (4-15) into Eq. (4-59) we have

$$l_A = \Delta H_{II} \cdot \left(\frac{H-h}{A}\right) + \Delta H_D \cdot \frac{\alpha_{22}}{2} + \Delta H_{12} \cdot \frac{\alpha_{12}}{2} \quad (4-60)$$

where A, H, and h are known, and  $\alpha_{22}$  and  $\alpha_{12}$  may be calculated from the equilibrium constants. [ see Eqs. (4-17) and (4-18) ].

Table 4-10 shows the values obtained for  $l_A$  in the various titrations, together with the values of  $\alpha_{II}$ ,  $\frac{\alpha_{12}}{2}$ , and  $\frac{\alpha_{22}}{2}$ .

TABLE 4-10

The calculation of  $l_A^*$  in titrations 1(a) and 1(b). Values of  $Q$  are taken from Table 4-8. The values of  $\alpha_{11}$ ,  $\frac{\alpha_{12}}{2}$ , and  $\frac{\alpha_{22}}{2}$  are tabulated also.

Point		$V_B$ (ml)	$V_T$ (ml)	$C_{HA}$ (mM)	$A$ (mM)	$n_A$ (mM)	Titration 1(a)		Titration 1(b)		$-l_A^*$ (cal/mole)	$\alpha_{11} \cdot 10^2$	$\frac{\alpha_{12}}{2} \cdot 10^2$	$\frac{\alpha_{22}}{2} \cdot 10^2$
1(a)	1(b)						$Q$ (cal)	$\sum Q$	$Q$ (cal)	$\sum Q$				
-	-	0.00	224.74	0.00	0.00	0.00	0.00	0.00	0.00	0.00	247.9	0.00	0.00	0.00
	4	0.92	225.66	40.35	40.35	9.106			2.257	2.257	241.3	97.14	0.027	0.726
1		1.93	226.67	84.27	84.27	19.102	4.609	4.609			246.3	96.04	0.038	1.460
	5	2.91	227.65	126.52	126.52	28.801			4.838	7.095	240.3	94.70	0.045	2.130
2		3.93	228.67	170.10	170.10	38.897	4.750	9.359			243.3	93.56	0.052	2.796
	6	4.91	229.65	211.61	211.61	48.596			4.730	11.825	238.3	92.48	0.056	3.400
3		5.93	230.67	254.44	254.44	58.692	4.629	13.988			239.4	91.25	0.059	3.980
	7	6.91	231.65	295.23	295.23	68.391			4.550	16.375	235.2	90.43	0.063	4.536
4		7.93	232.67	337.33	337.33	78.486	4.475	18.463			235.0	89.26	0.065	5.055
	8	8.91	233.65	377.43	377.43	88.186			4.353	20.728	231.4	88.29	0.067	5.531
5		9.93	234.67	418.81	418.81	98.281	4.279	22.742			231.9	87.51	0.070	6.026
	9	10.91	235.65	458.23	458.23	107.98			4.310	25.038	227.8	86.63	0.071	6.460
6		11.93	236.67	498.91	498.91	118.08	4.156	26.898			228.3	85.63	0.073	6.872
	10	12.91	237.65	537.66	537.66	127.78			4.129	29.167	224.1	84.87	0.074	7.278
7		13.93	238.67	577.66	577.66	137.87	3.996	30.894			224.7	84.24	0.075	7.710
	11	14.91	239.65	615.77	615.77	147.57			3.991	33.158	220.5	83.46	0.076	8.063
8		15.93	240.67	655.11	655.11	157.67	3.872	34.766			221.1	82.56	0.077	8.393
	12	16.91	241.65	692.59	692.59	167.37			3.841	36.999	216.8	82.04	0.078	8.761
9		17.93	242.67	731.28	731.28	177.46	3.715	38.481			217.4	81.36	0.079	9.097
	13	18.91	243.65	768.15	768.15	187.16			3.684	40.683	213.8	80.71	0.079	9.402
10		19.93	244.67	806.21	806.21	197.26	3.693	42.174			210.6	80.05	0.080	9.709
	14	20.91	245.65	842.48	842.48	206.96			3.542	44.225	209.9	79.39	0.081	9.985
11		21.93	246.67	879.92	879.92	217.05	3.533	45.707			209.0	78.85	0.081	10.28
	15	22.91	247.65	915.61	915.61	226.75			3.375	47.600	206.8	78.44	0.082	10.60
12		22.93	247.67	916.33	916.33	226.95	1.736	47.443			77.42	78.43	0.082	10.59
	16	24.91	249.65	987.56	987.56	246.54			3.381	50.981		77.42	0.083	11.13

TABLE 4-10

The calculation of  $l_A^*$  in titrations 2(a) and 2(b). Values of  $Q$  are taken from Table 4-9. The values of  $\alpha_{11}$ ,  $\frac{\alpha_{12}}{2}$ , and  $\frac{\alpha_{22}}{2}$  are tabulated also.

Point		$V_B$ (ml)	$V_T$ (ml)	$C_A$ (mM)	$C_{HA}$ (mM)	$A$ (mM)	$n_A$ (mM)	Titration 2(a)		Titration 2(b)		$-l_A^*$ (cal/mole)	$\alpha_{11} \cdot 10^2$	$\frac{\alpha_{12}}{2} \cdot 10^2$	$\frac{\alpha_{22}}{2} \cdot 10^2$
2(a)	2(b)							$Q$ (cal)	$\sum Q$	$Q$ (cal)	$\sum Q$				
-	-	0.00	224.74	500.00	0.00	500.00	112.37	0.00	0.00	0.00	0.00	0.00	0.00	0.00	0.00
	4	1.00	225.74	497.79	43.844	541.63	122.27			2.173	2.173	17.8	6.61	1.467	0.049
4		1.955	226.685	495.71	85.358	581.07	131.72	4.129	4.129			31.3	11.78	2.564	0.153
	5	3.00	227.74	493.41	130.38	623.79	142.06			4.219	6.392	45.0	16.68	3.562	0.326
5		3.955	228.685	491.37	171.17	662.54	151.51	4.089	8.218			54.2	20.51	4.298	0.526
	6	5.00	229.74	489.12	215.40	704.52	161.86			4.018	10.410	64.3	24.08	4.953	0.767
6		5.955	230.685	487.11	255.50	742.61	171.31	3.945	12.163			71.0	26.91	5.45	1.011
	7	7.00	231.74	484.90	298.96	783.86	181.65			3.897	14.307	78.8	29.64	5.88	1.295
7		7.955	232.685	482.93	338.37	821.30	191.10	3.793	15.956			83.5	31.86	6.23	1.567
	8	9.00	233.74	480.75	381.09	861.84	201.45			3.742	18.049	89.6	33.92	6.53	1.864
8		9.955	234.685	478.82	419.83	898.65	210.90	3.705	19.661			93.2	35.69	6.76	2.151
	9	11.00	235.74	476.67	461.83	938.50	221.24			3.629	21.678	98.0	37.33	6.96	2.457
9		11.955	236.685	474.76	499.92	974.68	230.69	3.514	23.175			100.5	38.68	7.10	2.744
	10	13.00	237.74	472.66	541.21	1013.9	241.04			3.540	25.218	105.0	40.04	7.23	3.054
10		13.955	238.685	470.79	578.66	1049.5	250.49	3.402	26.577			106.1	41.12	7.34	3.334
	11	15.00	239.74	468.72	619.26	1088.0	260.83			3.410	28.628	109.8	42.21	7.42	3.643
11		15.955	240.685	466.88	656.10	1123.0	270.28	3.306	29.883			110.6	43.11	7.48	3.922
	12	17.00	241.74	464.84	696.02	1160.9	280.63			3.282	31.910	113.7	43.98	7.53	4.221
12		17.955	242.685	463.03	732.26	1195.3	290.08	3.232	33.115			114.2	44.74	7.56	4.498
	13	19.00	243.74	461.02	771.52	1232.6	300.42			3.131	35.041	116.6	45.46	7.57	4.788
13		19.955	244.685	459.24	807.17	1266.4	309.87	3.113	36.228			116.9	46.08	7.58	5.06
	14	21.00	245.74	457.27	845.79	1303.0	320.22			3.082	38.123	119.1	46.65	7.58	5.33
14		21.955	246.685	455.52	880.87	1336.4	329.67	2.998	39.226			119.0	47.17	7.57	5.59
	15	23.00	247.74	453.58	918.87	1372.5	340.01			2.948	41.071	120.8	47.69	7.56	5.87
15		24.955	249.685	450.05	989.21	1439.3	359.36	4.258	43.484			121.0	48.50	7.51	6.37
	16	25.00	249.74	449.95	990.77	1440.7	359.81			2.841	43.912	122.0	48.54	7.52	6.38

TABLE 4-10

The calculation of  $l_A^*$  in titrations 3(a) and 3(b). Values of  $Q$  are taken from Table 4-9. The values of  $\alpha_{11}$ ,  $\frac{\alpha_{12}}{2}$ , and  $\frac{\alpha_{22}}{2}$  are tabulated also.

Point		$V_B$ (ml)	$V_T$ (ml)	$C_A$ (mM)	$C_{HClO_4}$ (mM)	$A$ (mM)	$n_A$ (mM)	Titration 3(a)		Titration 3(b)		$-l_A^*$ (cal/mole)	$\alpha_{11} \cdot 10^2$	$\frac{\alpha_{12}}{2} \cdot 10^2$	$\frac{\alpha_{22}}{2} \cdot 10^2$
3(a)	3(b)							$Q$ (cal)	$\sum Q$	$Q$ (cal)	$\sum Q$ (cal)				
-	-	0.00	224.74	25.00	0.00	25.00	5.6185	0.00	0.00	0.00	0.00	0.00	0.00	0.00	0.00
	1	1.00	225.74	24.89	2.18	24.89	5.6185			0.364	0.364	64.8	8.665	0.089	0.0035
4		2.00	226.74	24.78	4.34	24.78	5.6185	0.698	0.698			124.1	17.29	0.160	0.013
	2	3.00	227.74	24.67	6.48	24.67	5.6185			0.701	1.065	189.6	25.97	0.213	0.031
5		4.00	228.74	24.56	8.60	24.56	5.6185	0.711	1.409			250.8	34.62	0.249	0.055
	3	5.00	229.74	24.46	10.71	24.46	5.6185			0.719	1.784	317.5	43.27	0.268	0.086
6		6.00	230.74	24.35	12.79	24.35	5.6185	0.695	2.104			374.5	51.98	0.271	0.124
	4	7.00	231.74	24.25	14.86	24.25	5.6185			0.712	2.496	444.2	60.65	0.257	0.168
7		8.00	232.74	24.14	16.91	24.14	5.6185	0.700	2.804			499.1	69.35	0.226	0.218
	5	9.00	233.74	24.04	18.94	24.04	5.6185			0.681	3.177	565.5	77.83	0.180	0.274
8		10.00	234.74	23.94	20.96	23.94	5.6185	0.674	3.478			619.0	86.51	0.119	0.337
	6	11.00	235.74	23.83	22.95	23.83	5.6185			0.610	3.787	674.0	94.62	0.046	0.401
9		12.00	236.74	23.73	24.93	23.73	5.6185	0.542	4.020			715.5			
	7	13.00	237.74	23.63	26.90	23.63	5.6185			0.170	3.957	704.3			
10		14.00	238.74	23.53	28.85	23.53	5.6185	0.015	4.035			718.2			
	8	15.00	239.74	23.44	30.78	23.44	5.6185			0.008	3.965	705.7			
11		16.00	240.74	23.34	32.69	23.34	5.6185	0.068	4.103			730.3			
12		18.00	242.74	23.15	36.48	23.15	5.6185	-0.008	4.095			728.8			

In titration 1,  $n_0 = 0$ , and Eq. (4-54) reduces to

$$v_B A_T (l_A^* + \frac{L_T}{A_T} - l_A) = 0 \quad (4-61)$$

since for Eq. (4-54) to hold even for  $v_B = 0$ , the constant must be zero.

Thus

$$l_A = l_A^* + \frac{L_T}{A_T} \quad (4-62)$$

As a first approximation, we may neglect  $h$  and  $\frac{\alpha_{12}}{2}$  in Eq. (4-60), and since  $H = A$ , we may combine Eqs. (4-60) and (4-62) to give

$$l_A^* = (\Delta H_{II} - \frac{L_T}{A_T}) + \Delta H_D \frac{\alpha_{22}}{2} \quad (4-63).$$

A plot of  $l_A^*$  against  $\frac{\alpha_{22}}{2}$  gives  $(\Delta H_{II} - \frac{L_T}{A_T})$  as intercept and  $\Delta H_D$  as the slope. This plot is shown in Fig. 4-19, whence we find

$$\Delta H_{II} - \frac{L_T}{A_T} \approx -0.26 \text{ kcal.}$$

$$\Delta H_D \approx +0.47 \text{ kcal.}$$

In titration 2,  $H v_T = v_B A_T$  and

$$v_T A = n_0 + v_B A_T$$

At  $v_B = 0$ , we have, by definition,  $l = 0$ . Moreover  $l_A^* \rightarrow 0$  as  $n \rightarrow 0$ .

Thus the constant in Eq. (4-54) is  $n_0 \frac{L_T}{A_T}$ , and Eq. (4-60) gives

$$A(l_A^* + \frac{L_T}{A_T} - l_A) = (A-H) \frac{L_T}{A_T} \quad (4-64)$$

whence,

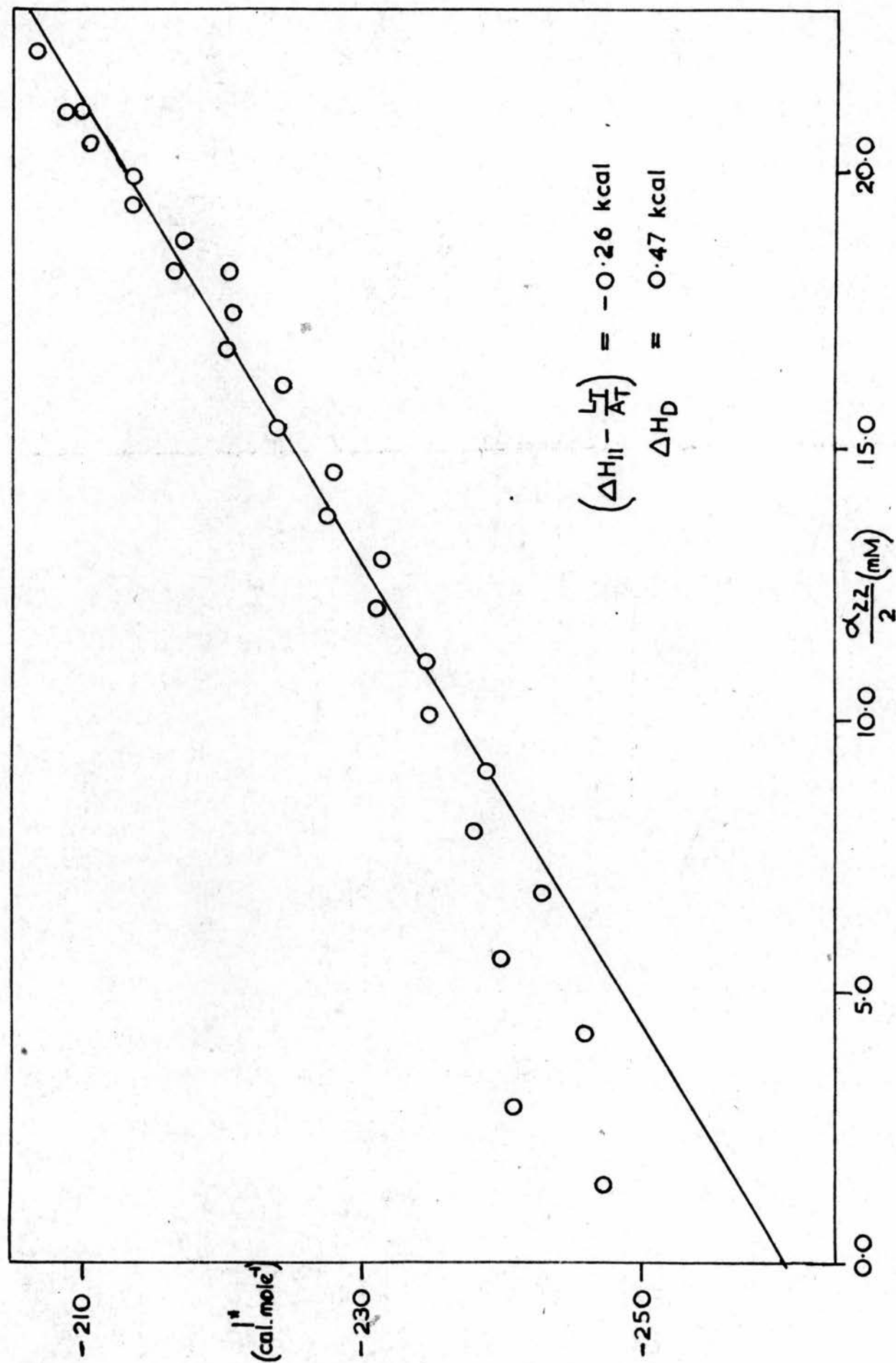
$$l_A = l_A^* + \frac{H}{A} \cdot \frac{L_T}{A_T} \quad (4-65)$$

Combining Eqs. (4-60) and (4-65), and neglecting  $h$ , which is small compared with other terms, we have



Fig 4.19

## TITRATION I

Evaluation of  $\left(\Delta H_{II} - \frac{L_I}{A_T}\right)$  and  $\Delta H_D$  using Eq.(4-63)

$$l_A^* - \frac{H}{A}(\Delta H_{II} - \frac{L_T}{A_T}) - \Delta H_D \frac{\alpha_{22}}{2} = \Delta H_{12} \frac{\alpha_{12}}{2} \quad (4-66)$$

Inserting the approximate values for  $(\Delta H_{II} - \frac{L_T}{A_T})$  and  $\Delta H_D$  we find

$$\Delta H_{12} \approx 0.3 \text{ kcal.}$$

In titration 3,  $L_T = 0$  by definition, so that  $l_A = l_A^*$ . From Eq. (4-60) we have, neglecting the small terms  $h$ ,  $\frac{\alpha_{12}}{2}$ , and  $\frac{\alpha_{22}}{2}$

$$l_A \approx \Delta H_{II} \cdot \frac{H}{A}$$

and  $\Delta H_{II} \approx -0.7 \text{ kcal.}$

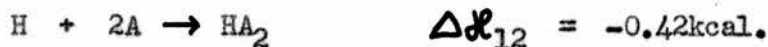
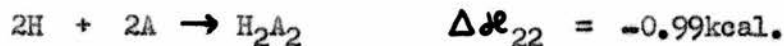
The values of  $\Delta H_{II}$ ,  $\Delta H_{12}$ , and  $\Delta H_D$  were then refined by successive approximations, using Eq. (4-60) from which the following values were obtained

$$\Delta H_{II} = -0.72 \pm 0.02 \text{ kcal.} \quad \Delta H_D = 0.45 \pm 0.02 \text{ kcal.} \quad (4-67)$$

$$\Delta H_{12} \approx 0.3 \text{ kcal.} \quad \frac{L_T}{A_T} = -0.46 \text{ kcal.}$$

The values of  $\Delta H_{12}$  increase slightly with concentration of  $HA_2$  and hence the value of 0.3 kcal. is approximate. This drift may be due to slight errors either in the analyses of solutions or in the equilibrium constants.

The values of  $\Delta H$  for the following reactions may now be calculated



The free energy change  $\Delta G$  and the entropy change  $\Delta S$  are related to the corresponding equilibrium constant by Eqs. (4-68) and (4-69) respectively, thus

$$\Delta G = -2.303RT \log K \quad (4-68)$$

$$\Delta S = 2.303R \log K + \frac{\Delta H}{T} \quad (4-69)$$

The values of the equilibrium constants and the corresponding values of  $\Delta G$ ,  $\Delta H$ , and  $\Delta S$  are summarised in Table 4-11.

TABLE 4-11

Thermodynamic functions for the acetic acid system in 3.00M sodium perchlorate at 25.00°C.

Reaction	Log (equilibrium constant)	$\Delta G$ kcal. mole <sup>-1</sup>	$\Delta H$ kcal. mole <sup>-1</sup>	$\Delta S$ cal. mole <sup>-1</sup> deg. <sup>-1</sup>
H+A → HA	+5.014	- 6.84	-0.72	+20.5
HA+A → HA <sub>2</sub>	-0.34	+ 0.46	+0.3	- 0.55
H+2A → HA <sub>2</sub>	+4.67	- 6.37	-0.42	+20.0
2HA → H <sub>2</sub> A <sub>2</sub>	-0.73	+ 1.00	+0.45	- 1.83
H+HA <sub>2</sub> → H <sub>2</sub> A <sub>2</sub>	+4.63	- 6.32	-0.57	+19.3
2H+2A → H <sub>2</sub> A <sub>2</sub>	+9.30	-12.69	-0.99	+39.2

4(c) DISCUSSION

The values of the equilibrium constants obtained for the four acids are tabulated in Table 4-12. This table also contains the equilibrium constants for higher aliphatic acids and for substituted acetic acids studied by Clarke and Rossotti<sup>214</sup>, and by Carson and Rossotti<sup>201</sup> respectively. The value of  $\beta_{II}^H$  tabulated is the value obtained using Eq. (4-8). The constants for iso-butyric acid have been evaluated on the assumption that successive association constants are equal [Hypothesis I, Sec. 2 (b), Eq. (2-76)]. Constants for pivalic acid and valeric acid were calculated using Hypotheses I-IV in Sec. 2 (b) and the tabulated values are the average of those obtained using these hypotheses.

The values of  $\beta_{II}^H$  are in the order of decreasing inductive effect of the substituent group except in the cases of phenylacetic acid, where hyperconjugation affects the strength of the acid, and propionic acid. Propionic acid is slightly weaker than n-butyric and iso-butyric acids. Dippy<sup>215</sup> has suggested that the terminal methyl group of butyric acid may interact with the carboxyl group forming a hydrogen bond thus:

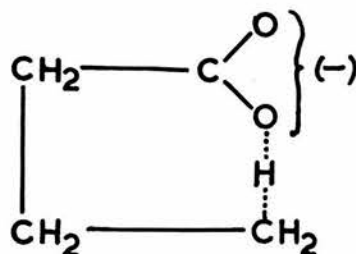


TABLE 4-12

Equilibrium constants for various carboxylic acid systems in 3.00M sodium perchlorate at 25.00°C.

Acid	Formic	Acetic	Pro- pionic	n- Butyric	iso- Butyric	Pivalic	Valeric	Cyano- acetic	Chloro- acetic	Phenyl- acetic	glycol- lactic	Methoxy- acetic
$\log \beta_{11}^H$	3.90	5.01	5.16	5.13	5.15	5.33	5.17	2.63	3.02	4.56	3.92	3.73
$\log \beta_{12}^H$	3.40	4.67	4.81	4.89	4.88	5.19	5.07	2.23	2.66	4.66	3.39	3.45
$\log \beta_{22}^H$	6.56	9.30	9.82	10.09	10.03	10.51	10.23	4.50	5.33	8.87	6.55	6.84
$\log \beta_{23}^H$	9.3		9.8	10.2	9.76	10.33	10.09					
$\log \beta_{33}^H$			14.5	15.0	14.91	15.66	15.26					
$\log \beta_{34}^H$					14.64	15.44	15.09					
$\log \beta_{44}^H$					19.79	20.76	20.25					
$\log K_{12}$	-0.50	-0.34	-0.35	-0.24	-0.27	-0.14	-0.10	-0.40	-0.36	+0.10	-0.53	-0.28
$\log K_{22}$	3.16	4.63	5.01	5.11	5.15	5.32	5.16	2.26	2.67	4.21	3.16	3.39
$\log K_{23}$			0.0	+0.2	-0.27	-0.18	-0.14					
$\log K_{33}$			4.7	4.8	5.15	5.23	5.20					
$\log K_D$	-1.24	-0.73	-0.50	-0.26	-0.27	-0.14	-0.10	-0.77	-0.71	-0.25	-1.29	-0.62
$\log K_{11}$			-1.0	-0.4	-0.54	-0.33	-0.22					
$\log \chi$	-0.24	-0.04	+0.20	+0.22	+0.27	+0.13	+0.09	+0.03	+0.01	-0.45	-0.23	-0.06
$\log \frac{K_{22}}{K_{11}}$	-0.74	-0.38	-0.15	-0.02	0.00	-0.01	-0.01	-0.37	-0.35	-0.35	-0.76	-0.34
$\log \frac{K_{11}}{K_D}$			-0.48	-0.13	-0.27	-0.19	-0.12					

There is thus some stabilisation of the anion causing  $\beta_{II}^H$  to fall. However, from a consideration of free energy and entropy changes of ionisation, Everett and co-workers<sup>216</sup> believe that propionic acid, not n-butyric acid, is anomalous. They find that there are smooth relationships in the series of acids between these quantities and chain length, but propionic acid, not n-butyric acid, deviates from these relationships.

The value of  $\beta_{II}^H$  for acetic acid has been measured at various ionic strengths, I, in sodium perchlorate media, by several workers. A plot of  $\log \beta_{II}^H$  against  $\sqrt{I}$  is shown in Fig. 420. The full line is the theoretical curve calculated by Ellilä<sup>217</sup>. A value of  $\log \beta_{II}^H = 5.025$  in a 3.00M sodium perchlorate medium has now been calculated from his data. This value agrees well with the value measured in this work. Unfortunately, there are insufficient data to give similar plots for the other acids.

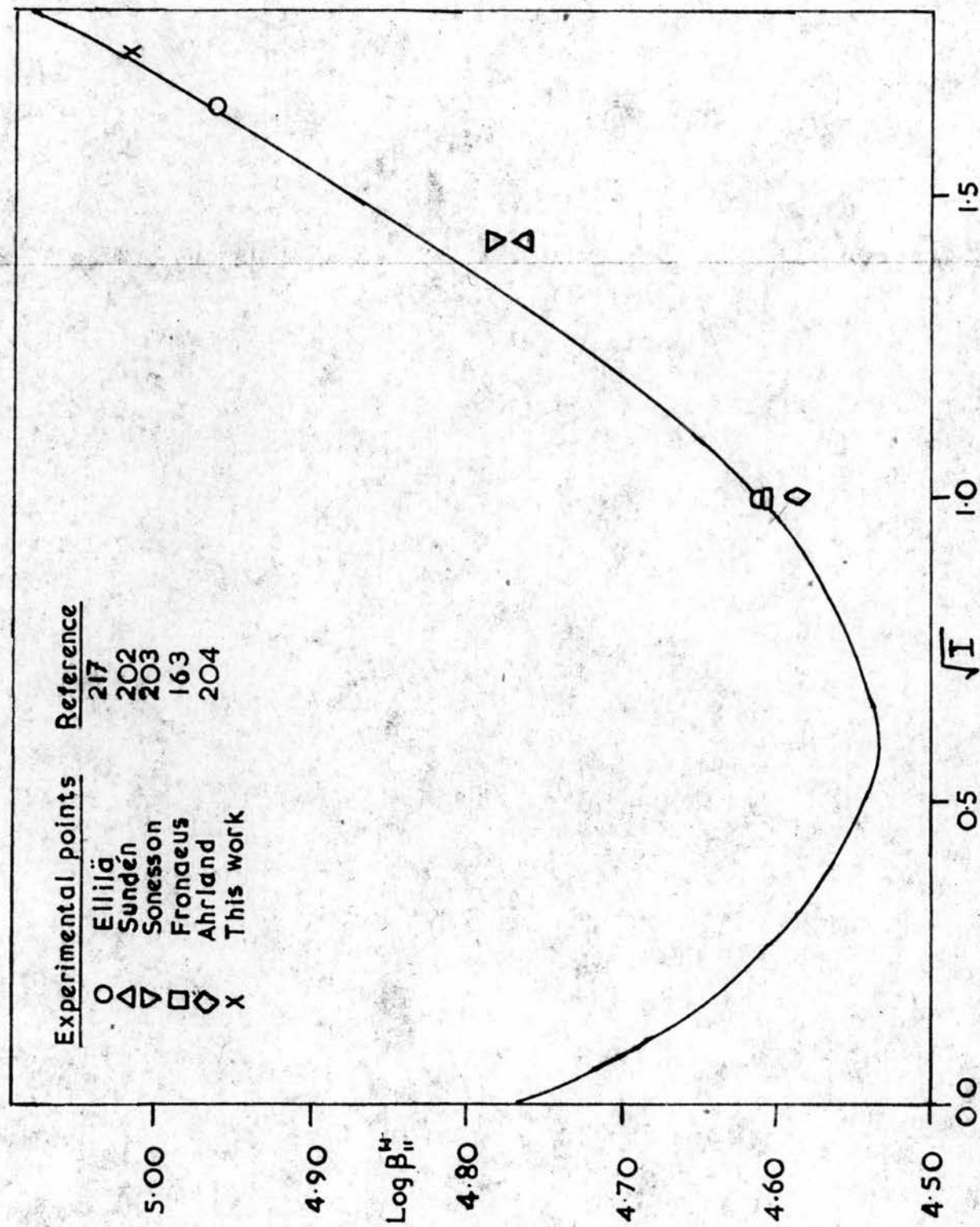
In the distribution curves, Figs. 4.4, 4.6, 4.9, 4.11, the maximum value of  $\alpha_{12}$  is about 0.10-0.12 at  $A = 700\text{mM}$  in each system. This maximum always occurs at a pH about  $\log \beta_{II}^H + 0.1$ . The neutral dimer  $H_2A_2$  is not formed appreciably until  $\alpha_{12}$  is about 0.05 i.e. at a pH about  $\log \beta_{II}^H + 0.5$ . Thereafter  $\alpha_{22}$  increases steadily with decrease in pH to a maximum. At  $A = 700\text{mM}$  the maximum values of  $\alpha_{22}$  are: formic acid, 0.067, (pH2); and acetic acid, 0.177, propionic acid, 0.247, n-butyric acid, 0.327, all at pH3. At these pH's the rest of the solution is composed almost entirely of monomeric HA with small amounts ( $< 1\%$ ) of a and  $HA_2$ .



Fig 4.20

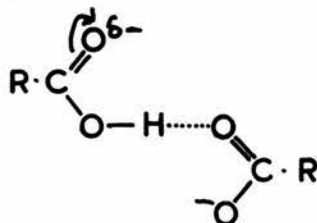
ACETIC ACID

Variation of  $\log \beta_{II}^H$  with ionic strength of the sodium perchlorate medium.  
The full line is the theoretical curve calculated after Ellilä (ref.217).



Evidence for the formation in solution of the hydrogen dicarboxylate ion  $\text{HA}_2$  has not been found previously except by Kolthoff and Bosch<sup>218</sup> who identified the hydrogen dibenzoate ion in aqueous solution. Speakman and co-workers have carried out X-ray diffraction measurements on several potassium hydrogen bicarboxylate crystals<sup>219-224</sup>. The dimer  $\text{HA}_2$  may be considered to be the chief structural unit in every acid salt investigated at Glasgow except the disalicylate and the p-nitrobenzoate. The hydrogen bond in all these salts except one<sup>224</sup> appears to be about 2.6-2.7 Å in length and to be symmetrical, at least statistically. The one exception is sodium hydrogen diacetate<sup>224</sup> where the  $\text{O} \cdots \text{H} \cdots \text{O}$  distance is  $2.40 \pm 0.03 \text{ Å}$ . This appears to be one of the shortest hydrogen bonds between oxygen atoms to have been measured with any precision and to come into the range where genuine, and not merely statistical, symmetry might be expected. A neutron diffraction study of potassium hydrogen bisphenylacetate<sup>225</sup> has yielded further evidence for a symmetrical hydrogen bond. Thus, some doubt is thrown on the interpretation of the infrared spectrum of this salt by Davies and Thomas<sup>226</sup> that the hydrogen bond is unsymmetrical. The dimeric ion  $\text{HA}_2$  exists in the extended form in these salts. As mentioned previously [Sec. 1(c)], crystalline formic and acetic acids exist as infinite chains in the extended form.

In solution, free rotation is possible about the hydrogen bond, but the ions  $\text{HA}_2$  are expected to exist predominantly in the extended form owing to electrostatic repulsion between the partial negative charges on the two carboxyl groups



The neutral dimers,  $H_2A_2$ , of these acids may exist in the extended form suggested by Fénéant<sup>86,92</sup>, in the cyclic form which occurs in the vapour state, or as an equilibrium mixture of the two forms. It can be seen in Table 4-12 that the values of  $K_{22}$  are also in the order of the inductive effect of the substituents. The inductive effect appears, therefore, to have a considerable bearing on the strength of the dimer.

The dimers are stronger acids than the monomers, though decreasingly so as the alkyl chain lengthens. This is illustrated by the trend in  $\frac{K_{22}}{K_{11}}$

as the series is ascended and it suggests that the structure of the dimer is the open form since the dissociation of the cyclic form to  $HA_2$  requires the rupture of a hydrogen bond. The value of  $\frac{K_{22}}{K_{11}}$  is almost zero for isobutyric, pivalic, and valeric acids but this is a result of the assumptions made in the calculation of the constants<sup>214</sup>. The value of  $\frac{K_{22}}{K_{11}}$  for the substituted acetic acids, except glycollic acid, is almost constant. Evidently substitution in acetic acid has little effect on the relative acidities of the monomer and dimer though the values of  $\beta_{11}^H$  and  $K_{22}$  may themselves be reduced by as much as  $10^{2.4}$ . Glycollic acid is an exception in this respect among the substituted acetic acids and it may be noted that the equilibrium constants for this acid and formic acid are identical within experimental error.

The enhanced stability conferred on a complex by ring formation is called the "chelate effect". A measure of this effect in these acids is provided by the equilibrium constant,  $\chi$ , for the reaction



The chelate effect is small.  $\log \chi$  is smallest for phenylacetic acid and within experimental error it is the same for acetic, cyanoacetic, chloroacetic,

and methoxyacetic acids.  $\log \chi$ , together with  $\frac{K_{22}}{K_{11}}$ , increases as the series of acids is ascended from formic to iso-butyric acids possibly indicating increasing stabilization of the cyclic dimer.

The thermodynamic data for acetic acid in Table 4-11 provide more evidence for the structure of the dimer. The heat and entropy changes for the formation of monomeric acetic acid have been measured before. Earlier workers found that in aqueous solution  $\Delta H \sim +0.10 \text{ kcal.}$  and  $\Delta S \sim +22.0 \text{ cal. mole}^{-1} \text{ deg.}^{-1}$  <sup>227</sup>. The change in medium in the present work to 3.00M sodium perchlorate appears to have had little effect on the values of  $\Delta H$  and  $\Delta S$ . The value of  $\Delta S$  is close to that predicted by Pitzer's rule for weak acids. Pitzer <sup>228</sup> found, both experimentally and from rough theoretical considerations, that the entropy change on the formation of monomeric weak acids was always about  $22 \text{ cal. mole}^{-1} \text{ deg.}^{-1}$ . It might be thought that the entropy change in this reaction should be negative but this is not so since the water molecules have greater freedom in the field around the molecule HA than they have in the field of the ions, H and A <sup>229</sup>.

The formation of  $\text{HA}_2$  from HA and A, and the dimerisation reaction are both endothermic and accompanied by loss of entropy which are unfavourable conditions for complex formation. This is the first time that these heats of reaction have been measured apart from some work by Davies and Griffiths <sup>96</sup> who found  $\Delta H$  for the dimerisation reaction to be zero. The entropy change for the reaction



is of some interest. This is a similar reaction to the reaction



and the experimental value of  $\Delta S$  is close to that predicted by Pitzer's

rule. However, if the structure of this dimer were the cyclic form  $\Delta S$  for reaction (4-71) would be less positive than  $\Delta S$  for reaction (4-72). It is possible to calculate the entropy change for these reactions using relationships derived by Cobble<sup>230</sup>. For neutral solutes

$$S^\circ(L) = 10 + 1.5R \ln M + 9.2N' - S_g^\circ - 0.22V \quad (4-73)$$

where  $S^\circ(L)$  = the standard entropy of the ligand on the molal scale

$M$  = the molecular weight

$N'$  = the total number of atoms excluding hydrogen

$S_g^\circ$  = an empirical structure factor

$V$  = molar volume in the pure liquid state at 25°C.

For charged organic ligands Cobble suggests a differential form of Eq. (4-73)

$$dS^\circ(L) = 1.5R d \ln M + 9.2 dN' - dS_g^\circ - 0.22 dV \quad (4-74)$$

Thus the entropy of some member of a series may be calculated from another simpler member by adding the entropy calculated using Eq. (4-74) for their <sup>in</sup> differences/structure, number of atoms, and molar volumes. Cobble has listed 54 compounds for which the observed and calculated values of  $S^\circ(L)$  agree to within  $\pm 3$  E.U. The value of  $S_{gS}^\circ$  for a double bond is +3.5 E.U. and for ring formation is +14 E.U. The value of  $S^\circ(L)$  for acetic acid monomer is +43 E.U. Cobble calculates 39 E.U. but this value appears to be erroneous. The value of  $S^\circ(L)$  for the open and cyclic forms of acetic acid dimer are +65.3 E.U. and +51.3 E.U. respectively. Now the entropy change for reaction (4-72) is

$$\Delta S_{11} = S^\circ(HA) - S^\circ(A) - S^\circ(H) \quad (4-75)$$

The value of  $S^\circ(A)$  is 20.8 E.U.<sup>230</sup> and the value of  $S^\circ(H)$  may be assumed to be 0.0 on the molal scale. Hence the calculated value of  $\Delta S$  for reaction (4-72) is 22.6 E.U. which compares well with the observed value of +20.5 E.U.



The value of  $\Delta S$  for reaction (4-71) is

$$\Delta S_{12} = S^\circ(H_2A_2) - S^\circ(HA_2) - S^\circ(H) \quad (4-76)$$

The calculated value of  $S^\circ(HA_2)$  using Eq. (4-74) is 43.4. If the cyclic form of  $H_2A_2$  is formed, then  $\Delta S_{12}$  is +7.9 E.U. whereas the formation of the open dimer leads to  $\Delta S_{12}$  of +21.9 E.U. The latter value agrees very well with the experimental value of +19.3 E.U.

Thus, there is substantial evidence that at least in acetic acid the open form of the neutral dimer  $H_2A_2$  plays an important part in the equilibria. Similar calorimetric measurements on the other acids might well yield further evidence about the structures of their neutral dimers. The calculated +22.3 E.U. in propionic acid, and +22.1 E.U. in n-butyric acid entropy change,  $\Delta S_{12}$ , for reaction (4-71) is +20.0 E.U. in formic acid, if the open form of  $H_2A_2$  is the main species present. In each case,  $\Delta S_{12}$  is 14 E.U. less than the values above if the cyclic dimer is formed. It is possible to calculate  $\Delta G$  for reaction (4-71) by substituting the value of  $K_{12}$  in Eq. (4-68). Then by substituting  $\Delta G$  and the above values of  $\Delta S$  in Eq. (4-69), a rough value of  $\Delta H_{12}$  may be calculated. The values of  $\Delta H_{12}$  calculated for the formation of the open and cyclic form respectively are (in kcal.): +1.65 and -2.52 for formic acid, +0.21 and -3.97 for acetic acid, -0.18 and -4.36 for propionic acid, -0.38 and -4.56 for n-butyric acid. The experimental value for acetic acid was -0.57 kcal. (Table 4-11) which is of the same order as the calculated value for the open form. These calculations provide further evidence for the existence of the open form of the dimer in propionic and n-butyric acids. The formation of the cyclic dimer would be accompanied by a heat change of totally different magnitude from that observed in acetic acid but as the three acids are closely related such a large heat change would appear to be rather improbable.



The assumptions made about the relationships between successive constants in the iso-butyric, pivalic, and methoxyacetic acid systems restrict discussion of the results for the trimers and tetramers. However, no such assumptions were made in the propionic and n-butyric acid systems and it can be seen from the values of  $K_{33}$  that the trimers are stronger acids than the dimers and monomers. The formation of the trimers  $H_2A_3$  and  $H_3A_3$  occurs more easily than the formation of  $HA_2$  and  $H_2A_2$ . This is shown by the fact that  $K_{23} > K_{12}$  and that  $\frac{K_T}{K_D}$ , the equilibrium constant for the reaction



is greater than  $K_D$ . This might be expected since the entropy loss for reaction (4-77) is less than that for the dimerisation of HA, for which  $K_D$  is the equilibrium constant. In the latter reaction, two monomer molecules lose some orientations whereas in reaction (4-77) one monomer only is added to the dimer<sup>231</sup>. The formation of the higher complexes  $H_2A_3$ ,  $H_3A_3$ , etc., is only possible through the extended form of  $H_2A_2$ . In general, the acids tend to polymerise more as the alkyl chain lengthens, pivalic and n-valeric acids being the most polymerised of the series.

SECTION 5.

METAL-CARBOXYLATE EQUILIBRIA IN WATER.

5 (a) POTENTIOMETRIC TITRATION RESULTS.

A precise equilibrium study has been made of copper(II) carboxylate systems in an attempt to obtain evidence for the existence of dinuclear and polynuclear complexes in aqueous solution. Since the carboxylate ligands are conjugate bases of weak acids the experimental approach was to follow the competition between protons and copper(II) ions for the carboxylate ions. In these systems, at least two buffers of the carboxylic acid and its sodium salt were usually titrated with three solutions of metal ion of concentrations between  $1 \times 10^{-2} M$  and  $1 \times 10^{-1} M$ . The data for a typical metal-carboxylate titration, performed as described in Sec. 3(c), are given in full in Table 5-1.

TABLE 5-1.

Experimental data for a typical metal-carboxylate titration.

Copper(II) formate.

B = 100.0mM

Composition of buffer: [HA] = 655.4mM  
[NaA] = 3000mM

V<sub>A</sub> = volume of buffer added.

E<sub>0</sub> = 261.1mV.

V <sub>A</sub> (ml)	V <sub>T</sub> (ml)	C <sub>NaA</sub> (mM)	C <sub>HA</sub> (mM)	C <sub>H</sub> <sup>+</sup> (mM)	E mV	pH	h (mM)	n <sub>H</sub>	a(mM)	-log a	n̄
0.00	39.40	0.00	0.00	1.546	249.2	2.811	1.546		0.00	3	0.00
0.05	39.50	3.797	0.8296	1.544	281.0	3.336	0.461		0.5405	3.267	0.022
0.10	39.60	7.576	1.655	1.543	294.2	3.560	0.276		1.353	2.869	0.050
0.20	39.80	15.08	3.293	1.540	305.1	3.744	0.180		3.258	2.487	0.105
0.40	40.20	29.85	6.522	1.534	311.2	3.847	0.142	0.531	6.972	2.157	0.215
0.60	40.60	44.34	9.686	1.523	314.4	3.901	0.126	0.500	10.72	1.970	0.319
1.00	41.40	72.46	15.83	1.517	318.8	3.975	0.106	0.456	20.45	1.689	0.505
1.50	42.40	106.1	23.19	1.503	322.0	4.029	0.093	0.423	33.29	1.478	0.812
2.00	43.40	138.3	30.20	1.490	324.8	4.077	0.084	0.398	47.34	1.325	0.890
2.50	44.40	168.9	36.90	1.478	327.2	4.117	0.076	0.378	62.30	1.206	1.045
3.00	45.40	198.2	43.31	1.466	329.2	4.151	0.071	0.362	77.71	1.110	1.181
4.50	48.40	278.9	60.94	1.276	334.0	4.232	0.059	0.321	129.0	0.889	1.524
6.00	51.40	350.2	76.51	1.207	337.2	4.286	0.052	0.301	176.3	0.754	1.687
7.00	53.40	393.3	85.92	1.165	339.0	4.317	0.048	0.289	208.8	0.680	1.780
8.00	55.40	433.2	94.64	1.127	340.4	4.340	0.046	0.280	239.6	0.621	1.860
10.00	59.40	505.1	110.3	1.057	342.2	4.371	0.043	0.267	296.3	0.528	1.983
12.00	63.40	567.8	124.1	0.996	344.0	4.401	0.040	0.256	351.0	0.455	2.036
14.00	67.40	623.2	136.1	0.943	345.2	4.422	0.038	0.250	396.2	0.402	2.111
17.00	73.40	694.8	151.8	0.873	346.7	4.447	0.036	0.241	461.6	0.336	2.133
20.00	79.40	755.7	165.1	0.815	347.8	4.466	0.034	0.237	511.5	0.291	2.209

The preliminary acid-base titration was continued till the pH of the solution was about 1 pH unit below the pH of the buffer. When the buffer and metal ion solution were added the pH slowly increased with increasing carboxylate concentration toward that of the buffer. Titrations were stopped when precipitation occurred or when large increments of buffer produced only small changes in potential. The term  $C'_H$  is the amount of perchloric acid present in solution, which although small, is usually significant. It arises from the unneutralised acid in the preliminary acid-base titration and from the acid present in the metal ion solution. The values of  $\bar{n}$  and  $a$  were calculated in the following way.

In the titrations under discussion metal ions and protons compete for carboxylate ions. At  $(A - \bar{n}B) \ll 50\text{mM}$  the only species present are metal-carboxylate complexes, free carboxylate ions, free protons, and the species HA. Provided that mixed species eg.  $B(HA_2)$  are not formed Eq. (2-17) reduces to

$$H = h + \beta_{11}^H ha \quad (5-1)$$

whence

$$a = \frac{H - h}{\beta_{11}^H h} \quad (5-2)$$

The value of  $\bar{n}$  may be calculated using Eq. (1-4).

$$\bar{n} = \sum_{n=1}^{n=N} n[BA_n]/B$$

The term  $\sum_{n=1}^{n=N} n[BA_n]$  is the amount of carboxylate ion bound to metal. Thus

Eq. (2-15) may be written

$$A = a + \beta_{11}^H ha + \bar{n}B \quad (5-3)$$

Substituting Eq. (5-2) into Eq. (5-3) we obtain

$$A = a + H - h + \bar{n}B \quad (5-4)$$

whence

$$\bar{n} = \frac{A - a - H + h}{B} \quad (5-5)$$

When  $50\text{mM} \leq (A - \bar{n}B) \leq 700\text{mM}$  the species present in solution are the metal carboxylate complexes, free carboxylate ions, free protons,  $\text{HA}$ ,  $\text{HA}_2$ , and  $\text{H}_2\text{A}_2$ . Eq. (2-15) may be written

$$A = a + \beta_{11}^H ha + 2\beta_{12}^H ha^2 + 2\beta_{22}^H h^2 a^2 + \bar{n}B \quad (5-6)$$

Combining Eq. (1-9) and Eq. (5-6) we obtain

$$A - \bar{n}B = \frac{H - h}{\bar{n}_H} \quad (5-7)$$

Assuming again that mixed species are not formed we have

$$H = h + \beta_{11}^H ha + \beta_{12}^H ha^2 + 2\beta_{22}^H h^2 a^2 \quad (2-17)$$

Subtracting Eq. (2-17) from Eq. (5-6) we obtain

$$A - \bar{n}B - H = a - h + \beta_{12}^H ha^2 \quad (5-8)$$

whence

$$a = \frac{-1 + \sqrt{1 + 4\beta_{12}^H(A - \bar{n}B - H + h)h}}{2\beta_{12}^H h} \quad (5-9)$$

For each experimental point,  $\bar{n}$  and  $a$  are evaluated by successive approximations, using Eqs. (5-7) and (5-9) and the appropriate value of  $\bar{n}_H(\log)_A$ . It was sometimes necessary to obtain the latter by a short graphical interpolation from the experimental data.

The experimental data for these metal-carboxylate titrations have been summarised in Tables 5-2 to 5-4, 5-6, and 5-7, and plotted in the form  $\bar{n}(\log)_B$  in Figs. 5-1, 5-5, 5-7 to 5-9. The shape of these curves can supply information about the complexes present. If the formation curve rises to a plateau at an integral

value,  $N$ , of  $\bar{n}$  then the highest complex formed is  $BA_N$ . However, it is often impossible to reach such a plateau so that the number of complexes present is not immediately evident from an inspection of the formation curve. For instance, in the case of copper(II) formate, Fig. 5.1, the maximum value of  $\bar{n}$  obtainable was 2.2 indicating that the highest complex is at least  $BA_3$ . Within the limits of the experimental data this formation curve gives no indication of forming a plateau. In some systems, the formation curve may form a plateau at say  $\bar{n} = 1$ , with  $\bar{n}$  remaining constant for a range of  $\log a$  and then the curve may rise to form another plateau at  $\bar{n} = 2$ . This type of behaviour indicates that the first complex is very much stronger than the second and  $K_1 \gg K_2$ .

The formation curve,  $\bar{n}(\log a)_B$  may sometimes be a function of the metal ion concentration,  $B$ . This indicates<sup>179</sup> that polynuclear species of the type  $BRA_Q$  are present, where  $R$  and  $Q$  are integers and  $R \gg 2$ .

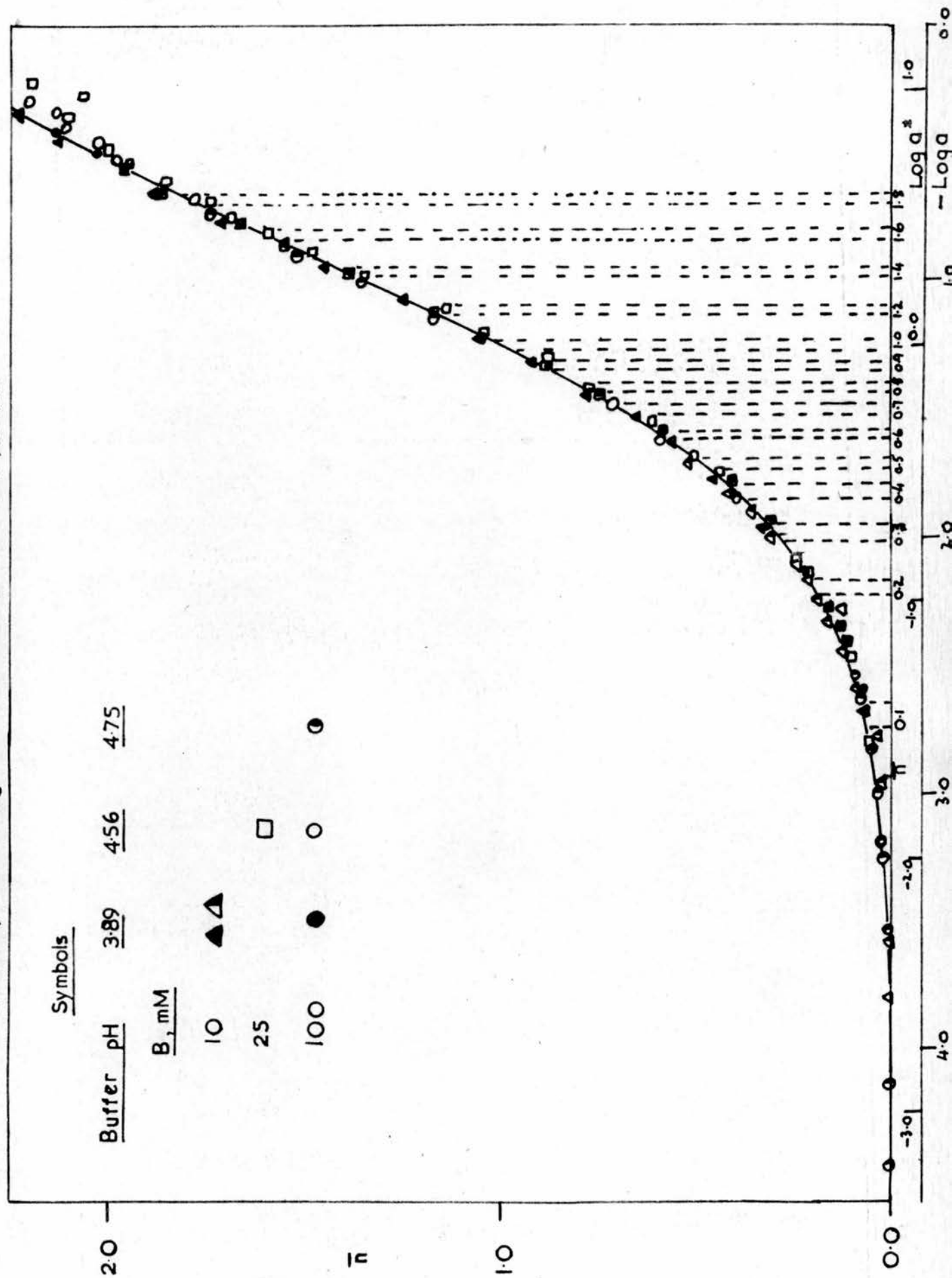
In the present work the equilibria between copper(II) ions and formate, acetate, propionate, and n-butyrate ions were studied. The cadmium(II) acetate system was also investigated as polynuclear species have been reported in solution<sup>178</sup>. The metal ion concentration,  $B$ , in a titration was kept constant between  $1 \times 10^{-2} M$  and  $1 \times 10^{-1} M$ . Thus, at most, the metal ion composed 3.3% of the ionic medium and under these conditions the activity coefficients of all species appear to remain constant<sup>196</sup>. Generally, the carboxylic acid - sodium carboxylate buffers used had pH between 4 and 5. The metal ions would meet intense competition from protons for the carboxylate ions in buffers of  $pH < 4$ . On the other hand, buffers with  $pH > 5$  could not be used since the Cu(II) ion begins to hydrolyse<sup>232</sup> between pH 4 and 5. The systems studied will now be considered separately.



**Fig 5-1** FORMATION CURVE FOR COPPER(II) FORMATE

The projection strip is on the abscissa.

For clarity about 25% of the data have not been plotted.



Copper(II) formate.

In this system titrations were made using buffers of pH 3.89, 4.56, and 4.75. (These figures refer to buffer solutions with  $A \leq 50\text{mM}$ ). The metal ion concentrations used were 0.010M, 0.025M, and 0.100M. The experimental data are summarised in Table 5-2. The range of concentration of free formate ion was  $3.5 \times 10^{-5}\text{M}$  to 0.5M. Precipitation did not occur during or after a titration.

TABLE 5-2.Copper(II) formate.

Experimental data  $\bar{n}(\log a)_B$  obtained from potentiometric titrations of metal ion solutions and formate buffers.

B(mM)	10				25	
	3046 3000		3046 3000		655.4 3000	
Buffer [HA]mM [NaA]mM	$\bar{n}$	$-\log a$	$\bar{n}$	$-\log a$	$\bar{n}$	$-\log a$
	0.068	2.679				
	0.126	2.283	-0.006	3.803	0.053	2.795
	0.246	2.109	0.000	3.583	0.114	2.419
	0.331	1.972	0.009	3.203	0.244	2.094
	0.460	1.775	0.024	2.960	0.444	1.752
	0.564	1.637	0.036	2.784	0.616	1.554
	0.651	1.532	0.053	2.663	0.774	1.419
	0.782	1.452	0.090	2.601	0.882	1.308
	0.926	1.321	0.124	2.446	1.139	1.118
	1.051	1.221	0.163	2.338	1.352	0.989
	1.250	1.075	0.193	2.247	1.485	0.888
	1.452	0.966	0.219	2.171	1.592	0.809
	1.550	0.852	0.255	2.113	1.744	0.688
	1.718	0.766	0.311	2.012	1.822	0.618
	1.883	0.660	0.361	1.910	2.000	0.476
	2.132	0.452	0.421	1.834	2.108	0.358
	2.243	0.371	0.522	1.718	2.064	0.279
					2.195	0.226

Table 5-2 (continued)

B(mM) Buffer [HA]mM [NaA]mM	100					
	3046 3000		655.4 3000		428.2 3000	
	$\bar{n}$	$-\log a$	$\bar{n}$	$-\log a$	$\bar{n}$	$-\log a$
	0.020	3.199	0.022	3.267	0.001	4.459
	0.048	2.834	0.050	2.869	0.002	4.142
	0.074	2.604	0.105	2.487	0.009	3.540
	0.103	2.471	0.215	2.157	0.019	3.246
	0.130	2.365	0.319	1.970	0.035	3.000
	0.158	2.278	0.505	1.689	0.060	2.803
	0.211	2.137	0.712	1.478	0.081	2.632
	0.313	1.935	0.890	1.325	0.101	2.537
	0.409	1.791	1.045	1.206	0.129	2.427
	0.589	1.592	1.181	1.110	0.163	2.315
	0.750	1.447	1.524	0.889	0.184	2.261
	0.890	1.330	1.687	0.754	0.227	2.136
	1.041	1.212	1.780	0.680	0.318	1.982
	1.170	1.116	1.860	0.621	0.401	1.850
	1.391	0.974	1.983	0.528	0.593	1.618
	1.553	0.865	2.036	0.455	0.770	1.462
	1.666	0.777	2.111	0.402	0.920	1.334
	1.868	0.657	2.133	0.336	1.171	1.144
	1.962	0.566	2.209	0.291	1.359	1.001
	2.027	0.499			1.523	0.896
	2.141	0.410			1.744	0.738
					1.873	0.623
					1.955	0.538

The formation curve (Fig. 5-1) is independent of metal ion concentration showing that the complexes formed are homonuclear. Since the concentration of metal ions used is small it seems reasonable to assume that these complexes are mononuclear. The formation curve does not form a plateau and the value of  $\bar{n}$  rises to 2.2. This indicates that the complexes formed are  $BA$ ,  $BA_2$ , and  $BA_3$  at least.

The stability constants were calculated using two methods. The projection strip was first prepared, see Sec. 2(b), and it is shown along the abscissa of Fig. 5-1. The strip was fitted to the family of curves  $\log p(\log a^*)_{\bar{n}}$  [Sec. 2(b), p. 37] but since  $N > 2$  the fit is bad at  $\bar{n} > 1.1$  of Fig. 5-2. In the position of best fit,  $\log p = 0.29 \pm 0.02$ ,

Fig 5.2

COPPER(II) FORMATE

Projection strip(Fig5.1) superimposed on normalised curves  
 $\log p(\log a^*)_{\bar{n}}$ , Eq.(2-12), in the position of best fit.

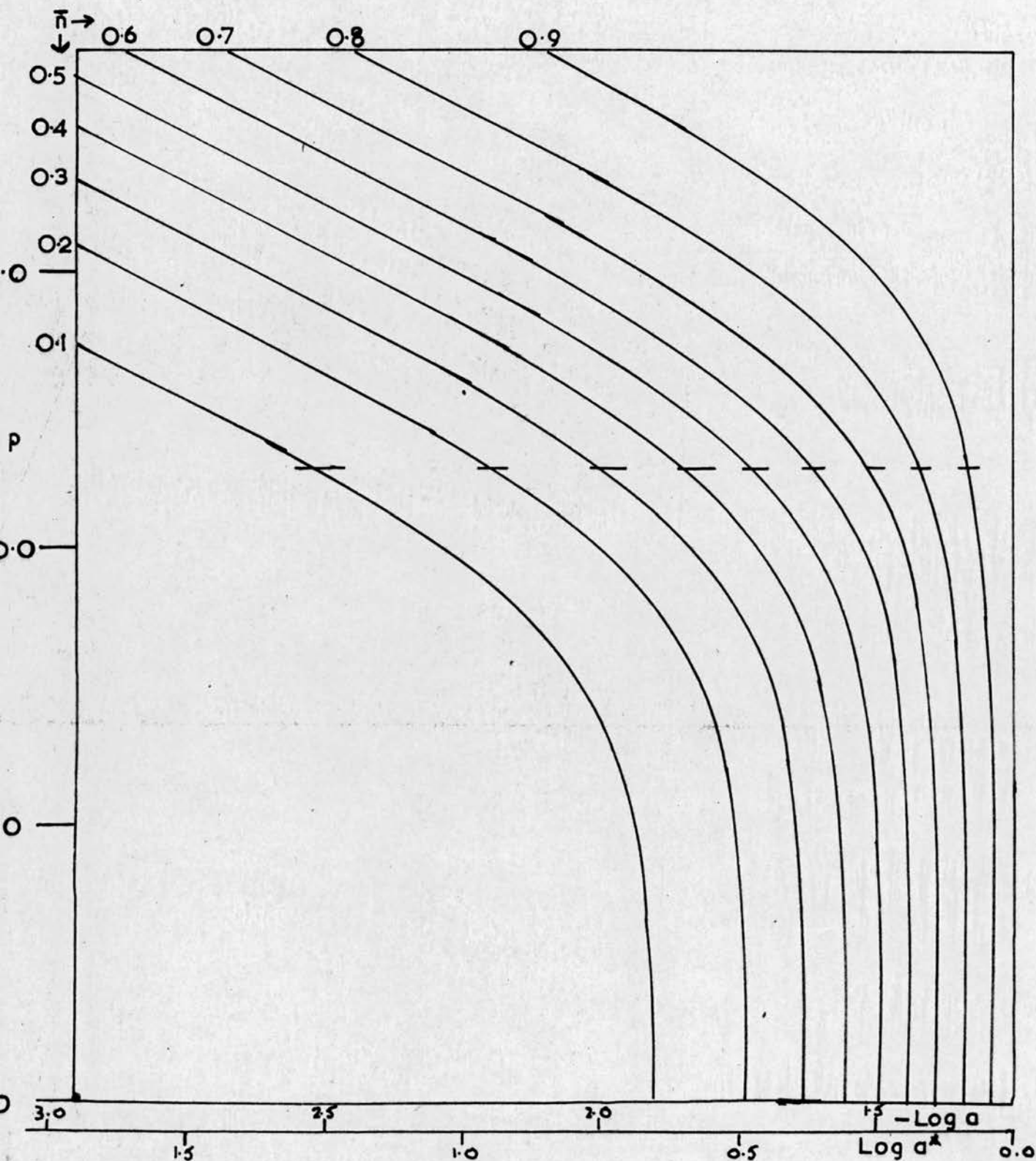
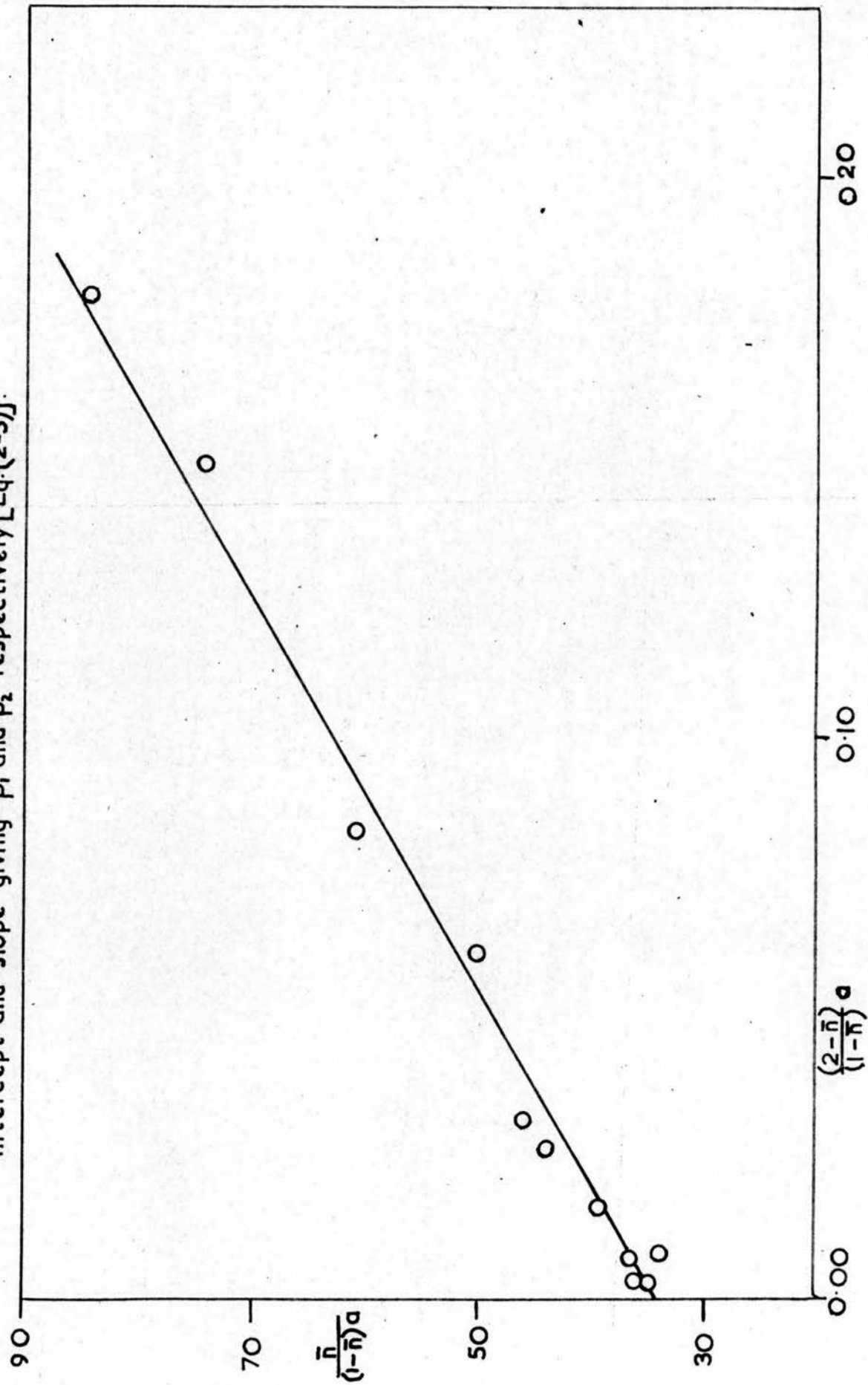


Fig 5.3

COPPER(II) FORMATE

First successive extrapolation in the evaluation of  $\beta_1, \beta_2, \dots, \beta_t$ .  
The best straight line is drawn through the experimental points, the intercept and slope giving  $\beta_1$  and  $\beta_2$  respectively [Eq. (2-5)].





and  $\log a^* - \log a = 1.25 \pm 0.02$ , and by substitution into Eqs. (2-11) and (2-10),

$$\begin{aligned}\log \beta_1 \beta_2^{-\frac{1}{2}} &= 0.29 \pm 0.02 \\ \log \beta_2^{\frac{1}{2}} &= 1.25 \pm 0.02\end{aligned}$$

whence

$$\log \beta_1 = 1.54 \pm 0.02_5, \quad \log \beta_2 = 2.50 \pm 0.02_5$$

Owing to the limit of the fit, these constants must be regarded as approximate.

The constants were refined using the successive extrapolations method of Rossotti and Rossotti<sup>182</sup> [Sec. 2 (a), p.34]. The first extrapolation is shown in Fig. 5-3, where the plot of  $\frac{\bar{n}}{(1-\bar{n})a}$  against  $\frac{(2-\bar{n})a}{(1-\bar{n})}$  gives

$\beta_1$  as intercept and  $\beta_2$  as slope. The value of  $\beta_3$  was refined in the third extrapolation where  $\left[ \frac{\bar{n} - (1-\bar{n})\beta_{1a}}{(2-\bar{n})a^2} - \beta_2 \right] / \frac{(3-\bar{n})}{(2-\bar{n})} a$

was plotted against  $\frac{(4-\bar{n})a}{(3-\bar{n})}$ . The slope of this plot was zero showing that

$\beta_4 = 0$ . The limits of error of the constants were estimated from the scatter of the points. The values of the stability constants are

$$\begin{aligned}\log \beta_1 &= 1.53 \pm 0.02_5 & \log K_2 &= 0.89 \pm 0.04 \\ \log \beta_2 &= 2.42 \pm 0.03 & \log K_3 &= 0.26 \pm 0.10 \\ \log \beta_3 &= 2.68 \pm 0.10\end{aligned}$$

If is possible to calculate a theoretical formation curve from these constants.

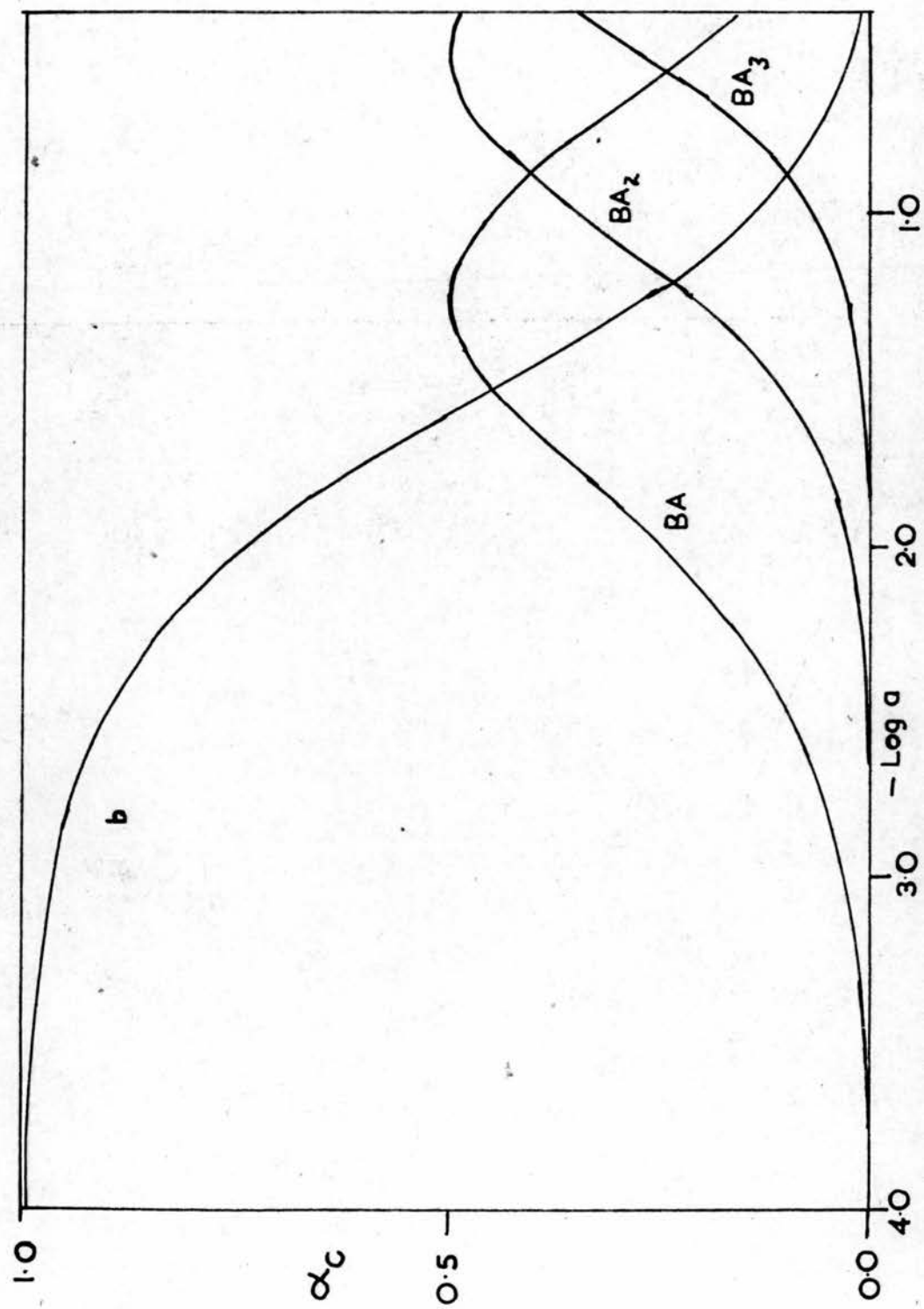
If the constants evaluated are those which best explain all the data then this curve should fit the plot of the data with high precision over the entire experimental range of  $\bar{n}$  and  $\log a$ . The curve is calculated using Eq. (1-5).



Fig 54

COPPER(II) FORMATE

Relative proportions of the species  $BA_n$  present in solution



$$\bar{n} = \frac{\sum_{n=1}^{n=3} n \beta_n a^n}{\sum_{n=0}^{n=3} \beta_n a^n}$$

$$= \frac{\beta_1 a + 2\beta_2 a^2 + 3\beta_3 a^3}{1 + \beta_1 a + \beta_2 a^2 + \beta_3 a^3} \quad (1-5a)$$

The full line of Fig. 5.1 is the theoretical formation curve which fits all the experimental data with high precision.

The fraction,  $\alpha_c$ , has been plotted against  $\log a$  in Fig. 5.4 . For a mononuclear complex

$$\alpha_c = \frac{BA_c}{b + BA + BA_2 + BA_3 + \dots + BA_N} = \frac{\beta_c a^c}{\sum_{n=0}^{n=N} \beta_n a^n} \quad (5-10)$$

#### Copper(II) acetate.

In this system titrations were made using buffers of pH 4.35, and 5.01, and solutions of metal ion of concentrations 0.025M, 0.050M, and 0.100M. The experimental data are summarised in Table 5-3. The range of concentration of free acetate ion was  $8.5 \times 10^{-6}M$  to 0.3M. Precipitation did not occur during a titration, but in some cases a precipitate was formed when titrated solutions were left overnight.

**TABLE 5-3.**

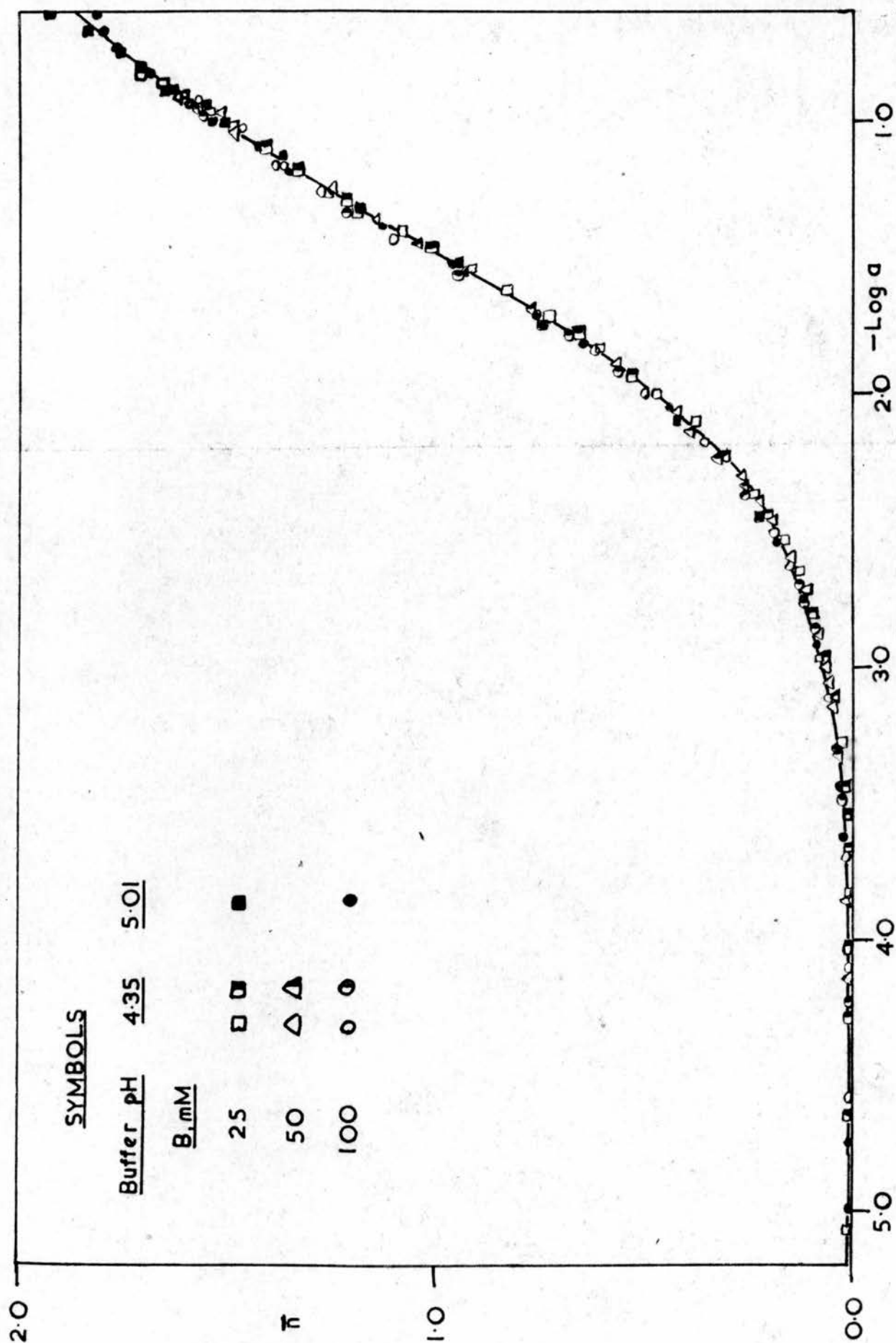
Copper(II) acetate.

Experimental data  $\bar{n}(\log a)_B$  obtained from potentiometric titrations of metal ion solutions and acetate buffers.

B(mM)		25		50		1000	
Buffer [HA]mM [NaA]mM	4260 918.3	4260 918.3	1951 1996	4260 918.3	4260 918.3	4260 918.3	4260 918.3
$\bar{n}$	$-\log a$	$\bar{n}$	$-\log a$	$\bar{n}$	$-\log a$	$\bar{n}$	$-\log a$
0.023	3.829	0.001	5.069	0.106	2.800	0.000	4.588
0.041	3.183	-0.008	4.649	0.218	2.450	0.003	4.113
0.070	2.959	-0.007	4.290	0.419	2.104	0.011	3.696
0.097	2.797	-0.005	4.030	0.742	1.748	0.021	3.452
0.122	2.678	-0.001	3.834	0.942	1.522	0.031	3.299
0.150	2.589	0.000	3.669	1.182	1.315	0.051	3.121
0.200	2.446	0.008	3.541	1.336	1.150	0.071	2.965
0.247	2.330	0.013	3.441	1.427	1.101	0.110	2.766
0.295	2.244	0.018	3.350	1.499	1.010	0.148	2.634
0.374	2.095	0.023	3.276	1.549	0.937	0.184	2.515
0.462	1.997	0.028	3.217	1.646	0.892	0.352	2.182
0.604	1.835	0.039	3.110	1.702	0.811	0.497	1.991
0.726	1.716	0.049	3.033	1.757	0.748	0.616	1.842
0.823	1.620	0.059	2.959	1.834	0.676	0.733	1.751
0.911	1.543	0.079	2.848	1.930	0.605	1.101	1.435
0.975	1.477	0.088	2.803			1.273	1.260
1.075	1.399	0.106	2.720			1.381	1.160
1.188	1.341	0.122	2.648			1.465	1.034
1.259	1.267	0.142	2.581			1.540	0.973
1.322	1.195	0.163	2.528			1.571	0.932
1.365	1.137	0.182	2.482				
1.407	1.091	0.200	2.440				
1.485	1.021	0.217	2.403				
1.537	0.969	0.232	2.369				
1.604	0.912	0.306	2.228				
1.657	0.872	0.527	1.925				
1.709	0.831	0.654	1.785				
		1.007	1.464				
		1.211	1.292				
		1.332	1.181				
		1.366	1.138				
		1.411	1.102				

Fig 55 FORMATION CURVE FOR COPPER(II) ACETATE

For clarity about 25% of the data have not been plotted



The formation curve (Fig. 5-5) is independent of B and it is assumed, therefore, that mononuclear complexes are present as in formic acid. As the curve does not seem to be forming a plateau at  $\bar{n} = 2$ , the complexes formed must be  $BA$ ,  $BA_2$ , and  $BA_3$  at least.

The stability constants were calculated in the same way as the copper(II) formate system. The projection strip could be fitted to the family of curves  $\log p(\log a^*)_{\bar{n}}$  up to  $\bar{n} = 1.5$ . In the position of best fit,  $\log p = 0.31 \pm 0.02$  and  $\log a^* - \log a = 1.48 \pm 0.01$ , and by substitution in Eqs. (2-11) and (2-10)

$$\log \beta_1 \beta_2^{-\frac{1}{2}} = 0.31 \pm 0.02$$

$$\log \beta_2^{\frac{1}{2}} = 1.48 \pm 0.01$$

Thus the approximate overall stability constants for the first two complexes are

$$\log \beta_1 = 1.79 \pm 0.025$$

$$\log \beta_2 = 2.96 \pm 0.015$$

These constants were refined by the method of successive extrapolations<sup>179</sup>.

The constants evaluated are

$$\log \beta_1 = 1.79 \pm 0.025$$

$$\log \beta_2 = 2.94 \pm 0.03$$

$$\log \beta_3 = 2.64 \pm 0.20$$

$$\log K_2 = 1.15 \pm 0.04$$

$$\log K_3 = -0.30 \pm 0.20$$

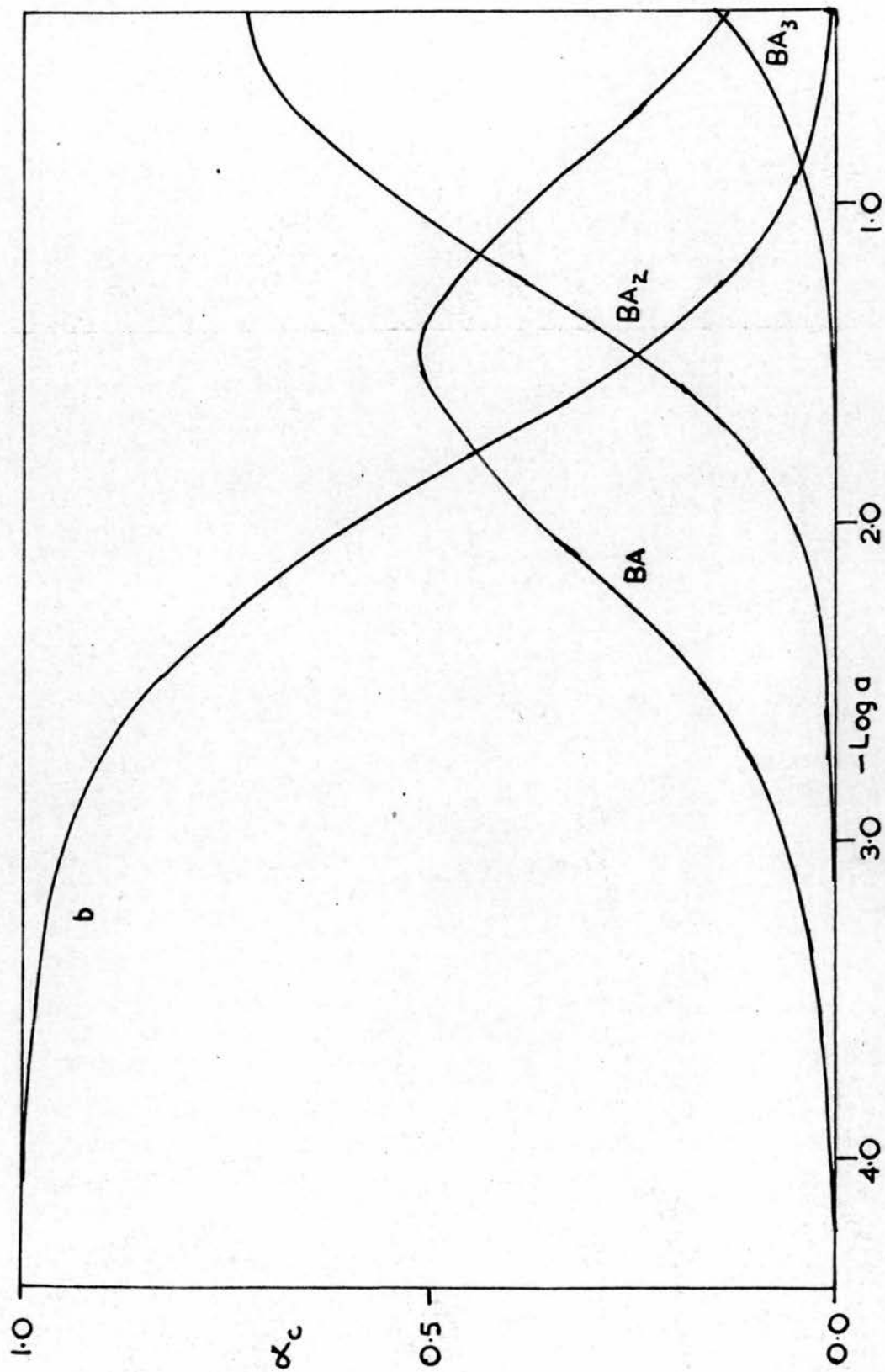
The full line in Fig. 5-5 is the theoretical formation curve calculated by substituting the above values in Eq. (1-5a). This curve fits all the experimental data excellently. Figure 5-6 shows the plot of  $\alpha_c$  against  $\log a$ .

After standing overnight, some concentrated titrated solutions deposited well-formed green-blue or green crystals. The solutions concerned were those of the buffer of pH 5.01 with copper concentrations of both 0.025M and 0.100M. The crystals were similar to those of copper(II) acetate monohydrate in appearance

Fig 5.6

COPPER(II) ACETATE

Relative proportions of the species  $BA_n$  present in solution.





Copper(II) propionate.

In this system titrations were made using buffers of pH 4.71 and 5.01, and solutions of metal ion of concentrations 0.025M, 0.050M, 0.075M, and 0.100M. The experimental data are summarised in Table 5-4. The range of concentration of free propionate ion was  $3.2 \times 10^{-6}$  M to 0.3M. Precipitation did not occur during a titration, but in some cases a precipitate appeared when titrated solutions were left overnight.

TABLE 5-4.

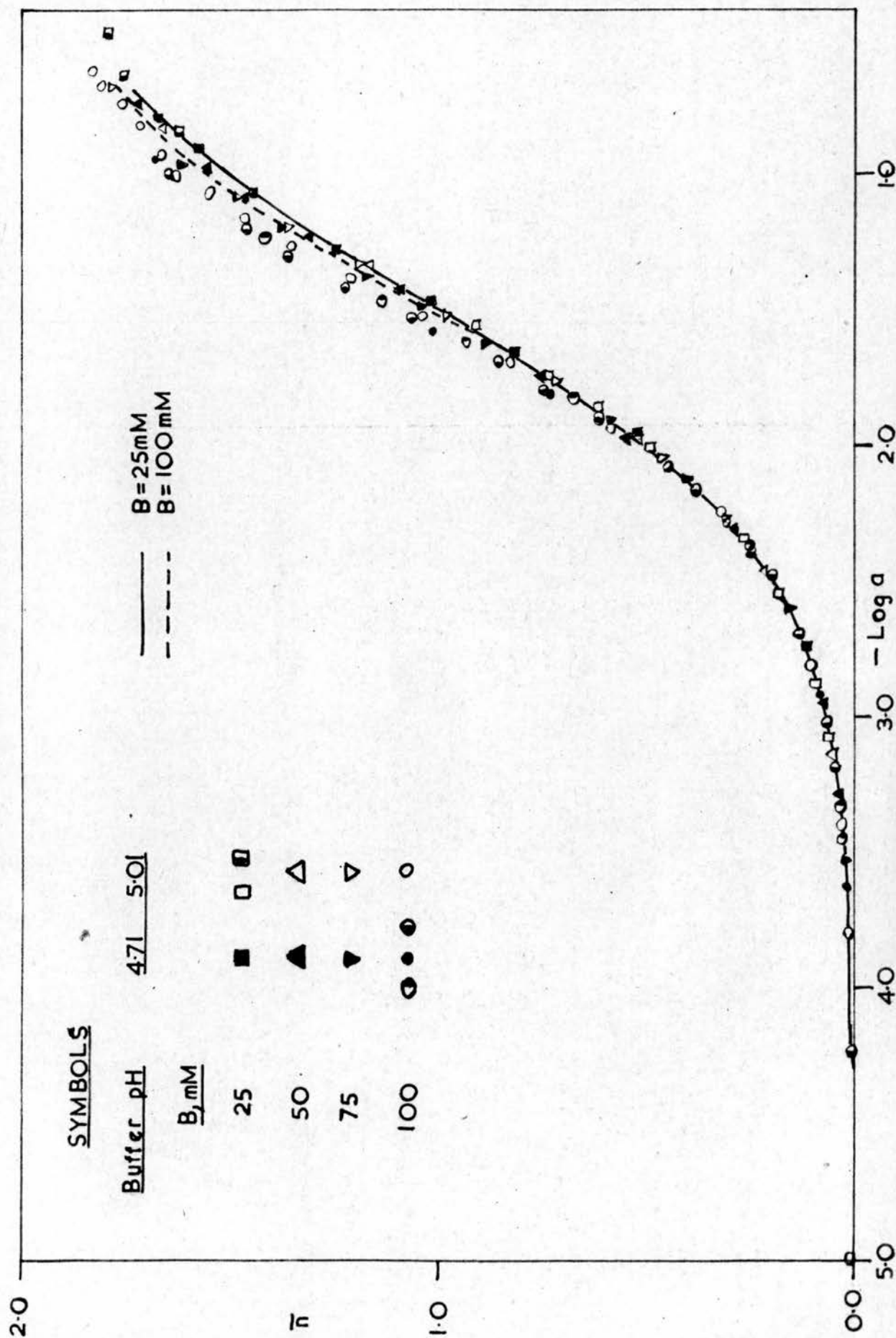
Copper(II) propionate.

Experimental data  $\bar{n}(\log a)_B$  obtained from potentiometric titrations of metal ion solutions and propionate buffers.

B(mM)	25						50						75						100							
Buffer [HA]mM [NaA]mM	5608 2000	4270 3000	4270 3000	5608 2000	4270 3000	4270 3000	5608 2000	4270 3000	5608 2000	4270 3000	5608 2000	4270 3000	5608 2000	4270 3000	5608 2000	4270 3000	5608 2000	4270 3000	5608 2000	4270 3000	5608 2000	4270 3000	5608 2000	4270 3000		
$\bar{n}$ -loga	$\bar{n}$ -loga	$\bar{n}$ -loga	$\bar{n}$ -loga	$\bar{n}$ -loga	$\bar{n}$ -loga	$\bar{n}$ -loga	$\bar{n}$ -loga	$\bar{n}$ -loga	$\bar{n}$ -loga	$\bar{n}$ -loga	$\bar{n}$ -loga	$\bar{n}$ -loga	$\bar{n}$ -loga	$\bar{n}$ -loga	$\bar{n}$ -loga	$\bar{n}$ -loga	$\bar{n}$ -loga	$\bar{n}$ -loga	$\bar{n}$ -loga	$\bar{n}$ -loga	$\bar{n}$ -loga	$\bar{n}$ -loga	$\bar{n}$ -loga			
0.056 3.079	0.093 2.879	0.096 2.906	0.036 3.293	0.048 3.140	0.020 3.528	0.039 3.282	0.000 5.114	0.018 3.629	0.017 3.619	0.031 3.396	0.004 4.229	0.082 2.920	0.024 3.451	0.063 3.062	0.011 3.803	0.246 2.405	0.031 3.320	0.189 2.533	0.046 3.177	0.470 2.059	0.038 3.238	0.310 2.293	0.064 3.023	0.738 1.812	0.056 3.037	0.588 1.938
0.116 2.735	0.183 2.553	0.186 2.561	0.074 2.952	0.219 2.460	0.047 3.145	0.080 2.942	0.082 2.896	0.015 1.593	0.074 2.910	0.827 1.699	0.016 1.664	0.488 2.009	0.500 2.021	0.633 1.874	0.074 2.910	0.738 1.812	0.056 3.037	0.588 1.938	0.099 2.810	1.221 1.417	0.111 2.735	1.035 1.527	0.064 3.023	0.738 1.812	0.056 3.037	0.588 1.938
0.521 1.960	0.266 2.351	0.274 2.370	0.289 2.310	0.515 1.980	0.074 2.944	0.161 2.612	0.099 2.810	1.221 1.417	0.111 2.735	1.035 1.527	0.521 1.960	0.488 2.009	0.500 2.021	0.633 1.874	0.074 2.910	0.738 1.812	0.056 3.037	0.588 1.938	0.082 2.896	0.015 1.593	0.074 2.910	0.827 1.699	0.064 3.023	0.738 1.812	0.056 3.037	0.588 1.938
0.816 1.664	0.488 2.009	0.500 2.021	0.551 1.982	0.897 1.588	0.154 2.600	0.312 2.256	0.082 2.896	0.015 1.593	0.074 2.910	0.827 1.699	0.521 1.960	0.488 2.009	0.500 2.021	0.633 1.874	0.074 2.910	0.738 1.812	0.056 3.037	0.588 1.938	0.099 2.810	1.221 1.417	0.111 2.735	1.035 1.527	0.064 3.023	0.738 1.812	0.056 3.037	0.588 1.938
1.014 1.474	0.615 1.860	0.633 1.874	0.754 1.750	1.161 1.351	0.257 2.354	0.457 2.053	0.082 2.896	0.015 1.593	0.074 2.910	0.827 1.699	0.521 1.960	0.488 2.009	0.500 2.021	0.633 1.874	0.074 2.910	0.738 1.812	0.056 3.037	0.588 1.938	0.099 2.810	1.221 1.417	0.111 2.735	1.035 1.527	0.064 3.023	0.738 1.812	0.056 3.037	0.588 1.938
1.243 1.290	0.728 1.744	0.752 1.758	1.089 1.433	1.335 1.183	0.404 2.122	0.713 1.763	0.082 2.896	0.015 1.593	0.074 2.910	0.827 1.699	0.521 1.960	0.488 2.009	0.500 2.021	0.633 1.874	0.074 2.910	0.738 1.812	0.056 3.037	0.588 1.938	0.099 2.810	1.221 1.417	0.111 2.735	1.035 1.527	0.064 3.023	0.738 1.812	0.056 3.037	0.588 1.938
1.442 1.077	0.909 1.564	0.904 1.562	1.307 1.241	1.562 0.967	0.582 1.909	0.976 1.517	0.082 2.896	0.015 1.593	0.074 2.910	0.827 1.699	0.521 1.960	0.488 2.009	0.500 2.021	0.633 1.874	0.074 2.910	0.738 1.812	0.056 3.037	0.588 1.938	0.099 2.810	1.221 1.417	0.111 2.735	1.035 1.527	0.064 3.023	0.738 1.812	0.056 3.037	0.588 1.938
1.568 0.908	1.058 1.433	1.043 1.429	1.459 1.094	1.637 0.821	0.745 1.755	1.188 1.338	0.082 2.896	0.015 1.593	0.074 2.910	0.827 1.699	0.521 1.960	0.488 2.009	0.500 2.021	0.633 1.874	0.074 2.910	0.738 1.812	0.056 3.037	0.588 1.938	0.099 2.810	1.221 1.417	0.111 2.735	1.035 1.527	0.064 3.023	0.738 1.812	0.056 3.037	0.588 1.938
1.671 0.803	1.172 1.328	1.164 1.327	1.552 0.987	1.699 0.721	0.889 1.627	1.359 1.201	0.082 2.896	0.015 1.593	0.074 2.910	0.827 1.699	0.521 1.960	0.488 2.009	0.500 2.021	0.633 1.874	0.074 2.910	0.738 1.812	0.056 3.037	0.588 1.938	0.099 2.810	1.221 1.417	0.111 2.735	1.035 1.527	0.064 3.023	0.738 1.812	0.056 3.037	0.588 1.938
0.8	1.319 1.208	1.384 1.141	1.662 0.843	1.734 0.646	1.037 1.487	1.481 1.084	0.082 2.896	0.015 1.593	0.074 2.910	0.827 1.699	0.521 1.960	0.488 2.009	0.500 2.021	0.633 1.874	0.074 2.910	0.738 1.812	0.056 3.037	0.588 1.938	0.099 2.810	1.221 1.417	0.111 2.735	1.035 1.527	0.064 3.023	0.738 1.812	0.056 3.037	0.588 1.938
	1.384 1.141	1.508 0.987	1.717 0.748		1.172 1.381	1.687 0.919	0.082 2.896	0.015 1.593	0.074 2.910	0.827 1.699	0.521 1.960	0.488 2.009	0.500 2.021	0.633 1.874	0.074 2.910	0.738 1.812	0.056 3.037	0.588 1.938	0.099 2.810	1.221 1.417	0.111 2.735	1.035 1.527	0.064 3.023	0.738 1.812	0.056 3.037	0.588 1.938
	1.472 1.059	1.615 0.850			1.374 1.206	1.728 0.780	0.082 2.896	0.015 1.593	0.074 2.910	0.827 1.699	0.521 1.960	0.488 2.009	0.500 2.021	0.633 1.874	0.074 2.910	0.738 1.812	0.056 3.037	0.588 1.938	0.099 2.810	1.221 1.417	0.111 2.735	1.035 1.527	0.064 3.023	0.738 1.812	0.056 3.037	0.588 1.938
	1.527 0.989	1.712 0.733			1.533 1.080	1.786 0.685	0.082 2.896	0.015 1.593	0.074 2.910	0.827 1.699	0.521 1.960	0.488 2.009	0.500 2.021	0.633 1.874	0.074 2.910	0.738 1.812	0.056 3.037	0.588 1.938	0.099 2.810	1.221 1.417	0.111 2.735	1.035 1.527	0.064 3.023	0.738 1.812	0.056 3.037	0.588 1.938
	1.579 0.931	1.752 0.648			1.619 0.972	1.872 0.553	0.082 2.896	0.015 1.593	0.074 2.910	0.827 1.699	0.521 1.960	0.488 2.009	0.500 2.021	0.633 1.874	0.074 2.910	0.738 1.812	0.056 3.037	0.588 1.938	0.099 2.810	1.221 1.417	0.111 2.735	1.035 1.527	0.064 3.023	0.738 1.812	0.056 3.037	0.588 1.938
	1.641 0.852	1.804 0.488			1.700 0.892	1.914 0.461	0.082 2.896	0.015 1.593	0.074 2.910	0.827 1.699	0.521 1.960	0.488 2.009	0.500 2.021	0.633 1.874	0.074 2.910	0.738 1.812	0.056 3.037	0.588 1.938	0.099 2.810	1.221 1.417	0.111 2.735	1.035 1.527	0.064 3.023	0.738 1.812	0.056 3.037	0.588 1.938
	1.688 0.787				1.723 0.818		0.082 2.896	0.015 1.593	0.074 2.910	0.827 1.699	0.521 1.960	0.488 2.009	0.500 2.021	0.633 1.874	0.074 2.910	0.738 1.812	0.056 3.037	0.588 1.938	0.099 2.810	1.221 1.417	0.111 2.735	1.035 1.527	0.064 3.023	0.738 1.812	0.056 3.037	0.588 1.938
	1.711 0.733						0.082 2.896	0.015 1.593	0.074 2.910	0.827 1.699	0.521 1.960	0.488 2.009	0.500 2.021	0.633 1.874	0.074 2.910	0.738 1.812	0.056 3.037	0.588 1.938	0.099 2.810	1.221 1.417	0.111 2.735	1.035 1.527	0.064 3.023	0.738 1.812	0.056 3.037	0.588 1.938
	1.729 0.687						0.082 2.896	0.015 1.593	0.074 2.910	0.827 1.699	0.521 1.960	0.488 2.009	0.500 2.021	0.633 1.874	0.074 2.910	0.738 1.812	0.056 3.037	0.588 1.938	0.099 2.810	1.221 1.417	0.111 2.735	1.035 1.527	0.064 3.023	0.738 1.812	0.056 3.037	0.588 1.938

Fig 5.7 FORMATION CURVES FOR COPPER(II) PROPIONATE

For clarity the formation curves at B=25mM and 100mM only have been drawn. About 40% of the data, mainly at high values of  $\pi$ , have not been plotted.



The formation curve (Fig. 5.7) is a function of  $B$ , although the curves for  $B = 0.025M$  and  $0.050M$  are rather similar to each other. It is apparent, therefore, that the species present are not homonuclear. The formation curve is independent of  $B$  up to the point  $(\log a, \bar{n}) = (-2.0, 0.5)$  and the projection strip method may be used to calculate  $\beta_1$  and  $\beta_2$ . The limits of error of  $\log p$  are rather wide but in the position of best fit  $\log p = 0.37 \pm 0.13$  and  $\log a^* - \log a = 1.49 \pm 0.10$ , and by substitution in Eqs. (2-11) and (2-10)

$$\log \beta_1 = 1.86 \pm 0.03$$

$$\log \beta_2 = 2.98 \pm 0.20$$

The reason for the large error in  $\log \beta_2$  is that at  $\bar{n} = 0.5$  almost no  $BA_2$  has been formed. If it is assumed that mononuclear complexes only are formed for  $B \leq 0.050M$  then a projection strip of the data for  $B = 0.025M$  and  $0.050M$  may be fitted to the calculated curves,  $\log p(\log a^*)_{\bar{n}}$ . In the position of best fit  $\log p = 0.35 \pm 0.02$  and  $\log a^* - \log a = 1.51 \pm 0.01$ , and by substitution in Eqs. (2-11) and (2-10)

$$\log \beta_1 = 1.85 \pm 0.02_5$$

$$\log \beta_2 = 3.02 \pm 0.02$$

These values have been refined and a value of  $\beta_3$  has been calculated by the method of successive extrapolations<sup>179</sup> which gives

$$\log \beta_1 = 1.86 \pm 0.02_5$$

$$\log \beta_2 = 3.00 \pm 0.03$$

$$\log \beta_3 = 2.50 \pm 0.10$$

The theoretical formation curve calculated from these constants using Eq. (1-5a) does not, of course, fit the data for  $B = 0.075M$  and  $0.100M$ , and it appears that polynuclear species are formed in the system. As a first approximation the assumption has been made that only one polynuclear species is formed and that it is dimeric, of the type  $B_2A_Q$  where  $Q$  is an integer  $\gg 1$ . In this case, assuming



that three mononuclear species are formed

$$B = \sum_0^3 \beta_n b a^n + 2 \beta_{2q} b^2 a^q \quad (5-11)$$

where  $\beta_{2q}$  is the overall stability constant for  $B_2A_q$  Equation (1-4) now becomes

$$\bar{n} = \left( \sum_0^3 n \beta_n a^n + q \beta_{2q} b^2 a^q \right) / B \quad (5-12)$$

Solving Eq. (5-11) for  $b$  and substituting into Eq. (5-12) we obtain

$$\bar{n}B = \frac{\sum_0^3 \beta_n a^n}{2 \beta_{2q} a^q} \left( \sqrt{\left( \sum_0^3 \beta_n a^n \right)^2 + 4B \beta_{2q} a^q} - \sum_0^3 \beta_n a^n \right) + \frac{q}{4 \beta_{2q} a^q} \left[ 2 \left( \sum_0^3 \beta_n a^n \right)^2 + 4B \beta_{2q} a^q - 2 \sum_0^3 \beta_n a^n \sqrt{\left( \sum_0^3 \beta_n a^n \right)^2 + 4B \beta_{2q} a^q} \right]$$

Setting  $C = \sum_0^3 \beta_n a^n$  (5-13)

$$D = \sum_0^3 n \beta_n a^n$$

and solving Eq. (5-13) for  $\beta_{2q}$ , we have

$$\beta_{2q} = \frac{(\bar{n}C - D)(qC - 2D)}{B(2\bar{n} - q^2) a^q} \quad (5-14)$$

It is now possible to gain some idea of the species present by substituting the experimental data,  $\bar{n}(\log a)_B$ , in Eq. (5-14). In Eq. (5-14) the term  $(\bar{n}C - D) \gg 0$ . If it is zero no polynuclear complexes are formed. Using the values of  $\beta_1$  and  $\beta_2$  calculated above by the projection strip method together with the data for  $B = 0.075M$  and  $0.100M$  in Table 5-4, we find that the value of  $\beta_{2q}$  is negative when Eq. (5-14) is solved with  $q=1$  or  $q=2$ , while with  $B_2A_2$  the value of  $\beta_{2q}$  is positive. The species  $B_2A$  and  $B_2A_2$  do not, therefore, appear to exist in

this system. The values of  $\beta_{2q}$  calculated with  $q = 3$  and  $q = 4$  are shown in Table 5-5. The values of  $\beta_{23}$  increase steadily with increase of  $\bar{n}$  and  $\log a$ , while the values of  $\beta_{24}$  are more constant, especially at higher concentrations.

TABLE 5-5.

Copper(II) propionate.

Values of  $\log \beta_{2q}$  calculated using Eq. (5-14) with  $q = 3$  and 4.

B(mM)	75		75			
Buffer [HA]mM [NaA]mM	5608 2000		4270 3000			
Symbol	▼		▽			
	$\bar{n}$	$\log \beta_{23}$	$\log \beta_{24}$	$\bar{n}$	$\log \beta_{23}$	$\log \beta_{24}$
	1.037	5.20	6.22	1.188	4.88	5.80
	1.172	5.64	6.59	1.359	5.80	6.34
	1.374	6.17	6.57	1.481	7.36	6.57
	1.533		6.80	1.687		6.90
	1.619		6.80	1.728		
	1.700		6.84	1.786		6.03
	1.723		6.55	1.872		6.23

The data are therefore consistent with the formation of a dimer  $B_2A_4$ . The value of  $\log \beta_{24}$  obtained in the above calculations is  $6.9 \pm 0.2$ . The formation curves calculated using this value fit the experimental data with fairly high precision for  $B = 0.075M$  and  $0.100M$  but not for  $B = 0.050M$  and  $0.025M$ . In the latter cases the experimental data fall below the calculated curves. Successive approximations have been used to obtain the values of  $\log \beta_3$  and  $\log \beta_{24}$  which best explain the data and these appear to be zero and  $6.50 \pm 0.20$  respectively. The formation curves calculated using this value of  $\log \beta_{24}$  fit the experimental data for  $B = 0.025M$  and  $0.050M$  with high precision

				100				
				5608 2000				
				5608 2000				
				4270 3000				
				●				
				●				
				⊙				
$\bar{n}$	$\log \beta_{23}$	$\log \beta_{24}$	$\bar{n}$	$\log \beta_{23}$	$\log \beta_{24}$	$\bar{n}$	$\log \beta_{23}$	$\log \beta_{24}$
1.062	5.98	6.98	1.015		7.26	1.035	5.66	6.84
1.228	6.23	6.97	1.221		7.06	1.210	6.30	6.82
1.360	6.64	7.02	1.676		6.87	1.349		6.78
1.461	7.52	7.06				1.545		6.74
1.648		7.15				1.664		6.72
						1.712		7.25
						1.759		6.26

and the data for  $B = 0.075M$  with somewhat lower precision. The experimental data for  $B = 0.100M$  fall slightly above the calculated curve and it is possible that a second polynuclear species is formed at this higher concentration of  $B$ . However the precision of the data does not justify a more extensive mathematical analysis.

Thus in this system two combinations of constants explain the experimental data with similar precision. First, the set

$$\log \beta_1 = 1.86 \pm 0.025$$

$$\log \beta_2 = 3.00 \pm 0.02$$

$$\log \beta_3 = 2.50$$

$$\log \beta_{24} = 6.9 \pm 0.2$$

Which represents the data for  $B = 0.100M$  with high precision, but does not represent the other data so well. The second set

$$\log \beta_1 = 1.86 \pm 0.025$$

$$\log \beta_2 = 3.00 \pm 0.02$$

$$\log \beta_{24} = 6.50 \pm 0.20$$

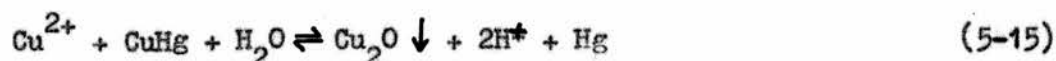
represents the data for  $B = 0.025M$  and  $0.050M$  with high precision, the data for  $B = 0.075M$  with moderately high precision, and the data for  $B = 0.100M$  with low precision. This set appears to explain the data better than the first set and these values are therefore taken as the preferred values of the constants. The full lines in Fig. 5.7 are the formation curves calculated using this set of constants.

After standing overnight, some concentrated titrated solutions deposited well-formed green crystals. These crystals were greener than those of copper(II) acetate and may possibly be crystals of the dimer.

The complexes existing in this system could be studied more easily if the



concentration,  $b$ , of the free metal ion could be measured. Such measurements are usually made with either a metal or a metal amalgam electrode. Biedermann<sup>232</sup> attempted to use a copper amalgam electrode in the study of the hydrolysis of the copper(II) ion. Even at low pH, where hydrolysis of the metal ion is negligible, the values of  $E$  drifted and small red crystals of  $\text{Cu}_2\text{O}$  appeared on the surface of the amalgam because of the reaction.



Measurements in the present system would have to be made at pH 4-5, close to the point where hydrolysis of the metal ion occurs. For this reason, and after discussion with Dr. Biedermann, it was not considered worthwhile to attempt to measure  $b$  in these solutions with an amalgam electrode. It is well known that copper metal electrodes are very slow in reaching equilibrium<sup>233</sup>.

#### Copper(II) n-butyrate

Titration were made using buffers of pH 4.84 and 5.13, and solutions of metal ion of concentrations 0.010M, 0.025M, and 0.100M. The experimental data are summarised in Table 5-6. The range of concentration of free butyrate ion was  $3 \times 10^{-5}\text{M}$  to  $4 \times 10^{-2}\text{M}$ . These titrations were limited by the low solubility of copper(II) n-butyrate in the ionic medium. When the metal ion concentration was 0.100M it was possible only to reach a point  $(\log a, \bar{n}) = (-2.25, 0.3)$  before precipitation occurred. Similarly, precipitation occurred at  $(\log a, \bar{n}) = (-1.9, 0.6)$  when  $B = 0.025\text{M}$ , and at  $(\log a, \bar{n}) \approx (-1.4, 1.1)$  when  $B = 0.010\text{M}$ . Precipitation was detected in the more concentrated solutions both visibly and by the fact that the value of  $E$  which, as usual, had increased for each addition of buffer, suddenly decreased. Precipitation was less easy to detect in the solutions with  $B = 0.010\text{M}$  since at first the precipitate was

TABLE 5-6

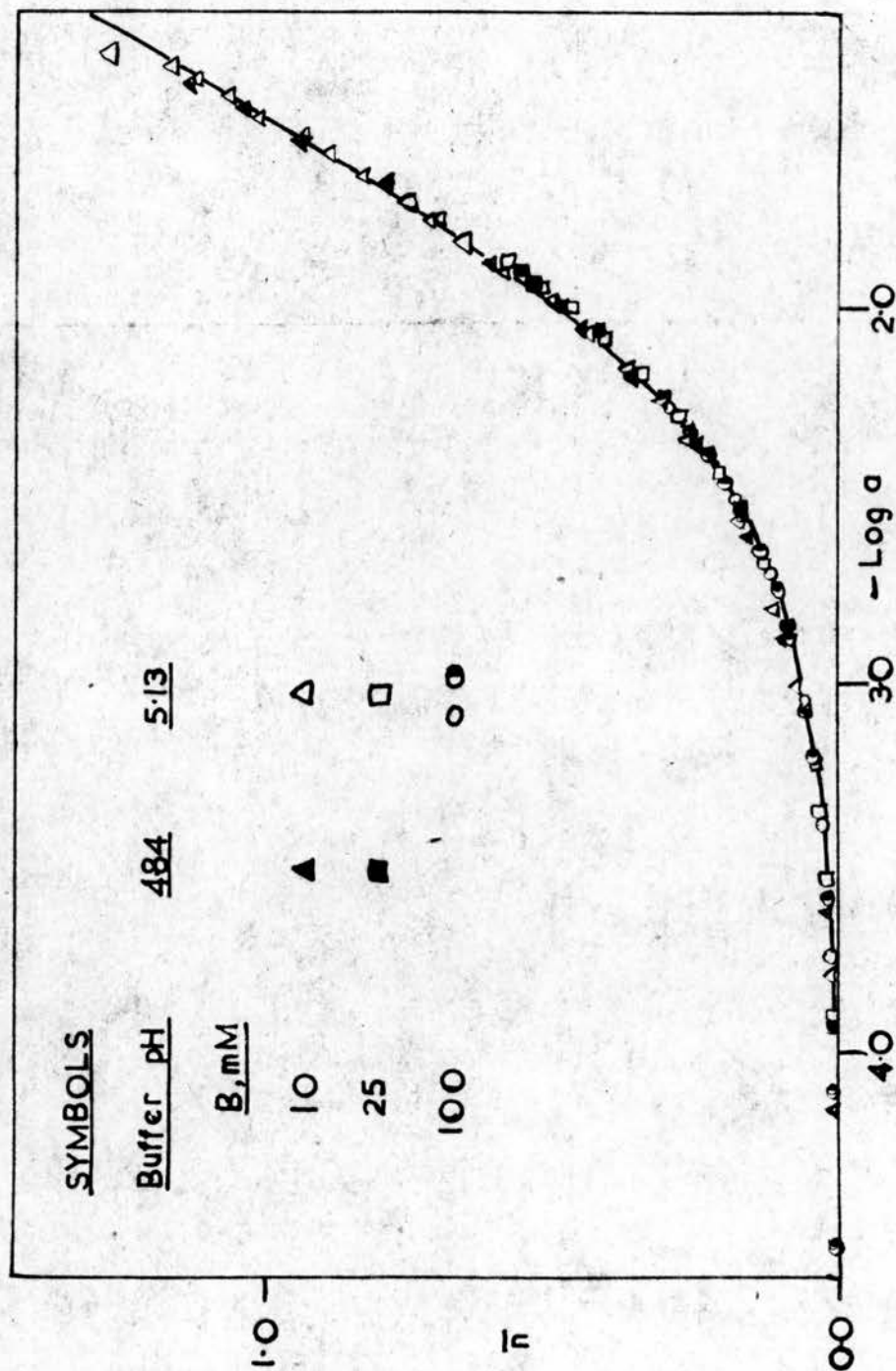
## Copper(II) n-butyrate.

Experimental data  $\bar{n}(\log a)_B$  obtained from potentiometric titrations of metal ion solutions and n-butyrate buffers.

B (mM)		10		25		100		100	
Buffer [HA] mM	[NaA] mM	$\bar{n}$	$-\log a$	$\bar{n}$	$-\log a$	$\bar{n}$	$-\log a$	$\bar{n}$	$-\log a$
582.5	300.0	0.008	4.157	0.021	3.791	0.008	3.916	0.030	3.388
		0.023	3.618	0.037	3.340	0.017	3.585	0.063	3.046
		0.098	2.880	0.078	3.011	0.054	3.084	0.125	2.708
		0.164	2.610	0.114	2.814	0.088	2.855	0.185	2.508
		0.257	2.365	0.177	2.566	0.170	2.550	0.303	2.258
		0.366	2.189	0.268	2.354	0.243	2.365		
		0.456	2.060	0.317	2.248	0.306	2.235		
		0.609	1.887	0.372	2.169	0.422	2.060		
		0.716	1.766	0.437	2.067	0.477	1.998		
		0.790	1.674	0.508	1.989	0.534	1.944		
		0.950	1.553	0.592	1.904	0.592	1.851		
		1.040	1.465	0.659	1.831	0.521	1.952		
		1.134	1.402	0.700	1.765	0.581	1.884		
				0.758	1.714				
				0.834	1.648				
				0.896	1.592				
				0.943	1.543				
				1.016	1.492				
				1.067	1.433				
				1.126	1.387				
				1.168	1.347				
				1.277	1.318				

Fig 5-8

FORMATION CURVE FOR COPPER(II) n-BUTYRATE.



not visible and the value of E did not decrease. However, the formation curve shows an anomalous break at  $(\log a, \bar{n}) = (-1.4, 1.1)$  indicating precipitation which was not detectable visibly until the last point shown on the curve, i.e.  $(\log a, \bar{n}) = (-1.2, 1.5)$ .

The formation curve is independent of B and extends beyond  $\bar{n} = 1$ . Therefore, the species formed are homonuclear, probably mononuclear as in the other systems, and there are two complexes at least. More experimental data, extending to higher values of  $\bar{n}$  and  $\log a$ , might be obtained by titrating with lower concentrations of B. However, the values of  $\bar{n}$  obtained would have a large uncertainty and it would be hazardous to draw any conclusions from such data. The maximum error in  $E - E_0$  is  $\pm 0.3 \text{ mV}$ , and in titrations with  $B = 0.010 \text{ M}$  the resultant error in  $\bar{n}$  is large, e.g.: for a typical measurement  $\bar{n} = 1.134 \pm 0.050$ . The error in  $\bar{n}$  increases with increase in  $\bar{n}$  and decrease in B.

As before, it was assumed that the two complexes present were  $BA$  and  $BA_2$ , and the projection strip method was used to calculate  $\beta_1$  and  $\beta_2$ . In the position of best fit,  $\log \beta = 0.33 \pm 0.02$  and  $\log a^* - \log a = 1.49 \pm 0.01$ , and by substitution in Eqs. (2-11) and (2-10),

$$\log \beta_1 = 1.82 \pm 0.02_5$$

$$\log \beta_2 = 2.98 \pm 0.03$$

The theoretical formation curve calculated by substituting these constants in (5-8)  
Eq. (1-5a) is the full line in Fig. / and it fits the data with high precision.

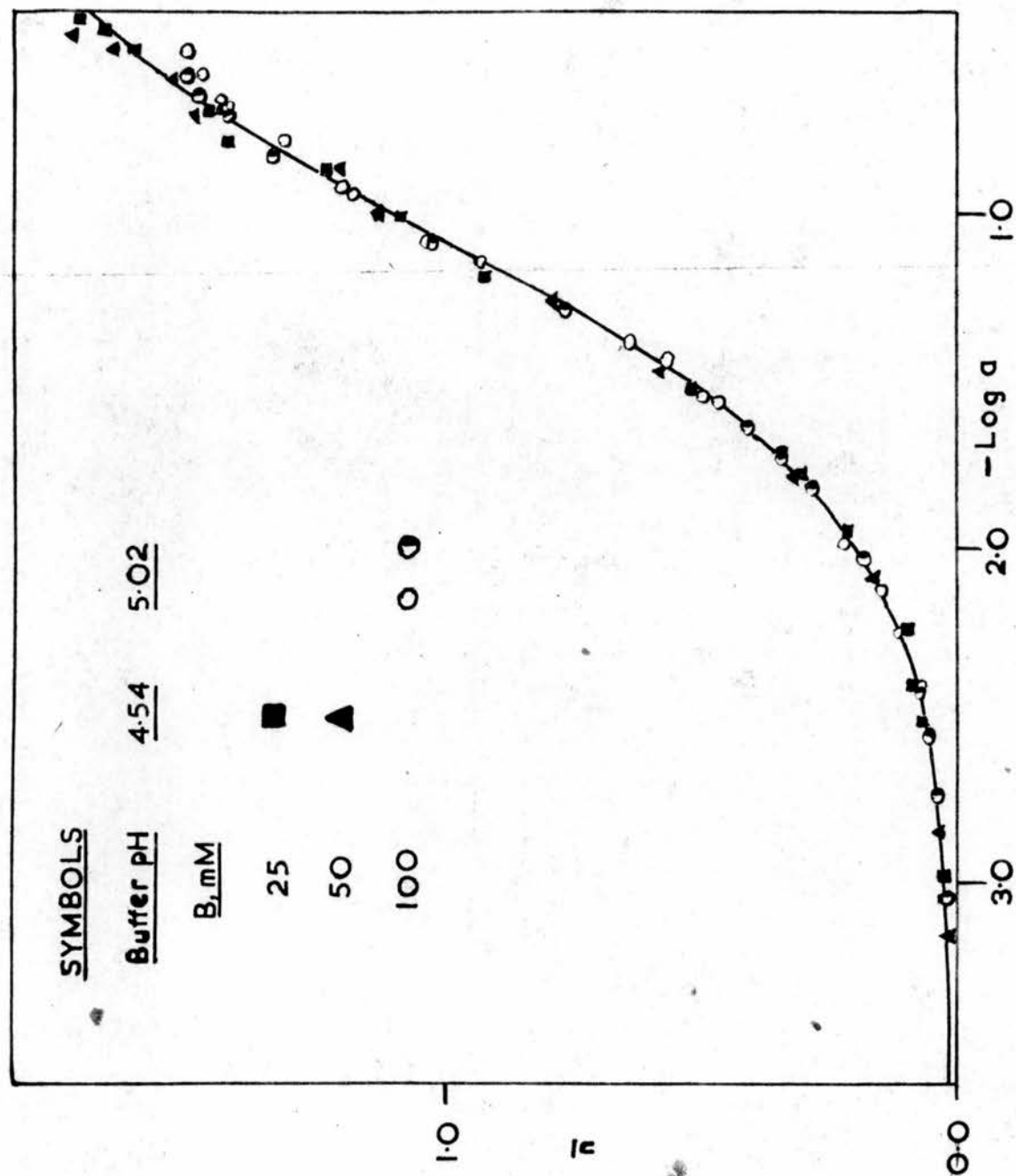
The precipitates formed in these titrations were light blue. A formal solubility product for the species  $BA_2$  has been calculated from the experimental data. The solubility product of  $B_p A_q$  is given by Eq. (5-16)

$$S_{B_p A_q} = b^p a^q \quad (5-16)$$

Now in copper(II) n-butyrate

Fig 59

FORMATION CURVE FOR CADMIUM(II) ACETATE





Now in copper(II) n-butyrate

$$B = \sum_{n=0}^{n=2} \beta_n b a^n$$

from which  $b$  may be calculated. The value of  $a$  used in the calculation is the value just before precipitation occurred. The values of  $S_{BA_2} \times 10^6$  obtained from one titration with  $B = 0.100M$  and two titrations with  $B = 0.025M$  are 2.211, 2.144, and 2.121 giving an average of  $2.16 \pm 0.04$ . It is interesting to note that the values obtained from the titrations with  $B = 0.010M$  are  $3.649 \times 10^{-6}$  and  $3.110 \times 10^{-6}$  which were calculated from the data when the precipitate was first detected visibly. To obtain the lower value of  $S_{BA_2}$  the value of  $a$  at  $K \approx 0.90$  must be used. Thus, this confirms that in the solutions with  $B = 0.010M$  precipitation occurred before the precipitate was visible and that the best method of detecting precipitation at low concentrations of metal ion is by the observation of anomalies in the formation curve.

#### Cadmium(II) acetate.

Titration were made using buffers of pH 4.54 and 5.02, and solutions of metal ion of concentrations 0.025M, 0.050M, and 0.100M. The experimental data are summarised in Table 5-7. The range of concentration of free acetate ion was  $7 \times 10^{-3}M$  to 0.3M. Precipitation did not occur either during or after a titration.

The formation curve (Fig. 5-9) is independent of  $B$  and it is assumed that mononuclear complexes up to  $BA_2$ , at least, are present. The values of  $\beta_1$  and  $\beta_2$  were calculated using the projection strip method. In the position of best fit  $\log p = 0.24 \pm 0.02$  and  $\log a^* - \log a = 1.095 \pm 0.01$ , and by substitution in Eqs. (2-11) and (2-10)

$$\log \beta_1 = 1.33 \pm 0.02_5$$

$$\log \beta_2 = 2.19 \pm 0.02$$

The full line in Fig. 5-9 is the theoretical formation curve calculated by substituting these constants in Eq. (1-5a). This curve fits the experimental data with high precision.



TABLE 5-7

Cadmium(II) acetate

Experimental data  $\bar{n}(\log a)_B$  obtained from potentiometric titrations of metal ion solutions and acetate buffers.

B (mM)	25	50	100
Buffer [HA] mM	44.60	44.60	1971
[NaA] mM	1500	1500	2000
$\bar{n}$	0.025	0.011	0.018
$\Delta$	2.982	3.154	3.045
$-\log a$	2.528	2.854	2.754
$\bar{n}$	0.068	0.040	0.038
$\Delta$	2.410	2.431	2.561
$-\log a$	2.253	2.416	2.434
$\bar{n}$	0.099	0.077	0.076
$\Delta$	1.952	2.099	2.254
$-\log a$	1.781	1.791	2.029
$\bar{n}$	0.308	0.317	0.185
$\Delta$	1.524	1.469	1.822
$-\log a$	1.297	1.256	1.723
$\bar{n}$	0.771	0.796	0.352
$\Delta$	1.189	0.999	1.642
$-\log a$	1.014	0.866	1.546
$\bar{n}$	1.221	1.345	0.503
$\Delta$	0.870	0.708	1.463
$-\log a$	0.793	0.601	1.293
$\bar{n}$	1.427	1.534	0.769
$\Delta$	0.703	0.512	1.152
$-\log a$	0.511	0.466	1.085
$\bar{n}$	1.605	1.649	1.030
$\Delta$	0.451	0.466	0.951
$-\log a$	0.417	0.466	0.835
$\bar{n}$	1.710	1.733	1.339
$\Delta$	0.417	0.466	0.705
$-\log a$	0.417	0.466	0.648
$\bar{n}$	1.710	1.733	1.479
$\Delta$	0.417	0.466	0.592
$-\log a$	0.417	0.466	0.592

5(b) DISCUSSION

The stability constants of the copper(II) carboxylates obtained in this work, by Carson and Rossotti<sup>201</sup>, and by Clarke and Rossotti<sup>214</sup>, are summarised in Table 5-8. A dimer has been detected only in copper(II) propionate solutions. This is somewhat surprising in view of the earlier measurements of Fronaeus<sup>163</sup> and Pedersen<sup>162</sup> both of whom reported that copper(II) acetate formed dimeric molecules. Pederson, however, reported only qualitative indications of polynuclear complex formation [cf. Sec. I(d)]. Fronaeus' experimental method was similar to that used in this work but he used 1.00M sodium perchlorate as the ionic medium in which the dimers would be expected to be less stable than in the 3.00M sodium perchlorate medium used in this work. Fronaeus's data have, therefore, been re-examined. His method of calculating  $\bar{n}$  and  $\alpha$  were slightly different from those in the present work and the formation of the species  $HA_2$  and  $H_2A_2$  was not realised. However, the Lund school of solution chemists believe the variation in potential of a carboxylate buffer with its concentration to be due to a liquid junction potential and Fronaeus corrected his results accordingly. The experimental measurements were plotted as  $\bar{n}/\alpha(a)_B$  and  $\bar{n}/\alpha(\log a)_B$  which were found to be functions of B. Fronaeus therefore postulated polynuclear complex formation. The data have now been re-plotted in the form  $\bar{n}(\log a)_B$  and constants calculated using the projection strip method and successive approximations. The projection strip fits the theoretical family of curves  $\log p(\log a^*)_{\bar{n}}$  up to  $\bar{n} = 1.2$ . In the position of best fit  $\log p = 0.305 \pm 0.015$  and  $\log a^* = \log a = 1.36 \pm 0.01$ , and by substitution in Eqs. (2-11) and (2-10)

$$\log \beta_1 = 1.665 \pm 0.02$$

$$\log \beta_2 = 2.72 \pm 0.02$$

These constants have been refined and a value of  $\beta_3$  evaluated by successive approximations. The theoretical curve calculated from the following set of constants fits the experimental data with high precision over the whole range

of concentration,

$$\log \beta_1 = 1.67 \pm 0.02$$

$$\log \beta_2 = 2.66 \pm 0.02$$

$$\log \beta_3 = 2.85 \pm 0.10$$

TABLE 5-8

Stability constants of copper(II) carboxylate complexes in 3.00M sodium perchlorate at 25.00°C.

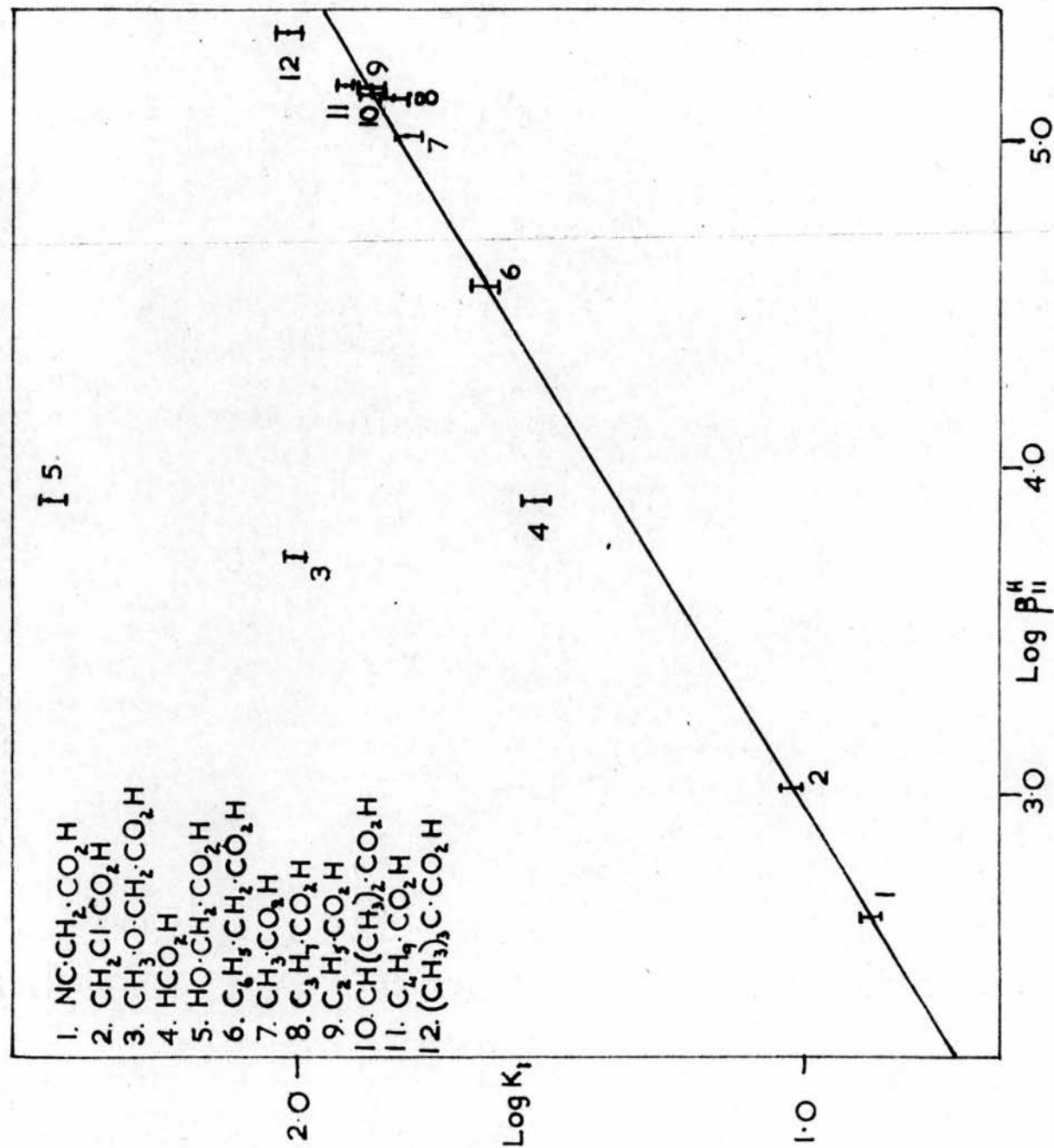
Ligand	$\log \beta_1$	$\log \beta_2$	$\log K_2$	$\log \beta_3$	$\log K_3$
Formate	1.53	2.42	0.89	2.68	0.26
Acetate	1.79	2.94	1.15	2.64	-0.30
Propionate	1.86	3.00	1.14		
n-Butyrate	1.82	2.98	1.16		
iso-Butyrate	1.87	$\leq 2.68$	$\leq 0.81$		
Valerate	1.92	$\leq 3.02$	$\leq 1.10$		
Pivalate	2.03	$\leq 3.68$	$\leq 1.65$		
Cyanoacetate	0.87	1.00	0.13		
Chloroacetate	1.02	1.43	0.41		
Phenylacetate	1.61	$\leq 2.4$	$\leq 0.8$		
Methoxyacetate	2.01	3.34	1.33		
Glycollate	2.50	4.02	1.52	4.27	0.25

The values of  $\beta_1$  and  $\beta_2$  are the same as those evaluated by Fronaeus while  $\beta_3$  is somewhat lower. There appears to be no justification for postulating the formation of dimeric species. At high values of  $\bar{n}$  the data do not fit the curve perfectly but the appreciable uncertainty in  $\bar{n}$  in this region may account for the observed discrepancies. The present method of plotting the data is preferable to Fronaeus's since the error in the term  $\bar{n}/a$  becomes very large as both  $\bar{n}$  and  $a$  tend to zero.

It can be seen in Tables 4-12 and 5-8 that the strengths of the metal complexes are inversely related to the strengths of the corresponding acids. A plot of  $\log K_1$  against  $\log \beta_{11}^H$  is shown in Fig. 5-10. There is a linear

Fig 5.10

$\log \beta_{II}^H$  AS A FUNCTION OF  $\log K_1$  FOR THE SERIES  
OF COPPER(II) CARBOXYLATE COMPLEXES.



relationship between these two constants except for the formate, methoxyacetate, and glycollate systems. Similar relationships have been noted for complexes formed by a given metal ion with a series of closely related ligands<sup>234</sup>. Steric effects often modify the relationship and these account for the deviations observed in this series. Formic acid, the first acid of the series, usually behaves anomalously, and the behaviour of copper(II) methoxyacetate and copper(II) glycollate is attributed to the formation of chelates<sup>201</sup>. The effect of chelation on the stability of complexes is illustrated by the copper(II) formate and copper(II) glycollate complexes. Formic acid and glycollic acid have almost identical equilibrium constants but  $\beta_1$  and  $K_2$  for copper(II) glycollate are respectively 10 times and 4 times more than the corresponding constants for copper(II) formate. This behaviour has been attributed to the chelation of copper(II) glycollate<sup>201</sup>.

In the series of complexes copper(II) acetate, -propionate, -n-butyrate, -n-valerate, the value of  $K_2$  is constant within experimental error indicating that the free energy of addition of the second carboxylate ion to the species  $\text{CuA}^+$  is the same throughout the series.

The values of  $\beta_1$  and  $\beta_2$  for the series of complexes are related linearly in the form

$$\log \beta_2 = 1.77 \log \beta_1 - 0.33$$

The constants for all the systems fall on or close to this line. The values of  $\beta_1$  and  $K_2$  are similarly related thus

$$\log K_2 = 0.77 \log \beta_1 - 0.33$$

though the points for iso-butyrate, pivalate, and glycollate fall some distance from this line. Rougher correlations may be drawn between  $K_{22}$  and  $K_2$ ,  $\beta_{12}^H$  and  $\beta_2$ , and  $\beta_{22}^H$  and  $\beta_2$ . The ligands formate, methoxyacetate, glycollate, iso-butyrate, and pivalate are excluded from the last three correlations.

In the copper(II) propionate system the value of the dimerisation constant,  $K_D$ , for reaction (5-16) is  $K_D = 10^{0.50}$ . The colours of the concentrated solutions of these copper(II) carboxylates are similar to those observed by other workers [cf. Sec. 1(d)]. Solutions of both copper(II) formate and copper(II) acetate were dark blue while those of copper(II) propionate in which dimers occurred, were green. The solutions of copper(II) n-butyrate were green also and it is likely that dimers would have been detected in them if the measurements had not been restricted by precipitation.

The silver(I) acetate system has recently been investigated<sup>235</sup> at 25°C. in the 3.00M constant ionic medium. The stability constants evaluated are

$$\log \beta_1 = 0.364 \pm 0.004$$

$$\log \beta_2 = 0.11 \pm 0.07$$

$$\log \beta_3 = -0.1 \pm 0.3$$

Thus, for the acetate system the stability of the metal complexes follows the order found in other systems<sup>181</sup>, viz,  $\text{Cu}^{++} > \text{Cd}^{++} > \text{Ag}^+$ .

Leden's data for cadmium(II) acetate<sup>178</sup> have been recalculated and plotted in the form  $\bar{n}(\log a)_B$ . Leden originally plotted these in the form  $\frac{\bar{n}}{a}(\log a)_B$  and concluded that dimeric species were present. However the replotting of the data shows that the formation curve is independent of B and that, therefore, mononuclear complexes only are present. The stability constants have been calculated using the projection strip method and successive approximations,

$$\log \beta_1 = 1.29 \pm 0.03$$

$$\log \beta_2 = 2.37 \pm 0.03$$

$$\log \beta_3 = 2.70$$



SECTION 6.

EQUILIBRIA IN 50% v/v AQUEOUS DIOXAN.

6(a) PRELIMINARY MEASUREMENTS.

Measurements in the 50% v/v dioxan-water mixture were made in the same way as those in aqueous solution. The constant ionic medium was 0.60M sodium perchlorate in which the variation of activity coefficient is small<sup>205</sup>. Some preliminary measurements were made of the liquid junction potential in acid solution and of the hydrolysis of the copper(II) ion.

Liquid junction potential.

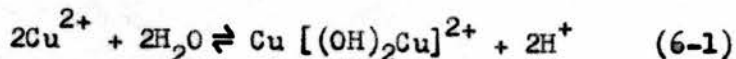
The determination of the variation of the liquid junction potential in acid solutions is important since the potential may be considerably larger in the organic solvent and in this ionic medium than it is in 3.00M aqueous sodium perchlorate. Measurements involving the copper(II) ion may have to be made in appreciably acid solutions in order to suppress hydrolysis of the metal ion. Solutions of 0.05M perchloric acid were therefore titrated with 0.1M sodium hydroxide in the presence of a constant concentration of copper. Titrations were made with B = 0.00M, 0.025M, 0.050M, and 0.100M. The liquid junction potential was found to be independent of B, and to be a linear function of h thus,

$$E_J = 26.2h \pm 0.4\text{mV/mole} \quad (3-15)$$

$E_J$  is significant, therefore, only for  $\text{pH} < 2$ .

Hydrolysis of the copper(II) ion.

The hydrolysis of the copper(II) ion has been investigated in aqueous 3.00M sodium perchlorate medium<sup>232</sup> and the following equilibrium was found to occur,



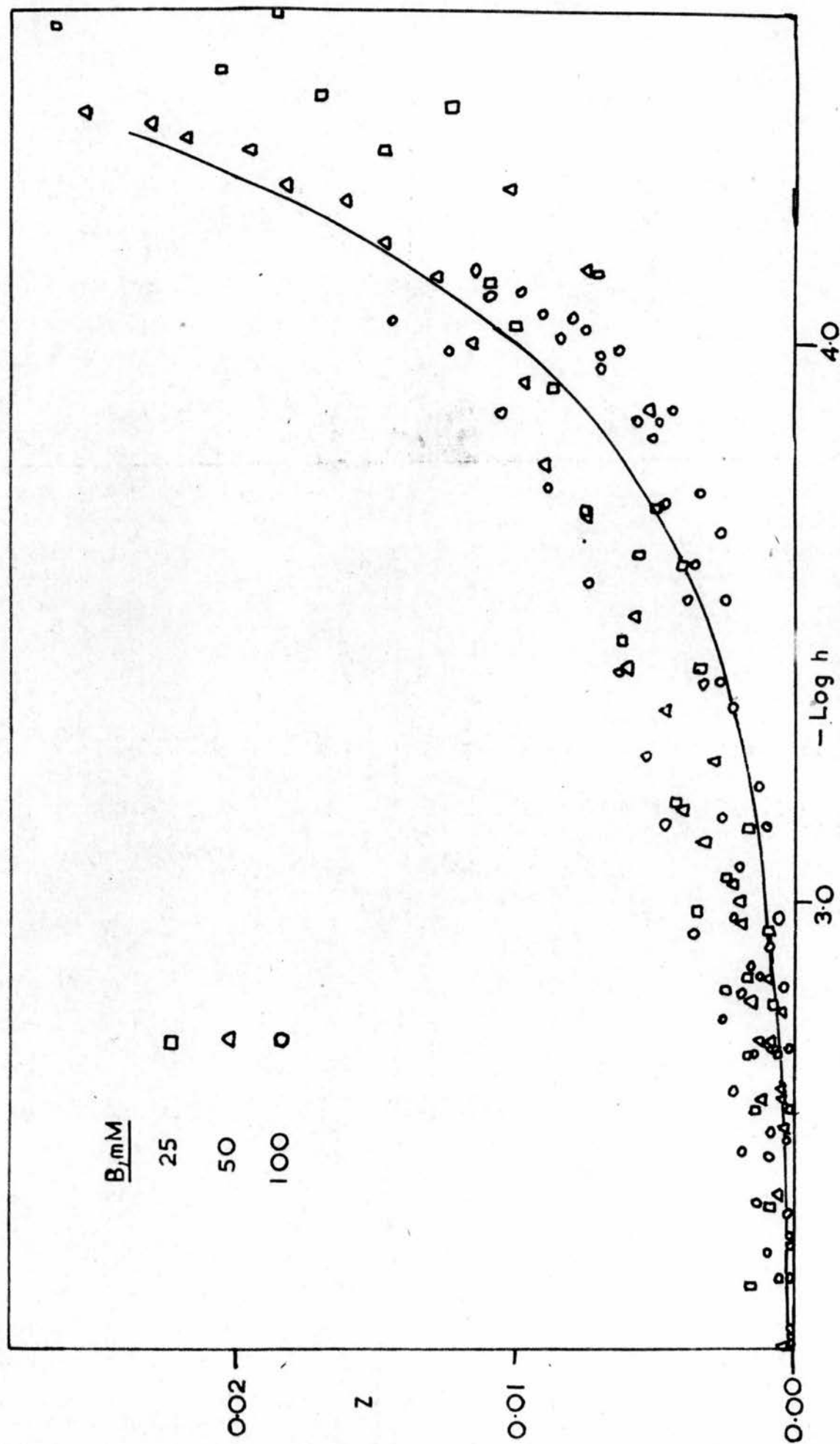
with hydrolysis constant  $\log k = -10.6 \pm 0.1$ .

In the present work acid-base titrations similar to those for the determination of the liquid junction potential have been made. The copper

Fig 6-1

HYDROLYSIS OF  $\text{Cu}^{2+}$  IN 50% v/v DIOXAN

Z plotted as a function of  $\log h$ . The curve calculated assuming that only the complex  $\text{CuOH}^+$  is formed, with  $k=1.0 \times 10^{-6}$

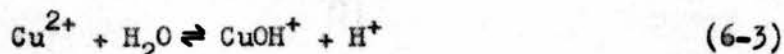


concentrations was kept constant at 0.025M, 0.050M, or 0.100M. Titrations were stopped when precipitation occurred. The average number,  $Z$ , of OH ions bound per copper atom may be calculated from  $B$ ,  $H$ , and  $h$  thus,

$$\frac{h - H - K_w h^{-1}}{B} = Z \quad (6-2)$$

In a 50% v/v dioxan-water mixture  $K_w$  is of the order<sup>205</sup> of  $1.8 \times 10^{-16}$ , and so the term  $K_w h^{-1}$  in Eq.(6-2) may be neglected since it is exceedingly small compared to the other terms. The experimental data are summarised in Table 6-1 and  $Z$  is plotted as a function of  $\log h$  in Fig. 6-1. The curves  $Z(\log h)_B$  appear to be independent of  $B$  and it was assumed that a mononuclear hydrolysis product is formed. The data are rather scattered owing to the nature of the calculation in which two similar large numbers,  $H$  and  $h$  are subtracted.

It was assumed that the following equilibrium occurred



for which the hydrolysis constant,  $k$ , is given by

$$k = \frac{[\text{CuOH}^+][\text{H}^+]}{[\text{Cu}^{2+}]} \quad (6-4)$$

The experimental data have been fitted to the calculated curve for one mononuclear complex only [Sec. 2(b), Eq. (2-7)]. The terms  $h$ ,  $k$ , and  $h^*$  in the present case correspond to  $a$ ,  $\beta_1$ , and  $a^*$  respectively in Eq.(2-7). In the position of best fit  $\log h = 0$  and  $\log h^* = -6.0 \pm 0.3$ , whence by Eq.(2-8)

$$\log k = -6.0 \pm 0.3$$

The full line drawn in Fig.6-1 is the curve calculated using  $\log k = -6.0$ .

Although hydrolysis appears to start at about pH2 it is not appreciable until pH3.7 where 0.5% of the copper is hydrolysed. Thus it would be desirable if copper(II) carboxylate titrations could be made within the range  $2.0 \leq \text{pH} \leq 3.7$  so that corrections for liquid junction potential and hydrolysis of the metal

ion need not be applied. In this medium the value of  $\log \beta_{11}^H$  for acetic acid is 5.618 [Sec. 6(b), p.175] and a buffer of pH 3.7 would have an acid to salt ratio of about 100 to 1. The copper ions would meet intense competition from protons for the acetate ions and copper(II) acetate complex formation would be rather slight. To achieve greater complex formation buffers of higher pH were therefore used.

TABLE 6-1

Hydrolysis of the copper(II) ion.

Experimental data (H, pH, h, Z) <sub>B</sub>											
B (mM)				25				25			
H	pH	h	Z	H	pH	h	Z	H	pH	h	Z
2.359	2.626	2.363	0.000	0.836	3.047	0.897	0.002	4.855	2.310	4.895	0.002
1.933	2.713	1.938	0.000	0.072	3.705	0.197	0.005	3.479	2.456	3.501	0.001
1.514	2.814	1.534	0.001	-0.103	4.128	0.075	0.007	2.337	2.625	2.373	0.001
1.101	2.949	1.124	0.001	-0.271	4.428	0.037	0.012	1.836	2.726	1.878	0.002
0.695	3.134	0.735	0.002	-0.434	4.595	0.027	0.018	1.374	2.843	1.436	0.002
0.296	3.421	0.379	0.003					0.947	2.985	1.035	0.004
0.098	3.624	0.238	0.006					0.551	3.183	0.657	0.004
-0.098	3.925	0.119	0.009					0.183	3.470	0.339	0.006
-0.195	4.112	0.077	0.011					0.009	3.707	0.197	0.008
-0.389	4.452	0.035	0.017					-0.160	4.035	0.092	0.010
-0.485	4.614	0.024	0.020					-0.323	4.351	0.045	0.015
								-0.481	4.498	0.032	0.021
								-0.633	4.574	0.027	0.026







6(b) ACETIC ACID EQUILIBRIA.

Buffers were prepared as described in Sec. 3(c) and the potentiometric titrations were made in the same way as before. The increments of buffer added were usually sufficient to increase A by 25mM or 50mM, up to a total carboxylate concentration of 600mM. Activity coefficients begin to vary significantly above this concentration<sup>205</sup>. Some titrations were stopped when A was less than 600mM since inconveniently large increments of rather dilute buffers would have had to be added in order to reach this concentration. These buffers could not be made more concentrated owing to solubility difficulties and the requirements of the constant ionic medium. A modified titration technique was used in order to overcome these difficulties and to obtain data at concentrations of A up to 600mM. The usual titration preceded by a determination of  $E_0$  was carried out first; the total concentration of A was usually 300-400mM. The glass electrode and J-tube of the salt bridge were removed carefully from this solution. Neither the electrode nor the tube was rinsed, or cleaned, or allowed to touch any surface before the next part of the measurements. Known volumes of buffer and 0.60M sodium perchlorate were then run into a second titration vessel so that the total carboxylate concentration was 600-800mM. The glass electrode and other fittings were then carefully inserted and the solution titrated with 0.60M sodium perchlorate. Readings of E were taken at 25mM intervals of A until the concentration of A had fallen to 200mM. The glass electrode and salt bridge were then removed from this solution and replaced in the first solution so that the last measurement of E in the first titration could be checked. No determination of  $E_0$  was made in the second titration and it was assumed that if the glass electrode and salt bridge were handled carefully during transfer from one

solution to another then  $E_0$  would not vary during these titrations. Any change in  $E_0$  would be shown by the check on the last measurement of the first titration. If a variation greater than the experimental error was detected then the second titration was rejected.

Duplicate readings of 6-8 points at concentrations of A between 200mM and 400mM were obtained using this "overlap" method of titration. The duplicate points also provide a check on the constancy of  $E_0$  and the method has been widely used in the study of various carboxylic acid equilibria in aqueous solution<sup>201, 214</sup>. In this system, however, there was always a difference in E between corresponding points in the two titrations even though the first check of  $E_0$  was satisfactory. The difference which was usually between 2.0 and 2.5mV was constant to within  $\pm 0.2$ mV in any pair of titrations. The only explanation for this phenomenon appears to be that  $E_0$  did, in fact, change when the glass electrode was transferred. The readings of E in the second titration have, therefore, been corrected by the constant difference to correspond with the readings of the first titration.

The values of  $\bar{n}_H$  and  $\log h$  were calculated using Eqs.(1-6) and (3-5) respectively. As mentioned above the term  $K_w h^{-1}$  may be neglected.

Tables 6-2A, 6-2B, and 6-2D contain a selection of the experimental data  $\bar{n}_H(\log h)_A$  for acetic acid obtained from the potentiometric titrations of the acetate buffers. The buffers of high acidity i.e. those in Table 6-2D were not examined until some time after the others and the data obtained from them have not been used in the subsequent calculations of the equilibrium constants. These constants are, however, consistent with the experimental data in the buffers of high acidity. The experimental data are plotted in the form  $\bar{n}_H(\log h)_A$  in Fig. 6-2.

Fig 6.2

FORMATION CURVES FOR ACETIC ACID IN 50% v/v DIOXAN

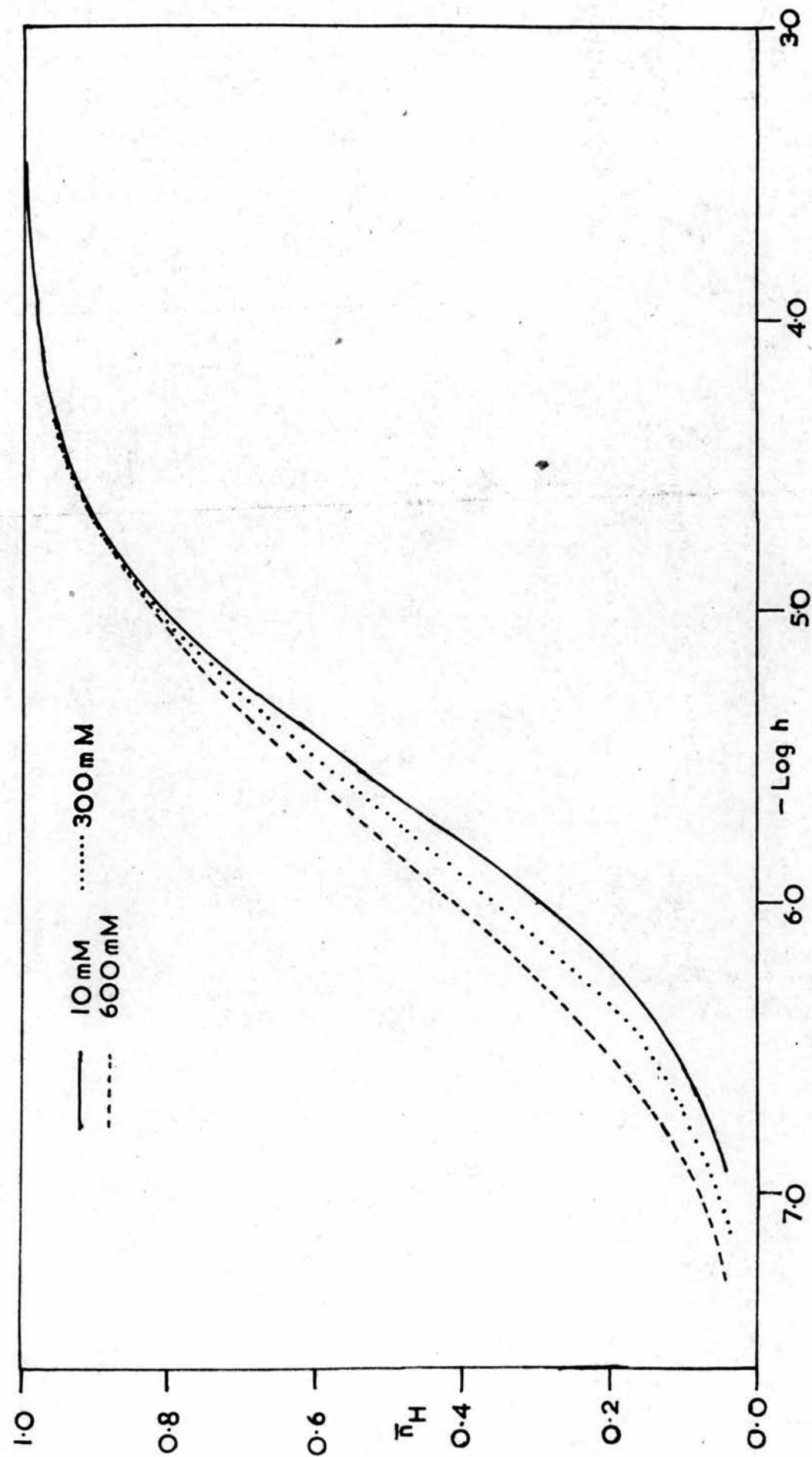


TABLE 6-2A

Acetic acid

Experimental data  $\bar{n}_H(\log h)_A$  obtained from potentiometric titrations of acetate buffers at  $A \leq 100\text{mM}$ . Duplicate titrations have not been tabulated.

Buffer	1			2			3		
[NaA]mM	597.2			600.0			586.0		
[HA]mM	28.02			83.05			140.1		
	A	$\bar{n}_H$	pH	A	$\bar{n}_H$	pH	A	$\bar{n}_H$	pH
	10.64	0.045	6.927	9.82	0.105	6.557	9.33	0.193	6.259
	14.54	0.045	6.927	13.94	0.112	6.529	15.42	0.193	6.249
	18.39	0.045	6.927	22.03	0.117	6.507	18.28	0.193	6.249
	26.41	0.045	6.927	27.32	0.122	6.504	21.40	0.193	6.249
	36.75	0.045	6.927	32.53	0.122	6.502	24.36	0.193	6.249
	46.84	0.045	6.930	37.65	0.122	6.502	27.29	0.193	6.249
	49.82	0.045	6.933	42.69	0.122	6.502	49.87	0.193	6.259
	100.0	0.045	6.974	50.10	0.122	6.502	100.4	0.193	6.284
				99.66	0.122	6.529			
	4			5			6		
	588.0			600.0			572.0		
	211.8			308.1			494.2		
	A	$\bar{n}_H$	pH	A	$\bar{n}_H$	pH	A	$\bar{n}_H$	pH
	10.28	0.265	6.056	9.74	0.339	5.928	9.17	0.463	5.688
	16.98	0.265	6.056	15.49	0.339	5.923	18.19	0.464	5.684
	23.57	0.265	6.056	19.28	0.339	5.923	27.05	0.464	5.684
	30.06	0.265	6.061	23.04	0.339	5.923	35.76	0.464	5.684
	50.39	0.265	6.073	30.46	0.339	5.923	50.67	0.464	5.688
	100.2	0.265	6.100	50.24	0.339	5.928	100.5	0.464	5.706
				99.93	0.339	5.951			
	7			8			9		
	572.0			600.0			568.0		
	759.1			1256			1620		
	A	$\bar{n}_H$	pH	A	$\bar{n}_H$	pH	A	$\bar{n}_H$	pH
	11.47	0.570	5.500	8.03	0.676	5.304	9.47	0.740	5.162
	17.14	0.570	5.500	12.02	0.677	5.299	18.86	0.740	5.159
	22.75	0.570	5.500	19.95	0.677	5.299	28.17	0.740	5.159
	28.32	0.570	5.500	31.72	0.677	5.299	37.39	0.740	5.159
	50.13	0.570	5.505	51.00	0.677	5.301	51.09	0.740	5.159
	99.10	0.570	5.517	99.28	0.677	5.311	99.85	0.740	5.165

TABLE 6-2A (CONTD.)

Buffer	10			11			12		
[NaA]mM	500.0			400.0			200.0		
[HA]mM	2393			3530			4002		
	A	$\bar{n}_H$	pH	A	$\bar{n}_H$	pH	A	$\bar{n}_H$	pH
12.52	0.814	4.969	8.52	0.871	4.728	9.12	0.911	4.521	
24.94	0.821	4.951	17.01	0.885	4.701	36.23	0.942	4.379	
37.25	0.823	4.947	25.46	0.889	4.694	54.11	0.945	4.364	
43.36	0.824	4.946	50.60	0.894	4.677	71.84	0.947	4.351	
49.45	0.824	4.946	67.18	0.895	4.673	98.15	0.948	4.344	
55.51	0.824	4.946	75.42	0.895	4.673				
61.55	0.825	4.946	83.62	0.896	4.673				
73.55	0.825	4.946	91.78	0.896	4.673				
97.24	0.826	4.946	99.92	0.896	4.673				

TABLE 6-2B

Acetic acid

Experimental data  $\bar{n}_H(\log h)_A$  obtained from potentiometric titrations of acetate buffers at  $100\text{mM} \leq A \leq 600\text{mM}$ . Duplicate titrations have not been tabulated.

Buffer	1			2			3		
[NaA]mM	597.2			600.0			586.0		
[HA]mM	28.02			83.05			140.1		
	A	$\bar{n}_H$	pH	A	$\bar{n}_H$	pH	A	$\bar{n}_H$	pH
100.0	0.045	6.974	99.66	0.122	6.529	100.4	0.193	6.284	
150.1	0.045	7.011	149.9	0.122	6.560	150.0	0.193	6.313	
199.8	0.045	7.048	200.2	0.122	6.590	199.8	0.193	6.344	
250.1	0.045	7.082	249.9	0.122	6.624	250.0	0.193	6.377	
299.9	0.045	7.119	300.0	0.122	6.656	300.2	0.193	6.406	
349.8	0.045	7.148	349.9	0.122	6.688	350.0	0.193	6.433	
400.1	0.045	7.177	400.0	0.122	6.720	399.9	0.193	6.465	
449.8	0.045	7.209	450.1	0.122	6.742	450.3	0.193	6.479	
500.2	0.045	7.239	500.4	0.122	6.761	499.9	0.193	6.507	
599.7	0.045	7.305	600.5	0.122	6.817	600.1	0.193	6.558	



TABLE 6-2B (CONTD.)

Buffer	4			5			6		
[NaA]mM	588.0			600.0			572.0		
[HA]mM	211.8			308.1			494.2		
	A	$\bar{n}_H$	pH	A	$\bar{n}_H$	pH	A	$\bar{n}_H$	pH
	100.2	0.265	6.100	99.933	0.339	5.951	100.5	0.464	5.706
	149.5	0.265	6.124	149.7	0.339	5.973	150.9	0.464	5.725
	200.3	0.265	6.153	199.8	0.339	5.997	200.9	0.464	5.743
	250.3	0.265	6.178	249.9	0.339	6.022	251.1	0.464	5.762
	299.5	0.265	6.207	299.6	0.339	6.044	300.6	0.464	5.781
	350.2	0.265	6.234	349.9	0.339	6.066	350.7	0.464	5.801
	399.9	0.265	6.261	399.4	0.339	6.093	401.1	0.464	5.820
	450.0	0.265	6.278	449.6	0.339	6.114	451.0	0.464	5.838
	499.9	0.265	6.301	500.1	0.339	6.137	500.6	0.464	5.856
	600.2	0.265	6.347				599.8	0.464	5.892
	7			8			9		
	572.0			600.0			568.0		
	759.1			1256			1620		
	A	$\bar{n}_H$	pH	A	$\bar{n}_H$	pH	A	$\bar{n}_H$	pH
	99.10	0.570	5.517	99.288	0.677	5.311	99.85	0.740	5.165
	149.0	0.570	5.532	151.9	0.677	5.317	150.6	0.740	5.169
	199.3	0.570	5.549	201.4	0.677	5.331	202.8	0.740	5.179
	249.3	0.570	5.563	251.2	0.677	5.341	248.7	0.740	5.186
	300.3	0.570	5.576	300.9	0.677	5.350	299.6	0.740	5.194
	349.8	0.570	5.590	350.2	0.677	5.361	351.3	0.740	5.201
	400.5	0.570	5.603	399.0	0.677	5.368	400.2	0.740	5.209
	450.1	0.570	5.618	449.4	0.677	5.380	449.6	0.740	5.216
	500.3	0.570	5.634	500.8	0.677	5.392	499.2	0.740	5.225
	600.4	0.570	5.664	600.4	0.677	5.412	600.4	0.740	5.240
	10			11			12		
	500.0			400.0			200.0		
	2393			3530			4002		
	A	$\bar{n}_H$	pH	A	$\bar{n}_H$	pH	A	$\bar{n}_H$	pH
	97.24	0.827	4.946	99.92	0.896	4.673	98.15	0.948	4.344
	149.1	0.827	4.947	148.0	0.897	4.673	149.8	0.950	4.330
	199.1	0.827	4.949	194.9	0.897	4.673	200.1	0.951	4.327
	252.6	0.827	4.952	248.1	0.897	4.673	249.2	0.951	4.324
	298.9	0.827	4.956	299.9	0.898	4.675	297.1	0.951	4.317
	348.5	0.827	4.961	350.2	0.898	4.677	351.6	0.951	4.315
	400.9	0.827	4.964	399.1	0.898	4.679	397.1	0.952	4.315
	451.2	0.827	4.968	453.4	0.898	4.680	448.8	0.952	4.313
	499.5	0.827	4.971	499.6	0.898	4.682	499.1	0.952	4.313
	598.5	0.827	4.979	600.7	0.898	4.684	602.6	0.952	4.312



TABLE 6-2C.

Acetic acid

Values of  $\log \beta''^H$  obtained from the pH of buffers at  $A \leq 20\text{mM}$  using Eq(4-8)

Buffer	$\log \beta''^H$	Buffer	$\log \beta''^H$
1	5.598	7	5.620
2	5.644	7a	5.623
3	5.627	8	5.620
3a	5.598	9	5.614
4	5.613	10	5.626
4a	5.595	11	5.632
5	5.633	12	5.615
6	5.621		

Buffers 3a, 4a, and 7a are buffers similar in composition to buffers 3, 4, and 7 respectively. The experimental data for these buffers have not been included in tables 6-2A and 6-2B.

TABLE 6-2D.

Acetic acid

Experimental data  $\bar{n}_H$  ( $\log h$ )<sub>A</sub> obtained from potentiometric titrations of acetate buffers of high acidity.

Buffer	13			14			15		
[NaA] mM	77.50			72.19			50.00		
[HA] mM	2267			2252			2386		
	A	$\bar{n}_H$	pH	A	$\bar{n}_H$	pH	A	$\bar{n}_H$	pH
	8.52	0.945	4.256	8.45	0.952	4.222	8.86	0.962	4.144
	16.99	0.956	4.239	49.81	0.966	4.214	17.65	0.970	4.102
	50.23	0.963	4.226	101.4	0.968	4.207	47.93	0.976	4.041
	98.36	0.965	4.220	150.7	0.968	4.207	98.12	0.978	4.019
	148.3	0.966	4.217	201.5	0.968	4.205	150.2	0.978	4.007
	199.6	0.966	4.217	249.9	0.968	4.204	199.9	0.979	4.002
	248.6	0.966	4.212	299.4	0.969	4.204	251.2	0.979	3.999
	298.6	0.966	4.207	349.6	0.969	4.202	300.1	0.979	3.994
	349.4	0.966	4.207	400.3	0.969	4.200	350.2	0.979	3.991
	400.7	0.967	4.205	451.2	0.969	4.200	401.0	0.979	3.989
	449.5	0.967	4.204	499.6	0.969	4.197	449.5	0.979	3.986
	501.1	0.967	4.204	600.8	0.969	4.190	501.3	0.979	3.984
	601.1	0.967	4.202				599.8	0.979	3.982

TABLE 6-2D.

Acetic acid (continued)

Buffer	[NaA] mM [HA] mM	16	17	18	19
		49.78 234.8	25.75 24.51	12.71 2506	2.47 2550
A		8.72 17.38 51.38 100.6 151.7 200.5 250.7 298.8 351.1 400.8 451.1 499.0 600.3	9.02 17.98 48.82 99.92 148.9 199.8 248.4 298.6 349.9 398.8 448.6 498.9 600.2	9.23 49.92 97.91 148.2 200.3 250.2 301.6 350.7 401.0 449.0 500.8 599.7	9.60 28.57 51.90 101.7 149.6 199.8 251.8 301.5 349.2 398.3 448.6 499.6 600.3
$\bar{\eta}_H$		0.968 0.973 0.977 0.978 0.979 0.979 0.979 0.979 0.979 0.979 0.979 0.979 0.979	0.989 0.989 0.990 0.990 0.990 0.990 0.990 0.990 0.990 0.990 0.990 0.990 0.990	0.998 0.997 0.996 0.996 0.996 0.996 0.996 0.995 0.995 0.995 0.995 0.995 0.995	1.004 1.000 0.999 0.999 0.999 0.999 0.999 0.999 0.999 0.999 0.999 0.999 0.999
pH		4.124 4.094 4.053 4.036 4.033 4.029 4.021 4.019 4.016 4.014 4.014 4.013 4.002	3.691 3.696 3.702 3.703 3.708 3.708 3.703 3.702 3.700 3.696 3.695 3.693 3.686	3.164 3.213 3.262 3.284 3.304 3.318 3.330 3.336 3.341 3.341 3.348 3.350	2.490 2.491 2.493 2.498 2.506 2.513 2.520 2.528 2.532 2.539 2.545 2.559 2.567

### Calculation of the equilibrium constants.

The shape of the formation curves is similar to that obtained in aqueous solution except that no isohydric point is evident. The pH of a buffer did not vary with concentration for  $A \leq 50\text{mM}$  in aqueous solution but in the organic solvent the pH is constant only for  $A \leq 20\text{mM}$ . Generally, there is also a larger variation of pH with A in the organic solvent than there was in water. Thus the organic solvent appears to have increased the polymerisation of the acid.

The value of  $\beta_{11}^H$ , the acid association constant, has been calculated by the following methods. (1) The formation curve ( $\bar{n}_H$ , logh) for  $A = 10\text{mM}$  fits exactly the normalised curve for a single complex, Eq. (2-7), and from Eq. (2-8),  $\log \beta_{11}^H = 5.620 \pm 0.010$ . (2) Where the pH of a buffer is constant at low concentrations of A,  $\log \beta_{11}^H$  has been calculated using Eq. (4-8). The values of  $\log \beta_{11}^H$  at  $A \leq 20\text{mM}$  for 15 buffers are shown in Table 6-2C. The average value of  $\log \beta_{11}^H = 5.618 \pm 0.013$ .

Values of  $\log \beta_{11}^H$  consistent with the above were found by various curve-fitting procedures described below. The preferred value of  $\log \beta_{11}^H$  is that obtained by method (2).

Clearly, species other than HA are present in this system and the first hypothesis made was that the species present were the same as in aqueous solution, namely HA,  $\text{HA}_2$ , and  $\text{H}_2\text{A}_2$ . The formation curves for all values of A appear to coalesce at  $\bar{n}_H = 0.95$  suggesting that there is an isohydric point there. Therefore, from Eq. (4-13)  $R = 0.474$ . As a first approximation the experimental data, plotted in the form  $\log A(\text{logh})_{\bar{n}_H}$ , were superimposed on the families of curves  $\log A^*(\text{logh}^*)_{\bar{n}_H, R}$ , calculated using Eq. (2-23), with  $R = 0.44$  and 0.50. In both cases the fit was extremely bad and it could be seen that

the experimental data could not be fitted to any family of normalised curves with  $R$  between 0.44 and 0.50. The experimental data for  $\bar{n}_H = 0.05, 0.10,$  and 0.15 at  $A \leq 300\text{mM}$  could be fitted with rather low precision to the family of normalised curves with  $R = 0.50$ . In the position of best fit, when  $(\log A^*, \log h^*) = (0, 0)$ ,  $(\log A, \log h) = (-0.28 \pm 0.04, -5.615 \pm 0.005)$ .

Whence, from Eqs. (2-24) and (2-25) and (2-28)

$$\log \beta_{11}^H = 5.615 \pm 0.005$$

$$\log \beta_{12}^H \sim 5.90$$

$$\log \beta_{22}^H \sim 11.20$$

The trend of the experimental data  $\log A(\log h)_{\bar{n}_H}$  for  $\bar{n}_H > 0.15$  in the above fit suggests that higher species than dimers are formed. The formation of such species restricts the use of curve-fitting techniques since these can be applied only to three parameters.

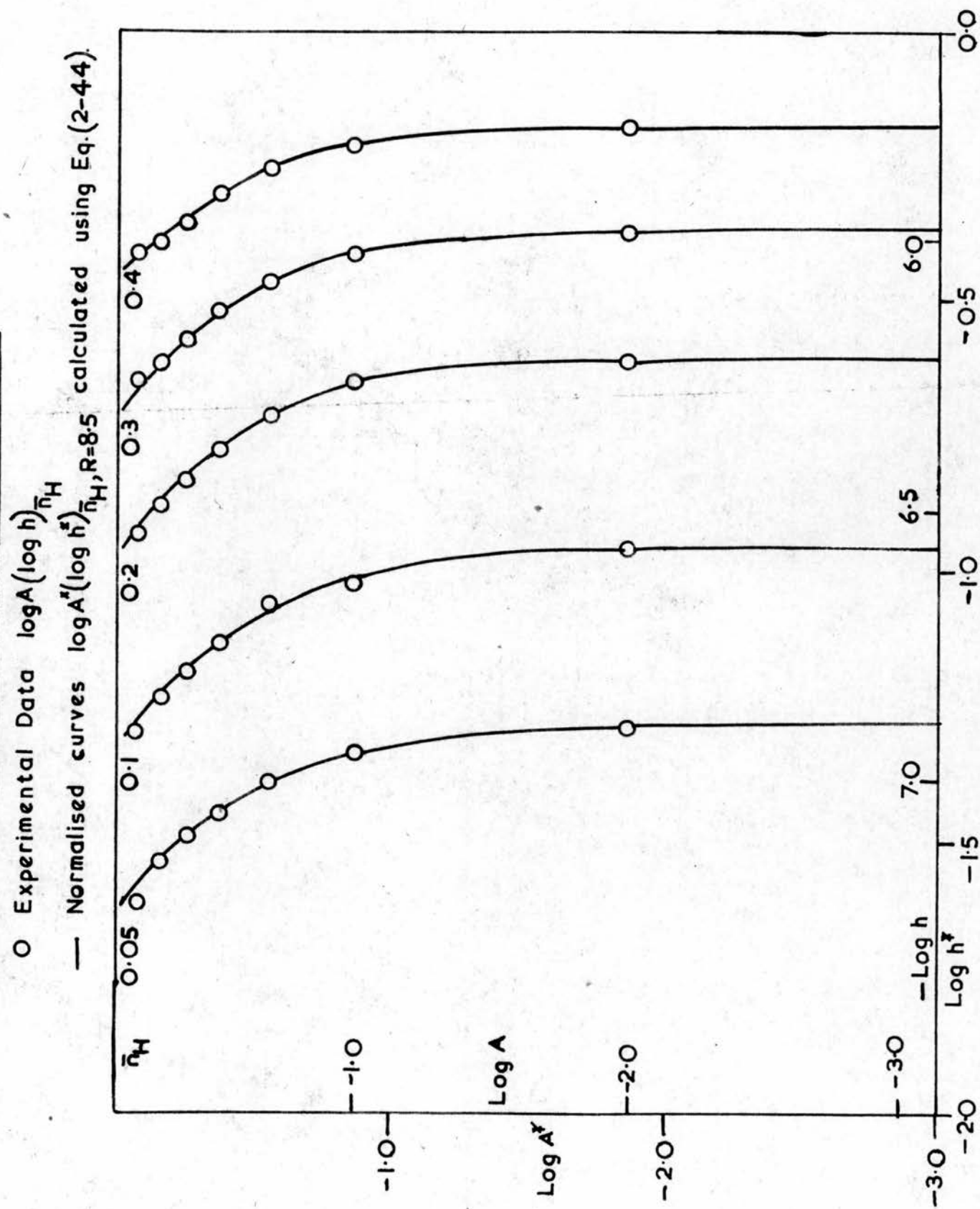
The species which appears most likely to be formed after the dimers, especially in the more alkaline solutions, is  $H_2A_3$ . At low values of  $\bar{n}_H$ , say  $\bar{n}_H \leq 0.30$ , it is unlikely that the neutral dimer  $H_2A_2$  is formed in appreciable amounts. Charged species will predominate in such solutions and therefore it was assumed that  $HA$ ,  $HA_2$ , and  $H_2A_3$  only were present at  $\bar{n}_H \leq 0.30$ . Families of normalised curves  $\log A^*(\log h^*)_{\bar{n}_H, R}$  were calculated using Eq. (2-44) and various values of  $R$ . When the experimental data,  $\log A(\log h)_{\bar{n}_H}$ , were superimposed on them acceptable fits could be obtained with  $7.5 \leq R \leq 9.75$ . The best fit was obtained with the family of curves with  $R = 8.5$ , Fig. 6-3 and in this position when  $(\log A^*, \log h^*) = (0, 0)$ ,  $(\log A, \log h) = (-0.133 \pm 0.012, -5.613 \pm 0.005)$ , whence from Eqs. (2-24), (2-25), and (2-28),

$$\log \beta_{11}^H = 5.613 \pm 0.005$$

$$\log \beta_{12}^H = 5.75 \pm 0.03$$

$$\log \beta_{23}^H = 12.43 \pm 0.05$$

Fig 6.3 ACETIC ACID IN 50% v/v DIOXAN





The best fit extends to  $\bar{n}_H = 0.40$  but  $H_2A_2$  is almost certainly formed to an appreciable extent at this point. Therefore the constants may be slightly in error.

The possibility of the formation of the charged species  $HA_2$  and  $HA_3$  in the most alkaline solutions must also be considered. The experimental data  $\log A(\log h)\bar{n}_H$  were superimposed on families of normalised curves,  $\log A^*(\log h^*)\bar{n}_{H,R}$ , calculated on the assumption that the species  $HA$ ,  $HA_2$ , and  $HA_3$  coexist. These curves were calculated using Eq. (2-52) for values of  $R$  between 0.10 and 10.0 but it was not possible to obtain an acceptable fit on any of the families of curves.

Calculation of the average composition of the oligomers and of the free ligand concentration.

The experimental data could not be explained completely by any of the above simple hypotheses and they were therefore analysed by methods which utilised all the data and not small portions of them. It is possible to obtain the average composition of the polynuclear species from the formation curves without any special assumptions about the complexes. The integration methods described in Sec. 2 (c) has been used.

The integrations have been carried out from the formation curves at given values of  $A$ . In order to evaluate  $A_1$ , Eq. (2-109), the slope  $(\delta \bar{n}_H / \delta \ln A)_h$  was assumed to be the average of the quotients  $(\Delta \bar{n}_H / \Delta \ln A)$  for two neighbouring intervals. The values of  $\left[ (\bar{n}_H - \bar{n}_{H(1)}) + \left( \frac{\delta \bar{n}_H}{\delta \ln A} \right)_h \right]_A$  and of  $\left( \frac{\delta \bar{n}_H}{\delta \log A} \right)_h$  were plotted against  $\log h$ . The integrals in Eq. (2-109) and (2-110) were evaluated graphically, thus enabling  $A_1$  and  $\bar{R}$  to be calculated. The lower limit of integration in each case was pH 9. The values of  $\bar{P}_{poly}$



TABLE 6-3A

Acetic acid

The calculation of  $\bar{p}_{\text{poly}}$ ,  $\bar{q}_{\text{poly}}$ , and  $a$ .

A = 400mm.

$-\log h$	$\bar{n}_H - \bar{n}_{H(1)}$	$\left( \frac{\delta \bar{n}_H}{\delta \ln A} \right)_h$	$\log \frac{A}{A_1}$	$A_1(\text{mm})$	$\bar{r}$	$\bar{p}_{\text{poly}}$	$\bar{q}_{\text{poly}}$	$\log \frac{A}{a}$	$a(\text{mm})$
8.6	0.001	0.001			1.000			0.000	4000.0
8.0	0.002	0.004	0.0024	397.8	0.996			0.0037	396.7
7.8	0.005	0.006	0.0039	396.4	0.994			0.0064	394.2
7.6	0.007	0.009	0.0064	394.1	0.991			0.0105	390.4
7.4	0.006	0.013	0.0105	390.4	0.986			0.0170	384.7
7.2	0.015	0.021	0.0164	385.2	0.978			0.0271	375.6
7.0	0.023	0.031	0.0250	377.6	0.967	1.03	2.46	0.0424	362.8
6.8	0.042	0.044	0.0391	365.6	0.950			0.0664	343.3
6.6	0.057	0.061	0.0594	348.8	0.927			0.1017	316.5
6.4	0.068	0.067	0.0855	328.5	0.898			0.1510	282.6
6.2	0.081	0.083	0.1163	306.0	0.862			0.2165	243.0
6.0	0.091	0.075	0.1497	283.2	0.824	1.52	2.51	0.2997	200.6
5.8	0.076	0.074	0.1810	263.5	0.793			0.4001	159.2
5.6	0.058	0.056	0.2081	247.7	0.766	1.73	2.60	0.5168	121.7
5.4	0.039	0.035	0.2270	237.0	0.746			0.6489	89.8
5.2	0.022	0.020	0.2386	230.8	0.733			0.7948	64.2
5.0	0.012	0.012	0.2451	227.4	0.725	2.29	2.76	0.9535	44.5
4.8	0.006	0.007	0.2488	225.4	0.721			1.1242	30.1
4.6	0.003	0.002	0.2505	224.6	0.719			1.3032	19.9
4.4	0.000	0.000	0.2510	224.3	0.718	2.63	2.78	1.4889	13.0

and  $\bar{q}_{\text{poly}}$  were then calculated using Eqs. (2-III) and (2-II2) respectively. This procedure was carried out for values of  $A = 400, 500, \text{ and } 600\text{mm}$  and an example of the various steps in the calculation is given in Table 6-3A. The values of  $\bar{p}_{\text{poly}}$  and  $\bar{q}_{\text{poly}}$  for  $A = 500$  and  $600\text{mm}$  are summarised in Table 6-3B. Both  $\bar{p}_{\text{poly}}$  and  $\bar{q}_{\text{poly}}$  rise to maximum values near 4 and thus it appears that species  $H_p A_q$ , where  $p$  and  $q$  are integers  $\leq 4$ , are present in this system. The values of  $\bar{p}_{\text{poly}}$  and  $\bar{q}_{\text{poly}}$  are usually within  $\pm 1$  of each other with  $\bar{p}_{\text{poly}}$  smaller than  $\bar{q}_{\text{poly}}$  which suggests that  $q - p$  is either zero or one. Thus the poly-nuclear species formed may be of the type  $HA_2, H_2A_2, H_2A_3, H_3A_3, H_3A_4, H_4A_4$  etc.

TABLE 6-3B

Acetic acidValues of  $\bar{p}_{\text{poly}}$  and  $\bar{q}_{\text{poly}}$ 

A(mm)	500		600	
	$\bar{p}_{\text{poly}}$	$\bar{q}_{\text{poly}}$	$\bar{p}_{\text{poly}}$	$\bar{q}_{\text{poly}}$
-log h				
7.0	1.12	2.93	1.40	3.01
6.0	1.68	2.81	1.68	2.83
5.6	2.00	2.94	2.06	3.00
5.2			2.60	3.31
5.0	2.72	3.28	2.89	3.45
4.8	2.89	3.31	3.10	3.55
4.6	3.05	3.33	3.31	3.60
4.4	3.13	3.32	3.42	3.62

The value of  $a$  may be calculated by Sillén's<sup>236</sup> method which requires only the data  $H$ ,  $A$ , and  $h$ .

The operational equation is

$$\log \frac{A}{a} = \left\{ \int_0^h \left[ \bar{n}_H + \left( \frac{\delta \bar{n}_H}{\delta \ln A} \right) h \right] d \log h \right\}_A \quad (6-5)$$

for a system which is mononuclear at the lower limit of integration. The integral is again evaluated graphically and an example of the various steps in the calculation is given in Table 6-3A. The lower limit of integration was taken as pH 9.0. Table 6-3C gives  $a$  for  $A = 100, 200, 300, 400, 500$ , and 600mM at various logh. A value of  $a$  may also be obtained from the value of  $A_1$  calculated using Eq. (2-109) thus

$$a = \frac{A_1}{1 + \beta_{11}^H h} \quad (6-6)$$

The values of  $a$  calculated using Eq. (6-6) for  $A = 400$ mM at pH's 6.8, 6.0, and 5.0 are 343.0, 200.1, and 44.16 which agree well with the values calculated using the present integration (see Table 6-3B). Several methods of calculating the equilibrium constants are now follow.

#### Curve-fitting methods

As a first approximation, it is postulated that the species HA, HA<sub>2</sub>, H<sub>2</sub>A<sub>2</sub>, H<sub>2</sub>A<sub>3</sub>, H<sub>3</sub>A<sub>3</sub>, H<sub>3</sub>A<sub>4</sub>, and H<sub>4</sub>A<sub>4</sub> coexist in this system. The value of  $\beta_{11}^H$  has been obtained already. The mass-balance equation for A, Eq. (2-16), may now be extended thus,

$$A = a + \beta_{11}^H ha + 2\beta_{12}^H ha^2 + 2\beta_{22}^H h^2 a^2 + 3\beta_{23}^H h^2 a^3 + 3\beta_{33}^H h^3 a^3 + 4\beta_{34}^H h^3 a^4 + 4\beta_{44}^H h^4 a^4 \quad (6-7)$$

whence

$$\frac{A - a - \beta_{11}^H ha}{ha^2} = (2\beta_{12}^H + 2\beta_{22}^H h) + (3\beta_{23}^H h + 3\beta_{33}^H h^2)a + (4\beta_{34}^H h^2 + 4\beta_{44}^H h^3)a^2 \quad (6-8)$$

Thus we have an equation of the type

$$f(a) = k_0 + k_1 a + k_2 a^2 \quad (6-9)$$

TABLE 6-3C

Acetic acidValues of  $a(\log h)_A$ 

A(mm)	100	200	300	400	500	600
-log h						
8.6	100.0	200.0	300.0	400.0	500.0	599.1
8.0	99.9	199.2	298.4	396.7	496.0	591.7
7.8	99.6	198.6	297.0	394.2	492.1	586.0
7.6	99.2	197.4	294.8	390.4	486.2	576.6
7.4	98.4	195.6	291.5	384.7	476.7	562.6
7.2	97.2	192.8	286.4	375.8	462.0	542.4
7.0	95.5	188.4	278.6	362.8	440.7	514.2
6.8	92.8	181.8	266.2	343.3	411.3	476.4
6.6	88.7	172.0	248.0	316.5	374.0	428.2
6.4	83.1	158.4	224.5	282.6	329.6	372.3
6.2	75.5	140.9	196.0	243.0	280.4	312.6
6.0	66.2	120.1	164.4	200.6	229.6	253.2
5.8	55.5	98.7	132.2	159.2	180.5	197.2
5.6	44.4	77.5	102.8	121.7	136.6	148.2
5.4	33.9	58.2	76.5	88.8	99.7	107.5
5.2	24.7	42.0	54.9	64.2	70.6	75.6
5.0	17.3	29.3	38.2	44.5	48.7	51.9
4.8	11.7	19.9	25.9	30.1	32.8	34.9
4.6	7.78	13.2	17.1	19.9	21.7	23.0
4.4	5.07	8.63	11.2	13.0	14.2	15.0

where

$$k_0 = 2\beta_{12}^H + 2\beta_{22}^H h \quad (6-10a)$$

$$k_1 = 3\beta_{23}^H h + 3\beta_{33}^H h^2 \quad (6-10b)$$

$$k_2 = 4\beta_{34}^H h^2 + 4\beta_{44}^H h^3 \quad (6-10c)$$

Using the values of  $a$  calculated by integration the term  $\log\left(\frac{A - a - \beta_{11}^H ha}{ha^2}\right)$

was calculated for  $A = 100, 200, 300, 400, 500$ , and  $600\text{mM}$  at various values of  $\log h$  and plotted against  $\log a$ . The experimental data,  $\log f(\log a)_h$  were then superimposed on families of normalised curves  $\log f^*(\log a^*)_{g_3}$ .

Setting the normalised variables as follows:

$$\log f^* = g_1 + \log f = \log(1 + g_3 v + v^2) \quad (6-11)$$

$$\log a^* = g_2 + \log a = \log v$$

where  $v$  is an auxiliary variable, and solving Eqs. (6-9), and (6-11) for  $g_1$ ,  $g_2$ , and  $g_3$ , we find

$$g_1 = -\log k_0 \quad (6-12a)$$

$$g_2 = \frac{1}{2}\log k_2 - \frac{1}{2}\log k_0 \quad (6-12b)$$

$$\log g_3 = \log k_1 - \frac{1}{2}\log k_0 - \frac{1}{2}\log k_2 \quad (6-12c)$$

The experimental data fitted the normalised curves over a range of values of  $g_3$ . Data in the region  $4.4 \leq \text{pH} \leq 5.2$  could be fitted to curves with  $0 \leq g_3 \leq 2$ , Fig. 6-4. Data at  $\text{pH} > 5.2$  could be fitted to curves with  $g_3$  ranging from zero to at least 50. The latter data were therefore not considered further. The values of  $k_0$ ,  $k_1$ , and  $k_2$  evaluated for data at  $4.4 \leq \text{pH} \leq 5.2$  are summarised in Table 6-4. The values of  $\log k_0$  and  $\log k_2$  vary with  $h$ . The values of  $\log k_1$  are those evaluated with  $g_3 = 2$  i.e. they are maximum values which also vary with  $h$ .

Fig 6.4

Family of normalised curves  $\log r^*(\log a^*)_{g_3}$ , calculated using Eq.(6-11), for finding coefficients of polynomials  $k_0 + k_1 a + k_2 a^2$ .

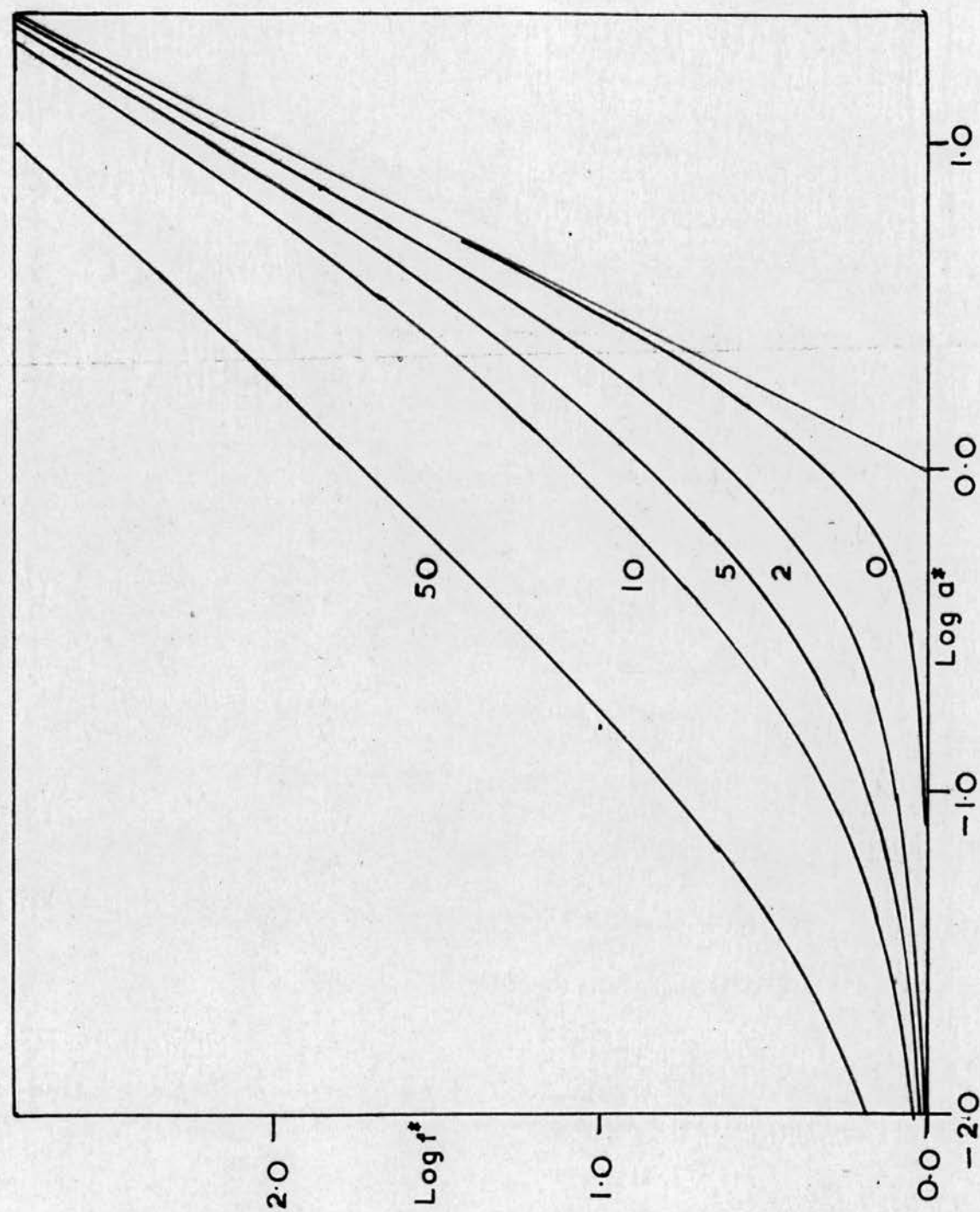




TABLE 6-4Acetic acid

Values of  $k_0$ ,  $k_1$ , and  $k_2$  in Eq. (6-9) evaluated using the normalised curves, Eq. (6-11).

$-\log h$	$\log k_0$	$\log k_1$	$\log k_2$
4.4	6.72+0.17	$\leq 9.0$	10.92+0.18
4.6	6.56+0.18	$\leq 8.6$	10.37+0.18
4.8	6.42+0.16	$\leq 8.3$	9.85+0.18
5.0	6.27+0.22	$\leq 8.0$	9.38+0.18
5.2	6.13+0.21	$\leq 7.7$	8.94+0.18

The terms  $k_0$ ,  $k_1$ , and  $k_2$  are each the sum of two constants which may be evaluated by further curve-fitting.

We have

$$k_0 = 2\beta_{12}^H + 2\beta_{22}^H h \quad (6-10a)$$

and rearranging Eqs. (6-10b) and (6-10c)

$$\frac{k_1}{3h} = \beta_{23}^H + \beta_{33}^H h \quad (6-13a)$$

$$\frac{k_2}{4h^2} = \beta_{34}^H + \beta_{44}^H h \quad (6-13b)$$

These equations are all of the type

$$f(a^1) = k_0^1 + k_1^1 a^1 \quad (6-14)$$

which is a special case of Eq. (6-9) when  $k_2 = 0$ . Using the same normalised variables as before we have

$$\begin{aligned} \log f^* &= \log g_1 + \log f = \log(1+v) \\ \log a^* &= \log g_2 + \log a^1 = \log v \end{aligned} \quad (6-15)$$

Solving Eqs. (6-14) and (6-15) for  $g_1$  and  $g_2$  we find

$$g_1 = -\log k_0^1 \quad (6-16a)$$

$$g_2 = \log k_1^1 - \log k_0^1 \quad (6-16b)$$

The data  $\log k_0(\log h)$ ,  $\log \frac{k_1}{3h}(\log h)$ , and  $\log \frac{k_2}{4h^2}(\log h)$  may all be fitted to

this normalised curve. As the data cover a small range of  $\log h$  and the normalised curve is rather shallow the data could be fitted between wide limits. The constants obtained from these curve-fits are in Table 6-6.

In Eqs. (6-10a), (6-13a), and (6-13b),  $k_0$ ,  $\frac{k_1}{3h}$ , and  $\frac{k_2}{4h^2}$  may also be plotted

against  $h$  and the constants obtained as the intercepts and slopes of straight lines. The values obtained by this method are also in Table 6-6.

The mass-balance equation, Eq. (2-16), may also be rearranged thus

$$\frac{A - a - \beta_{11}^H ha}{ha^3} = (2\beta_{12}^H + 2\beta_{22}^H h)a^{-1} + (3\beta_{23}^H h + 3\beta_{33}^H h^2) + (4\beta_{34}^H h^2 + 4\beta_{44}^H h^3)a \quad (6-17)$$

Equation (6-17) is of the type

$$f(a^{-1}) = k_0 + k_1 a + k_2 a^2 \quad (6-18)$$

Plots of  $\log\left(\frac{A - a - \beta_{11}^H ha}{ha^3}\right)$  against  $\log a$  at constant values of  $h$  may

be curve-fitted to normalised curves  $\log f^*(\log a^*)_{g_3}$

In this case the normalised variables are

$$\begin{aligned} \log f^* &= \log fa^{-1} + g_1 = \log(v^{-1} + g_3 + v) \\ \log a^* &= \log a + g_2 = \log v \end{aligned} \quad (6-19)$$

Eqs. (6-12a), (6-12b), and (6-12c) are still valid. The normalised curves are similar in shape to those in Fig. 6.4 .

The experimental data fitted these curves over a wide range of values of  $g_3$ . Data in the region  $4.4 \leq pH \leq 5.2$  could be fitted to curves with  $0 \leq g_3 \leq 2$ . Data at  $pH > 5.2$  could be fitted to curves with  $g_3$  ranging from zero to at least 50 and were not therefore considered further. The terms

$k_0$ ,  $k_1$ , and  $k_2$  are each the sum of two constants. In principle, these constants may be evaluated by further curve-fitting or by the use of straight-line plots as above. However, it was found that the experimental data could not be fitted to the calculated curves and the plots of  $k_0$ ,  $\frac{k_1}{3h}$ , and  $\frac{k_2}{4h^2}$  against  $h$  were not straight lines.

The mass-balance equation for H, Eq. (2-17), may be extended thus

$$H = h + \beta_{11}^H ha + \beta_{12}^H ha^2 + 2\beta_{22}^H h^2 a^2 + 2\beta_{23}^H h^2 a^3 + 3\beta_{33}^H h^3 a^3 + 3\beta_{34}^H h^3 a^4 + 4\beta_{44}^H h^4 a^4 \quad (6-20)$$

whence,

$$\frac{H - h - \beta_{11}^H ha}{ha^2} = (\beta_{12}^H + 2\beta_{22}^H h) + (2\beta_{23}^H h + 3\beta_{33}^H h^2)a + (3\beta_{34}^H h^2 + 4\beta_{44}^H h^3)a^2 \quad (6-21)$$

The value of  $\log \beta_{11}^H$  is again taken to be 5.618, and values of  $a$  used were those obtained from the integration method. The plots of  $\log\left(\frac{H - h - \beta_{11}^H ha}{ha^2}\right)$  against  $\log a$  were fitted to the set of normalised curves  $\log f^*(\log a^*)_{g_3}$ , Eq. (6-11).

The equilibrium constants were evaluated by the same methods as before i.e. the secondary curve-fitting and the straight-line plot. These constants and their limits of error are given in Table 6-6.

Equation (6-7) may be rewritten

$$A = (\beta_{11}^H ha + 2\beta_{22}^H h^2 a^2 + 3\beta_{33}^H h^3 a^3 + 4\beta_{44}^H h^4 a^4) + h^{-1}(ha + 2\beta_{12}^H h^2 a^2 + 3\beta_{23}^H h^3 a^3 + 4\beta_{34}^H h^4 a^4) \quad (6-22)$$

$$A = \left( [HA] + \frac{2\beta_{22}^H [HA]^2}{(\beta_{11}^H)^2} + \frac{3\beta_{33}^H [HA]^3}{(\beta_{11}^H)^3} + \frac{4\beta_{44}^H [HA]^4}{(\beta_{11}^H)^4} \right) + h^{-1} \left( \frac{[HA]}{\beta_{11}^H} + \frac{2\beta_{12}^H [HA]^2}{(\beta_{11}^H)^2} + \frac{3\beta_{23}^H [HA]^3}{(\beta_{11}^H)^3} + \frac{4\beta_{34}^H [HA]^4}{(\beta_{11}^H)^4} \right) \quad (6-23)$$

$$= \sum_q \beta_{qq}^H (\beta_{11}^H)^{-q} [HA]^q + h^{-1} \sum_q \beta_{q-1,q}^H (\beta_{11}^H)^{-q} [HA]^q \quad (6-24)$$

$$= f_0(HA) + h^{-1} f_1(HA) \quad (6-25)$$

where

$$f_0 = \sum_q \beta_{qq}^H (\beta_{11}^H)^{-q} [HA]^q \quad (6-26)$$

$$f_1 = \sum_q \beta_{q-1,q}^H (\beta_{11}^H)^{-q} [HA]^q \quad (6-27)$$

Equation (2-17) may be extended to include terms for  $H_2A_3$ ,  $H_3A_3$ ,  $H_3A_4$ , and  $H_4A_4$ , then combined with Eq. (1-6) and rearranged similarly to the above. Thus

$$A\bar{n}_H = \sum_q \beta_{qq}^H (\beta_{11}^H)^{-q} [HA]^q + h^{-1} \sum_q (q-1) \beta_{q-1,q}^H (\beta_{11}^H)^{-q} [HA]^q \quad (6-28)$$

Combining Eqs. (6-24) and (6-28), and rearranging

$$Ah(1-\bar{n}_H) = \sum_q \beta_{q-1,q}^H (\beta_{11}^H)^{-q} [HA]^q \quad (6-29)$$

which is constant when  $[HA]$  is constant. A plot of  $A$  against  $h^{-1}$  at constant  $[HA]$  i.e. constant  $Ah(1-\bar{n}_H)$  will give  $f_0$  as intercept and  $f_1$  as slope.

Values of  $Ah(1-\bar{n}_H)$  were calculated using the formation curves  $(\bar{n}_H, \log h)_A$  at  $A = 100, 200, \dots, 600$  mM. Curves  $[Ah(1-\bar{n}_H), h]_A$  were plotted and values of  $h$  interpolated at a number of values of  $Ah(1-\bar{n}_H)$ . Thus  $A$  could then be plotted against  $h^{-1}$  at constant values of  $Ah(1-\bar{n}_H)$ , and  $f_0$  and  $f_1$  calculated from the intercept and slope respectively of these lines. A summary of the values of  $f_0$  and  $f_1$  is given in Table 6-5.

From Eq. (6-29)

$$\frac{d[Ah(1-\bar{n}_H)]}{d\ln[HA]} = \sum q \beta_{q-1,q}^H (\beta_{11}^H)^{-q} [HA]^q = f_1(HA) \quad (6-30)$$

Hence, integration of the graph of  $\frac{1}{f_1}$  against  $Ah(1-\bar{n}_H)$  will lead to a value of  $\ln[HA]$ . However, it is impossible to integrate from  $Ah(1-\bar{n}_H) = 0$  as the lowest experimental value of this term is  $0.02 \times 10^{-6}$ . The amount of  $[HA]$  formed between  $Ah(1-\bar{n}_H) = 0$  and  $0.02 \times 10^{-6}$  may be calculated using the mononuclear formation curve by taking various values of  $A$  between 0 and 20mM. For each of these values of  $A$ , the corresponding values of  $\bar{n}_H$  and  $\log h$  which make  $Ah(1-\bar{n}_H) = 0.02 \times 10^{-6}$  are read off the formation curve. The value of  $[HA]$  is now easily calculated since  $A\bar{n}_H = [HA]$  when the acid is mononuclear [Eq. (1-4)]. The average value of  $[HA]$  for 12 values of  $A$  is  $8.25 \pm 0.7$ mM. The values of  $[HA]$  at higher values of  $Ah(1-\bar{n}_H)$  may now be calculated and are shown in Table 6-5.

Neglecting the tetramers  $H_3A_4$  and  $H_4A_4$ , we have

$$\frac{f_1}{[HA]} = \frac{1}{\beta_{11}^H} + \frac{2\beta_{12}^H}{(\beta_{11}^H)^2} [HA] + \frac{3\beta_{23}^H}{(\beta_{11}^H)^3} [HA]^2 \quad (6-31)$$

This curve is of the familiar form,

$$f(HA) = k_0 + k_1[HA] + k_2[HA]^2 \quad \text{cf. Eq. (6-9)}$$

Thus the plot of  $\log \frac{f_1}{[HA]}$  against  $\log[HA]$  may be curve fitted to the family of

curves  $\log f^*(\log a^*)_{g_3}$ , Eq. (6-11). The experimental data fit curves with  $0.80 \leq g_3 \leq 1.50$ , the best fit being obtained with  $g_3 = 1.00$ . The values of  $k_0$ ,  $k_1$ , and  $k_2$ , i.e.,  $\frac{1}{\beta_{11}^H}$ ,  $\frac{2\beta_{12}^H}{(\beta_{11}^H)^2}$ , and  $\frac{3\beta_{23}^H}{(\beta_{11}^H)^3}$  respectively, may be calculated

in the usual way. The values of the constants are given in Table 6-6.

TABLE 6-5

Acetic acidValues of  $f_0$ ,  $f_1$ , and  $[HA]$  at selected values of  $Ah(1-\bar{\alpha}_H)$ .

$Ah(1-\bar{\alpha}_H) \times 10^6$	$f_0$	$f_1 \times 10^6$	$[HA]$ mM
0.02	0.008	0.021	8.25
0.03	0.012	0.031	12.2
0.04	0.016	0.041	16.2
0.05	0.020	0.052	20.7
0.06	0.025	0.063	23.9
0.07	0.028	0.074	27.6
0.08	0.030	0.086	31.3
0.09	0.035	0.098	34.8
0.10	0.038	0.110	38.4
0.11	0.040	0.123	41.8
0.12	0.045	0.135	45.2
0.14	0.052	0.162	51.9
0.16	0.057	0.191	58.2
0.20	0.073	0.245	70.1
0.24	0.088	0.298	81.3
0.28	0.105	0.355	91.9
0.32	0.125	0.409	102.1
0.36	0.145	0.465	111.9
0.40	0.160	0.539	121.3
0.44	0.175	0.603	130.2
0.48	0.188	0.680	138.5
0.52	0.202	0.744	146.5
0.56	0.220	0.817	154.2
0.60	0.233	0.901	161.6
0.64	0.245	0.983	168.5
0.68	0.252	1.089	175.1
0.72	0.274	1.156	180.5
0.76	0.299	1.194	186.7



Rearranging Eq. (6-26) we obtain

$$\frac{\frac{f_0}{[HA]} - 1}{[HA]} = \frac{2\beta_{22}^H}{(\beta_{11}^H)^2} + \frac{3\beta_{33}^H}{(\beta_{11}^H)^3} [HA] + \frac{4\beta_{44}^H}{(\beta_{11}^H)^4} [HA]^2 \quad (6-32)$$

Hence a plot of  $\log \frac{\frac{f_0}{[HA]} - 1}{[HA]}$  against  $\log[HA]$  may be fitted to the same set

of normalised curves,  $\log f^*(\log a^*)_{g_3}$ , Eq. (6-11), used previously. However the data  $\log \frac{\frac{f_0}{[HA]} - 1}{[HA]}$  cover a very small range (about 0.5 unit) which is not

enough to enable a satisfactory fit to be made. I

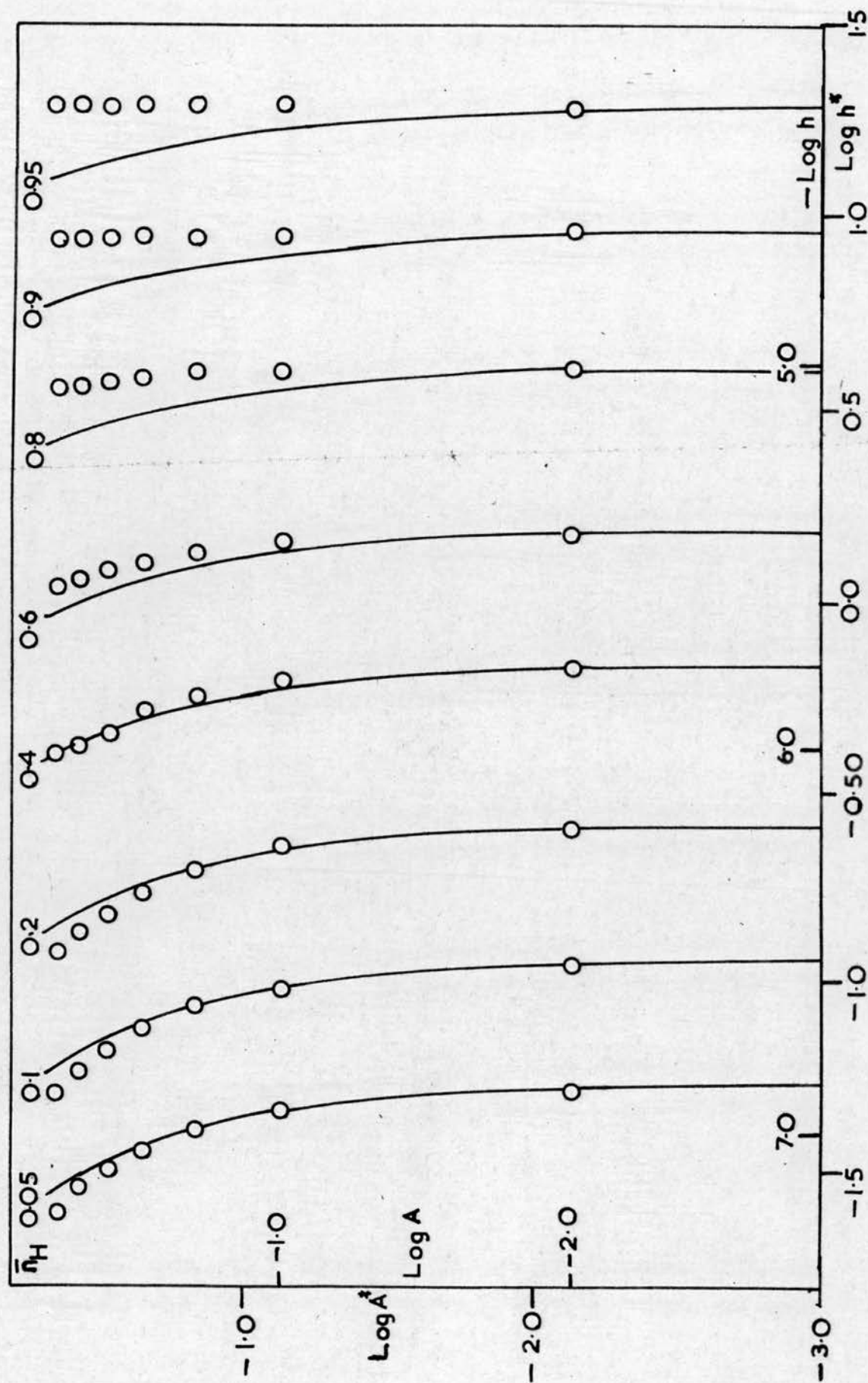
In attempting to explain the data we have been forced to introduce no fewer than nine parameters. It may be possible to explain the data by assuming that ratios of equilibrium constant are related one to another e.g.

$$\frac{\beta_{44}^H}{\beta_{33}^H} = \frac{\beta_{33}^H}{\beta_{22}^H} = \frac{\beta_{22}^H}{\beta_{11}^H} = \beta_{11}^H. \quad \text{Four such assumptions which reduce the number of}$$

parameters to a more manageable total, have been tested. The methods of calculating families of normalised curves for these hypotheses have been described in Sec.2 (b), p.45. The experimental data,  $\bar{n}_H(\log h)_A$ , were fitted to the family of normalised curves for each hypothesis. In no case was an acceptable fit obtained. The fit for Hypothesis II is shown in Fig. 6.5. It may be noted, however, that these hypotheses have been used to obtain the equilibrium constants in the systems, iso-butyric acid, n-valeric acid, and pivalic acid in 3.00M sodium perchlorate<sup>214</sup>.

Fig 6.5

ACETIC ACID IN 50% v/v DIOXAN

O Experimental Data  $\log A(\log h)_{\bar{n}_H}$ — Normalised curves  $\log A^*(\log h^*)_{\bar{n}_H}$ , calculated using Hypothesis II, Eq.(2-92).

# Acetic acid

Values of the equilibrium constant obtained by the various methods. For ease of tabulation the methods are identified by their operational equations.

Method of Computation	$\log \beta_{11}^H$	$\log \beta_{12}^H$	$\log \beta_{22}^H$	$\log \beta_{23}^H$	$\log \beta_{33}^H$	$\log \beta_{34}^H$	$\log \beta_{44}^H$
Preferred value of $\log \beta_{11}^H$	5.618 $\pm$ 0.013						
Eq. (2-23), $A \leq 300\text{mm}$	5.615	$\sim 5.90$	$\sim 11.20$				
Eq. (2-44), $\bar{n}_H \leq 0.4$	5.613	5.75 $\pm$ 0.03		12.43 $\pm$ 0.05			
Eq. (6-8)(6-11) and (6-15)		$\leq 5.9$ best fit 5.45	$> 10.5$ ; $\leq 10.88$ best fit 10.80	$\leq 12.42$	$\leq 17.32$	18.6 $\pm$ 0.2	23.3 $\pm$ 0.2
Eq. (6-11), (6-10a) and (6-13a,b)		5.65 $\pm$ 0.14	10.74 $\pm$ 0.17	$\leq 12.19$	$\leq 17.24$	18.6 $\pm$ 0.2	23.3 $\pm$ 0.2
Eqs. (6-21), (6-11), and (6-15)		$\leq 5.85$	$\geq 10.75$ ; $\leq 10.87$	$\leq 12.47$	$\leq 17.30$	18.5	23.4
Eqs. (6-21), (6-11), (6-10a), and (6-13a,b)		5.65 $\pm$ 0.20	10.81 $\pm$ 0.17	$\leq 12.08$	$\leq 17.29$	18.5 $\pm$ 0.3	23.4 $\pm$ 0.2
and							
Eqs. (6-31) and (6-11)	5.63 $\pm$ 0.01	6.01 $\pm$ 0.07		12.09 $\pm$ 0.10			

TABLE 6-6

Successive approximations

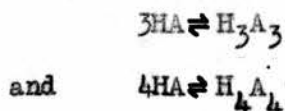
A summary of the equilibrium constants obtained by the various curve-fitting methods is given in Table 6-6. It now remains to obtain the combination of constants which explain all the data best. The constants in Table 6-6 have been refined by successive approximations. At values of A, 200, 300, ..... 600mM, the right-hand side of Eq. (6-7) has been calculated at 0.2 pH unit intervals between pH 4.4 and 7.0 using the values of a calculated by the integration method. Various combinations of constants were used in an attempt to obtain equality between the right- and left-hand sides of Eq. (6-7) over the entire range of the experimental data. The set of constants which explain the data best is

$$\begin{array}{ll}
 \log \beta_{11}^H = 5.618 & \\
 \log \beta_{22}^H = 10.70 & \log \beta_{12}^H = 5.85 \\
 \log \beta_{33}^H = 16.8 & \log \beta_{23}^H = 12.20 \\
 \log \beta_{44}^H = 23.5 & \log \beta_{34}^H = 18.1
 \end{array}$$

whence

$$\begin{array}{ll}
 \log K_{12} = 0.23 & \log K_{33} = 4.60 \\
 \log K_{22} = 4.85 & \log K_{44} = 5.40 \\
 \log K_D = -0.54 &
 \end{array}$$

The equilibrium constants for the reactions



are  $K_T$  and  $K_{TT}$  respectively.  $\log K_T = -0.05$ ;  $\log K_{TT} = +1.03$ .

It can be seen in Table 6-7 that this set of constants explains the data

with high precision. For each value of A, the value of the right-hand side of Eq. (6-7) was calculated for 14 values of pH between 4.4 and 7.0, and the averages of these values are given in the table.

TABLE 6-7

Acetic acid

Comparison of the values of A and of the right-hand side of Eq. (6-7), calculated using the preferred set of constants.

A mm	R.H.S. Eq.(6-7) mm
200	201.7 $\pm$ 1.3
300	303.3 $\pm$ 2.7
400	399.9 $\pm$ 4.3
500	484.4 $\pm$ 3.3
600	561.4 $\pm$ 8.1

The agreement between the corresponding values in Table 6-7 is excellent except for A = 600mm where activity coefficients may be varying appreciably. The difference between the two terms at A = 500mm is somewhat greater than at lower concentrations but even so the difference is only 3% in A.

Attempts were made to explain the data by other combinations involving fewer species e.g. the combination HA, HA<sub>2</sub>, H<sub>2</sub>A<sub>2</sub>, and H<sub>2</sub>A<sub>3</sub>, but none of these was as successful as the above combination.

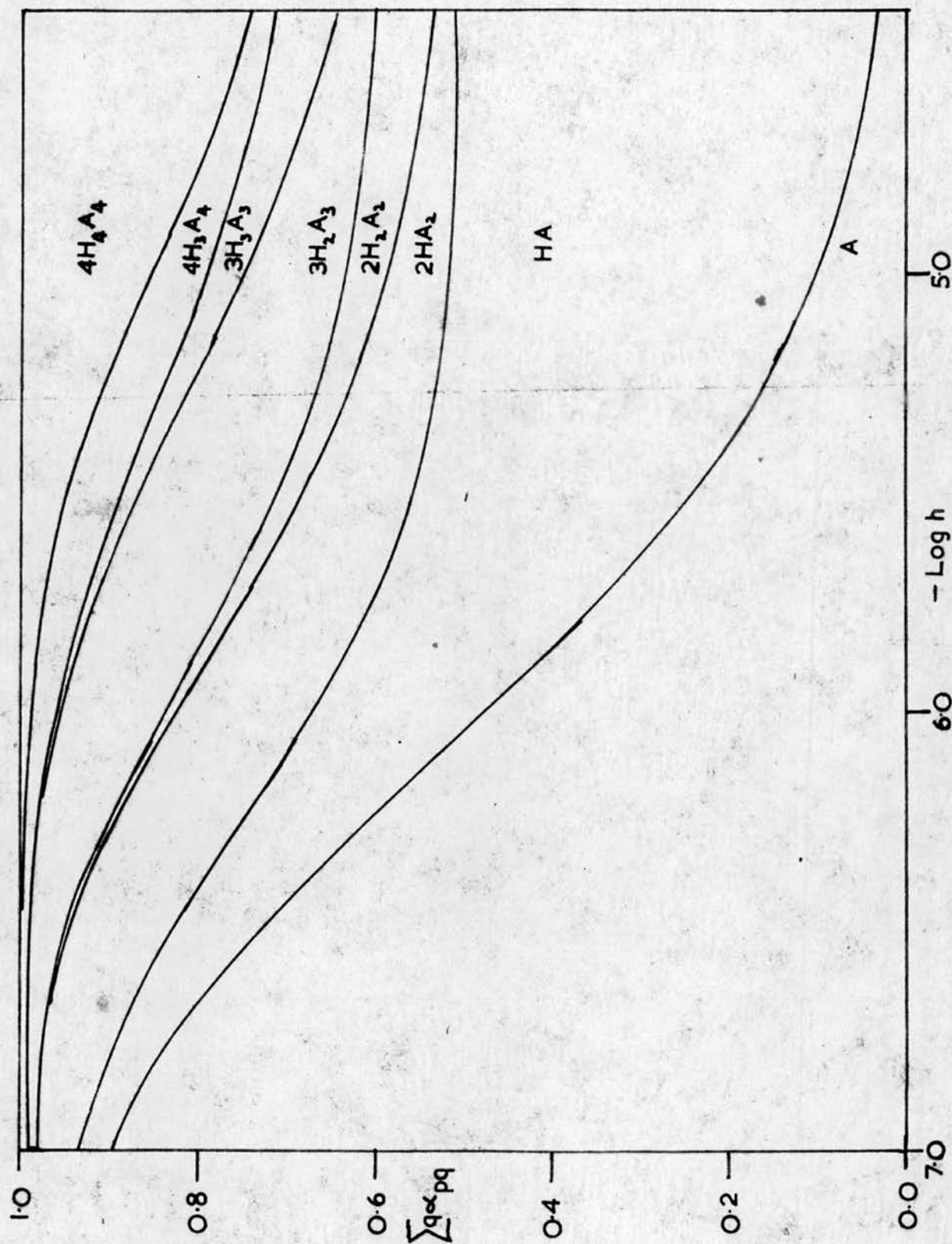
The values of  $\alpha_{pq}$  have been calculated in the usual way and are plotted against pH in Fig. 66. It can be seen that  $\alpha_{12}$  has a slightly higher maximum value in this solvent than in water. The principal species in the more acid solutions are HA and H<sub>4</sub>A<sub>4</sub> with smaller, nearly equal, amounts of H<sub>2</sub>A<sub>2</sub> and H<sub>3</sub>A<sub>3</sub>.

Although the dissociation of acetic acid in dioxan-water mixtures has been studied previously<sup>205</sup>, the formation of oligomers of the acid in this



Fig 66 ACETIC ACID IN 50% v/v DIOXAN

Relative proportions of the species  $H_pA_q$  present in solution at  $A=500\text{mM}$ :





solvent has not been reported before. Comparisons of the behaviour of acetic acid in water and in the organic mixture must be somewhat tentative. Not only are there differences in the constant ionic medium but there are also differences in solvation. The value of  $\log \beta_{11}^H$  is higher in the 50% v/v aqueous dioxan mixture than in water and this is expected since  $\log \beta_{11}^H$  generally increases with decreasing dielectric constant of the medium (Table 1-2 ). The dimer is again a stronger acid than the monomer, and the trimer is slightly stronger than the dimer. The tetramer, however, is weaker than both dimer and trimer. The value of  $K_D$  is almost ten times less than  $\frac{K_T}{K_D}$ , the constant

for the reaction



which in turn is appreciably less than  $\frac{K_{TT}}{K_D}$ , the constant for the reaction



Thus it is far more difficult for two molecules of HA to associate to form a dimer than it is for a molecule of HA to add to an associated complex  $(HA)_n$  to form  $(HA)_{n+1}$ . This behaviour is exactly that predicted by Sarol&e-Mathot<sup>231</sup> from theoretical considerations and it has already been noted in propionic and n-butyric acids in water [Sec 4(c)] where, however, there are not such large differences between  $K_D$  and  $K_T$  as there are in the present case. The structure of the trimers and tetramers must be the extended form, and it is probable that the dimer is predominately of the open form too. The difference in the acidities of monomer and dimer is given by  $\log \frac{K_{22}}{K_{11}}$  which is -0.38 in

aqueous solution, and is -0.77 in 50% v/v aqueous dioxan. Thus there seems to be a greater concentration of the extended form of the dimer in the organic solvent.

6(c) Copper(II) acetate.

The copper(II) acetate system in the mixed organic solvent was studied in the same way as in aqueous solution. After a preliminary acid-base titration, from which  $E_0$  was obtained, metal perchlorate solutions were titrated with acetate buffers. The value of B was kept constant at 0.025, 0.050, or 0.100M, and buffers of pH 4.61, 4.91, and 5.32 were used. (These figures are valid for buffer solutions with  $A \leq 20\text{mM}$ ). Titrations were stopped when large increments of buffer produced only small changes in potential or when precipitation occurred.

The experimental data are summarised in the form  $\bar{n}(\log a)_B$  in Table 6-8. Methods of computation, similar to those employed in the systems in aqueous solution, were used to obtain values of  $a$  and  $\bar{n}$ . When  $(A - \bar{n}B) \leq 20\text{mM}$ , Eqs. (5-2) and (5-5) may still be used to calculate  $\bar{n}$ ,  $a$  provided that no mixed species are formed. When  $20\text{mM} \leq A - \bar{n}B \leq 500\text{mM}$ , Eqs. (5-6) and (2-15) must be extended to include the additional oligomers of  $H_qA_q$  and  $H_{q-1}A_q$  which exist in the mixed organic solvent. Equation (5-7) is unaltered but Eq. (5-8) now becomes  $A - \bar{n}B - H = a - h + \beta_{12}^H h a^2 + \beta_{23}^H h^2 a^3 + \beta_{34}^H h^3 a^4$  (6-35)

For each experimental point,  $\bar{n}$  and  $a$  are evaluated by successive approximations using Eqs. (5-7) and (6-35) and the appropriate value of  $\bar{n}_H(\log h)_A$ . It was sometimes necessary to obtain the latter by a short graphical interpolation from the experimental data.

The experimental data have been plotted in the form  $\bar{n}(\log a)_B$  in Fig. 6-7.

The formation curves are a function of B showing that polynuclear species  $B_R A_Q$  may exist, where Q and R are integers ( $R \geq 2$ ). The curves are also a function of h which indicates that mixed complexes  $B_R H_P A_Q$  or hydroxo complexes  $B_R(OH)_n A_Q$  (where n, P, Q, and R are integers  $\geq 1$ ) may be present in the system. The formation curve is unique for  $\bar{n} \leq 0.1$  and it is reasonable to assume that only BA is formed at such low free ligand concentrations. In this region

## Copper(II) acetate

Experimental data  $\bar{n}(\log a)_B$  obtained from potentiometric titrations of metal ion solutions and acetate buffers.

B(mM)		1196		1196		1403		3045		4117		4117		1196		1524	
Buffer HA mM NaA mM		600.0		600.0		276.6		600.0		400.0		400.0		600.0		300.0	
$\bar{n}$	$-\log a$	$\bar{n}$	$-\log a$	$\bar{n}$	$-\log a$	$\bar{n}$	$-\log a$	$\bar{n}$	$-\log a$	$\bar{n}$	$-\log a$	$\bar{n}$	$-\log a$	$\bar{n}$	$-\log a$	$\bar{n}$	$-\log a$
-0.019	5.904	-0.024	5.881	-0.002	5.808	0.008	5.564	0.000	5.500	0.002	5.496	-0.008	5.876	-0.001	6.805	-0.001	6.805
-0.012	5.585	-0.004	5.613	-0.003	5.461	0.010	5.169	-0.001	5.142	0.003	5.144	-0.004	5.556	0.000	5.243	0.000	5.243
-0.013	5.110	0.003	5.144	-0.003	5.049	0.011	4.881	0.003	4.740	0.004	4.917	0.001	5.101	0.002	5.086	0.002	5.086
-0.006	4.672	0.004	4.926	0.001	4.472	0.019	4.640	0.031	4.163	0.014	4.418	0.009	4.687	0.002	4.924	0.002	4.924
0.047	3.877	0.005	4.426	0.047	3.958	0.043	4.138	0.092	3.714	0.063	3.916	0.028	4.292	0.005	4.795	0.005	4.795
0.146	3.415	0.079	3.692	0.105	3.608	0.095	3.711	0.261	3.233	0.180	3.421	0.058	3.962	0.008	4.673	0.008	4.673
0.284	3.105	0.217	3.250	0.168	3.386	0.161	3.438	0.428	2.984	0.349	2.993	0.093	3.745	0.011	4.549	0.011	4.549
0.413	2.875	0.350	2.987	0.290	3.106	0.297	3.110	0.582	2.811	0.511	2.886	0.165	3.455	0.016	4.449	0.016	4.449
0.539	2.718	0.470	2.798	0.407	2.917	0.428	2.896	0.723	2.677	0.657	2.733	0.237	3.265	0.020	4.334	0.020	4.334
0.703	2.514	0.623	2.604	0.512	2.773	0.553	2.740	0.903	2.517	0.821	2.585	0.373	3.006	0.032	4.161	0.032	4.161
0.938	2.257	0.829	2.377	0.698	2.560	0.725	2.551	1.059	2.393	0.985	2.447	0.500	2.818	0.046	4.012	0.046	4.012
1.122	2.065	1.037	2.150	0.891	2.372	0.882	2.397	1.187	2.292	1.127	2.336	0.729	2.549	0.062	3.883	0.062	3.883
1.343	1.806	1.232	1.912	1.052	2.232	1.016	2.271	1.371	2.172	1.283	2.221	0.947	2.327	0.079	3.783	0.079	3.783
1.442	1.637	1.377	1.704	1.267	2.042	1.129	2.169					1.149	2.140	0.096	3.694	0.096	3.694
1.486	1.438	1.438	1.511	1.402	1.918	1.225	2.084					1.304	1.990	0.163	3.446	0.163	3.446
1.457	1.325	1.427	1.365	1.497	1.798	1.337	1.989					1.484	1.766	0.259	3.226	0.259	3.226
1.404	1.223	1.335	1.257	1.558	1.723	1.438	1.891					1.572	1.613	0.341	3.086	0.341	3.086
1.360	1.144	1.285	1.172	1.597	1.656	1.490	1.813					1.621	1.467	0.471	2.909	0.471	2.909
1.290	1.095	1.236	1.109	1.630	1.599	1.566	1.694					1.623	1.368	0.533	2.839	0.533	2.839
						1.617	1.616					1.604	1.286	0.644	2.725	0.644	2.725
												1.597	1.236	0.764	2.614	0.764	2.614
														0.868	2.521	0.868	2.521
														1.066	2.361	1.066	2.361
														1.143	2.303	1.143	2.303
														1.230	2.236	1.230	2.236
														1.361	2.140	1.361	2.140
														1.412	2.101	1.412	2.101
														1.464	2.058	1.464	2.058
														1.512	2.023	1.512	2.023



1403 276.6		1828 178.7		1196 600.0		1196 600.0		3045 600.0		3045 600.0		4117 400.0		4117 400.0	
$\bar{n}$	$-\log a$	$\bar{n}$	$-\log a$	$\bar{n}$	$-\log a$	$\bar{n}$	$-\log a$	$\bar{n}$	$-\log a$	$\bar{n}$	$-\log a$	$\bar{n}$	$-\log a$	$\bar{n}$	$-\log a$
-0.001	5.920	0.000	5.877	-0.002	5.963	-0.005	5.903	0.002	5.685	-0.001	5.642	0.000	5.582	0.001	5.434
0.001	5.590	0.000	5.551	-0.003	5.583	-0.003	5.591	0.003	5.317	-0.001	5.276	0.001	5.254	0.001	5.225
0.001	5.218	0.004	5.227	-0.001	5.146	0.002	4.974	0.007	4.894	0.001	5.047	0.006	4.902	0.002	5.013
0.009	4.754	0.007	4.844	0.004	4.771	0.007	4.550	0.025	4.305	0.012	4.550	0.017	4.483	0.009	4.612
0.043	4.248	0.023	4.379	0.013	4.438	0.020	4.314	0.056	3.944	0.038	4.083	0.053	4.034	0.034	4.159
0.118	3.570	0.047	4.028	0.028	4.184	0.045	3.997	0.091	3.727	0.072	3.804	0.096	3.767	0.077	3.843
0.210	3.286	0.080	3.783	0.063	3.860	0.081	3.754	0.162	3.470	0.127	3.576	0.140	3.623	0.122	3.670
0.310	3.089	0.117	3.619	0.100	3.659	0.135	3.516	0.217	3.316	0.197	3.384	0.203	3.484	0.188	3.515
0.414	2.935	0.162	3.481	0.171	3.405	0.205	3.316	0.296	3.207	0.264	3.257	0.282	3.368	0.250	3.415
0.518	2.807	0.206	3.384	0.239	3.248	0.304	3.117	0.445	3.021	0.373	3.101	0.412	3.224	0.335	3.312
0.618	2.696	0.325	3.229	0.366	3.020	0.438	2.918	0.577	2.896	0.513	2.948			0.459	3.156
0.717	2.604	0.426	3.092	0.507	2.833	0.570	2.766	0.693	2.794	0.636	2.839				
0.810	2.515	0.532	2.971	0.631	2.701	0.740	2.594	0.796	2.714	0.746	2.753				
0.897	2.441	0.621	2.885	0.840	2.501	0.925	2.425	0.889	2.647	0.844	2.680				
0.977	2.371	0.695	2.818	1.008	2.361	1.080	2.304								
1.047	2.317	0.757	2.766	1.144	2.240	1.230	2.183								
1.126	2.252	0.832	2.701	1.300	2.110	1.344	2.084								
1.192	2.202			1.382	2.040	1.417	2.016								
1.251	2.156			1.447	1.980	1.491	1.942								
1.309	2.103			1.528	1.900	1.556	1.864								
				1.581	1.820	1.587	1.836								
						1.611	1.790								
						1.635	1.757								
						1.662	1.708								

the formation curve fits exactly the normalised curve for a single complex Eq. (2-7), and from Eq. (2-8) the value of  $\log \beta_1 = 2.70 \pm 0.08$ .  
species

If mixed, hydroxo, or copper hydrolysis/are present then Eqs. (1-4), (2-17), (5-2), and (5-9) are no longer valid, and the values of  $\bar{n}$  and  $\log a$  in Table 6-8 must be regarded as first approximations to the correct values. It may be possible to neglect the effect of the copper hydrolysis products since at the pH's at which these are likely to exist, there is also the maximum complex formation with acetate. The concentration of free metal ion is, therefore, likely to be rather low. In the titrations with the buffer of pH 4.91 the titration with B = 0.100M was stopped at pH 3.6 ( $\bar{n} = 0.9$ ,  $Z = 0.004$ ), that with B = 0.050 at pH 4.2 ( $\bar{n} = 1.45$ ,  $Z = 0.016$ ), and that with B = 0.025 at pH 4.6 ( $\bar{n} = 1.6$ ,  $Z \sim 0.036$ ). Thus even in the last titration only  $\sim 4\%$  of the free metal ion is hydrolysed and since  $\bar{n} = 1.6$ , b will be rather small. However, more information is required before one may decide what polynuclear, mixed, and hydroxo complexes are formed. It would be useful to know b but the difficulties in the use of copper and copper amalgam electrodes have already been mentioned. It is possible that if titrations were made with very acid buffers the formation curves might be independent of h and functions of B only. The mononuclear and polynuclear species present could then be identified provided, of course, that there were appreciable complex formation. The metal ion would meet intense competition from protons for the carboxylate ions in titrations with such acid buffers. A study of the equilibria in 25% v/v dioxan-water mixture might be useful since fewer polynuclear species are likely to be formed in this medium of higher dielectric constant. Certainly it does not seem possible at present to elucidate the equilibria in the copper(II) acetate system in 50% dioxan-water mixture without further information.

BIBLIOGRAPHY

1. Guldberg, C.M., and Waage, P., "Etudes sur les affinités Chimiques", Christiania, 1867.
2. Morse, H., Z. phys. Chem., 1902, 41, 709.
3. Sherrill, M.S., Z. phys. Chem., 1903, 43, 705.
4. Bodländer, G., and Fittig, R., Z. phys. Chem., 1902, 39, 597.
5. Grossmann, H., Z. anorg. Chem., 1905, 43, 356.
6. Bjerrum, N., Kgl. danske Videnskab. Selskab Skrifter, nat.-mat. Afdel., 1915, 7, 66.
7. Bjerrum, N., Z. anorg. Chem., 1921, 119, 179.
8. Bjerrum, J., "Metal Ammine Formation in Aqueous Solution", P. Haase & Son, Copenhagen, 1941.
9. Leden, I., Z. phys. Chem., 1941, 188A, 160.
10. Allen, G., and Caldin, E.F., Quart. Rev., 1953, 7, 255.
11. Bineau, --, Ann. Chim. Phys., 1846, 18, 228.
12. Ramsay, W., and Young, S., J. Chem. Soc., 1886, 49, 790.
13. Gibbs, J.W., Amer. J. Sci., [3], 1879, 18, 277.
14. Ramsperger, H.C., and Porter, C.W., J. Amer. Chem. Soc., 1928, 50, 3036.
15. Pettersson, O., and Ekstrand, G., Ber., 1880, 13, 1191.
16. Ramsperger, H.C., and Porter, C.W., J. Amer. Chem. Soc., 1926, 48, 1267.
17. Coolidge, A.S., J. Amer. Chem. Soc., 1928, 50, 2166.
18. Wrewsky, M.S., and Glagoleva, A.A., Z. phys. Chem., 1928, 133, 370.
19. Herman, R.C., J. Chem. Phys., 1940, 8, 252.
20. Halford, J.O., J. Chem. Phys., 1942, 10, 582.
21. Foz, O.R., and Morcillo, J., Anales real. Soc. españ. Fis. Quím., 1949, 45A, 525.
22. Gross, E.F., and Val'kov, V.I., Doklady Akad. Nauk S.S.S.R., 1949, 68, 1013.



23. Shubin, A.A., Izvest. Akad. Nauk S.S.S.R., Ser. Fiz., 1950, 14, 442.
24. Taylor, M.D., and Bruton, J., J. Amer. Chem. Soc., 1952, 74, 4151.
25. Young, S., Sci. Proc. Royal Dublin Soc., 1910, 12, 374.
26. Fenton, T.M., and Garner, W.E., J. Chem. Soc., 1930, 694.
27. Zawidski, J. von, Z. phys. Chem., 1900, 35, 129.
28. Bakr, A.M., and McBain, J.W., J. Amer. Chem. Soc., 1924, 46, 2718.
29. Nernst, W., and Wartenberg, H. von, Z. Electrochem., 1916, 22, 37.
30. Trautz, M., and Moschel, W., Z. anorg. Chem., 1926, 155, 13.
31. MacDougall, F.H., J. Amer. Chem. Soc., 1936, 58, 2585.
32. Badger, R.M., and Bauer, S.H., J. Chem. Phys., 1937, 5, 839.
33. Halford, J.O., J. Chem. Phys., 1941, 9, 859.
34. Ritter, H.L., and Simons, J.H., J. Amer. Chem. Soc., 1945, 67, 757.
35. Potter, A.E. (Jr.), Bender, P., and Ritter, H.L., J. Phys. Chem., 1955, 59, 250.
36. Johnson, E.W., and Nash, L.K., J. Amer. Chem. Soc., 1950, 72, 547.
37. Taylor, M.D., J. Amer. Chem. Soc., 1951, 73, 315.
38. Morcillo, J., and Pérez-Masiá, A., Anales real Soc. españ. Fis Quím., 1952, 48B, 631.
39. Reiser, A., Kimla, A., and Hájek, J., Chem. Listy, 1953, 47, 1265.
40. Weltner, W. (Jr.), J. Amer. Chem. Soc., 1955, 77, 3941.
41. Herman, R.C., and Hofstadter, R., J. Chem. Phys., 1938, 6, 534.
42. MacDougall, F.H., J. Amer. Chem. Soc., 1941, 63, 3420.
43. Freedman, E., J. Chem. Phys., 1953, 21, 1784.
44. Lamb, J., and Huddart, D.H.A., Trans. Faraday Soc., 1950, 46, 540.
45. Herman, R.C., and Hofstadter, R., J. Chem. Phys., 1939, 7, 460.
46. Lundin, R.E., Harris, F.E., and Nash, L.K., J. Amer. Chem. Soc., 1952, 74, 743.

47. Pimentel, G.C., and McClellan, A.L., "The Hydrogen Bond". W.H. Freeman & Co., San Francisco, 1960.
48. Pauling, L., and Brockway, L.O., Proc. Nat. Acad. Sci. U.S.A., 1934, 20, 336.
49. Karle, J., and Brockway, L.O., J. Amer. Chem. Soc., 1944, 66, 574.
50. Holtzberg, F., Post, B., and Fankuchen, I., Acta Cryst., 1953, 6, 127.
51. Johnson, J.F., and Cole, R.H., J. Amer. Chem. Soc., 1951, 73, 4536.
52. Rigaux, C., Compt. rend., 1954, 238, 783.
53. Jones, R.E., and Templeton, D.H., Acta Cryst., 1958, 11, 484.
54. Beckmann, E., Z. phys. Chem., 1890, 6, 437.
55. Nernst, W., Z. phys. Chem., 1891, 8, 110.
56. Hendrixson, W.S., Z. anorg. Chem., 1897, 13, 73.
57. Auwers, K., Z. phys. Chem., 1893, 12, 689.
58. Beckmann, E., Z. phys. Chem., 1897, 22, 609.
59. Herz, W., and Fischer, H., Ber., 1905, 38, 1138.
60. Hantzsch, A., Ber., 1917, 50, 1422.
61. Waentig, P., and Pescheck, G., Z. phys. Chem., 1919, 93, 529.
62. Badger, R.M., and Bauer, S.H., J. Chem. Phys., 1937, 5, 369.
63. Kinsey, E.L., and Ellis, J.W., J. Chem. Phys., 1937, 5, 399.
64. Batuev, M.I., Izvest. Akad. Nauk S.S.S.R., Ser. Fiz., 1948, 12, 611.
65. Chulanovskii, V.M., and Simova, P.D., Doklady Akad. Nauk S.S.S.R., 1949, 68, 1033.
66. Chapman, D., J. Chem. Soc., 1956, 225.
67. Pohl, H.A., Hobbs, M.E., and Gross, P.M., J. Chem. Phys., 1941, 9, 408.
68. Wilson, C.J., and Wenzke, H.H., J. Chem. Phys., 1934, 2, 546.
69. Batuev, M.I., Compt. rend. Acad. Sci. U.R.S.S., 1946, 53, 507.
70. Huggins, M.L., J. Org. Chem., 1937, 1, 407.
71. Kumler, W.D., J. Amer. Chem. Soc., 1935, 57, 600.
72. Batuev, M.I., Compt. rend. Acad. Sci. U.R.S.S., 1946, 52, 401.

73. Blinc, M., and Blinc, R., J. Polymer Sci., 1958, 32, 506.
74. Peddle, C.J., and Turner, W.E.S., J. Chem. Soc., 1911, 99, 685.
75. Saxton, B., and Darken, L.S., J. Amer. Chem. Soc., 1940, 62, 846.
76. Katchalsky, A., Eisenberg, H., and Lifson, S., J. Amer. Chem. Soc., 1951, 73, 5889.
77. Cartwright, D.R., and Monk, C.B., J. Chem. Soc., 1955, 2500.
78. Smyth, C.P., and Rogers, H.E., J. Amer. Chem. Soc., 1930, 52, 1824.
79. Broughton, G., Trans Faraday Soc., 1934, 30, 367.
80. Moelwyn-Hughes, E.A., J. Chem. Soc., 1940, 850.
81. Davies, M., Jones, P., Patnaik, D., and Moelwyn-Hughes, E.A., J. Chem. Soc., 1951, 1249.
82. Smith, A.A., and Elgin, J.C., J. Phys. Chem., 1935, 39, 1149.
83. Vandoni, R., and Chazeau, M., Mém. Services chim. État, 1948, 34, 97.
84. Reeves, L.W., and Schneider, W.G., Trans. Faraday Soc., 1958, 54, 314.
85. Tokareva, G.A., and Kozlov, V.N., Trudy Inst. Khim., Akad. Nauk S.S.S.R., Ural. Filial, Sbornik Rabot, 1958, 2, 19.
86. Fénéant, S., Mém. Services chim. État, 1952, 37, 297.
87. Fénéant, S., J. Phys. Radium, 1954, 15, 325.
88. Batuer, M.I., Doklady, Akad. Nauk S.S.S.R., 1948, 59, 1117.
89. Osipov, O.A., and Shelomov, I.K., Zhur. fiz. Khim., 1956, 30, 608.
90. Kovalenko, K.N., Trifonov, N.A., and Tissen, D.S., Zhur. obshchei Khim., 1956, 26, 403.
91. Richards, R.E., and Thompson, H.W., J. Chem. Soc., 1947, 1248.
92. Fénéant, S., Compt. rend., 1952, 235, 240.
93. Izmaïlov, N.A., and Kutsyna, L.M., Izvest. Akad. Nauk S.S.S.R., Ser. Fiz., 1953, 17, 740.
94. Herz, W., and Lewy, M., Z. Electrochem., 1905, 11, 818.
95. Meisenheimer, J., and Dorner, O., Annalen, 1936, 523, 299.
96. Davies, M., and Griffiths, D.M.L., Z. phys. Chem. (Frankfurt), 1954, 2, 353.

97. Sarkadi, D.S., and Boer, J.H. de, Rec. Trav chim., 1957, 76, 628.
98. Herz, W., and Kurzer, A., Z. Electrochem., 1910, 16, 240.
99. Davies, M.M., and Sutherland, G.B.B.M., J. Chem. Phys., 1938, 6, 767.
100. Harris, J.T. (Jr.), and Hobbs, M.E., J. Amer. Chem. Soc., 1954, 76, 1419.
101. Wenograd, J. and Spurr, R.A., J. Amer. Chem. Soc., 1957, 79, 5844.
102. Barrow, G.M., and Yerger, E.A., J. Amer. Chem. Soc., 1954, 76, 5248.
103. Brown, C.P., and Mathieson, A.R., J. Phys. Chem., 1954, 58, 1057.
104. Wolf, K.L., and Metzger, G., Annalen, 1949, 563, 157.
105. Allen, G., and Caldin, E.F., Trans. Faraday Soc., 1953, 49, 895.
106. Rothmund, V., and Wilsmore, N.T.M., Z. phys. Chem., 1902, 40, 611.
107. Jones, E.R., and Bury, C.R., Phil. Mag., [vii], 1927, 4, 841.
108. Goebel, J.B., Z. phys. Chem., 1912, 78, 244.
109. Nash, G.R., and Monk, C.B., J. Chem. Soc., 1957, 4274.
110. Kipling, J.J., J. Chem. Soc., 1952, 2858.
111. MacDougall, F.H., and Blumer, D.R., J. Amer. Chem. Soc., 1933, 55, 2236.
112. Traynard, P., Bull. Soc. chim France, 1947, 316.
113. Traynard, P., Compt. rend., 1946, 223, 202.
114. Latimer, W.M., and Rodebush, W.H., J. Amer. Chem. Soc., 1920, 42, 1419.
115. Lamb, J., and Pinkerton, J.M.M., Proc. Roy. Soc., 1949, A199, 114.
116. Fénéant, S., Compt. rend., 1952, 235, 1292.
117. Harris, F.E., and Alder, B.J., J. Chem. Phys., 1953, 21, 1306.
118. Ragni, A., Ferrari, G., and Papoff, P., Ann. Chim. (Italy), 1955, 45, 960.
119. Cucurezeanu, I., Acad. rep. populare Romine, Bul. științ. Sect. științe mat. fiz., 1957, 2, 187.
120. Cucurezeanu, I., Rev. Phys. (Acad. R.P.R.), 1957, 2, 243.
121. Cucurezeanu, I., Acad. rep. populare Romine, Inst. fiz. atomică și Inst. fiz. Studii cercetări fiz., 1958, 2, 269.
122. Smith, H.W., and White, T.A., J. Phys. Chem., 1929, 33, 1953.

123. Davies, M., and Griffiths, D.M.L., Z. phys. Chem. (Frankfurt), 1956, 6, 143.
124. Bektourov, A., Zhur. obshchei Khim., 1939, 9, 1717.
125. Dyrssen, D., Acta Chem. Scand., 1957, 11, 1771.
126. Seidell, A., "Solubilities of Organic Compounds," D. van Nostrand Co. Inc., New York, 1941.
127. Griffiths, D.M.L., Thesis, University of Wales, 1952.
128. Grindley, J., and Bury, C.R., J. Chem. Soc., 1929, 679.
129. Bury, C.R., and Davies, D.G., J. Chem. Soc., 1932, 2413.
130. White, P., Moule, D., and Benson, G.C., Trans. Faraday Soc., 1958, 54, 1638.
131. Moule, D., and Benson, G.C., Canad. J. Chem., 1959, 37, 2083.
132. Niekerk, J.N. van, and Schoening, F.R.L., Acta Cryst., 1953, 6, 227.
133. Lifschitz, J., and Rosenbohm, E., Z. Electrochem., 1915, 21, 499.
134. Bhatnagar, S.S., Singh, B., and Ghani, A., Indian J. Phys., 1932, 7, 323.
135. Amiel, J., Compt. rend., 1938, 207, 1097.
136. Mookerjee, A., Indian J. Phys., 1945, 19, 63.
137. Guha, B.C., Proc. Roy. Soc., 1951, A206, 353.
138. Foëx, G., Karantassis, T., and Perakis, N., Compt. rend. 1953, 237, 982.
139. Ploquin, J., and Vergneau, C., Bull. Soc. chim. France, 1951, 757.
140. Amiel, J., Ploquin, J., and Dixmier, J.A., Compt. rend., 1951, 232, 2097.
141. Bleaney, B., and Bowers, K.D., Proc. Roy. Soc., 1952, A214, 451.
142. Lancaster, F.W., and Gordy, W., J. Chem. Phys., 1951, 19, 1181.
143. Bleaney, B., and Bowers, K.D., Phil. Mag., 1952, 43, 372.
144. Kumagai, H., Abe, H., and Shimada, J., Phys. Rev., 1952, 87, 385.
145. Abe, H., and Shimada, J., Phys., Rev., 1953, 90, 316.
146. Nakomoto, K., Fujita, J., Tanaka, S., and Kobayashi, M., J. Amer. Chem. Soc., 1957, 79, 4904.
147. Costa, G., Pauluzzi, E., and Puxeddu, A., Gazzetta, 1957, 87, 885.



148. Figgis, B.N., and Martin, R.L., J. Chem. Soc., 1956, 3837.
149. Abe, H., Phys. Rev., 1953, 92, 1572.
150. Abe, H., J. Phys. Soc. Japan, 1958, 13, 987.
151. Martin, R.L., and Waterman, H., J. Chem. Soc., 1957, 2545.
152. Tsuchida, R., and Yamada, S., Nature, 1955, 176, 1171.
153. Yamada, S., Nakamura, H., and Tsuchida, R., Bull. Chem. Soc. Japan, 1957, 30, 953.
154. Yamada, S., Nakamura, H., and Tsuchida, R., Bull. Chem. Soc. Japan, 1958, 31, 303.
155. Tsuchida, R., Yamada, S., and Nakamura, H., Nature, 1958, 181, 479.
156. Tsuchida, R., and Yamada, S., Nature, 1958, 182, 1230.
157. Tsuchida, R., Yamada, S., and Nakamura, H., Nature, 1956, 178, 1192.
158. Martin, R.L., and Whitley, A., J. Chem. Soc., 1958, 1394.
159. Kondo, M., and Kubo, M., J. Phys. Chem., 1958, 62, 468.
160. Graddon, D.P., J. Inorg. Nuclear Chem., 1959, 11, 337.
161. Graddon, D.P., Nature, 1960, 186, 715.
162. Pedersen, K.J., Kgl. danske Videnskab. Selskab, Mat.-fys. Medd., 1945, 22, No. 12.
163. Fronaeus, S., Doctoral Diss., Lund 1948.
164. Fronaeus, S., Acta Chem. Scand., 1951, 5, 859.
165. Doucet, Y., and Cogniac, R., Compt. rend., 1955, 240, 968.
166. Sircar, S.C., Adyita, S., and Prasad, B., J. Indian Chem. Soc., 1953, 30, 633.
167. Doucet, Y., and Marion, G.W., Compt. rend., 1955, 240, 1616.
168. Lloyd, M., Wycherley, V., and Monk, C.B., J. Chem. Soc., 1951, 1786.
169. Gregor, H.P., Luttinger, L.B., and Loebel, E.M., J. Phys. Chem., 1955, 59, 34.
170. Kiriya, R., Ibamoto, H., and Matsuo, K., Acta Cryst., 1954, 7, 482.
171. Hershenson, H.M., Brooks, R.T., and Murphy, M.E., J. Amer. Chem. Soc., 1957, 79, 2046.
172. Martin, R.L., and Waterman, H., J. Chem. Soc., 1959, 1359.



173. Martin, R.L., and Waterman, H., J. Chem. Soc., 1959, 2960.
174. Ewan, T., Proc. Roy. Soc., 1894, 57, 117.
175. Sidgwick, N.V., and Tizard, H.T., J. Chem. Soc., 1908, 93, 187.
176. Sidgwick, N.V., and Tizard, H.T., J. Chem. Soc., 1910, 97, 957.
177. Jones, H.C., and Uhler, H.S., Amer. Chem. J., 1907, 37, 126, 207, 244.
178. Leden, I., Doctoral Diss., Lund, 1943.
179. Rossotti, F.J.C., and Rossotti, H.S., "The Determination of Stability Constants," McGraw-Hill, New York, in the press.
180. Irving, H., and Rossotti, H.S., J. Chem. Soc., 1953, 3397.
181. Rossotti, F.J.C., in "Modern Co-ordination Chemistry," Lewis, J., and Wilkins, R.G. eds., Interscience, New York, 1960.
182. Rossotti, F.J.C., and Rossotti, H.S., Acta Chem. Scand., 1955, 9, 1166.
183. Sillén, L.G., Acta Chem. Scand., 1956, 10, 186.
184. Rossotti, F.J.C., Rossotti, H.S., and Sillén, L.G., Acta Chem. Scand., 1956, 10, 203.
185. Rossotti, F.J.C., and Rossotti, H.S., J. Phys. Chem., 1959, 63, 1041.
186. Sillén, L.G., Acta Chem. Scand., 1956, 10, 803.
187. Ingri, N., Lagerström, G., Frydman, M., and Sillén, L.G., Acta Chem. Scand., 1957, 11, 1034.
188. Sillén, L.G., unpublished work.
189. Brown, A.S., J. Amer. Chem. Soc., 1934, 56, 646.
190. Rosin, J., "Reagent Chemicals and Standards," D. Van Nostrand Co. Inc., New York, 1946.
191. Vogel, A.I., "A Textbook of Quantitative Inorganic Analysis," Longmans, Green & Co., London, 1953.
192. Forsling, W., Hietanen, S., and Sillén, L.G., Acta Chem. Scand., 1952, 6, 901.
193. Schlyter, K., Trans. Royal Inst. Tech. Stockholm, No. 132, 1959.
194. Lange, J., and Bergä, J., Monatsh, 1950, 81, 921.
195. Leden, I., Acta Chem. Scand., 1952, 6, 971.
196. Biedermann, G., and Sillén, L.G., Arkiv Kemi, 1953, 5, 425.

197. Stability Constants, Part II; Inorganic Ligands, The Chemical Society, London, 1958.
198. Gran, G., Analyst, 1952, 77, 661.
199. Rossotti, F.J.C., and Rossotti, H.S., Acta Chem. Scand., 1956, 10, 957.
200. Büchi, P.F., Z. Electrochem., 1924, 30, 443.
201. Carson, J.D.E., and Rossotti, F.J.C., unpublished work.
202. Sundén, N., Svensk kem. Tidskr., 1953, 65, 257.
203. Sonesson, A., Acta Chem. Scand., 1958, 12, 165.
204. Åhrland, S., Acta Chem. Scand., 1951, 5, 199.
205. Harned, H.S., and Owen, B.B., "The Physical Chemistry of Electrolytic Solutions," Reinhold, New York, 1958.
206. Guggenheim, E.A., Phil. Mag., 1935, 19, 588.
207. Carpeni, G., Bull. Soc. chim. France, 1948, 629.
208. Carpeni, G., Compt. rend., 1948, 226, 807.
209. Byé, J., Bull. Soc. chim. France, 1953, 390.
210. Reilly, J., and Rae, W.N., "Physico-Chemical Methods," 1954, Vol. I, p. 175, Methuen, London.
211. Cramér, H., "Mathematical Methods of Statistics," 1945, p. 560, Uppsala.
212. Schlyter, K., unpublished work.
213. Schlyter, K., Trans. Royal. Inst. Tech. Stockholm, 1960, No. 152.
214. Clarke, J.J., and Rossotti, F.J.C., unpublished work.
215. Dippy, J.F.J., Chem. Rev., 1939, 25, 151.
216. Everett, D.H., Landsman, D.A., and Pinsent, B.R.W., Proc. Roy. Soc., 1952, A215, 403.
217. Ellilä, A., Ann. Acad. Sci. Fennicae, Ser A., 1953, 11, No. 51.
218. Kolthoff, I.M., and Bosch, W., J. Phys. Chem., 1932, 36, 1685.
219. Speakman, J.C., Nature, 1948, 162, 695.
220. Speakman, J.C., J. Chem. Soc., 1949, 3357.
221. Skinner, J.M., and Speakman, J.C., J. Chem. Soc., 1951, 185.

222. Skinner, J.M., Stewart, G.M.D., and Speakman, J.C., J. Chem. Soc., 1954, 180.
223. Downie, T.C., and Speakman, J.C., J. Chem. Soc., 1954, 787.
224. Speakman, J.C., Proc. Chem. Soc., 1959, 316.
225. Bacon, G.E., and Curry, N.A., Acta Cryst., 1957, 10, 524.
226. Davies, M., and Thomas, W.J.O., J. Chem. Soc., 1951, 2058.
227. Canady, W.J., Papée, H.M., and Laidler, K.J., Trans. Faraday Soc., 1958, 54, 502, and references therein.
228. Pitzer, K.S., J. Amer. Chem. Soc., 1937, 59, 2365.
229. King, E.L., J. Chem. Educ., 1953, 30, 71.
230. Cobble, J.W., J. Chem. Phys., 1953, 21, 1451.
231. Sarolëa-Mathot, L., Trans. Faraday Soc., 1953, 49, 8.
232. Berecki-Biedermann, C., Arkiv Kemi, 1956, 9, 175.
233. Dobbie, H., Kermack, W.O., and Rees, H., Biochem J., 1955, 59, 240.
234. Irving, H., and Rossotti, H.S., Acta Chem. Scand., 1956, 10, 72.
235. Rossotti, F.J.C., and Watson, E., unpublished work.
236. Sillén, L.G., unpublished work.

# The Hydrogen-bonding of Monocarboxylates in Aqueous Solution

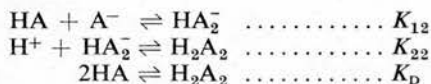
By D. L. MARTIN and F. J. C. ROSSOTTI

(DEPARTMENT OF CHEMISTRY, UNIVERSITY OF EDINBURGH)

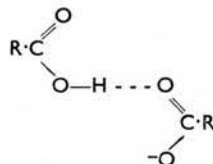
DIMERIC formic, acetic, propionic, and *n*-butyric acid have been reported to exist in aqueous solution<sup>1</sup> but previous attempts to study the equilibria have been hampered by variations in activity coefficients. The hydrogen-ion concentrations, *h*, of sodium carboxylate-carboxylic acid buffers in 3*M*-sodium (perchlorate) have been measured potentiometrically at 25° ± 0.05°. Data obtained for a wide range of *h* and of total carboxylate concentration, *A*, were analysed by methods developed in studying isopolyacids.<sup>2,3</sup> The single mononuclear association



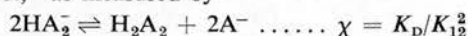
predominates for  $A \lesssim 5 \times 10^{-2}M$ , but the polynuclear equilibria



are also apparent at higher concentrations. Further association (to  $H_2A_3^-$ ,  $H_3A_3$ , etc.) appears to occur in the range  $0.7M \leq A \leq 1.0M$  with propionate and butyrate, but not in the formate and acetate systems. Values of the stoichiometric equilibrium constants are tabulated. These equilibrium constants indicate,



in the solid.<sup>5</sup> Although free rotation is possible about the hydrogen bond in solution, the ions  $HA_2^-$  are expected to exist predominantly in the extended form owing to electrostatic repulsion. The dimers may also exist in the extended form, in the cyclic form which occurs in the vapour, or as an equilibrium mixture of both configurations. The trends  $K_{11} > K_{22} > K_{12} > K_D$ , which are also in the expected order for ion-ion, ion-dipole, and dipole-dipole interactions, suggest that the dimers are predominantly in the extended form. The absence of a marked "chelate effect," as measured by



appears to support this hypothesis. However, the increase of  $K_{22}/K_{11}$ ,  $K_D/K_{12}$ , and  $\chi$  with increasing chain length is compatible with increasing stabilisation of the cyclic form.

Crystalline formic<sup>6</sup> and acetic acid<sup>7</sup> exist as infinite chains in the extended form, whereas  $\beta$ -nitropropionic<sup>8</sup> and long-chain fatty acids<sup>9</sup> consist of cyclic

Acid	log $K_{11}$	log $K_{12}$	log $K_{22}$	log $K_D$
H-CO <sub>2</sub> H	3.900 ± 0.005	-0.50 ± 0.04	3.16 ± 0.01	-1.24 ± 0.04
Me-CO <sub>2</sub> H	5.014 ± 0.009	-0.34 ± 0.03	4.63 ± 0.01	-0.73 ± 0.03
Et-CO <sub>2</sub> H	5.161 ± 0.006	-0.35 ± 0.03	5.01 ± 0.03	-0.50 ± 0.04
Pr <sup>n</sup> -CO <sub>2</sub> H	5.132 ± 0.007	-0.24 ± 0.03	5.11 ± 0.03	-0.26 ± 0.04

for example, that a maximal amount of ~10% is in the form  $HA_2^-$  in all the 1:1 buffers at  $A = 0.7M$ , and that the amount of  $H_2A_2$  in the acids increases from ~10% in formic acid to ~33% in butyric acid at the same concentration.

The species are assumed to associate by hydrogen-bonding rather than by micellar interaction of alkyl tails. The hydrogen dibenzoate ion has previously been identified in solution,<sup>4</sup> and is shown to exist in the extended form

dimers. Raman spectra<sup>10</sup> are consistent with the same structural differences in dioxan solution. The formation of higher complexes  $H_2A_3^-$ ,  $H_3A_3$ , etc., is only possible via the extended form of  $H_2A_2$ . Many physicochemical properties of concentrated aqueous solutions of the lower fatty acids indicate extensive oligomerisation.

We thank Professor L. G. Sillén for his interest and the Department of Scientific and Industrial Research for financial support.

(Received, January 8th, 1959.)

<sup>1</sup> Nash and Monk, *J.*, 1957, 4274, and references therein.

<sup>2</sup> Rossotti and Rossotti, *Acta Chem. Scand.*, 1956, 10, 957.

<sup>3</sup> Ingri, Lagerström, Frydman, and Sillén, *ibid.*, 1957, 11, 1034.

<sup>4</sup> Kolthoff and Bosch, *J. Phys. Chem.*, 1932, 36, 1685.

<sup>5</sup> Skinner, Stewart, and Speakman, *J.*, 1954, 180.

<sup>6</sup> Holtzberg, Post, and Fankuchen, *Acta Cryst.*, 1953, 6, 127.

<sup>7</sup> Jones and Templeton, *ibid.*, 1958, 11, 484.

<sup>8</sup> Sutor, Calvert, and Llewellyn, *ibid.*, 1954, 7, 767.

<sup>9</sup> von Sydow, *Arkiv Kemi*, 1956, 9, 231.

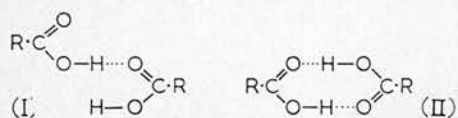
<sup>10</sup> Batuev, *Izvest. Akad. Nauk, S.S.S.R., Ser. Fiz.*, 1947, 11, 336; 1948, 12, 611.

## The Structure of Dimeric Acetic Acid in Aqueous Solution

By D. L. MARTIN and F. J. C. ROSSOTTI

(DEPARTMENT OF CHEMISTRY, UNIVERSITY OF EDINBURGH)

THE existence of the hydrogen diacetate ion  $\text{HA}_2^-$  in aqueous solution was suggested in 1930 by Dawson and Spivey<sup>1</sup> in order to explain an unexpected cross-term  $[\text{HA}][\text{A}^-]$  in the expression for the rate of oxidation of acetone in acetate buffers.<sup>2</sup> Preliminary



reports have been given<sup>3</sup> of potentiometric evidence for this species and also for the neutral dimer  $\text{H}_2\text{A}_2$ , together with formation constants valid in a 3M sodium (perchlorate) ionic medium at 25°. As the

In collaboration with Dr. Schlyter,<sup>4</sup> we have now confirmed our description of proton-acetate catenation by a method of enthalpy titration<sup>5</sup> at 25°, using the Stockholm adiabatic calorimeter. Enthalpies<sup>4</sup> and entropies of association have been calculated, and thermodynamic functions for the relevant reactions are listed in the annexed Table.

Comparison of these values suggests that reactions (1) and (2) are strictly analogous and that the latter is not a cyclisation. This conclusion is reinforced by comparing the thermodynamic functions for reactions (3) and (4). It is also noteworthy that  $\Delta S_1$  and  $\Delta S_2$  approximate to the value required by Pitzer's

Reaction	$\Delta G$ (kcal./mole)	$\Delta H$ (kcal./mole)	$\Delta S$ (e.u.)
(1) $\text{H}^+ + \text{A}^- \rightleftharpoons \text{HA}$	$-6.839 \pm 0.012$	$-0.721 \pm 0.006$	$20.53 \pm 0.06$
(2) $\text{H}^+ + \text{HA}_2^- \rightleftharpoons \text{H}_2\text{A}_2$	$-6.315 \pm 0.014$	$-0.596 \pm 0.135$	$19.2 \pm 0.5$
(3) $\text{HA} + \text{A}^- \rightleftharpoons \text{HA}_2^-$	$0.46 \pm 0.04$	$0.300 \pm 0.106$	$-0.5 \pm 0.5$
(4) $\text{HA} + \text{HA} \rightleftharpoons \text{H}_2\text{A}_2$	$1.00 \pm 0.04$	$0.425 \pm 0.047$	$-1.9 \pm 0.3$

dimer proved to be a stronger acid than the monomer, it was suggested that the dimer exists predominantly in the open (I) rather than in the cyclic form (II).

rule<sup>6</sup> for monobasic acids, in spite of the unconventional standard state.<sup>7</sup>

If the neutral dimer exists in the extended form (I)

<sup>1</sup> Dawson and Spivey, *J.*, 1930, 2180.

<sup>2</sup> Cf. Rossotti, *Nature*, 1960, 188, 936.

<sup>3</sup> Martin and Rossotti, *Proc. Chem. Soc.*, 1959, 60; *Chem. Soc. Special Publ.* No. 13, 1959, p. 182.

<sup>4</sup> Schlyter and Martin, *Kgl. Tekn. Högskolans Handl.*, in the press.

<sup>5</sup> Schlyter, *Kgl. Tekn. Högskolans Handl.*, 1959, no. 132; 1960, no. 152; Schlyter and Sillén, *Acta Chem. Scand.*, 1959, 13, 385.

<sup>6</sup> Pitzer, *J. Amer. Chem. Soc.*, 1937, 59, 2365.

<sup>7</sup> Cf. Rossotti, in "Modern Co-ordination Chemistry," ed. Lewis and Wilkins, Interscience Publ. Inc., New York, 1960.



like the ion  $\text{HA}_2^-$ , then the following approximate relationship might be expected between the partial molar entropies:

$$S_{\text{H}_2\text{A}_2}^\circ - S_{\text{HA}}^\circ \approx S_{\text{H}_2\text{A}_2}^\circ - S_{\text{A}}^\circ \quad (5)$$

whence

$$\Delta S_1 \approx \Delta S_2. \quad (6)$$

If we calculate the conventional partial molar entropies from Cobble's empirical equations for neutral and ionic organic solutes,<sup>8</sup> the approximate eqns. (5) and (6) are exact and equal to 22 e.u. However, reactions (1) and (2) will be accompanied by an increase in the configurational entropy of the organic solutes and a release of water from the hydration spheres of the ionic reactants. The former effect will be expected to be more marked for reaction (2), whereas the latter effect should be less pronounced for reaction (2) owing to hydrogen-bonding of water to the centre of the dimer. Our experimental result,  $\Delta S_1 > \Delta S_2$ , appears to be significant and, indeed, some analogous reactions suggest that the dehydration factor is the more important of the two. The entropies of protonation,  $\Delta S_1$ , of monomeric acetate,<sup>9</sup> butyrate,<sup>9</sup> and methoxyacetate<sup>10</sup> ions are

22.0, 24.5, and 19.6 e.u. respectively in the conventional standard state. The increase in  $\Delta S_1$  with increasing chain length has been ascribed to the configurational effect,<sup>11</sup> and the lower value of  $\Delta S_1$  in the methoxyacetate system to the dehydration effect.<sup>10</sup>

It is difficult to predict a value of  $\Delta S_2$  for the formation of a cyclic dimer (II) by reaction (2) owing to the impossibility of assessing differences in hydration between molecules (I) and (II). However, as  $S_{\text{H}_2\text{O}}^\circ$  is 16.7 e.u., and the entropy of cyclisation about  $-14$  e.u.,  $\Delta S_2$  would probably be greater than  $\Delta S_1$ . It therefore appears to be most likely that dimeric acetic acid exists predominantly in the open form (I) in aqueous solution.

We thank the D.S.I.R. and the Post-graduate Studentship Committee of Edinburgh University for financial assistance, and Dr. K. Schlyter and Professor L. G. Sillén for their help with the calorimetry.

(Received, December 9th, 1960)

<sup>8</sup> Cobble, *J. Chem. Phys.*, 1953, **21**, 1451.

<sup>9</sup> Canady, Papée, and Laidler, *Trans. Faraday Soc.*, 1958, **54**, 502.

<sup>10</sup> King, *J. Amer. Chem. Soc.*, 1960, **82**, 3575.

<sup>11</sup> Evans and Hamann, *Trans. Faraday Soc.*, 1951, **47**, 34.